UNLIMITED DISTRIBUTION

National Defence Défense nationale

Research and Development Branch Bureau de Recherche et Développement

CR/89/414

PARAMETERIZATION OF DIRECTIONAL SPECTRA

by
Barbara-Ann Juszko

JUSZKO SCIENTIFIC SERVICES
483 Sue Mar Place
Victoria, British Columbia, Canada
V9C 3E1

Scientific Authority
Ross Graham

Contract Number
W7707-8-1049/01-OCS

31 March 1989

CONTRACTOR REPORT
Prepared for

Defence Research Establishment Atlantic

Centre de Recherches pour la Défense Atlantique

ABSTRACT

High-resolution directional wave spectra, obtained from a WAVEC buoy moored on the Grand Banks in 1984, were modelled using various directional parameterizations. Consistent with most approaches in the literature, a two-part parameterization was attempted. Initially, the Ochi and Hubble (1976) six-parameter amplitude model (OH model) was fitted to the data amplitude spectrum. Parameterization of the directional component was then examined using a basic two-parameter cosine-power model upon which various limitations on the parameters were introduced. The model was assessed by its ability to reproduce the data spectrum based on a least-squares residual statistic. A 10-parameter model, for which the amplitude and direction parameters were fitted simultaneously, was then developed as an extension to the OH model. It was shown to outperform any equivalent, two-part parameterization and could acceptably reproduce over 90% of the data records.

RÉSUMÉ

Des spectres directionnels d'ondes haute résolution mesurés en 1984 par une bouée WAVEC amarrée dans les Grands Bancs ont été modélisés au moyen de diverses paramétrisations directionnelles. On a adopté une paramétrisation en deux parties, ce qui correspond à la plupart des approches suggérées dans la littérature. On a commencé par ajuster le spectre d'amplitude des données au moyen du modèle d'amplitude à six paramètres de Ochi et Hubble (modèle OH, 1976). On a ensuite étudié la paramétrisation de la composante directionnelle au moyen d'un modèle de base à deux paramètres et à puissances du cosinus, auquel sont appliquées les diverses contraintes sur les paramètres. On a évalué la faculté de reproduction du spectre de données par le modèle, au moyen d'une statistique résiduelle à moindres carrés. On a développé un modèle à 10 paramètres prolongeant le modèle OH et pour lequel les paramètres d'amplitude et de direction ont été ajustés simultanément. On a démontré que ce modèle est plus performant que toute paramétrisation équivalente en deux parties et peut reproduire adéquatement plus de 90% des articles de données.

TABLE OF CONTENTS

LIST OF FIGURES

LIST OF TABLES

1. INTRODUCTION

The information contained in directional wave spectra, whether obtained directly from field measurements or predicted by wave hindcast models, can be used in numerous applications. The parameterization of this information is often desired, in both theoretical and applied marine research, to allow for simple incorporation into models and to answer certain computer storage and operational demands. Different parameterizations will result in varying degrees of information loss with a corresponding increase in errors. A rejection criterion should be established in order to decide whether or not the chosen parameterization is acceptable for the desired application. Providing a limit on an objectively determined bulk error statistic which describes the overall spectrum, would allow for a rapid screening of any data/model set prior to implementation.

In the winter of 1984, Datawell WAVEC heave/slope data were collected near the Hibernia C-96 drill site. These data have recently been processed using newly developed, high-resolution directional analysis techniques. This study will assess how well a simple directional parameterization, linked to an existing six-parameter heave model, describes the real data spectrum.

2. STUDY BACKGROUND

2.1 Study Objective

The major objective of this study is to provide a simple description of a directional wave spectrum using a limited number of parameters. As each directional spectrum consists of N frequencies X M directions values, large data storage capabilities may be required for some applications. This is particularly true when examining hindcast model spectra whose time series may extend over many years. Limiting the number of parameters to ten, for example, may reduce these storage demands by one to two orders of magnitude. As the chosen parameters may show functional relationships between themselves, or with measured environmental signals, their values may be predictable or could be used to characterize classes of spectral types, useful in both theoretical and practical applications.

In this study, the analysis will be performed on field data collected in 1984. This data set was chosen as its characteristics were well known, the study location was relatively fetch unlimited, and the time series contain periods of widely varying energy and direction signals. This allows for an assessment of model behavior for a range of conditions and on a data set expected to contain a high degree of stochastic variability thereby providing the worst case results. If the parameterization works acceptably under these conditions, the application to hindcast model spectra should pose no problem. Following sections will describe in greater detail, the study

location, data set and the approach that will be used to develop an appropriate parameterization to the complete frequency/direction spectrum.

2.2 Study Location

Directional wave data were collected using a Datawell slope-following WAVEC buoy, moored in approximately 85 meters of water, near the Hibernia C-96 drill site on Newfoundland's Grand Banks. This buoy was assigned MEDS (Marine Environmental Data Service) Station No. 249 at location 46 deg. 44.83 min. North, 48 deg. 49.75 min. West (see Figure 1). The data set covers the recording period from February 28 to April 3, 1984. The buoy sampled for 34 minutes, every three hours at a frequency of 1.28 Hz.(ie. every 0.78125 sec). During storms, the sampling was continuous. Wave information was telemetered to receiving equipment located aboard the West Venture mobile drilling unit, operated by Mobil oil Canada Ltd. and stationed at 46 Deg. 45.17 min. N., 48 Deg. 44.59 min. W., approximately five kilometers from the buoy. Meteorological information was also available from this drilling platform.

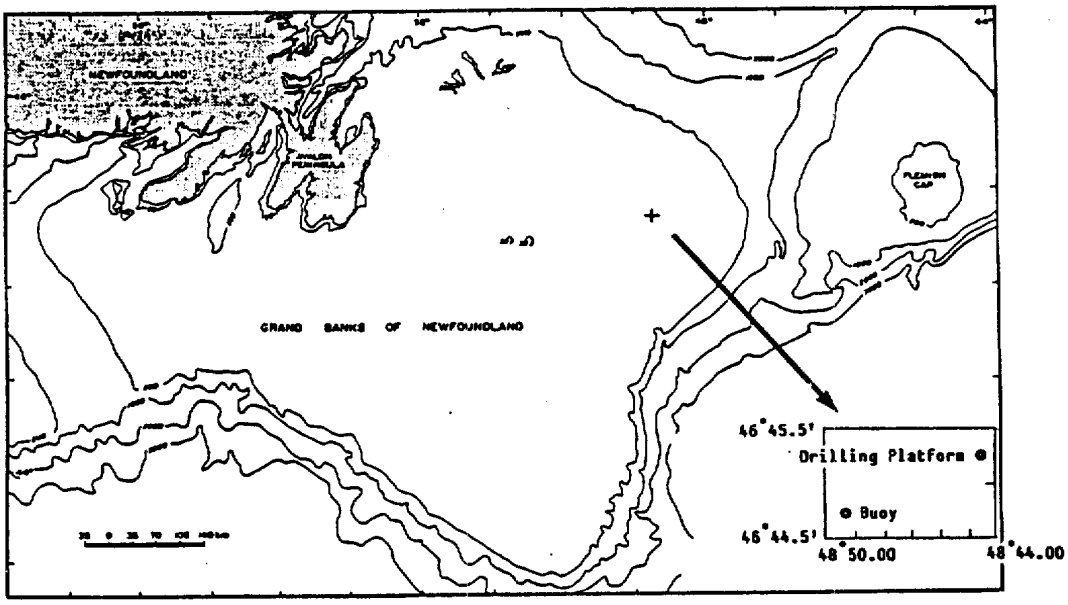

Fig. 1 Study location

The buoy location was particularly favorable for this study as it provided fetch unlimited conditions from North to West (270 degrees of azimuth) and limited to about 200 kms. from West to North. Most of the

other existing WAVEC data were collected in reduced fetch conditions. The major limitation of the study site was the water depth of 85 meters which may influence long period swell contributions to the wave spectrum.

2.3 Data Set

The directional spectra were available from earlier studies (see Juszko, 1988 and 1989 for details). The time series of wave heave and two slopes were processed, using standard Fourier analysis techniques, to obtain the cross-spectral matrix, with a frequency resolution of 0.062832 radians/sec (0.01 Hz). Normally, 20 groups were ensemble averaged to provide 40 degrees of freedom per spectral estimate. Records with less then ten groups were rejected. There were 560 acceptable data runs.

The cross-spectral matrix was processed to directional spectra using the data-adaptive techniques of either Oltman-Shay and Guza(1985) (Iterative Maximum Likelihood Method, IMLM) or of Marsden and Juszko (1987) Iterative Eigenvector Method, IEIG). The direction was resolved to four degrees. This data adaptive spectrum will be referred to through the text as the MJ spectrum. The choice of technique depended on the presence of double peaks in the directional spectra and the noise-to-signal ratio, both determined after an initial processing with the non-iterative Eigenvector technique. The IMLM technique was used only for single peaked spectra when the noise-to-signal ratio was less than 20%. The noise represents the background isotropic energy present at each frequency. For each frequency, the directional parameters P (an indication of directional spread) and Θm (the mean direction), described by Hasselmann et. al. (1980) and based on the Longuet-Higgins et. al. (1963) model spectrum (COS2P-LH):

$$S(\theta) = A \cos^{2P}\left(\frac{\theta-\theta m}{2}\right) \qquad (1)$$

were calculated. These were obtained using the relationships:

$$\theta m = \mathrm{TAN}^{-1}(QD13/QD12) \qquad K^2 = \frac{CO22+CO33}{CO11}$$

$$P = \frac{RTEMP}{1-RTEMP} \qquad RTEMP = \frac{\sqrt{(QD12^2+QD13^2)}}{K(CO11)}$$

where 1, 2 and 3 represent the heave and two slope signals, CO## and QD## are the co- and quad-spectral values between the respective numbered signals, and K is the wavenumber at the given frequency. Similar directional parameters were obtained through a non-linear

least-squares fit to the directional spectra (COS2P-FIT) by minimizing the residual:

$$\delta^2 = \sum_{I=1}^{N} [\, Sd(\theta_I) - (A \cos^{2P}(\frac{\theta_I - \theta m}{2}) + \alpha)]^2$$

where Sd is the estimated data spectrum, N is the number of direction bins and α is the isotropic noise contribution. A measure of the accuracy of the fit-was given by:

$$RES = \frac{\sum_{I=1}^{N} [Sd(\theta_I) - S(\theta_I)]^2}{\sum_{I=1}^{N} [Sd(\theta_I)]^2} \qquad (2)$$

and a value of RES= 0.05 was suggested for the rejection criteria. The calculation of the COS2P-LH spectra permits intercomparison of the MJ based COS2P-FIT with standards for directional spectra established in the physical oceanographic literature.

When calculating the MJ spectrum, the errors in this data-adaptive model cross-spectral matrix, as well as the two COS2P models were determined. The error in the cross-spectral matrix supplies a statistic for evaluating how well the model reproduces the actual data cross-spectral matrix. Its calculation is discussed in Marsden and Juszko (1987). Given a model estimate of the cross-spectral matrix, $\vec{d}$, and the actual data cross-spectral matrix, $\vec{\hat{d}}$, the stochastic error is given by $\rho^2 = \vec{e}^T V^{-1} \vec{e}$ where $\vec{e} = \vec{d} - \vec{\hat{d}}$ and V is the expected co-variance of $\vec{d}$ and calculated according to Long (1980). If the difference between the matrices is small (ie. $\vec{e}$ is small), ρ^2 should follow a chi-squared distribution. This statistic is only used as a rejection criteria. For this application, a value of 9.8 represents rejection at the 80% confidence level (ie. models whose ρ^2 is greater than 9.8 can be rejected with 80% confidence). An attempt will be made to use this statistic to examine the relative behavior of different directional parameterizations proposed in this study.

All of the above information was available prior to the commencement of this study. During the course of this work, it was found that a smoothed, or band-averaged spectra would be required in order to reduce the variability in the model parameters. For this purpose, the heave spectrum and directional spectrum were band-averaged. The calculated directional spectra could not be

band-averaged directly as many of the calculated statistics are non-linear. The cross-spectral matrices were band-averaged and reprocessed in the manner described above. The averaging provided a frequency resolution of 0.1884955 radians/sec (0.03 Hz) and generally, 120 degrees of freedom to each spectral estimate. The frequency range extended from 0.314 to 3.14 radians/sec (ie. 0.05 to 0.50 Hz).

2.4 Methodology

There are numerous parameterizations in the literature to describe the amplitude spectrum (eg. Pearson-Moskowitz spectrum, JONSWAP spectrum) while the direction component, treated separately, has generally been considered to be frequency dependent and described by a mean direction and spread parameter, as described in the previous section. Our ultimate goal is a single expression to describe the frequency/direction information. To do this, a hierarchy of models will be developed and evaluated.

The parameterization of the amplitude spectrum, expressed by the Ochi and Hubble (1976) model

$$S(\omega) = \frac{1}{4} \sum_{i=1}^{2} \frac{\left(\frac{4\lambda_i + 1}{4}\, \omega m_i^4\right)^{\lambda_i} \delta_i^2 \, e^{-\left(\frac{4\lambda_i+1}{4}\right)\left(\frac{\omega m_i}{\omega}\right)^4}}{\Gamma(\lambda_i)\omega^{4\lambda_i+1}} \qquad (3)$$

will be used as the basic model for the study. This will be referred to as the OH model or spectrum throughout the report. The direction information will then be incorporated in various levels in order to provide greater generalization at each stage. The OH model will then be extended to include the direction information (also suggested by Hogben and Cobb, 1986) in the form

$$M(\omega,\theta) = \frac{1}{4} \sum_{i=1}^{2} \frac{\left(\frac{4\lambda_i + 1}{4}\, \omega m_i^4\right)^{\lambda_i} \delta_i^2 \, e^{-\left(\frac{4\lambda_i+1}{4}\right)\left(\frac{\omega m_i}{\omega}\right)^4} * \cos^{2p_i}\left(\frac{\theta - \theta m_i}{2}\right)}{\Gamma(\lambda_i)\omega^{4\lambda_i+1}} \qquad (4)$$

This model will be referred to as the ten-parameter model. Finally, an attempt will be made to obtain a functional relationship between the directional and the OH model parameters.

The stages that will be followed, and which reflect the organization of this report are:

1. The OH model will be fit to the amplitude spectrum and its behavior evaluated. The fit procedure, for both this stage and the 10-parameter model are similar and described in Section 2.5 .

2. Level 1 parameterization. The COS2P-LH and COS2P-FIT (egs. 1 and 2) parameters were previously calculated independently at each frequency which required a normalization of the direction distribution to the data amplitude spectrum. In Level 1, the existing directional distributions will be normalized to the OH model amplitude spectrum to investigate the error being introduced by the new fitted spectral densities. Both the mean direction and spread are allowed to vary with frequency. This provides baseline statistics for later comparison.

3. Level 2, 3 and 4 parameterization. In these levels, the direction parameters, particularly the directional spreads, will have increased restrictions placed on them. In Level 2, the mean direction associated with $\omega m1$ and $\omega m2$, will be kept constant with frequency and the P1 and P2 value, associated with the COS2P-FIT results at $\omega m1$ and $\omega m2$, will be varied with frequency using a known functional relationship based on $\omega/\omega mi$. P1 and P2 will be allowed to vary from one 35 minute record to the next. Level 3 is similar to Level 2, however a constant value for P1 and P2 will be chosen over all the samples, though still varied with frequency. In Level 4, P1 and P2 will no longer be allowed to vary with frequency.

4. The 10-parameter model of equ. 4 will be fit to the complete directional spectrum. Neither the mean direction nor the directional spread are explicitly allowed to vary with frequency.

5. A regression analysis between the COS2P-FIT P1 and P2 values and the OH model parameters will be performed to determine a predictive relationship thereby allowing for a further reduction in the number of parameters for storage.

2.5 Fit Procedure

Equations 3 and 4 represent non-linear models of the parameters, ωm, λ, δ, Θm and P which must be solved using iterative techniques. Here a first guess to each parameter is used to calculate a fit residual, given by

$$\sum_{I=1}^{N} [E(\omega_I) - S(\omega_I)]^2 \quad \text{OR} \quad \sum_{I=1}^{N} \sum_{J=1}^{M} [D(\omega_I,\theta_J) - M(\omega_I,\theta_J)]^2$$

The parameters are modified slightly, based on the method of steepest descent, and then the new fit residual examined. If the residual decreases, the new parameter values are taken as the second guess and the process is repeated until a "stop" criteria is met. All non-linear

methods are sensitive to the choice of first guess and different guesses may result in no convergence or convergence to widely different parameter values. This can be visualized if one considers the iterative series of residuals, each residual representing one realization of the set of model parameters, of which there are an infinite number, as peaks and canyons of different heights and depths. If the first guess happens to find itself in a "canyon", not necessarily the deepest, any change in the parameters will result in a residual increase and thereby be rejected.

The Levenberg-Marquardt method was used for the iteration as it is one of the steepest descent methods which is least sensitive to the choice of the first guess while providing reasonably rapid convergence. The software to perform the fit is available in the "Numerical Recipes" mathematical library and described in Press et. al. (1986). The routine, as written, has no constraints on the predicted parameter values. It was soon found that the program would often converge to physically unrealistic values and the routine was modified for this application. The user has to supply a function subroutine which contains the model equation as well as the derivatives of the function with respect to each parameter being varied. The algorithms used are given in Appendix 1 .

Considerable time was spent on determining appropriate first guesses and parameter constraints. These are described in the appropriate sections later in the report.

2.6 Model Evaluation

Objective statistics are required to assess the relative performance of the different models. In the case of the fit of the energy spectrum to the OH model a residual error of the form

$$\mathrm{RESH} = \frac{\sum_{I=1}^{N} [E(\omega_I) - S(\omega_I)]^2}{\sum_{I=1}^{N} [E(\omega_I)]^2} \qquad (5)$$

was used, Here, N is the number of frequencies, E represents the data spectrum and S the model spectrum. RESH is normalized by the total energy thereby allowing for inter-spectral comparison.

To assess the directional spectrum, a similar least-squares residual statistic will be calculated as:

$$RESD = \frac{\sum_{i=1}^{N}\sum_{j=1}^{M}[D(\omega_i,\theta_j) - M(\omega_i,\theta_j)]^2}{\sum_{i=1}^{N}\sum_{j=1}^{M}[D(\omega_i,\theta_j)]^2} \quad (6)$$

where D represents the "best" directional spectrum (ie, the MJ spectrum) and M the model spectrum and the error is summed over all frequency and direction bins. The residual error, RESD, is not to be confused with RES discussed earlier (eq. 2). which describes the least-squares fit of the COS2P-FIT model at each frequency.

A second statistic is given by:

$$WXS = \frac{\sum_{i=1}^{N}\rho^2 E(\omega_i)}{\sum_{i=1}^{N}E(\omega_i)} \quad (7)$$

Here, ρ^2 represents the error in the cross-spectral matrix for each frequency i. The WXS statistic thus provides a energy weighted mean of ρ^2 and can be considered to be a representative value of the accuracy of the model in reproducing the data cross-spectral matrix over a 35 minute sampling period.

3. FIT OF OCHI AND HUBBLE SIX PARAMETER SPECTRA

3.1 Model Description

The Ochi and Hubble (1976) model considers the heave (ie. surface displacement) spectrum to be composed of a low-frequency "swell" and a high-frequency "sea" component. In actuality, this distinction, between sea and swell, can become blurred for many actual data spectra. Each component is described using three parameters: a modal frequency (ωm), a significant wave height (δ) and a shape parameter (λ). The two components are then added together to generate the complete spectrum having the functional form:

$$S(\omega) = \frac{1}{4}\sum_{i=1}^{2}\frac{\left(\frac{4\lambda_i+1}{4}\,\omega m_i^4\right)^{\lambda_i}\,\delta_i^2\; e^{-\left(\frac{4\lambda_i+1}{4}\right)\left(\frac{\omega m_i}{\omega}\right)^4}}{\Gamma(\lambda_i)\omega^{4\lambda_i+1}} \quad (8)$$

Ochi and Hubble (1976) found that this form acceptably reproduces spectra over a large range of energy and shape conditions. It will not

be able to handle spectra containing more than two distinctive peaks. The fit was performed on all 560 records of the data set.

3.2 Fitting Procedure

The general fit procedure was described in Section 2.5 . Various first guesses were tried including constant values for the six-parameters, values obtained from characteristics of the spectrum (eg. peak frequency and significant wave height) and using the parameter values from a previous record as the first guess for the current record (assuming little change between the time series of heave spectra). It was found that the fit was most sensitive to the initial estimate of the two modal frequencies. The simplest, and generally most reliable, method finally used was to scan for the position of peaks. The frequencies associated with the two largest peaks were taken as the first guesses for $\omega m1$ and $\omega m2$ ($\omega m1 < \omega m2$). The first guess for the values of $\delta 1$ and $\delta 2$ were calculated from the spectrum according to:

$$\delta_1 = 4.0 * \mathrm{SQRT} \left(\int_{\omega_1}^{\omega_2} E(\omega) d\omega \right) \qquad \omega_1 = 0.25$$

$$\delta_2 = 4.0 * \mathrm{SQRT} \left(\int_{\omega_2}^{\omega_3} E(\omega) d\omega \right) \qquad \omega_2 = (\omega m_1 + \omega m_2) * 0.5$$

$$\omega_3 = 3.14$$

The first guesses for the shape parameters, $\lambda 1$ and $\lambda 2$, were taken as constant at 2.5 and 1.0 respectively which seemed to be representative values according to the results of Ochi and Hubble (1976).

It was necessary to set limits on the fit parameters for convergence to occur at realistic values. These limits were:

$$0 < \omega m_1, \omega m_2, \delta_1, \delta_2, \lambda_1, \lambda_2 < 20$$

$$\omega m_1 \leq \omega m_2$$

$$0.25 \leq \omega m_1 \quad \omega m_2 < 3.14$$

Various other limits were tested, but the above were the least stringent that still supplied acceptable fits. The "stop" criteria was set at 100 iterations or 15 iterations in a row resulting in a relative change in the fit residual of less than 2.E-5.

3.3 Fit Assessment

Figure 2 contains the time series plots of wind speed and direction, the measured significant wave height, the RESH value (EQ. 5) and the six model parameters. The time series of model parameters are quite "spiky", particularly for the shape values. A portion of the

variability can be explained by the dominant parameters (ie. containing most of the energy) alternating between the "low" and "high" frequency assignment. One must also question whether the model is fitting to features in the data spectrum which result from the physical variability of the sea or are due to stochastic errors inherent in the power spectral estimate. As later in the study, one would like to develop a functional relationship between the OH parameters and the directional parameters, the noisiness of the fit parameters could make this difficult. Smoothing the energy spectrum by band-averaging was found to reduce the stochastic noise.

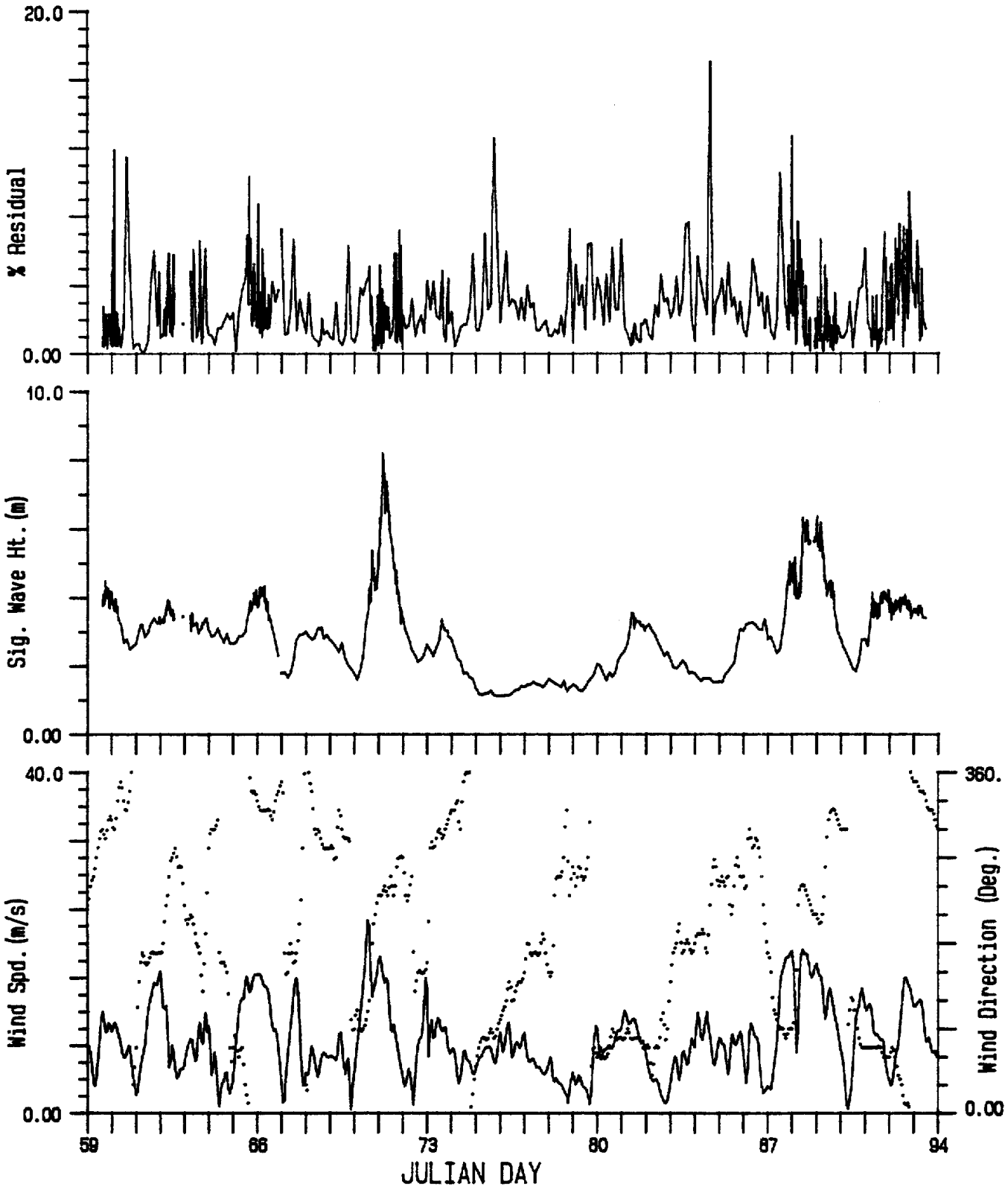

Fig. 2 Time series of fit residual, environmental and model parameters

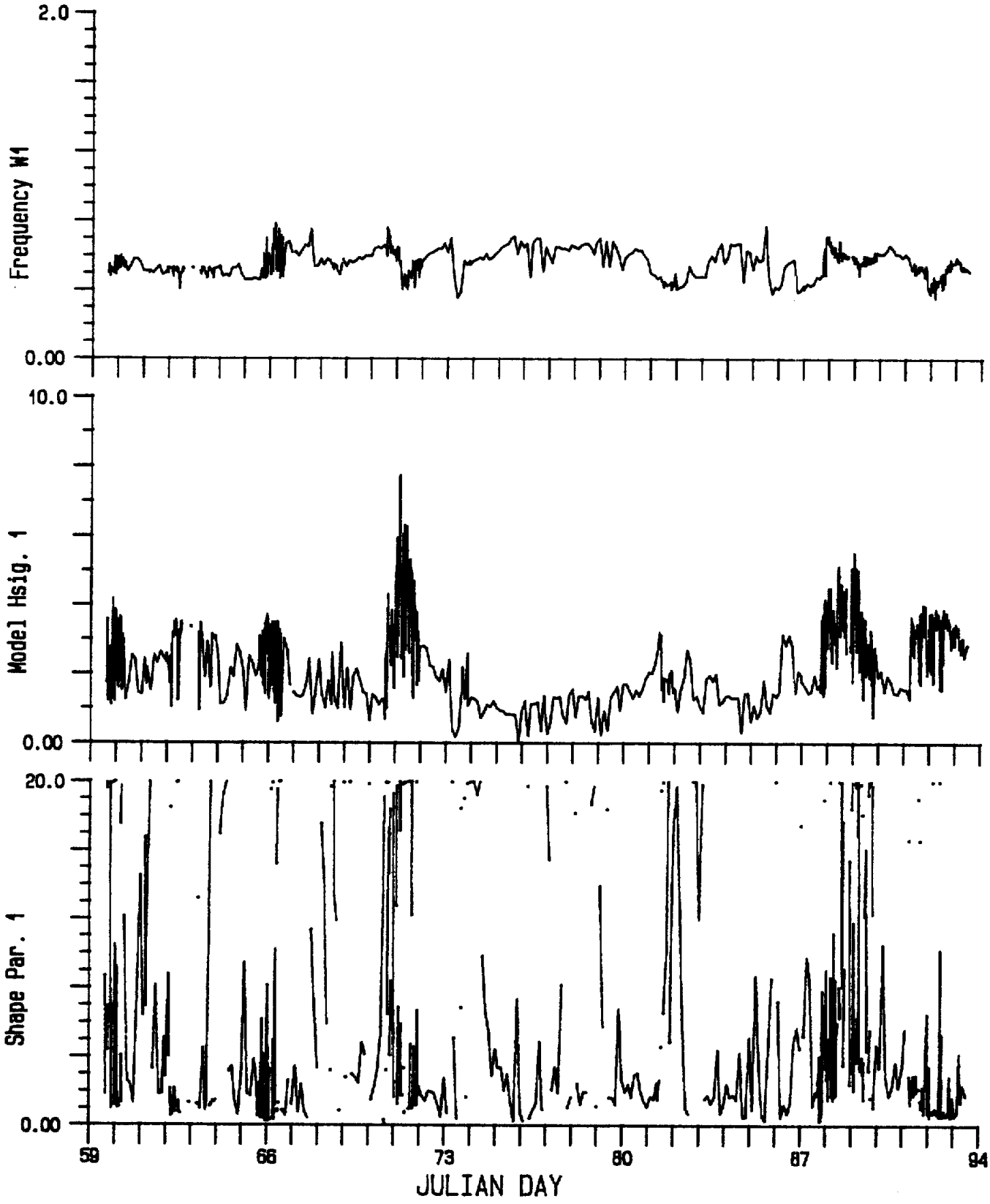

Fig. 2 (continued)

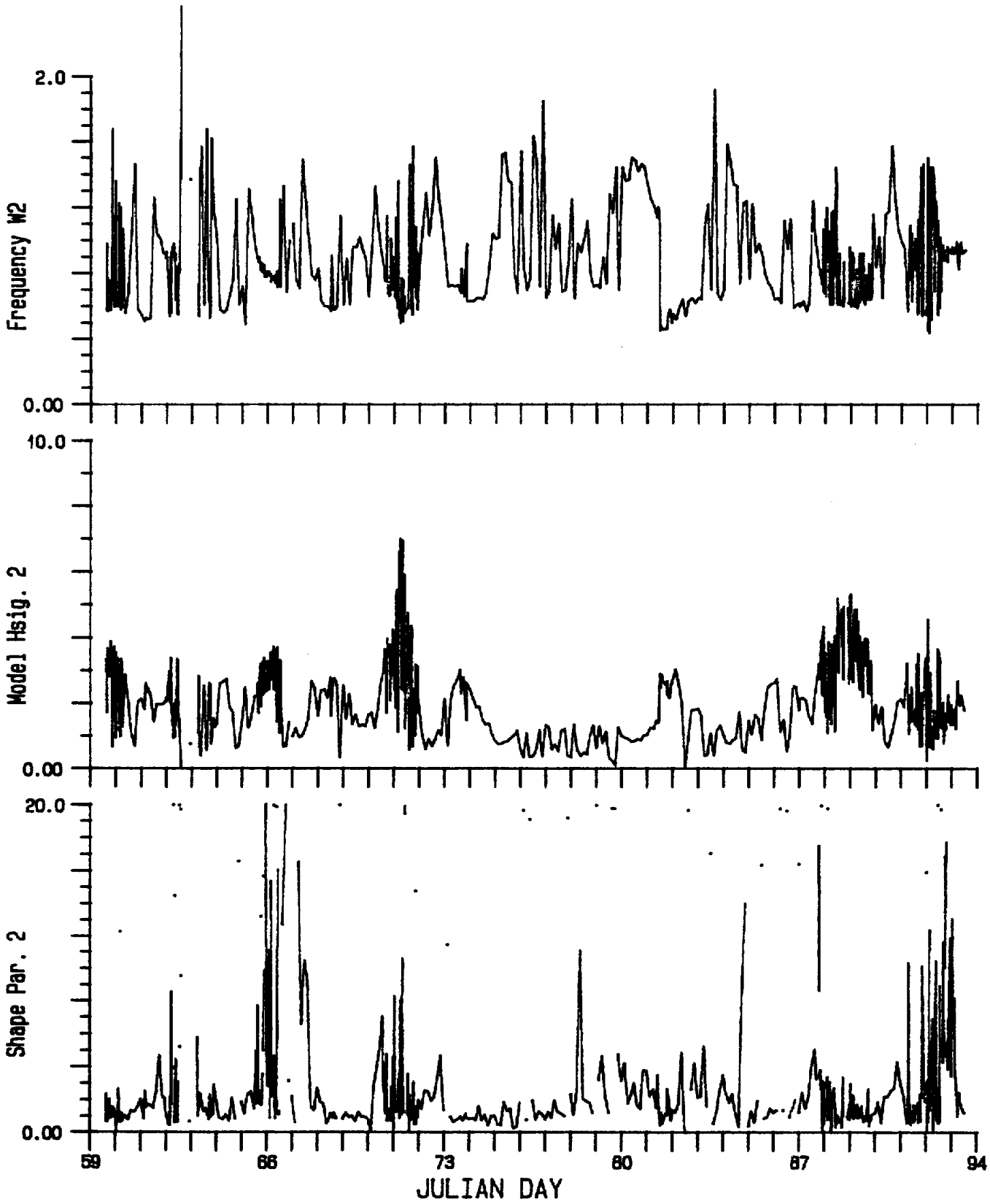

Fig. 2 (continued)

The original data spectrum was smoothed using a three-point averaging and a new fit to the model calculated. These fit results are shown in Figure 3 . The RESH value was calculated between the model and smoothed data spectrum and is reduced from the original analysis results. The fit parameters for the "swell" component are considerably less noisy. The second set of parameters still contain a high degree of variability though they are now generally associated with lower energy.

Appendix 2 and Figure 4 contain examples of the OH fits to both the original (left) and smoothed (right) data spectra for the two storms encountered during the study (Storm 1: Day 70-72; Storm 2: Day 87-89). Also shown on the plots are the RESH values for the respective model fit and the 95% confidence limits (dots) on the data spectrum (solid line). It can be seen that the fitting procedure works well for both single peaked (Eg. 1500 day 88) and double-peaked spectra (Eg. 600, 900 day 70) though the model may fall off too steeply to the right of the second peak. Such a shoulder could only be handled using a third wave component. It is often difficult to distinguish the model fit to the spectrum from the spectrum itself. The model does not handle well spectra with more than two large peaks (Eg. 1200 day 87). In general, the fit to the smooth spectrum does not drop off as quickly on the high frequency side of the peak though it may miss some low frequency energy.

An assessment was made of the model fit at each frequency. This is reflected in Fig. 5a which contains the plot of RESH as a function of frequency with the solid line representing the fit to the original data and the dotted line the fit to the band-averaged spectrum. Here, the RESH calculation, similar to eq.5 is summed over all the records, at a given frequency, instead of over frequency for each record. This figure indicates the frequency range over which the greatest confidence in the model results can be placed. Both the original and smooth fit indicate poor handling of the first three frequency bands (ω<0.44). The fit to the original spectra shows a rapid rise in RESH for frequencies above 1.0 radians/sec which does not occur until 1.5 radians/sec in the smooth case. The larger errors at high frequency result because energy levels are low in this region and a small absolute difference between the model and the data can represent a large relative difference. If the energy maximum, as opposed to the energy at each frequency, is used to replace the denominator in the RESH calculation, an implicit weighting of the error as a function of the relative energy contribution to the spectrum of the given frequency is included. The results of this calculation are shown in Figure 5b and, in this case, the RESH values never exceed 1%.

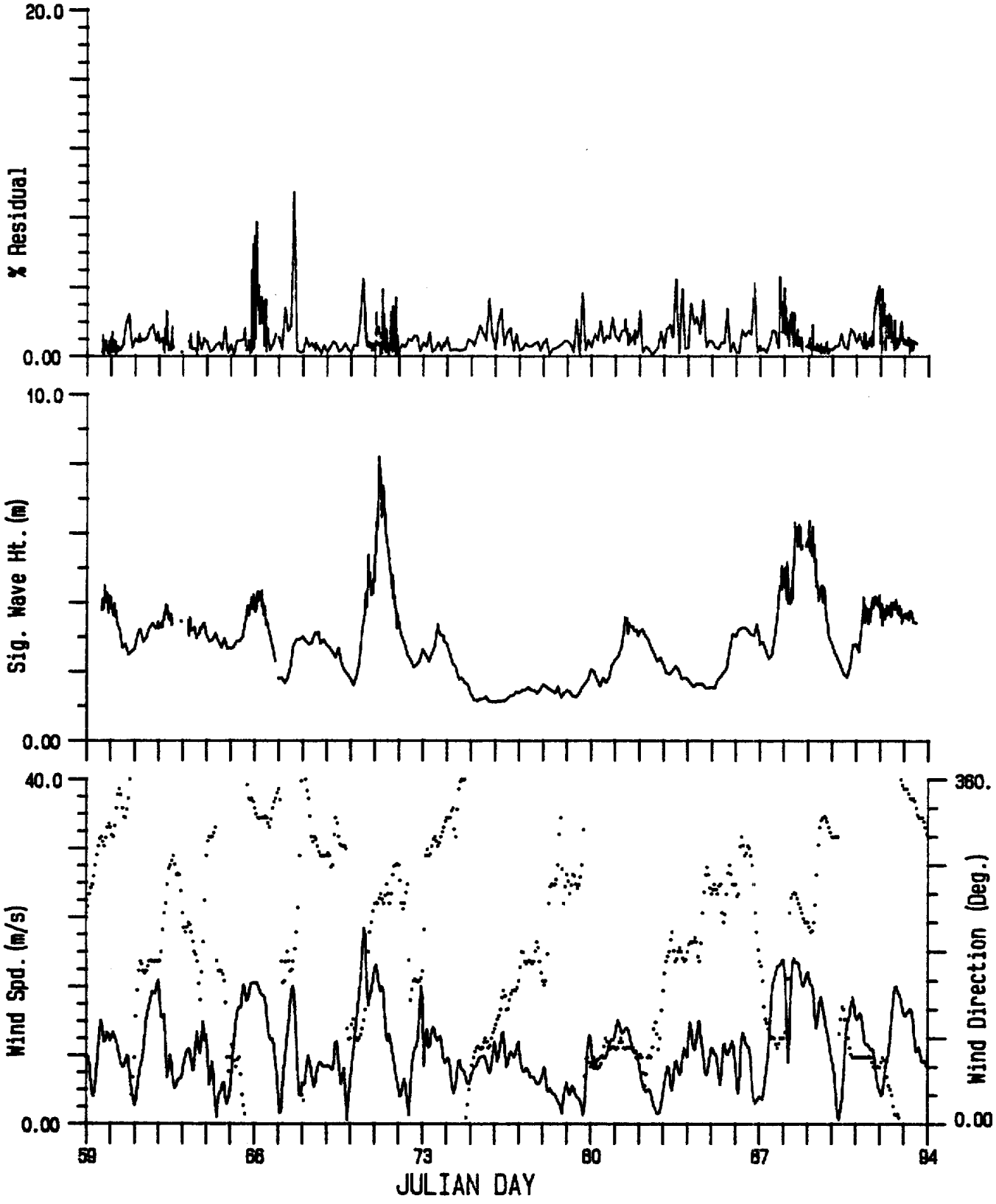

Fig. 3 Time series of fit residual, environmental and model parameters for the smoothed spectrum

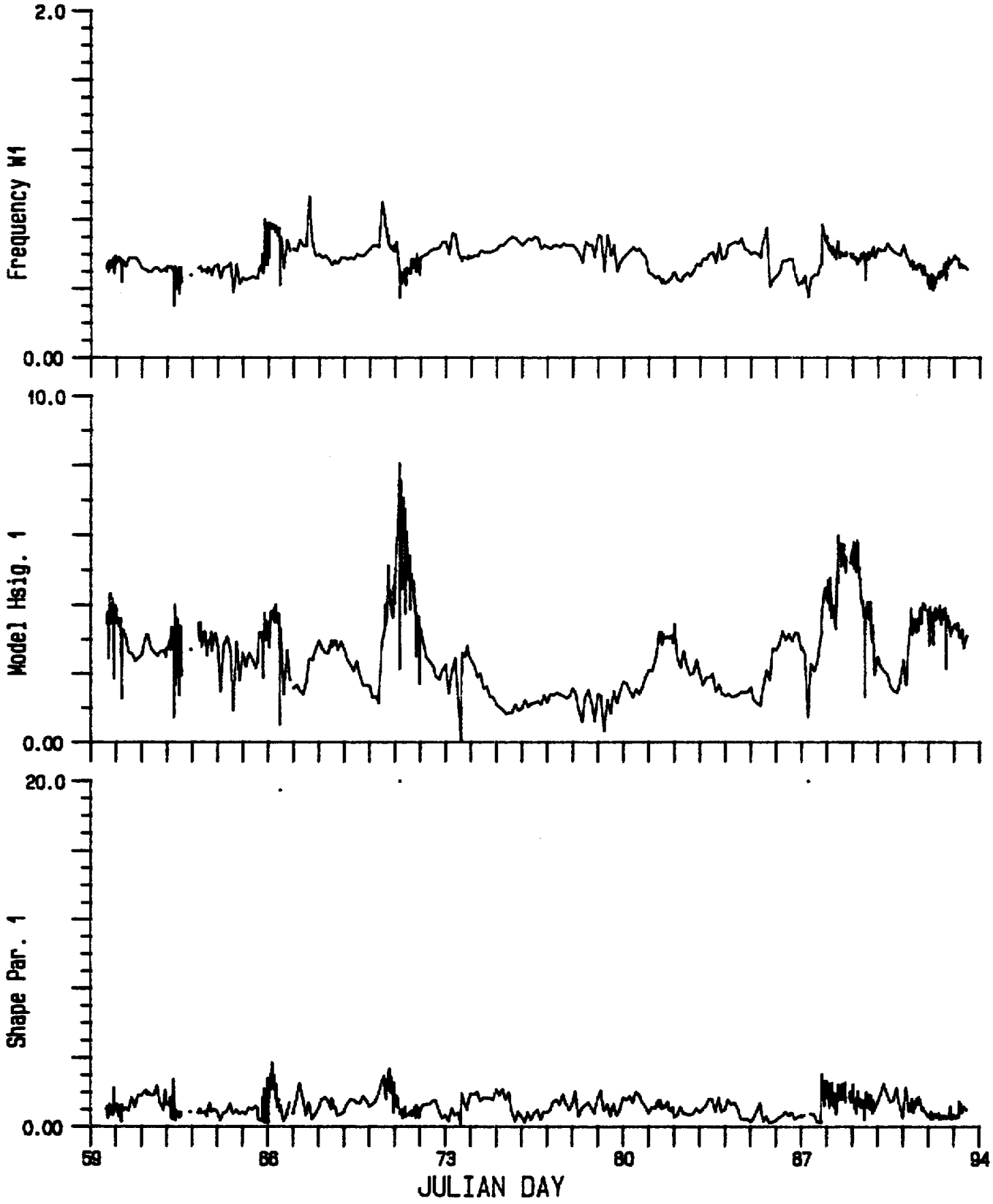

Fig. 3 (continued)

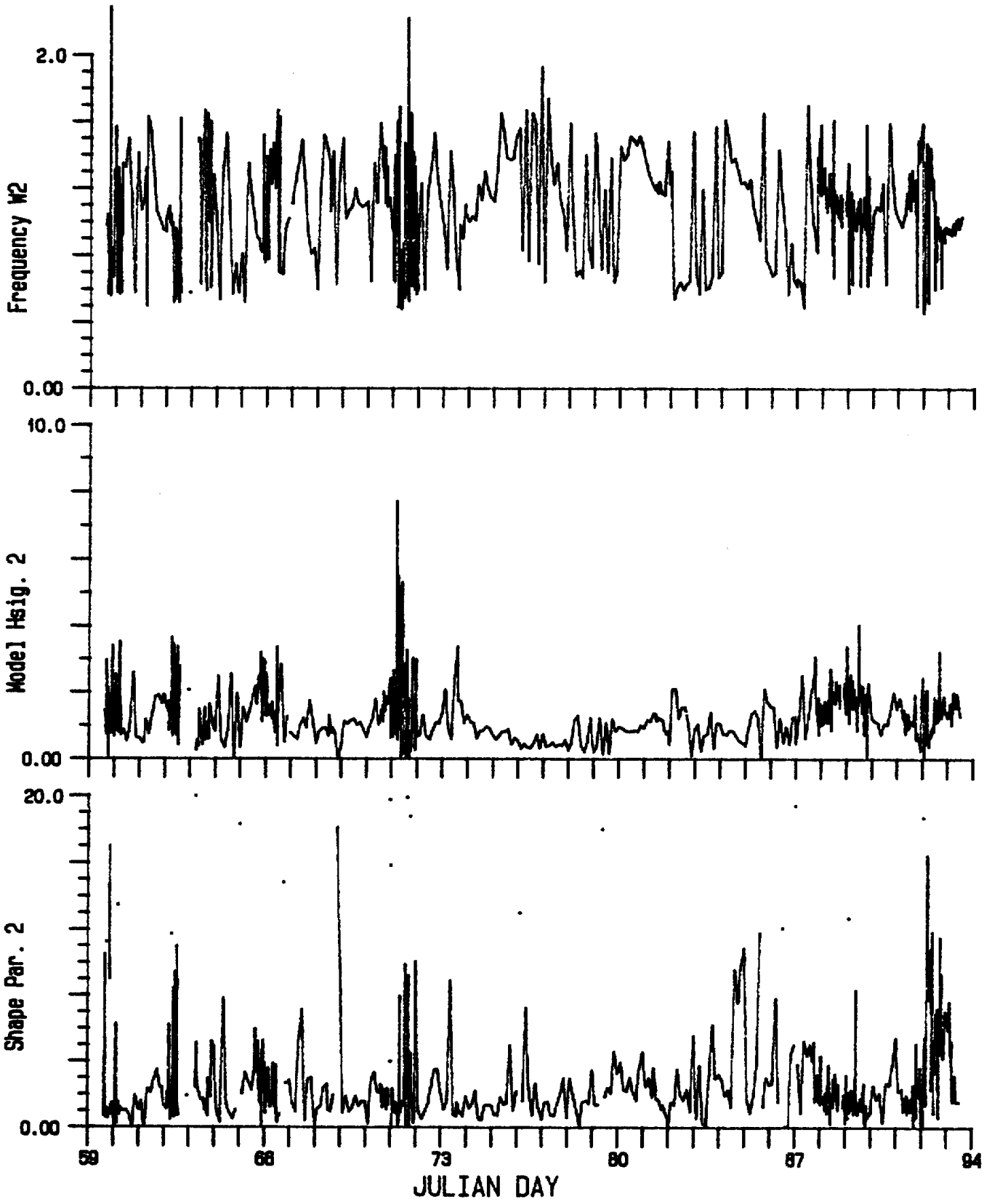

Fig. 3 (continued)

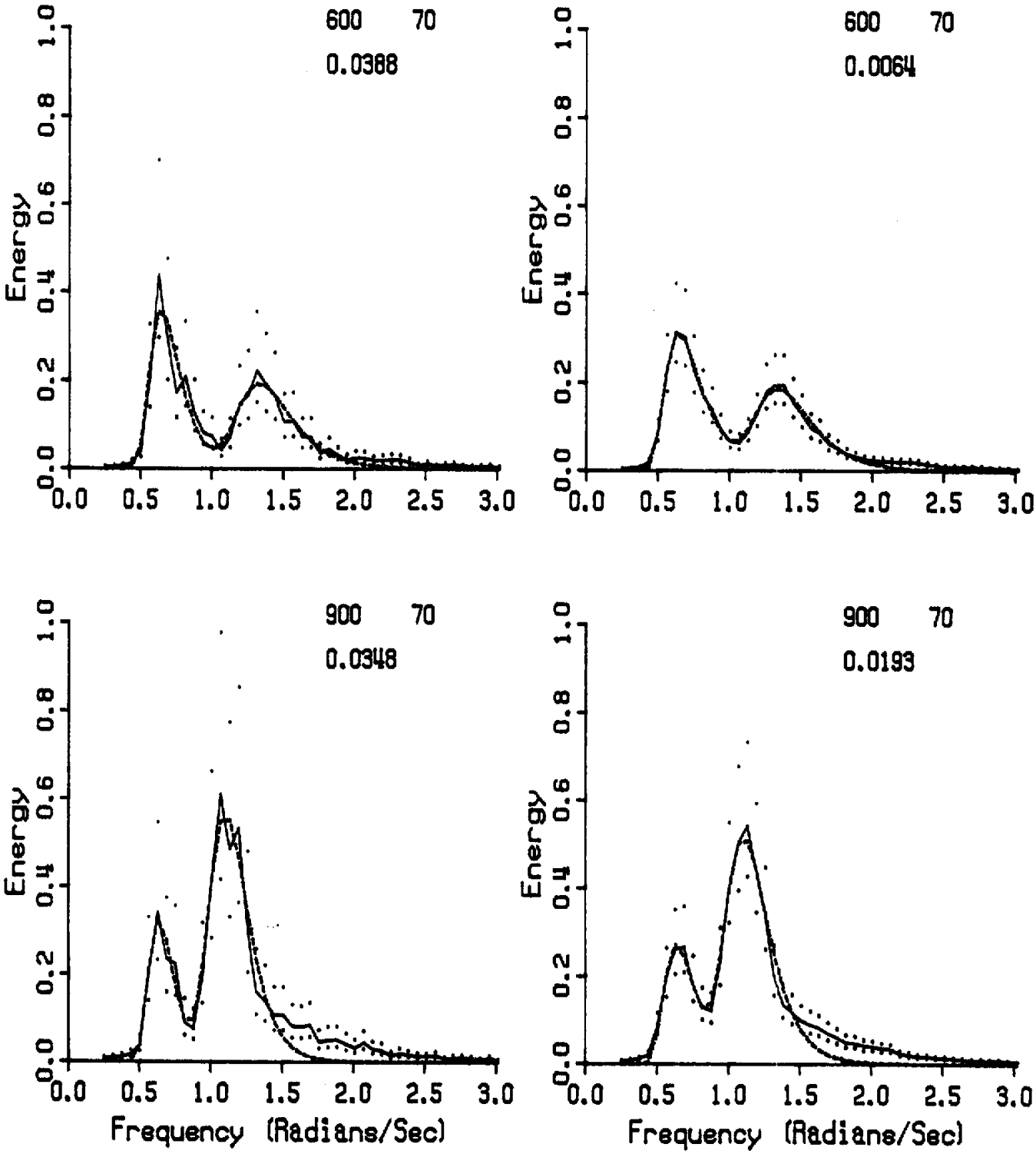

Fig. 4 Sample overlayed heave spectra - Solid: Data; Long dash: Original fit; Short dash: Smooth fit; Dots: 95% confidence limits on original (left) and smoothed (right) data spectrum.

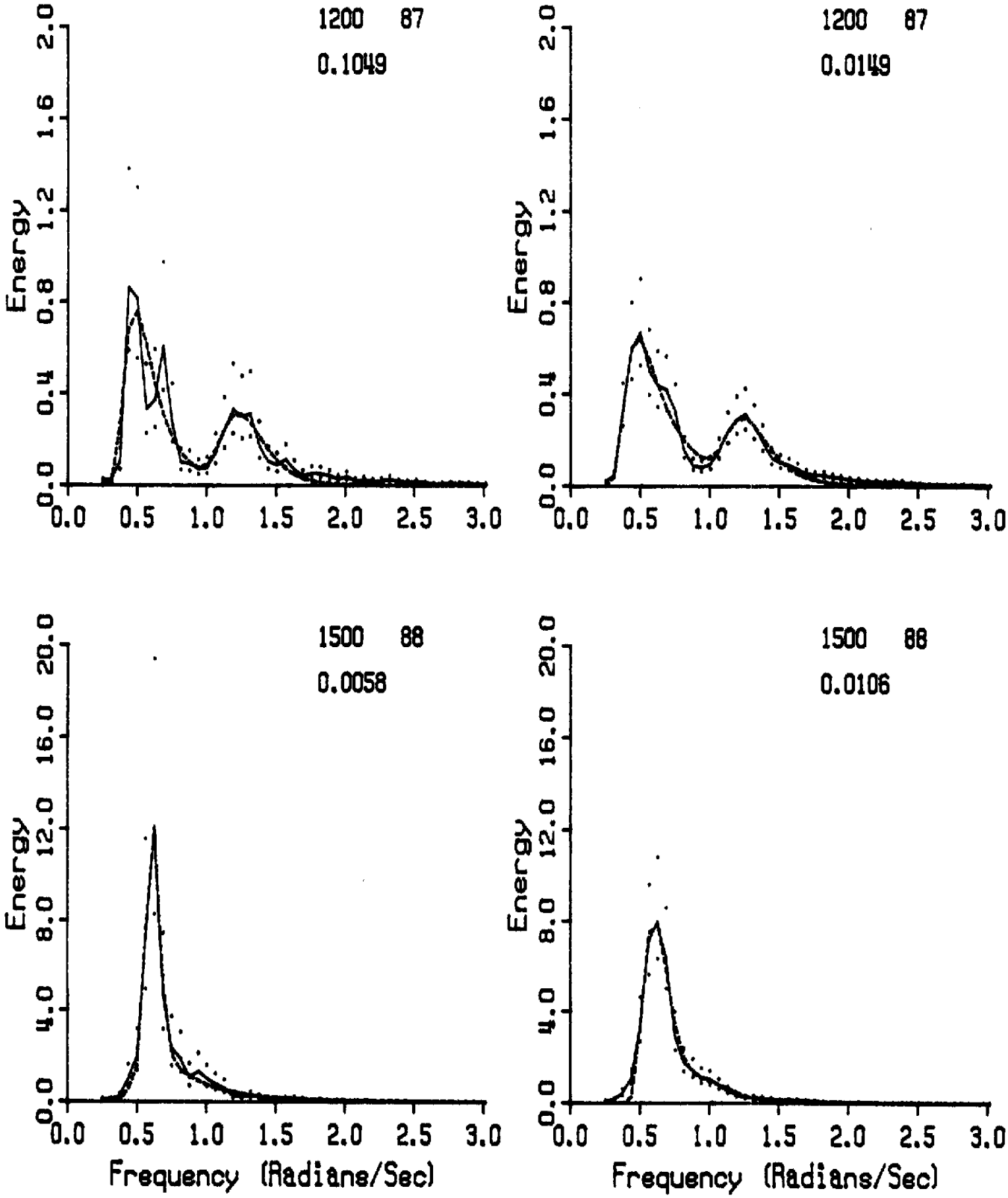

Fig. 4 (continued)

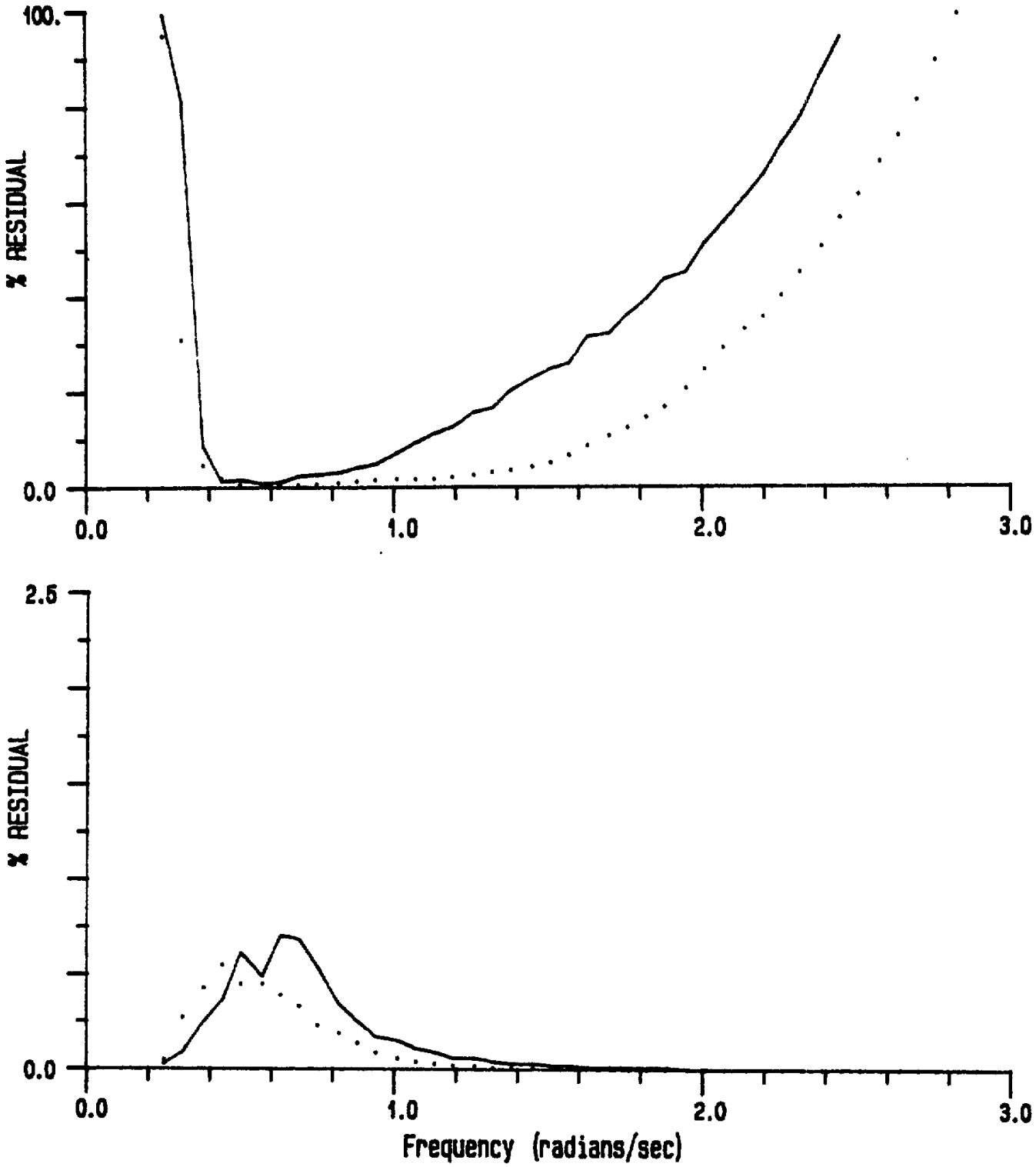

Fig. 5 Fit residual as a function of frequency - Solid: Original fit; Dotted line: Smooth fit. A) Upper weighting by E(w) B) Lower - weighting by EMAX

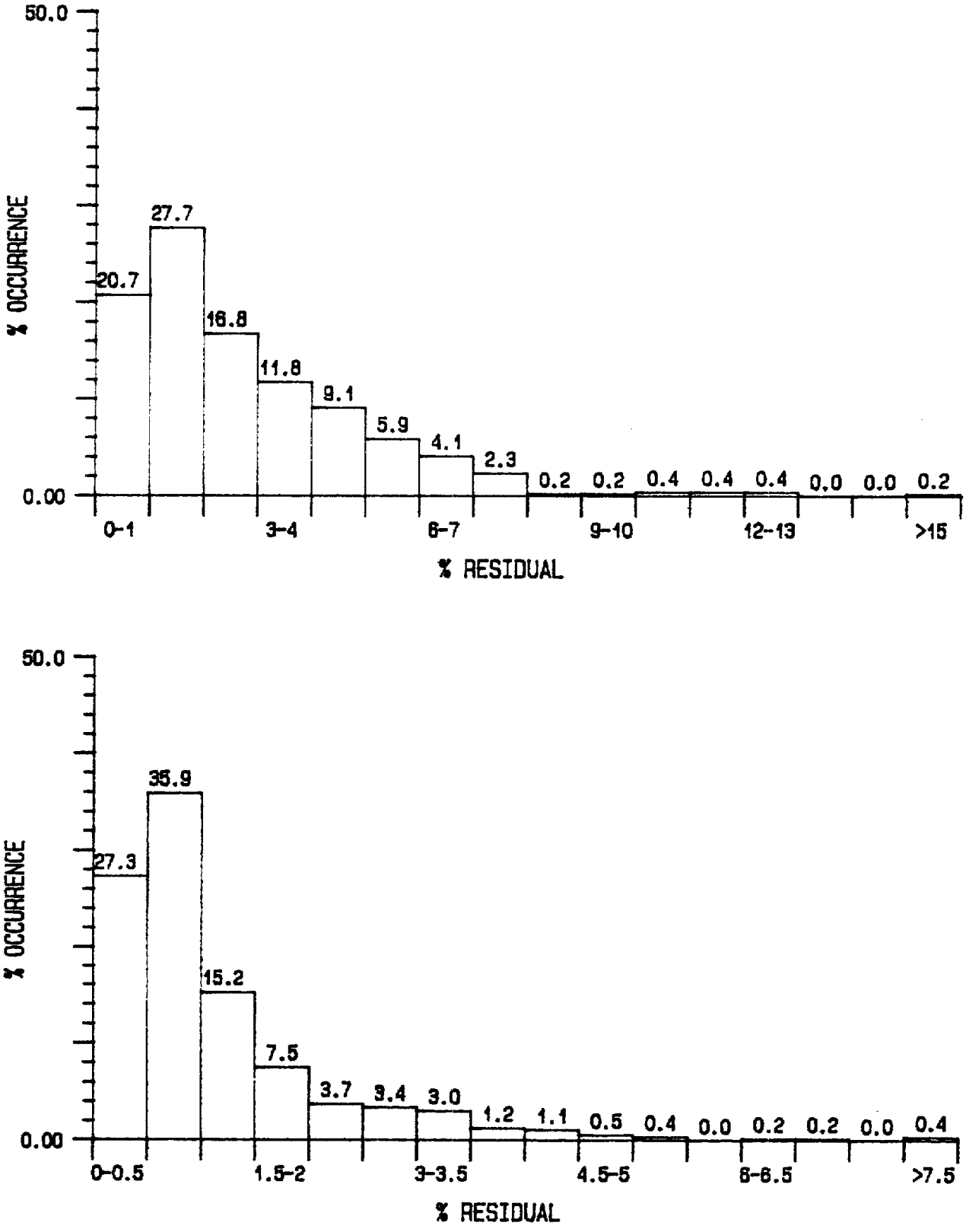

Fig. 6 Percent occurrence of RESH. Upper - Original fit; Lower - Smooth fit.

Figure 6 contains the histograms of the percent occurrence of records having a given RESH value. The upper plot is for the fit to the original spectrum and the lower plot is for the fit to the band-averaged spectrum. After examining numerous spectra, a rejection criteria of 8 to 10% would seem appropriate. This implies that 1.8% and 0.4% of the records would be rejected when fitted to the original or smoothed spectrum, respectively. The criteria of 8% was used in later analyses. These statistics indicate that the chosen fitting procedure is capable of handling spectra containing different levels of stochastic variability. The smoothing that was used may not be necessary when applying the fit to hindcast model results and this application should not pose any problems.

From the reduced variability in the parameters indicated in fig.3 , the improved behavior with frequency indicated in fig.5 a and b , as well as the low RESH values shown in fig.6 , it appears that band-averaging helps to reduce unwanted stochastic variability and thus provides a better basis for later analysis. Henceforth, all spectra examined will be taken as band-averaged.

4. DIRECTIONAL PARAMETERIZATION - LEVEL 1

4.1 Model Description

In section 3 , the OH fit parameters were obtained independently of any direction information. For Level 1 parameterization, an initial attempt was made to integrate the directional distribution of the wave energy into the overall spectrum. The directional model chosen for this study was the COS2P form discussed in Longuet-Higgins et. al.(1963) and Hasselmann et. al.(1980) and given in Eq.1 with parameter values, P and Θm. This expression has found numerous application in the literature though it is not the only form that has been examined. The values for P and Θm were previously calculated using the Hasselmann formulation and by least-squares fit (discussed in Section 2.3). The amplitudes of these distributions were initially normalized so that the spectral density of the frequency band equals the spectral density of the data spectrum. In Level 1 parameterization, the direction distributions were normalized to the OH model energy and not the data. This allowed for an error assessment due to the modelling of the amplitude spectrum. Both the mean direction and P value were allowed to vary with frequency.

It is recognized that this formulation is not the desired final parameterization, however it is a critical first step in model development. These models, as well as the data adaptive MJ spectra, already contain a certain level of error when compared to the real, and unknown, data spectrum. Examination of these errors will provide baseline statistics for later comparison as higher degrees of

parameterization are tested. The two error statistics calculated are the WXS and RESD errors given by Eqs. 7 and 6 and which assess the ability of the model to reproduce the data cross-spectral matrix and the directional spectrum, respectively. The WXS error, representing a weighted average error in the cross-spectral matrix, is examined to ascertain that the MJ spectrum is properly reproducing the average data cross-spectral matrix, and can be used as the "best spectrum" for comparison and calculation of the RESD error. It allows for an observation of the relative behavior of the different models. It is expected that most of the models will be statistically unacceptable as the WXS error is very sensitive to slight changes in the cross-spectral matrix however this does not preclude the use of the chosen model if it reproduces the desired features of the directional spectrum. This in turn is assessed using the RESD error which provides a weighted difference error between the model spectrum and the chosen "best spectrum". The interpretation of the RESD error is more straightforward and has the advantage of weighting the calculation to the higher energy components of the spectrum which is, generally, the region of greater interest.

Table 1 lists the various cases that were examined and which will be described further in the fit assessment. The errors were calculated only over the frequencies for which parameters were available. Errors 4, 8, and 11 were included to check for any improvement of the fit when one excludes frequencies for which the model is a poor candidate. Errors 5, 9 and 12 were originally calculated as a response to the fit behavior of the OH model as a function of frequency indicated in fig, 5a . Errors 10, 11 and 12 would assess the relative importance of representing isotropic noise in the directional model.

4.2 WXS Error Assessment

Figure 7a contains time series of the WXS errors for normalization of the directional spectra to the data COll (ie, energy density) values. Error 1 is the WXS error of the initial directional spectrum. No parameterization errors can be lower than these and they can be considered as the underlying measurement error or precision of the experiment. Note that virtually all errors are below 9.8 which was the rejection criteria for an individual spectral estimate. Error 2 is the WXS when the COS2P-LH model is used. This gives an estimate of the error using calculated directional parameters that are generally accepted in the literature. Note the mean error is about 100 with virtually no cases below 10. Error 3 is the WXS error for the COS2P-FIT model while error 4 is similar to 3 only excluding cases when the RES error between the fit and the data (eq.2) was greater than 0.05. Juszko (1989) found that the single peak direction model

was inappropriate for most of these cases. Clearly, the COS2P-FIT to the MJ spectrum is superior to the COS2P-LH fit. Although the mean is above the 9.8 rejection criteria, the results are well below 100 and there are numerous cases below the 9.8 mark.

Figure 7b contains the time series of WXS errors associated with normalizing the power spectral density to the OH model spectrum. The error in the cross-spectral matrix is very sensitive to slight changes in CO11 (the heave spectral density). Consequently, one expects large errors where the initial OH fit was weak. Error 6 is the WXS error for the COS2P-LH model. The features of Error 2 are generally reproduced with the mean value about 100. The errors can vary over 5 orders of magnitude. Error 8 shows the WXS error for a COS2P-FIT. The mean is similar to that for Errors 3 and 4. The increased occurrence of very large errors reflect the influence of the OH parameterization. The COS2P-FIT contains the parameter alpha to describe the background noise. Error 11 shows the results when this noise component is not included. Here the mean error increases to about 100 similar to the COS2P-LH fit. Thus the simple COS2P no noise model adds considerable intrinsic error to the modelling process. Errors 7 and 10 were not included as they were noisier then 8 and 11, respectively. There was no significant difference between Errors 8 and 9, and Errors 11 and 12 possibly reflecting the improved behavior of the OH fit to the smooth heave spectrum at slightly higher frequencies.

4.3 RESD Error Assessment

From the previous section, it is clear that the only directional spectral model which provides a statistically acceptable spectrum is the MJ directional spectral estimate. Furthermore, all candidate parameterizations produce similar large WXS errors that are well above the 9.8 rejection criteria. The WXS error is valid for small errors in the cross-spectral matrix. The observed large values suggest that the errors in the matrix are large and the statistic would not serve as an appropriate assessment tool. The underlying assumption in the RESD estimate, however, is that the MJ spectrum is accurate and the model candidates will be judged in terms of their ability to reproduce the MJ model and not to reproduce the unknown data spectrum represented by the cross-spectral matrix.

Figure 8 contains the time series of RESD values for several cases. This statistic shows more consistent behavior than WXS and, by its nature, is more limited in range, which are desired features for a statistic that will eventually be used as a measure of acceptance. The reduced noise reflects the fact that RESD behavior is primarily being determined by the high energy portion of the spectrum while, even though WXS is also weighted, the error can take on extremely large

values at high frequencies, where the model fit is relatively poor. Again, the COS2P-FIT model errors, 3 and 4, are lower than for the COS2P-LH model, the latter showing little change between Errors 2 and 6 with a mean RESD value of about 25%.

TABLE 1. Error Number Convention

1	Original data spectrum
2	Original heave energy, COS2P-LH direction model, all cases
3	Original heave energy, COS2P-FIT direction model, complete expression, all cases
4	Original heave energy, COS2P-FIT direction model, complete expression, excluding cases when RES>0.05
5	Original heave energy, COS2P-FIT direction model, complete expression, excluding cases when RES>0.05, ω>1.26 RPS
6	OH model heave energy, COS2P-LH direction model, all cases
7	OH model heave energy, COS2P-FIT direction model, complete expression, all cases
8	OH model heave energy, COS2P-FIT direction model, complete expression, excluding cases when RES>0.05
9	OH model heave energy, COS2P-FIT direction model, complete expression, excluding cases when RES>0.05, ω>1.26 RPS
10	OH model heave energy, COS2P-FIT direction model, no noise, all cases
11	OH model heave energy, COS2P-FIT direction model, no noise, excluding cases when RES>0.05
12	OH model heave energy, COS2P-FIT direction model, no noise, excluding cases when RES>0.05, ω>1.26 RPS

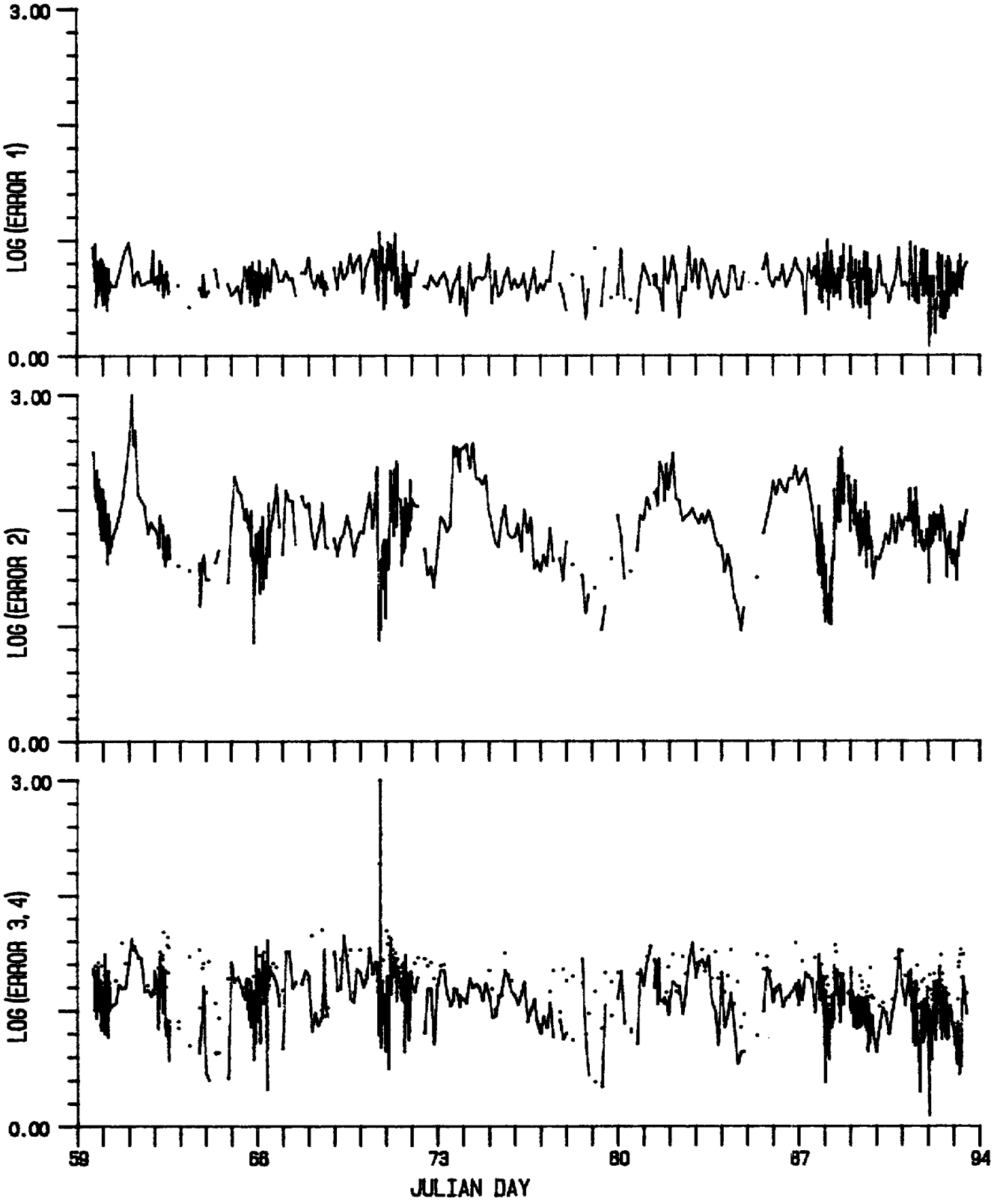

Fig. 7a Time series of WXS errors normalized to data spectrum (Errors 1,2 and 4 solid; Error 3 dotted)

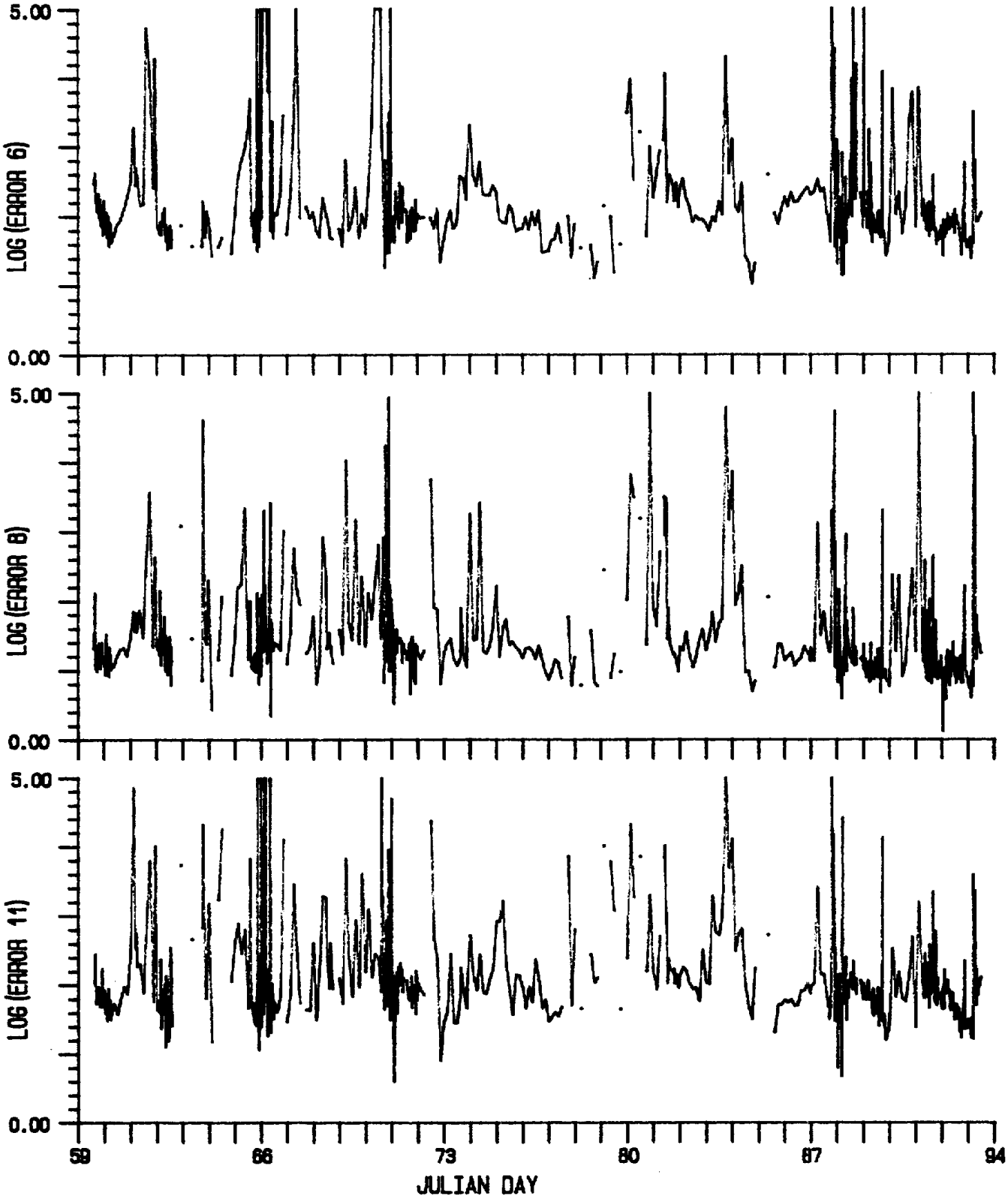

Fig. 7b Time series of WXS errors normalized to OH model spectrum

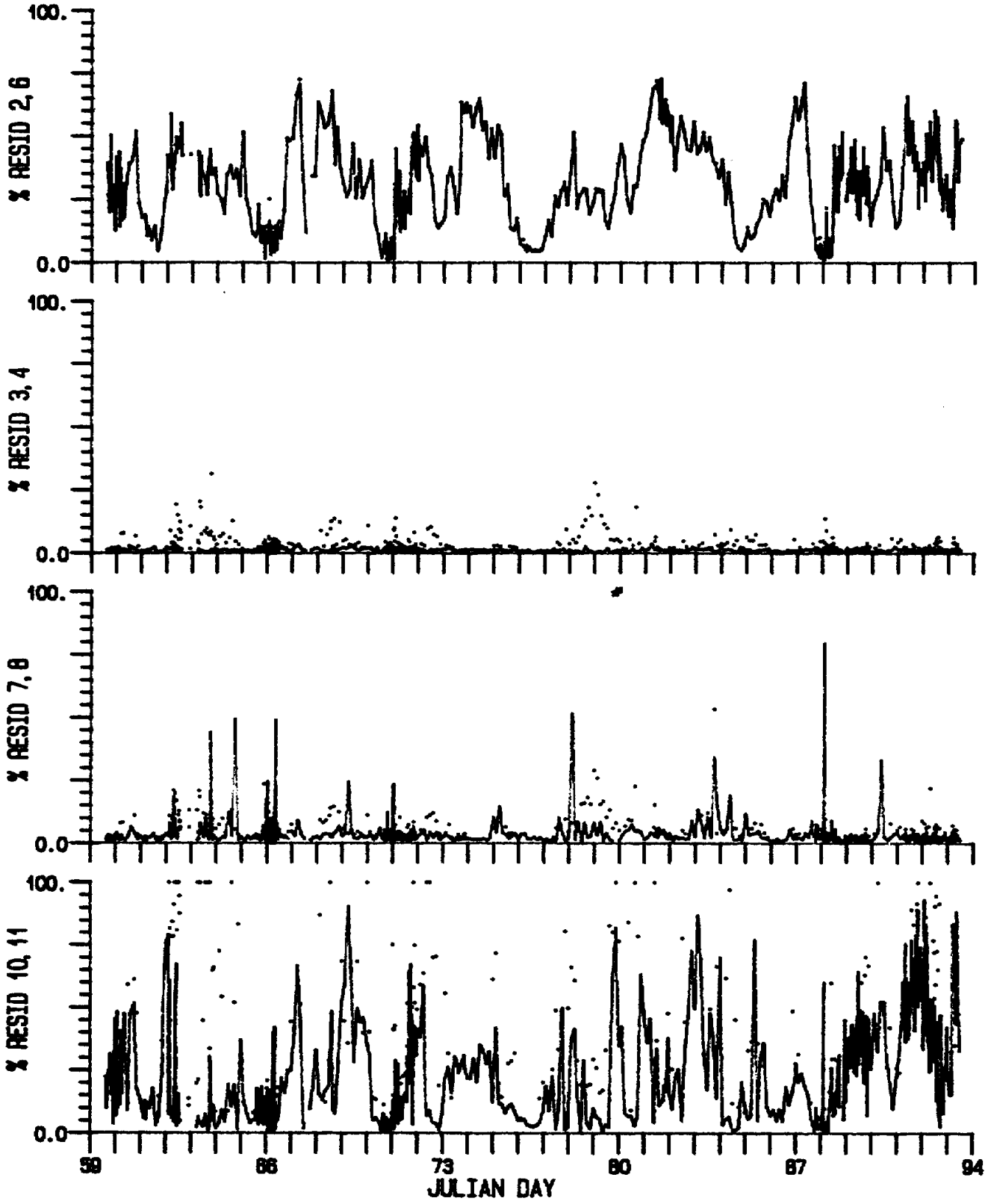

Fig. 8 Time series of RESD errors (Errors 6,3,7,and 10 dotted; Errors 2,4,8 and 11 dotted)

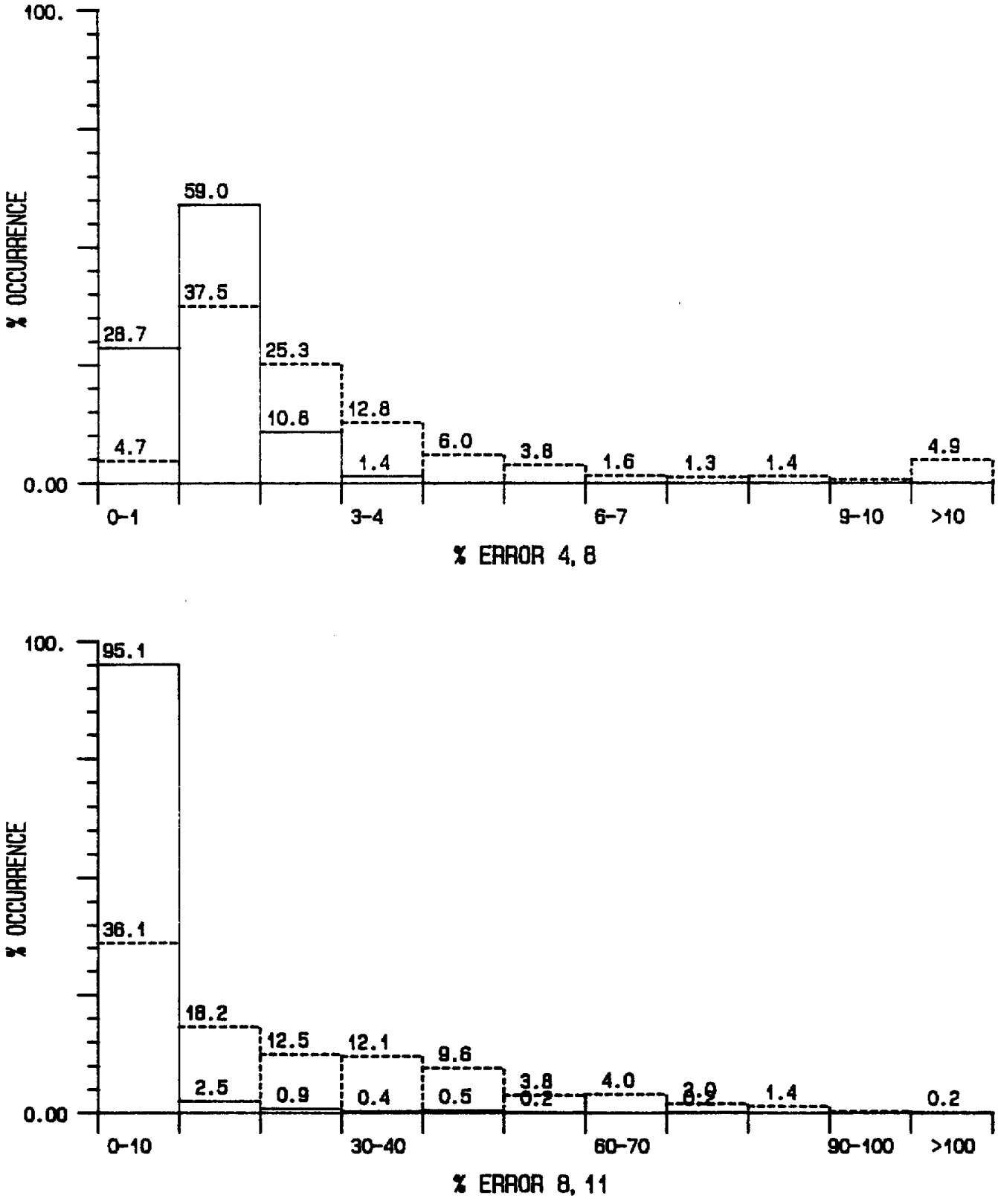

Fig. 9 Percent occurrence of RESD errors.
Errors 8 (upper) and 11 (lower) are dashed.

There was only a marginal increase in the RESD values when the COS2P-FIT model was normalized to the OH spectrum (Errors 7 and 8). Not explicitly including the noise input, Errors 10 and 11, significantly increases the error. The noise contribution effectively broadens the directional distribution for a given P value. The error is reduced when frequencies for which RES > 5% are excluded from the calculation (Errors 8 and 11). There was little difference between Errors 8 and 9, 11 and 12 reflecting the nature of the weighting (ie, excluding high frequencies, where there is little energy anyway). The time series indicate, best seen in Error 11, that the errors are lowest during storm build-up and higher energy conditions (see Days mid-65 to mid-66, 70 to mid-71, late 87 to 88) and increase during the decay phase (Day late-66, late-71 to 72, day 89). This is somewhat to be expected as during storm build-up and at the storm peaks, the frequency and directional spectra are generally well defined often consisting of a single sea peak and a single dominant wave direction which can best be modelled by the parameterization chosen.

A histogram of the percent occurrence of records having a given RESD value is much more suited than a time series plot for inter-comparison between models, Figure 9 contains such a display for COS2P-FIT with the upper plot representing the "baseline" distribution (Error 4, with Error 8 overlayed for comparison) and the lower plot the Level 1 results with and without noise included (Errors 8 and 11). These are the lowest errors one can expect for this particular data set using a COS2P directional model. As RESD values behave better than WXS, the rest of the study will only refer to the RESD results.

Appendix 3 contains selected contoured directional spectra for the two major storms of March 1984 (Storm 1 Day 70-72; Storm 2 Day 87-90). For each record, the MJ or "best" spectrum (labelled A), and the Level 1 COS2P-FIT spectrum (labelled B), with noise, are shown on the first page, Later plots show the results for higher levels of parameterization. The percent residual listed on the figures were calculated only for frequencies where FIT parameters were available and are, therefore, screening out many bi-modal conditions. All existing FIT parameters were used, ie. not excluding frequencies where RES > 5% but excluding frequencies where a fit was not possible. High RES values were generally associated with small P's trying to account for bi-modal spectra at high frequency which would not be modelled by higher levels of parameterization and it was felt that a better basis for comparison would be to include them. These figures will be referred to during later discussion.

5. DIRECTIONAL PARAMETERIZATION - LEVEL 2, 3 AND 4

5.1 Model Description

In section 4 , the value of the direction parameters, P and Om, varied with frequency based upon the fit to the MJ spectrum. For the levels 2, 3 and 4 parameterizations, increased restrictions will be placed on the variation of these parameters. Level 2 and 3 parameterizations assume that P is a function of $\omega/\omega m$. For Level 2, this function can vary from record to record while in Level 3, one general functional form was used for all runs. In Level 4, P was not allowed to vary with frequency.

The P parameter was varied with frequency, in Level 2 and 3, using the functional form:

$$P = P_1 (\omega/\omega m_1)^D$$

Two sets of values for D were tested. The first was found using the COS2P-FIT results on this data set as part of an earlier study (Juszko, 1989) and given as:

$$\text{SET 1: } D = -1.27 \quad \text{IF} \quad \omega/\omega m \geq 1$$
$$D = 5.64 \quad \text{IF} \quad \omega/\omega m < 1$$

The second was determined by Hasselmann et. al. (1980) as:

$$\text{SET 2: } D = -2.34 \quad \text{IF} \quad \omega/\omega m \geq 1$$
$$D = 4.06 \quad \text{IF} \quad \omega/\omega m < 1$$

In Level 2, P1 and P2 were obtained from the COS2P-FIT results at the frequencies nearest to $\omega m1$ and $\omega m2$ and would vary from record to record. If either P1 or P2 were missing the record was not analyzed. In Level 3, representative values for P1 and P2 were chosen. In Level 4, both the COS2P-FIT determined and representative P1 and P2 were used but, in this case, not allowed to vary with frequency. The FIT directions or, if these were not available, the Longuet-Higgins directions, associated with the frequencies nearest $\omega m1$ and $\omega m2$, were taken and kept constant with frequency for all three levels.

The model was assessed using a constant 0%, 5% and 10% background noise component. The procedure to re-constitute the modelled directional spectra was as follows:

1. Treat the two OH parameter sets (swell and sea) separately

2. Determine the $H1(\omega)$ (heave energy) and $H2(\omega)$ values

3. Calculate $Sig1(\omega)$ (ie. signal) and $Noise1(\omega)$, $Sig2(\omega)$ and $Noise2(\omega)$ assuming 0, 5, and 10% noise-to-signal contributions (ie. at 0%, $Sig(\omega)=H(\omega)$; at 5%, $1.05*Sig(\omega)=H(\omega)$; and at 10%, $1.10*Sig(\omega)=H(\omega)$).

4. Calculate P1 and P2 using either set of D values discussed earlier; or kept constant for Level 4 analysis

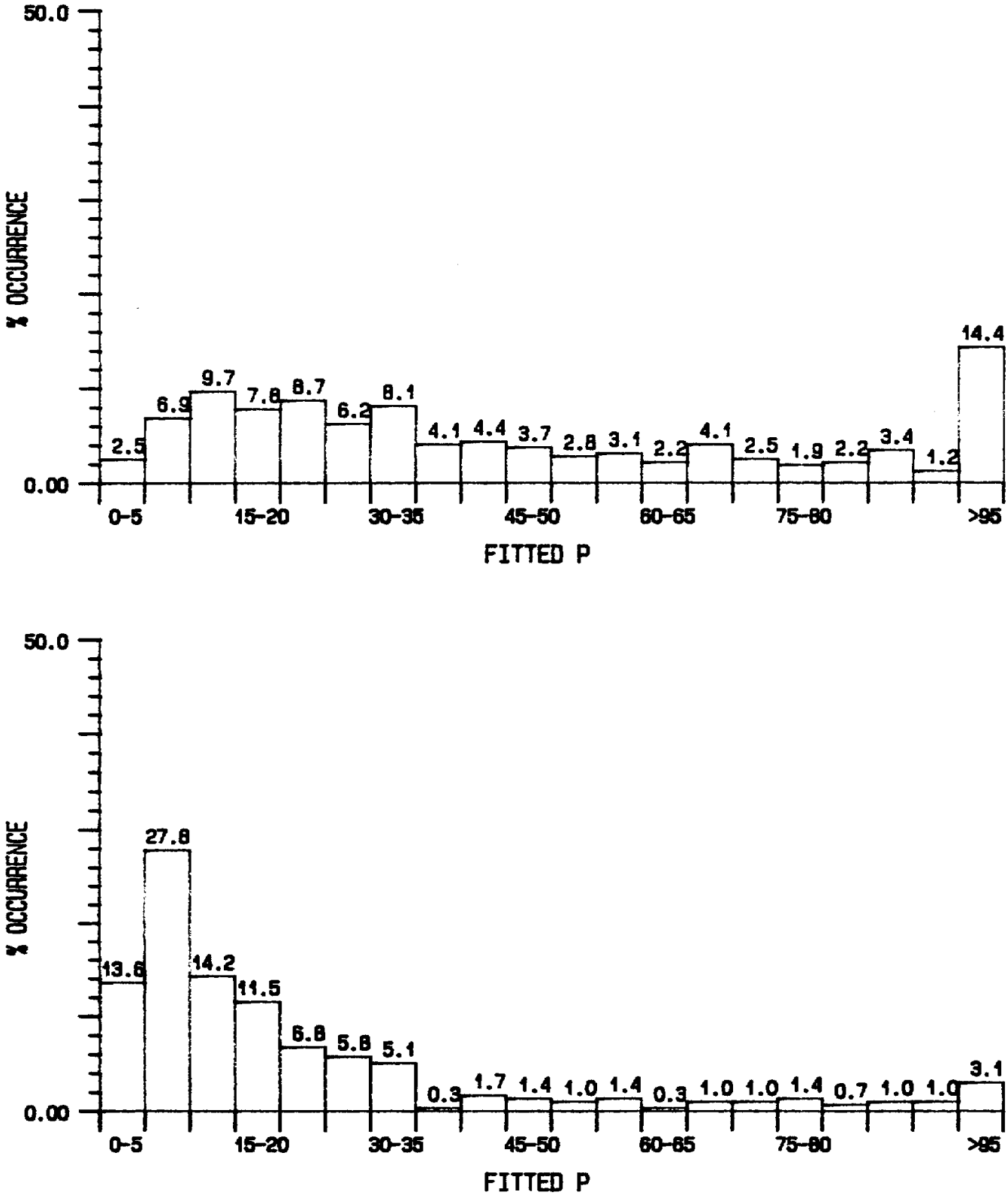

Fig. 10a Percent occurrence of P at ω1(upper) and ω2 (lower) from the original data spectrum.

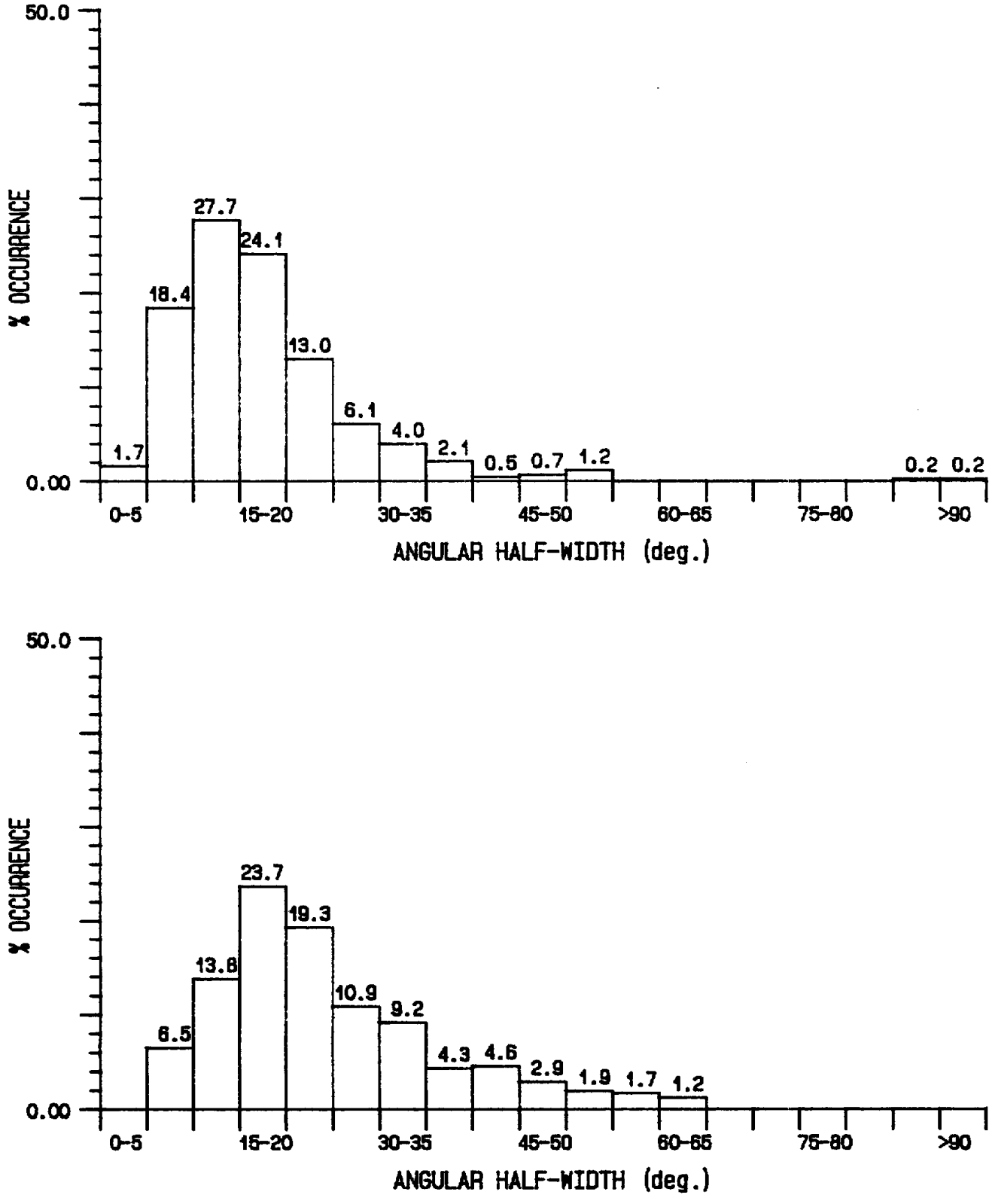

Fig. 10b Percent occurrence of angular half-width at ω1 (upper) and ω2(lower)

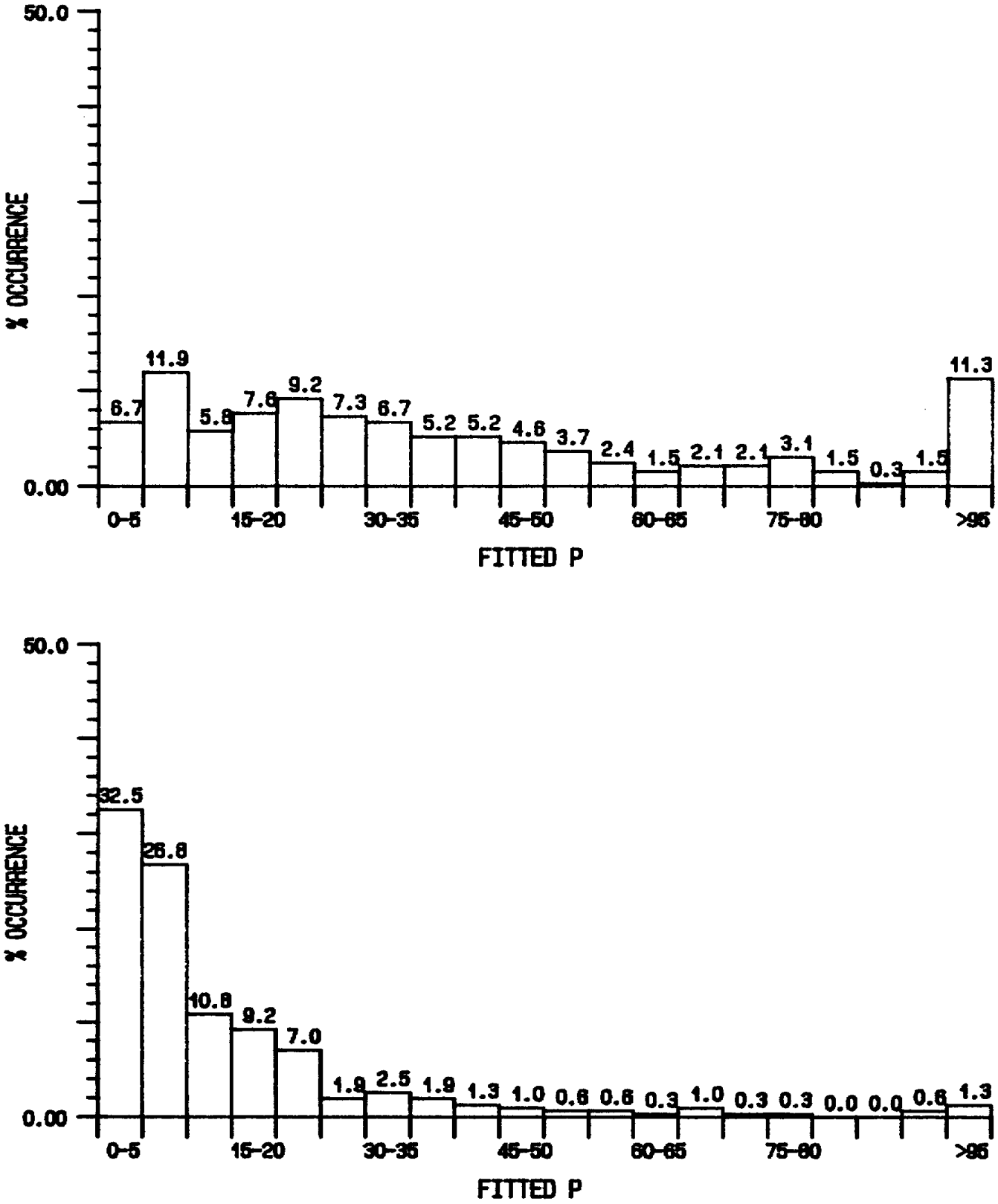

Fig. 11a Percent occurrence of P at ω1(upper) and ω2 (lower) from the band-averaged data spectrum

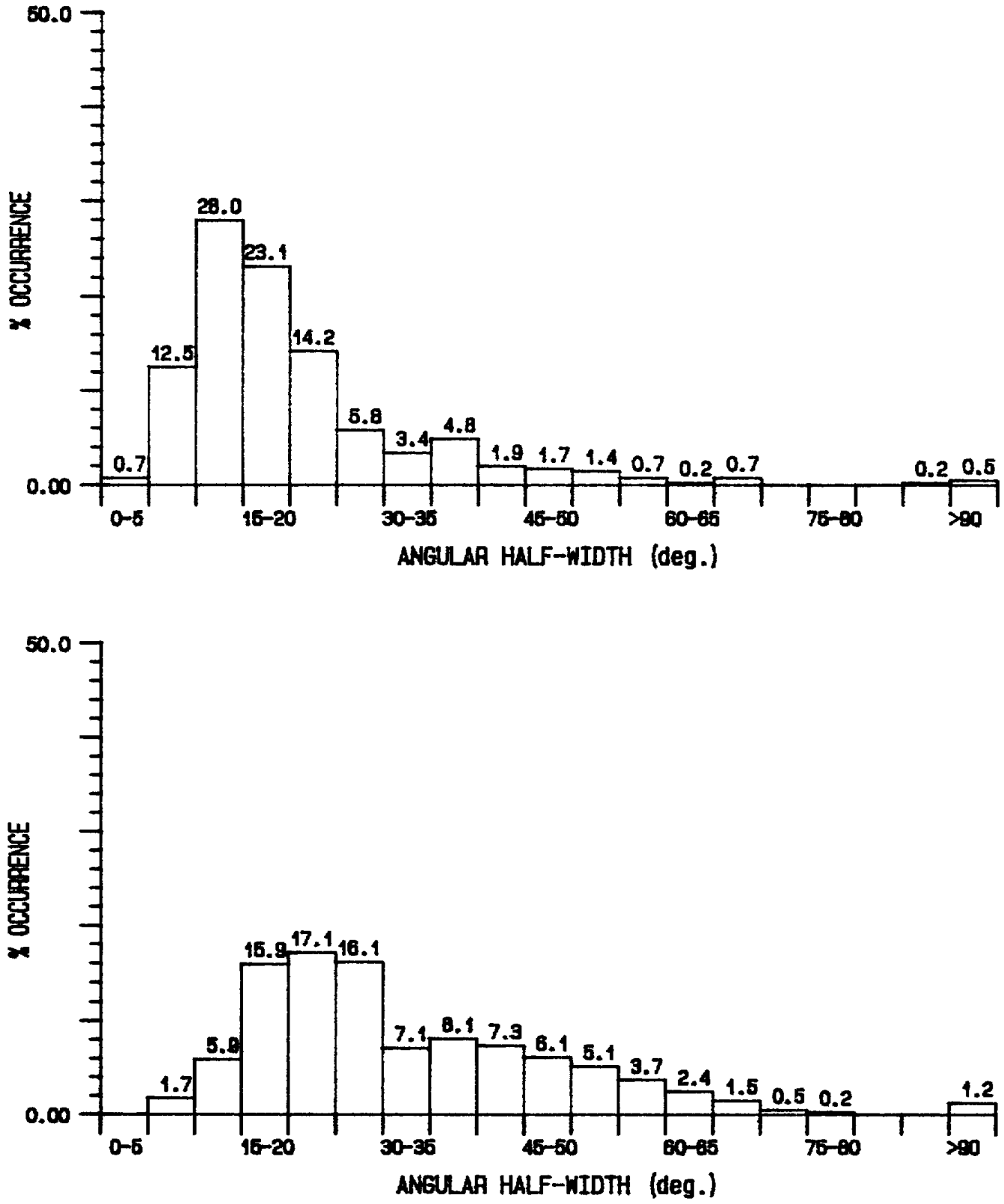

Fig. 11b Percent occurrence of angular half-width at ω1 (upper) and ω2(lower)

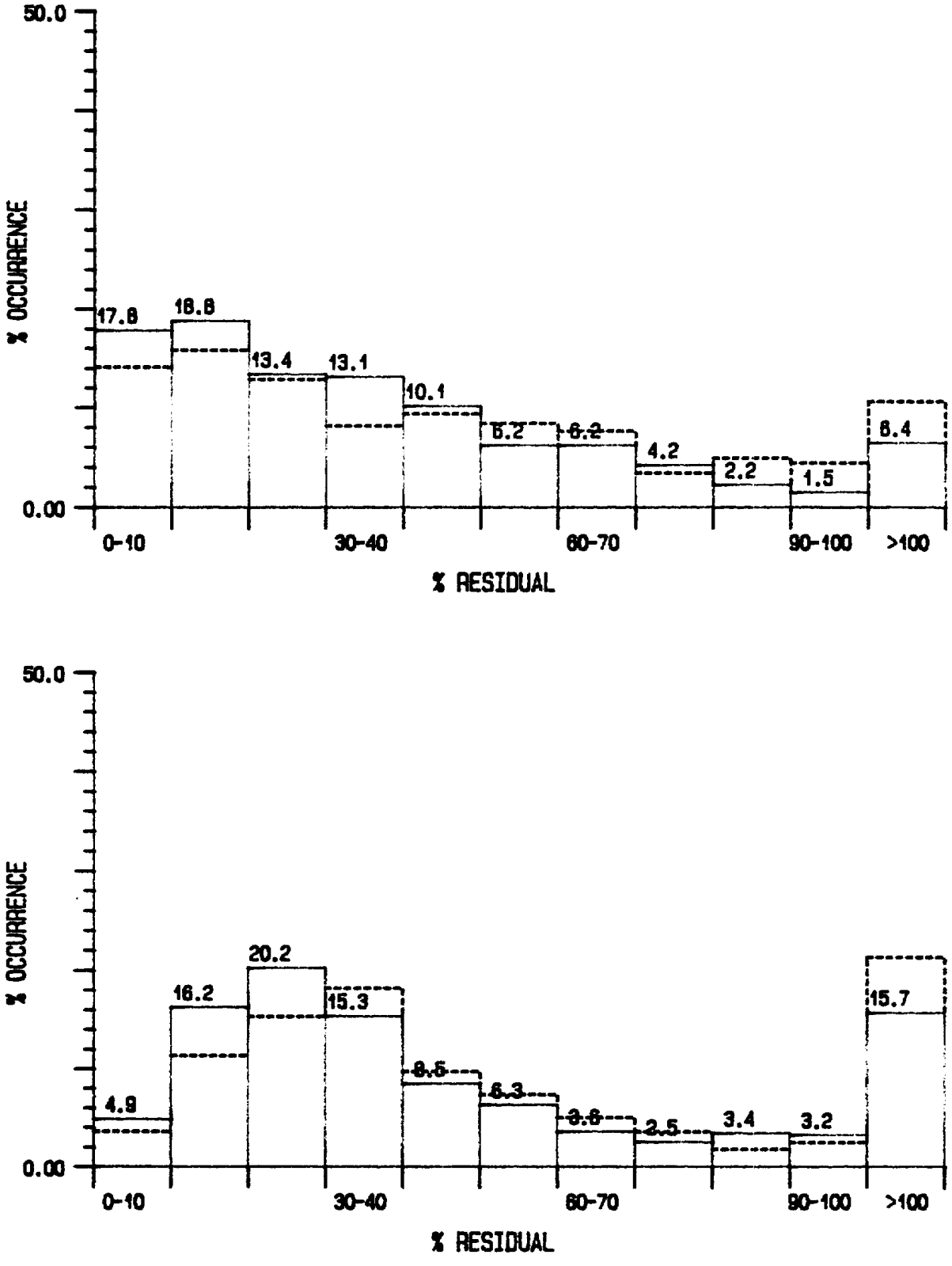

Fig. 12 Percent occurrence of RESD for Level 2(upper), Level 3(lower) parameterization with(solid) and without(dashed) 10% noise added(Set 1; P1=20; P2=7.5)

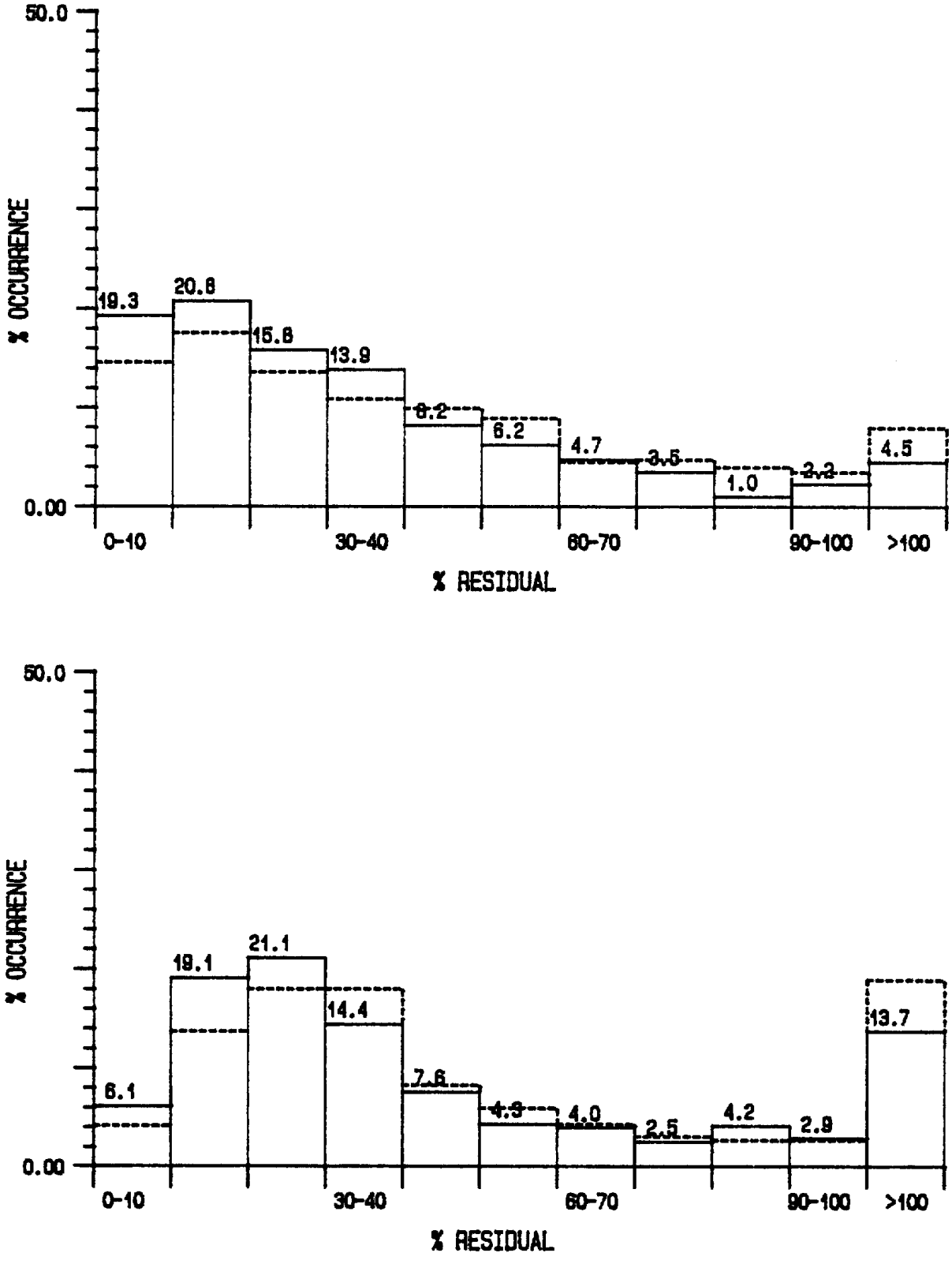

Fig. 13 Percent occurrence of RESD for Level 2(upper), Level 3(Lower) parameterization with(solid) and without(dashed) 10% noise added(Set 2; P1=20; P2=7.5)

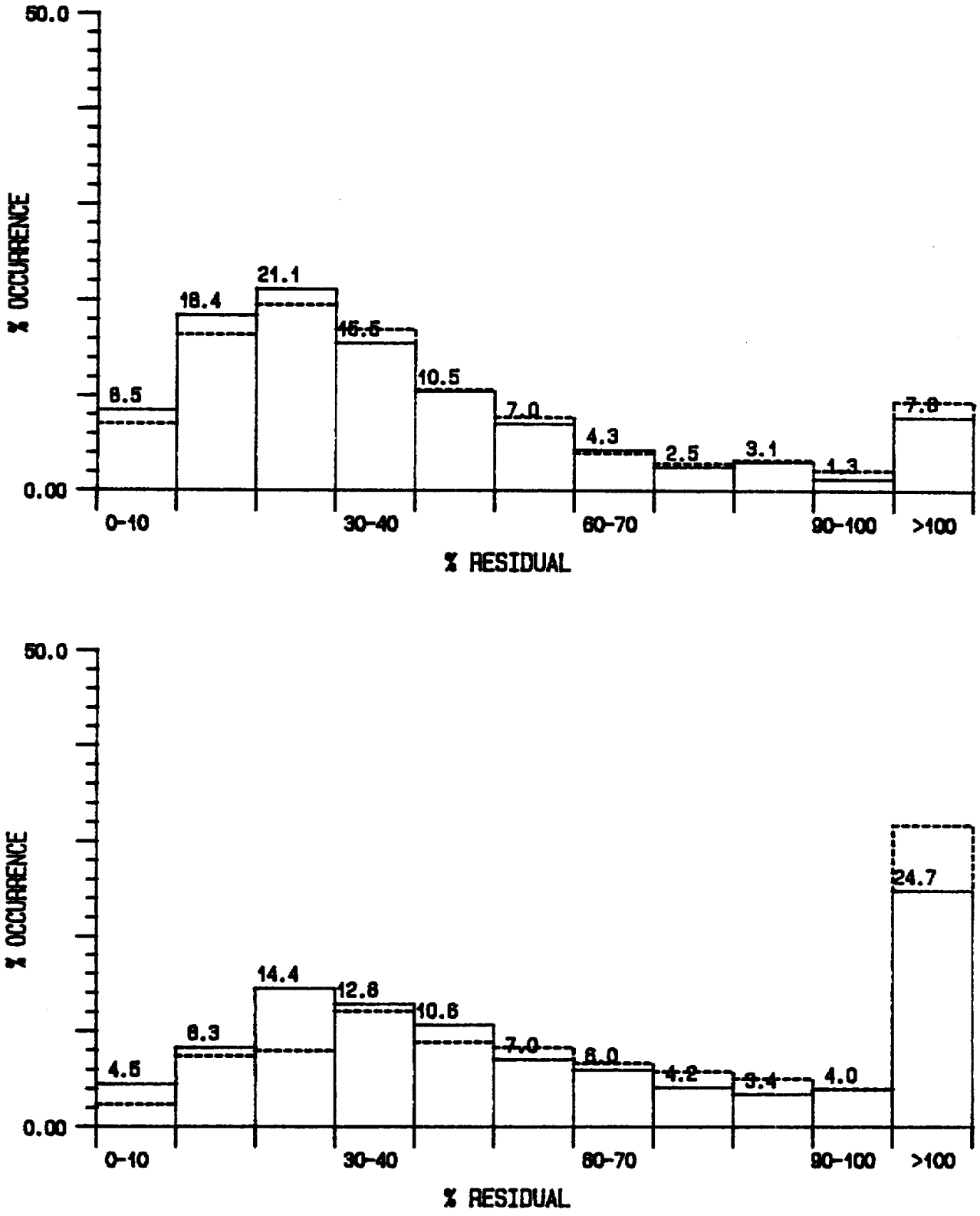

Fig. 14 Percent occurrence of RESD for Level 3 model with(solid) and without(dashed) 10% noise added (Upper: P1=10 and P2=4.0;Lower: P1=40 and P2=7.5)

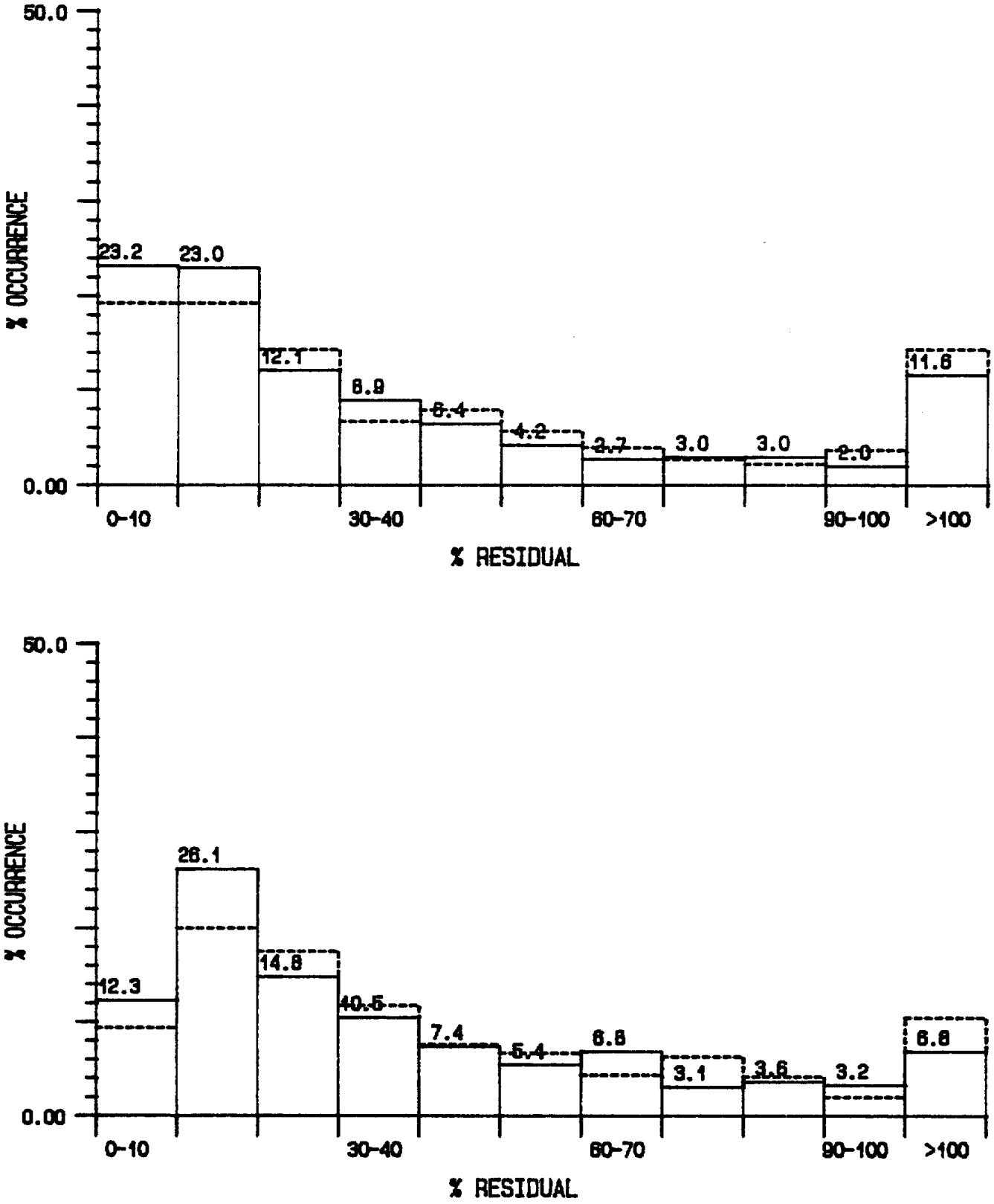

Fig. 15 As Fig. 13 for unimodal spectra only

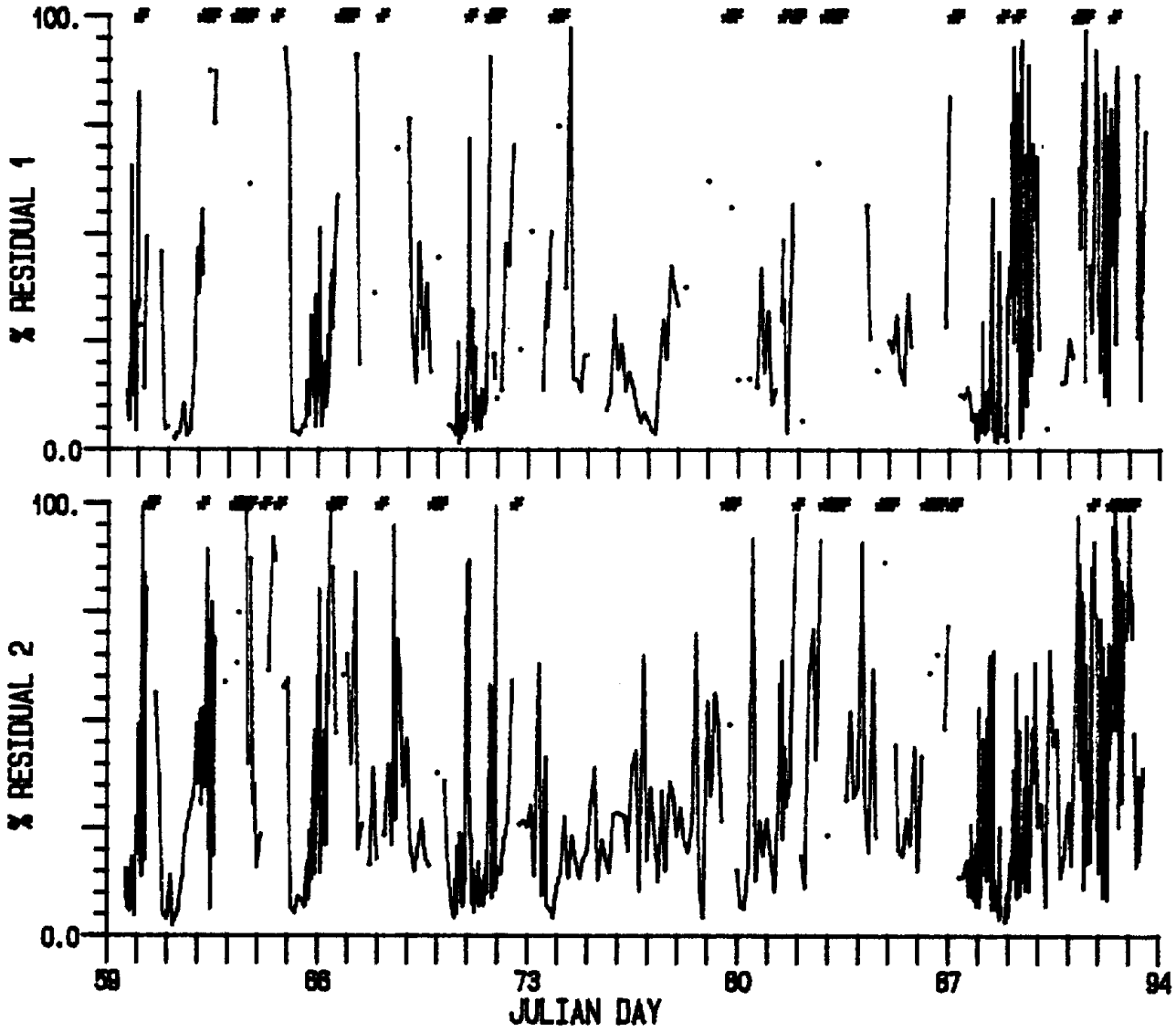

Fig. 16 Time series of RESD for Level 2(upper) and Level 3(lower) parameterization, including 10% noise (Set 2; P1=20 and P2=7.5; * >100%)

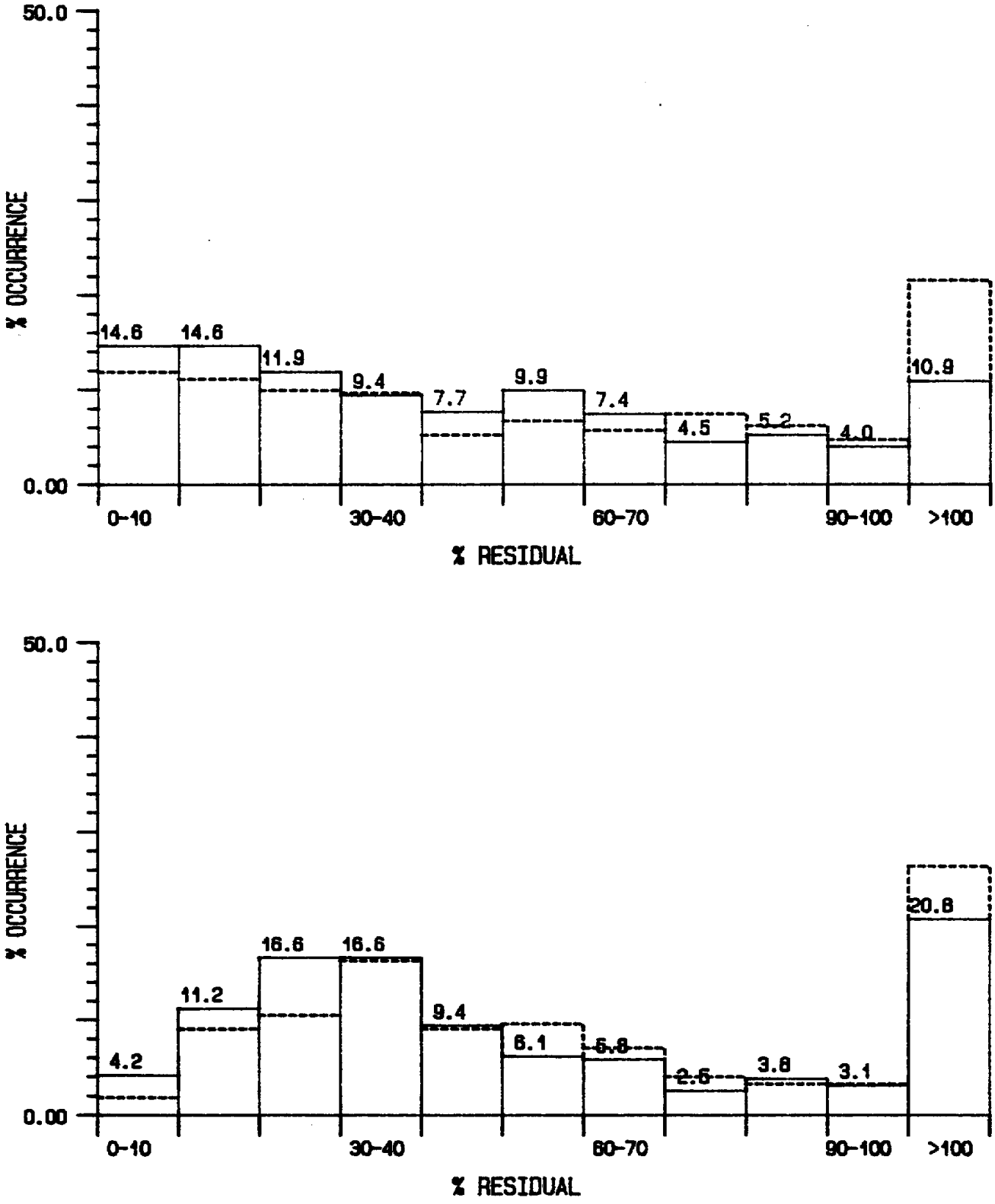

Fig. 17 Percent occurrence of RESD for Level 4 model with(solid) and without(dashed) 10% noise added (Upper: Fitted P; Lower: P1=20 and P2=7.5)

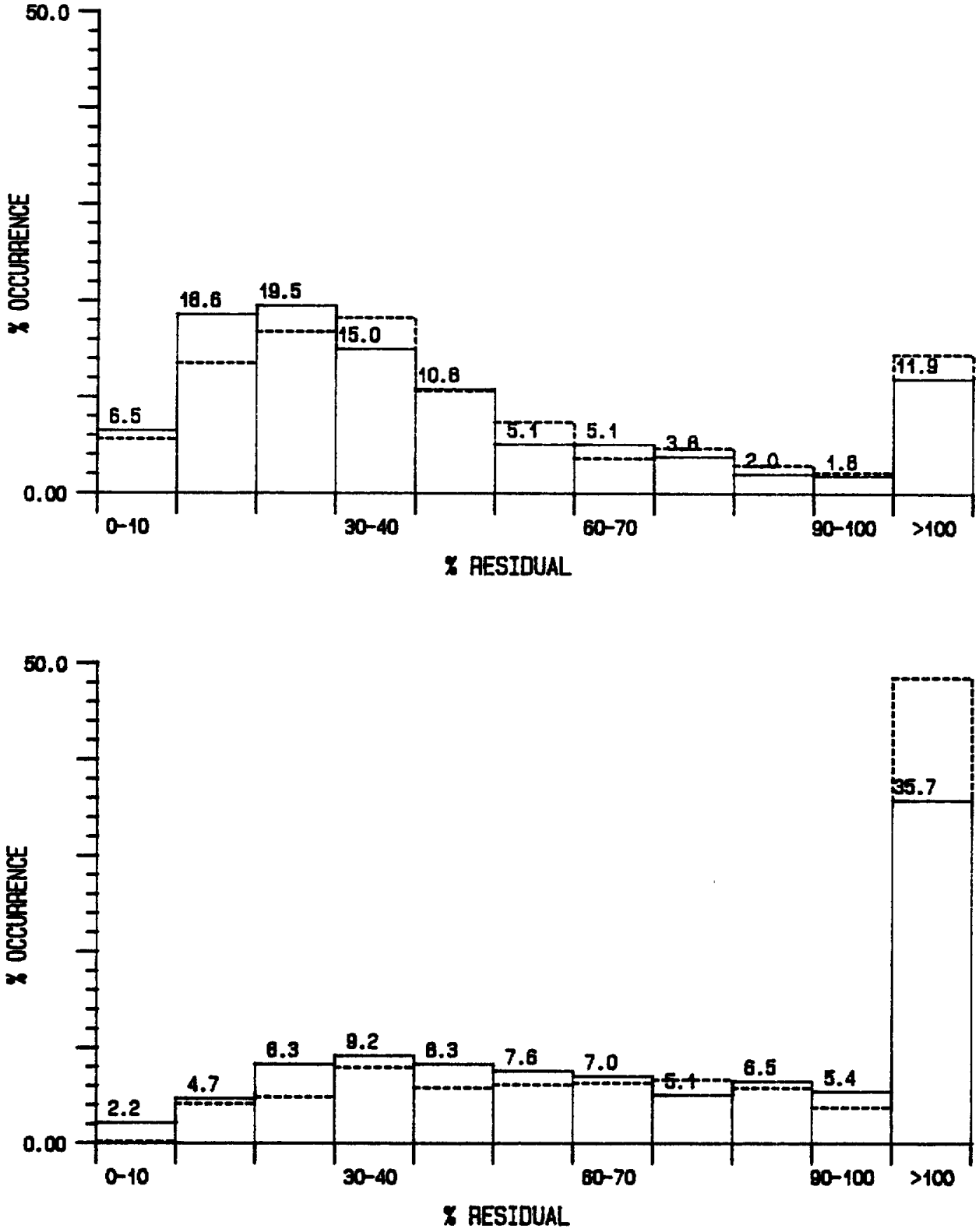

Fig. 18 Percent occurrence of RESD for Level 4 model with(solid) and without(dashed) 10% noise added (Upper: P1=10 and P2=4.0; Lower: P1=40 and P2=7.5)

5. Set up directional spectra at this frequency, ie.

$$E_1(\theta) = \cos^{2P_1}\left(\frac{\theta - \theta m_1}{2}\right)$$

$$E_2(\theta) = \cos^{2P_2}\left(\frac{\theta - \theta m_2}{2}\right)$$

6. Integrate under the directional spectra and normalize the areas Int1(ω) and Int2(ω) to Sig1(ω) and Sig2(ω), respectively

7. Calculate the normalized, complete directional spectra including any noise contributions, given as:

$$M(\omega,\theta) = Sig1(\omega)/Int1(\omega) * \cos^{2P_1(\omega)}\left(\frac{\theta - \theta m_1}{2}\right) + Noise1/2\pi$$
$$+ Sig2(\omega)/Int2(\omega) * \cos^{2P_2(\omega)}\left(\frac{\theta - \theta m_2}{2}\right) + Noise2/2\pi$$

Figure 10a shows the percent occurrence of a given P value obtained from the original directional spectrum (for fits where RES < 5%) associated with ωm1 (upper) and ωm2 (lower). For comparison, Fig. 10b shows the distribution of the corresponding, measured angular half-widths at half energy. Fig. 11 a and b are the equivalent displays for P and half-width determined from the band-averaged directional spectra. The angular half-widths were examined to see if they behaved in a more predictable manner than the P parameter which is non-linear (ie. a linear change in P is not reflected by a corresponding linear change in angular half-width). Representative P values of P1= 10, 20 and 40 (approx. 27, 20 and 15 degrees half-width) and P2 = 4.0 and 7.5 (approx. 45 and 35 degrees half-width) were chosen for the Level 3 and 4 analyses to describe a range of spread conditions.

5.2 Fit Assessment

Figure 12 contains the histograms of % occurrence of a given RESD for the Level 2 (upper) and Level 3 (lower) parameterization using the SET 1 functional form to calculate P(ω) and constant values P1=20 and P2=7.5 (for Level 3). The solid bars have 10% noise included while the dashed have no noise (5% noise results lie in between these two). Fig. 13 shows similar plots except using the SET 2 functional form to calculate P(ω). Fig. 14 is similar to Fig. 13 except for varying the P values in the Level 3 analysis to P1=10 and P2=4.0 (upper) and P1=40 and P2=7.5 (lower) with the broader distribution (ie. smaller Pi) showing better results. In all cases, including a noise component improved the overall model fit. These figures indicate that, as expected, the error increases with increasing

parameterization (Level 3 over Level 2; and Level 2 over Level 1 - Fig. 9). However, the number of records examined in each case are not the same because COS2P-FIT parameters were not always available, effectively screening out records for which the model is a poor candidate. This would tend to bias the Level 2 errors low compared to Level 3. The P values used in Level 2 were taken from the nearest frequency in the band-averaged spectrum. This analysis had also been performed using the P values from the original directional spectrum and the RESD values were poorer than for Level 3. This is another indication of intrinsic "noise" in the P parameter.

Use of the SET 2 functional form to calculate P(ω) also improved the overall fit. This is not surprising as the Hasselmann et. al. (1980) expression was determined using spectra having lower directional resolution and is in effect better suited to the parameterization being tested in this study.

The directional parameterization cannot properly handle bi-modal spectra which are independent of the swell and sea being modelled. Therefore, calculating RESD only over frequencies having unidirectional distributions should reduce the error. This was performed and the results shown in Fig. 15 (P1=20, P2= 7.5. Set 2). There is some improvement particularly for the Level 3 analysis (in Level 2 many of the worst conditions may have already been screened out). The time series of these RESD values are shown in Figure 16 . As in Fig. 8 (Error 11), there appears to be better behavior during the early and peak stages of the two storms.

The results for the Level 4 analysis (ie. P not varying with frequency) are shown in Figs. 17 and 18 . in Fig. 17 , the upper plot used the COS2P-FIT model P values for frequencies nearest to ωm1 and ωm2, allowed to vary between records, and the lower plot used a constant P1=20 and P2=7.5. In fig, 18 , constant value of P1=10 and P2=4.0 (upper) and P1=40 and P2=7.5 (lower) were used. An increase in the RESD values occurs for the narrower distributions (ie. larger Pi) with little change when using P1=10 and P2=4.0 compared to the corresponding Level 3 results. This implies that the majority of the error is resulting from discrepancies in a narrow frequency and direction region about the peaks, where the energy is largest.

For Levels 2, 3 and 4 (P1=10, P2=4.0), between 40 and 60% of the records had RESD values less than 30%. The sources of error could be due to errors in the heave energy obtained from the OH model, the choice for P1 and P2. any errors in D which varies P with frequency, and if the COS2P model is inappropriate, particularly in the case of bi-modal spectra, selected contoured directional spectra for the Level 2, Level 3 and Level 4 model results, with 10% noise, are displayed in

Appendix 3 and labelled C, D and E, respectively. Generally, much of the error results from either an inability to handle bi-modal spectra or slight changes in energy levels near the peaks. Bi-modal spectra are present both in the swell regime and at high frequencies during high energy conditions. The former introduces large errors as the model either assigns an intermediate direction or ignores one of the peaks and there is significant energy in this region. If one of the peaks is ignored, the error may be compounded by the necessity to normalize the spectra according to the energy at that frequency thereby forcing the single peak to account for all the energy. The bi-modal spectra at high frequency are associated with lower energy, locally, and do not have as much influence on the errors. The choice of P = f(ω/ωm)**D tends to handle the directional spreads near the storm peak frequency well, however it seems to provide too broad a distribution for higher frequencies (approx. 1.0 radians/sec or more above the peak). The constant P model often provides too narrow a distribution in this region. In these figures, 10% noise was added to all frequencies while a slightly reduced amount at the peak may be more appropriate. The noise component helps to reduce the residual as the original P calculations explicitly included a parameter to describe it thereby allowing for larger P values in the fit.

6. TEN-PARAMETER MODEL

6.1 Model Description

In this section, we will be performing the full 10-parameter, non-linear, least-squares fit to the data of the model:

$$M(\omega,\theta) = \frac{1}{4}\sum_{i=1}^{2}\frac{\left(\frac{4\lambda_i+1}{4}\,\omega m_i^4\right)^{\lambda_i}\,\delta_i^2\; e^{-\left(\frac{4\lambda_i+1}{4}\right)\left(\frac{\omega m_i}{\omega}\right)^4} * \cos^{2P_i}\left(\frac{\theta-\theta m_i}{2}\right)}{\Gamma(\lambda_i)\omega^{4\lambda_i+1}}$$

This is a simple extension of the OH model to describe the directional spectra as opposed to the frequency spectra alone. Both Θm and P are assumed constant with frequency.

6.2 Fit Procedure

The procedure used was similar to that used for fitting the six-parameter OH model, discussed in Section 2.5 . Increasing the number of parameters significantly increased the processing time/record. The core of the analysis requires, for each iteration, the inversion of an N X N matrix and the calculation, at each data point, of M(ω,Θ), δM(ω,Θ)/δAi, and (M(ω,Θ)-D(ω,Θ))**2. Previously,

the matrix was 6X6 and there were 50 data points. For the 10-parameter model, the matrix is 10X10 and there are, in the case of the band-averaged directional spectrum, 16X90 (ie. 1440) data points. Methods to reduce the processing time were required. This was done by first reducing the directional resolution to eight degrees (ie. 45 direction bands instead of 90). It was also noticed, that if one tried to fit the 10-parameter model directly, using the same first guesses for the six heave parameters, as described in Section 3.2 , and new first guesses (discussed later) for the four direction parameters, the fitting to the "heave" portion dominated the iteration, the process was very slow, and little change, away from the first guess, of the direction parameters occurred. A three stage approach to the fit was designed which seems to work more quickly and does improve the final overall residual value. The procedure used was as follows:

- Stage 1. Fit the six-parameter OH model to the heave portion of the spectra. (These parameters were already calculated and were used directly in Stage 2.)

- Stage 2. An initial fit of the 10-parameter model is performed whereby the six heave parameters are kept constant and only the four direction parameters allowed to vary. This allows for the fit to "home in" on the appropriate spread and direction values.

- Stage 3. All 10 parameters are allowed to vary with the first guesses being the final values of Stage 2.

This analysis approach takes approximately 10-15 min./record. A first guess to the direction parameters is required in Stage 2. A considerable amount of time was spent in devising a general method for obtaining the first guess to the two direction parameters as the fit was most sensitive to these parameters. Initially, the first guesses for the two mean directions were obtained by scanning the direction spectra at the frequencies nearest to $\omega m1$ and $\omega m2$ for the direction associated with the energy maximum. When the nearest frequencies to $\omega m1$ and $\omega m2$ were the same, the mean wave direction was calculated and assigned to each frequency, with a corresponding P value of 1.0. In cases where two peak directions were present at this frequency, the iteration procedure generally resulted in the assignment of one direction to one frequency and the second direction to the other, thereby allowing for the modelling of some bi-modal directional spectra. The first guesses for P1 and P2 were otherwise obtained by performing a "quick" fit to the linear expression:

$$LN(S(\theta)) = P*LN(\cos^2(\frac{\theta - \theta m}{2}))$$

emphasized about the peak by limiting the fit to energies above 10% of the peak energy. If the P value returned was less than 0.1 it was set

to 1.0 (ie. a cosine-squared distribution). The directional spectra should be re-centered about the new mean directions between each iteration, for the appropriate frequencies (ie. Θm1 was used for 0< ω < ωhalf, Θm2 used for ωhalf < ω < 3.14, where ωhalf= 0.5*(ωm1+ωm2)). For cases where ωm1 and ωm2 were the same, the distribution was centered about a mean direction only once. The re-centering procedure handles the circular nature of the direction function which must be treated as linear during the fit. Some test spectra were modelled without re-centering between iterations and it was found that for conditions when more than one distinct wave direction at a given frequency is observed, the procedure would not necessarily converge to the lowest residual fit. This can be visualized as the fit direction parameter Jumping from one centered direction to the other. The distribution is then no longer centered, and the fit process may have difficulty in determining the remaining four parameters associated with the new peak direction. The fit limits for the heave parameters were the same as in the OH model fit. The P parameters were forced to be between 0 and 100, and the fit directions between -pi and pi. The stop criteria was made less stringent than for the six-parameter fit to reduce the computation time. The iterations were stopped after 50 or if the change in the chi-square residual was less than 0.1% for seven iterations in a row.

6.3 Fit Assessment

Figure 19 contains the time series plot of the residual (ie RESD), environmental parameters, the 10-model parameters and the measured angular half-widths. The angular half-width was obtained through a scanning of the modelled directional spectrum at the given modal frequencies ωm1 and ωm2. If one compares the modal frequency, significant wave height and shape parameters with those from the six-parameter model (Fig.3). It can be seen that some adjustment to the parameters has occurred to account for the direction distribution. This is particularly true for the significant wave height and shape parameters as these terms are including an implicit normalization factor associated with the direction model. In other words, in the case of the six-parameter fit, the SQRT(HS1**2+HS2**2) should equal the total significant wave height for the record if energy is being conserved. However, in the 10-parameter fit, this is not true but it is the SQRT((HS1/A1)**2+(HS2/A2)**2) which equals the record significant wave height where A1 and A2 are determined from the expression:

$$1 = A1 \int_0^{2\pi} \cos^{2P1}\left(\frac{\theta - \theta m1}{2}\right) d\theta$$

This factor has to be corrected for when performing any comparison with the six-parameter model or when doing a regression of one parameter against another.

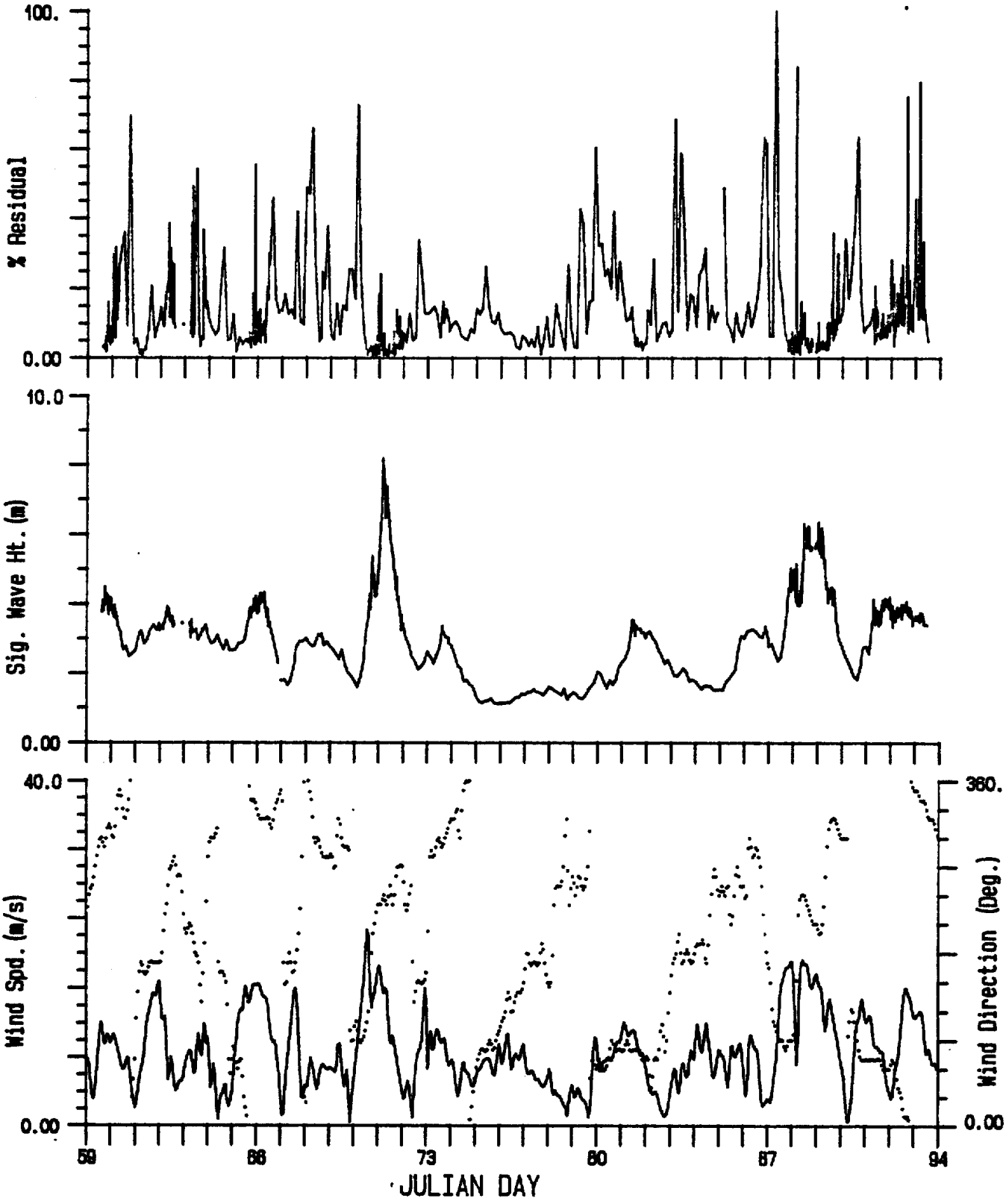

Fig. 19 Time series of fit residual(RESD), environmental and model parameters for the 10-parameter model

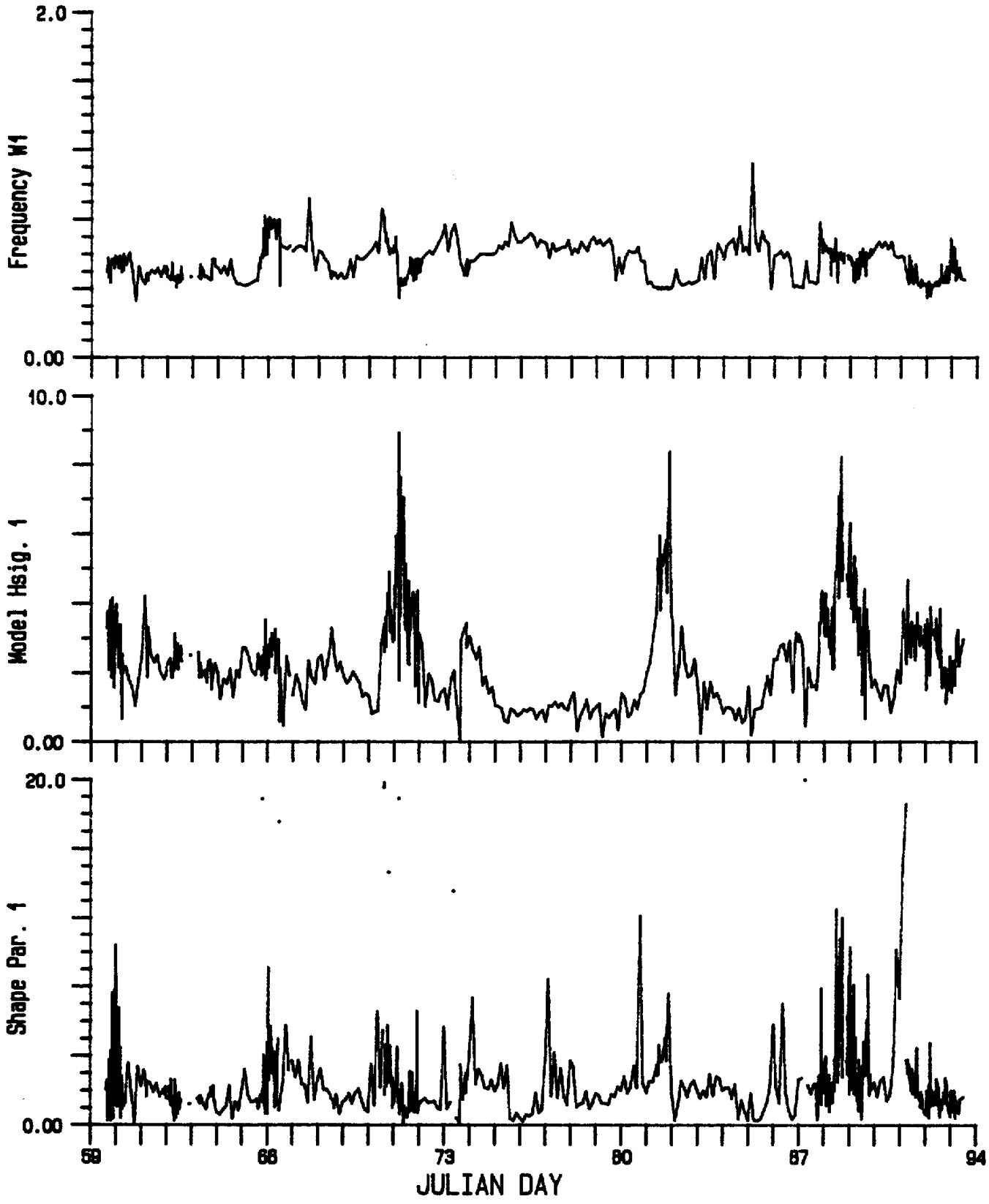

Fig. 19 (continued)

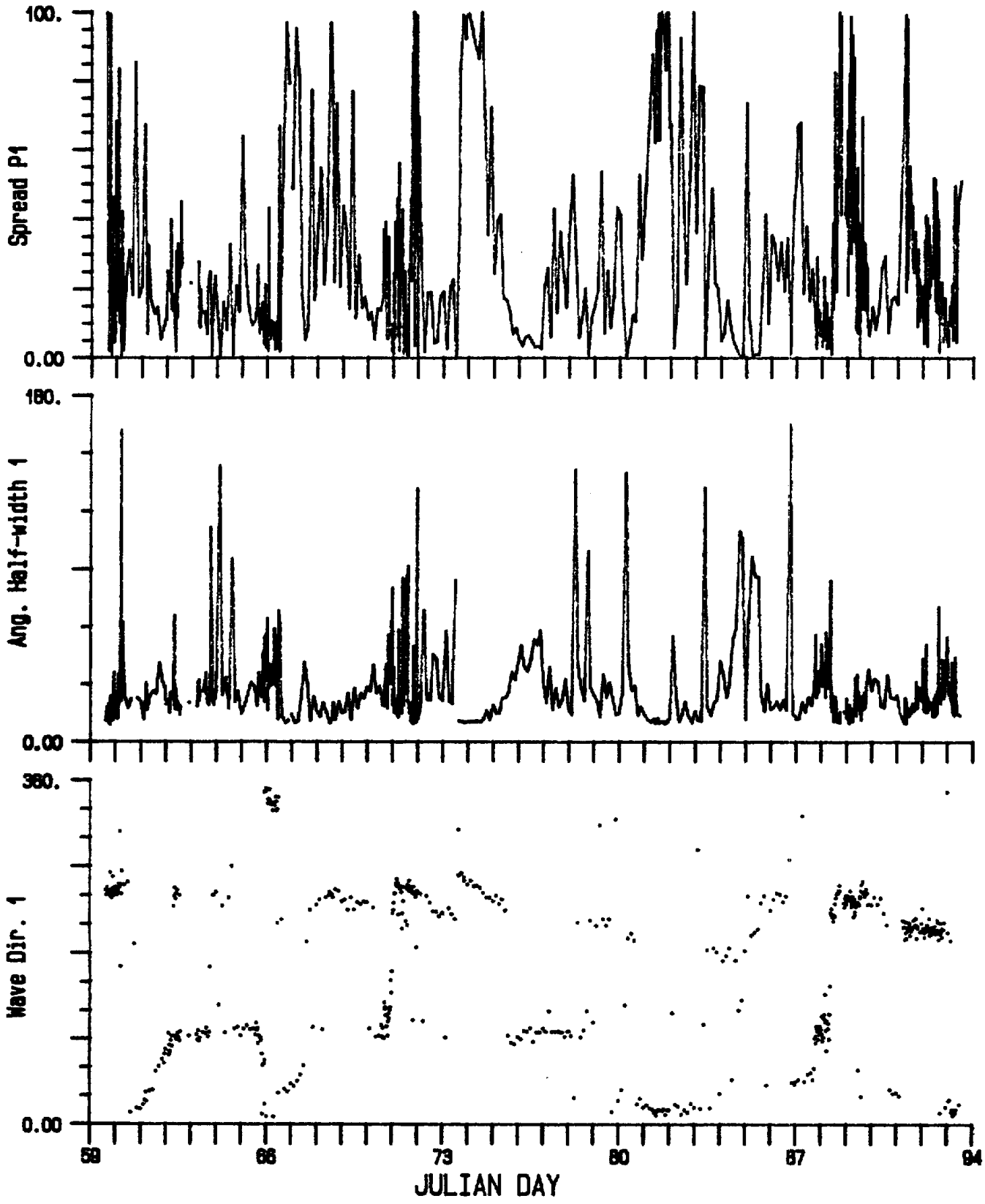

Fig. 19 (continued)

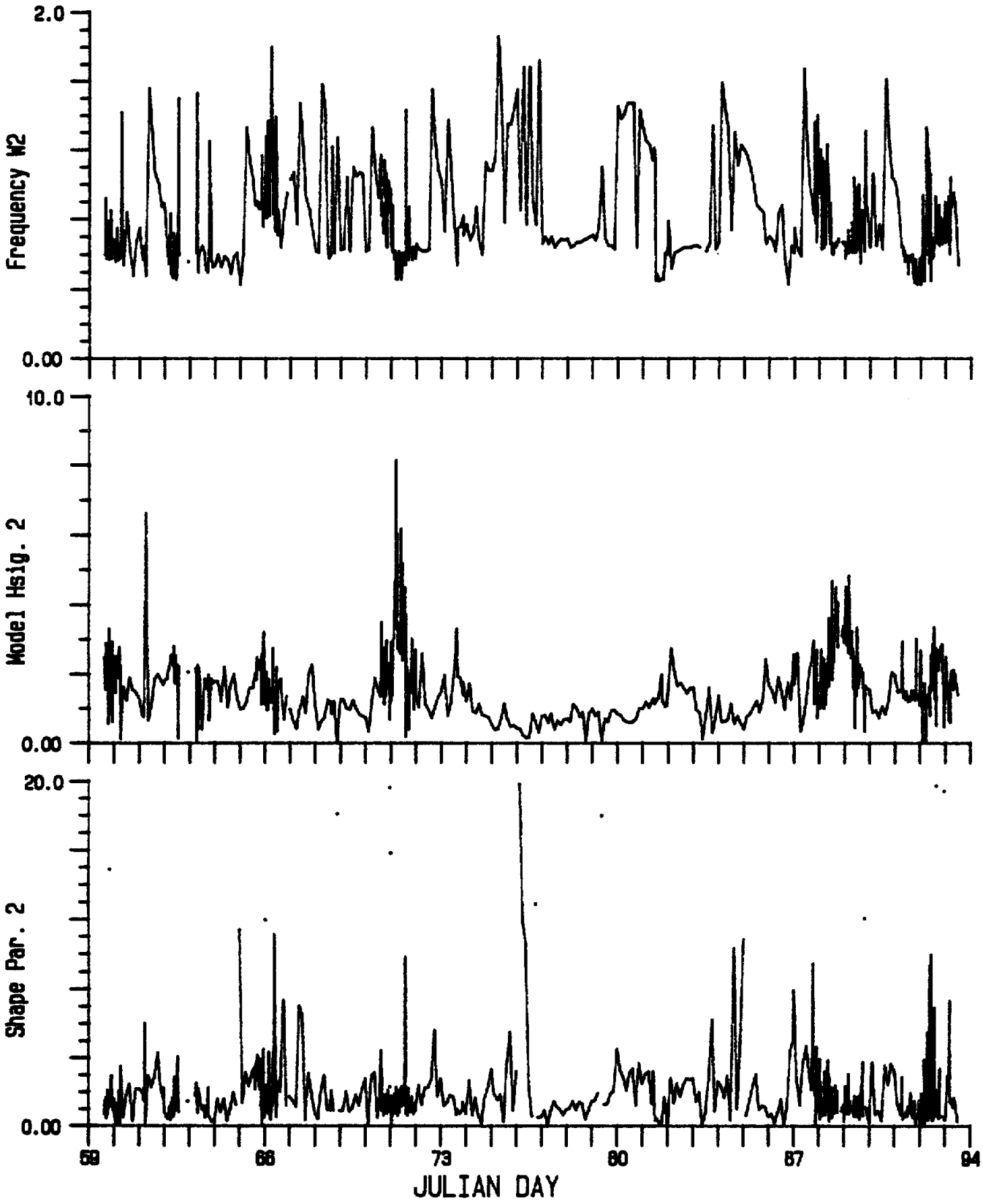

Fig. 19 (continued)

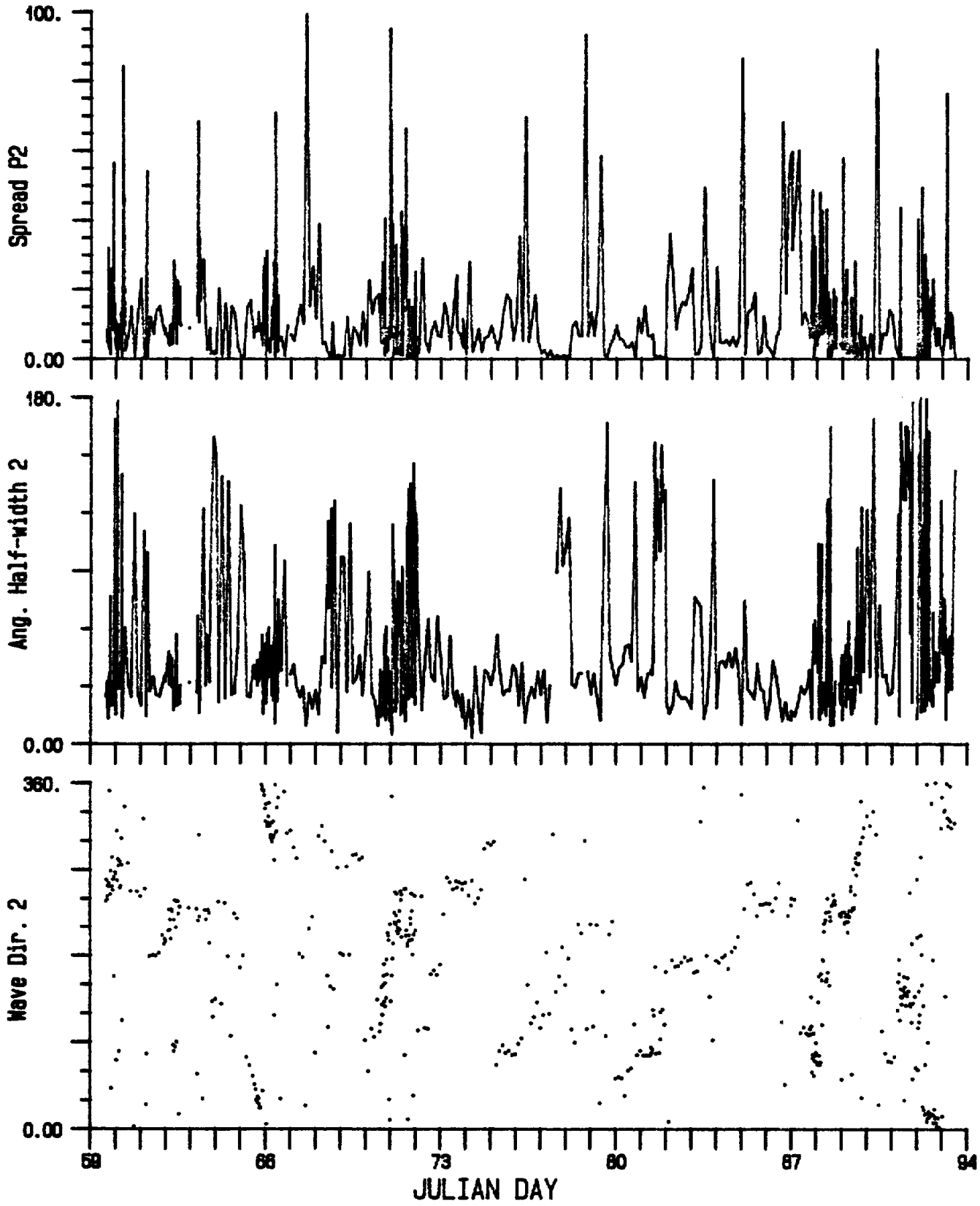

Fig. 19 (continued)

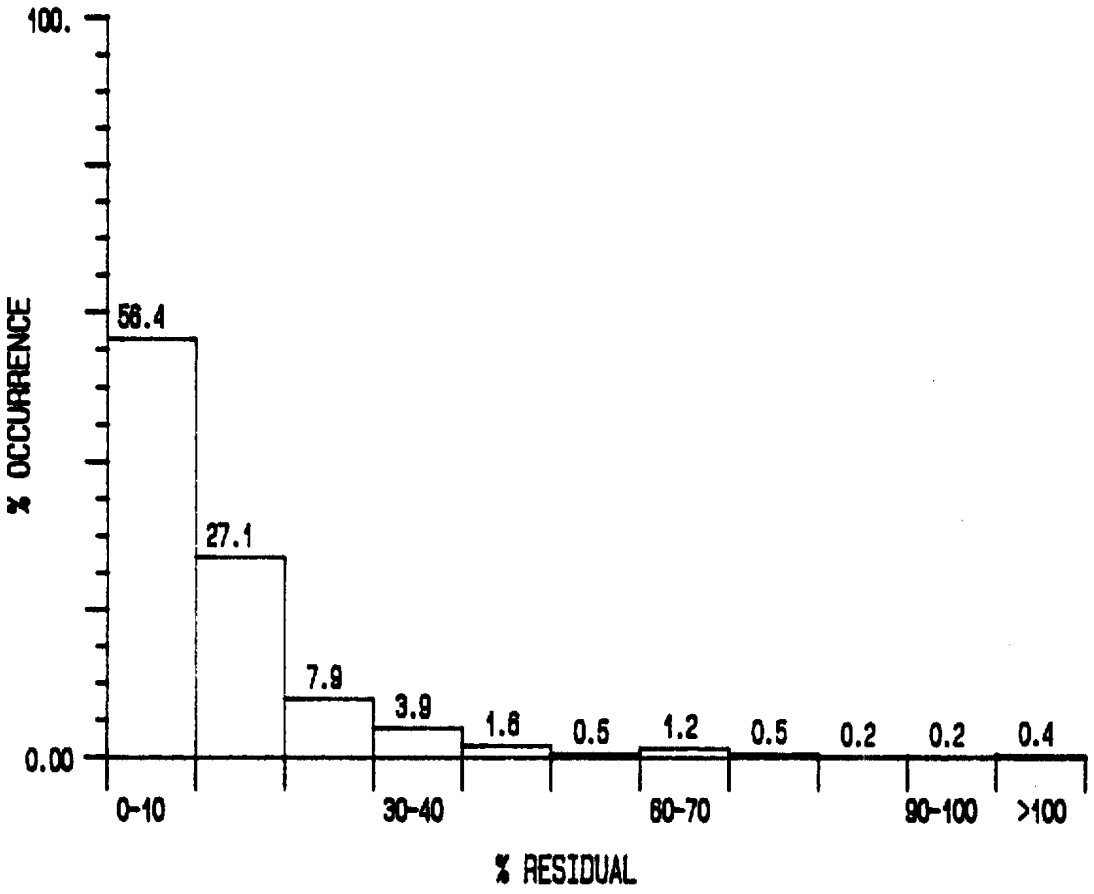

Fig. 20 Percent occurrence of RESD for 10-parameter model

Fig. 20 contains the percent occurrence of RESD. The adjustment of the parameters during the fit of the complete expression, results in a better fit to the original data than either the Level 2 or Level 3 parameterizations. The fit is better than the Level 1 parameterization when noise is not included (Fig.9 , error 11), as it is implicitly including a certain level of noise. In fact, if one considers the intrinsic limitations to the model and that the RESD values for Level 1 were only calculated for frequencies whose RES value was less than or equal to 5%, which effectively excludes very poor fits from the calculation, the 10-parameter model results are very good. Keeping P constant with frequency, did not seriously affect the errors as the model is fitting very well at the energy peaks and more poorly away from these peaks which contributes little to the overall error calculation. Some adjustment may be provided by the shape parameter which is allowing for changes in the energy level to compensate for P being kept constant. Very large errors (>80%)

generally resulted when the 10X10 matrix was singular and thus could not be inverted and the iteration was stopped prematurely.

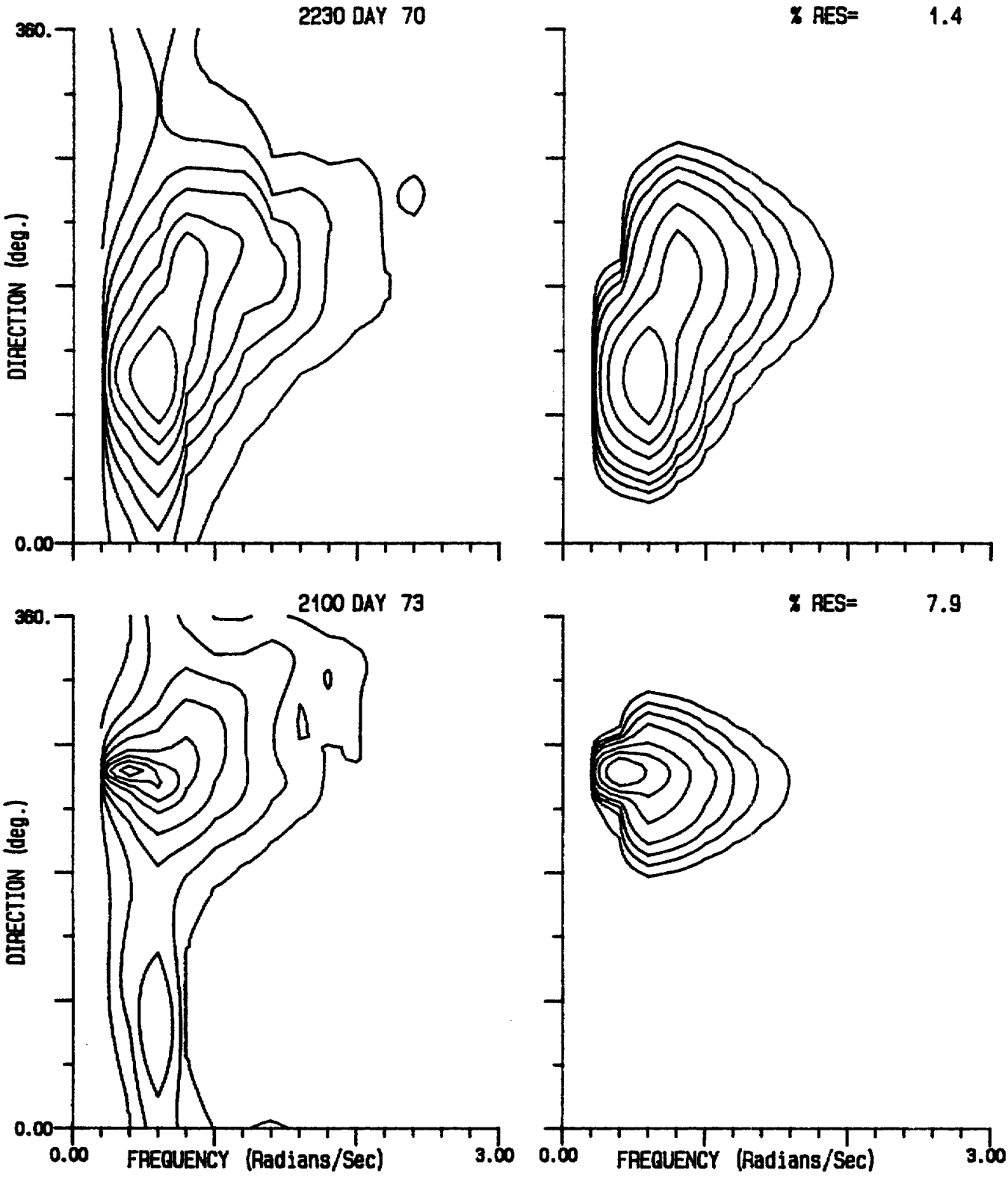

Fig. 21 Selected contoured data(left) and 10-parameter model directional spectra. (Contour intervals as in Appendix 3)

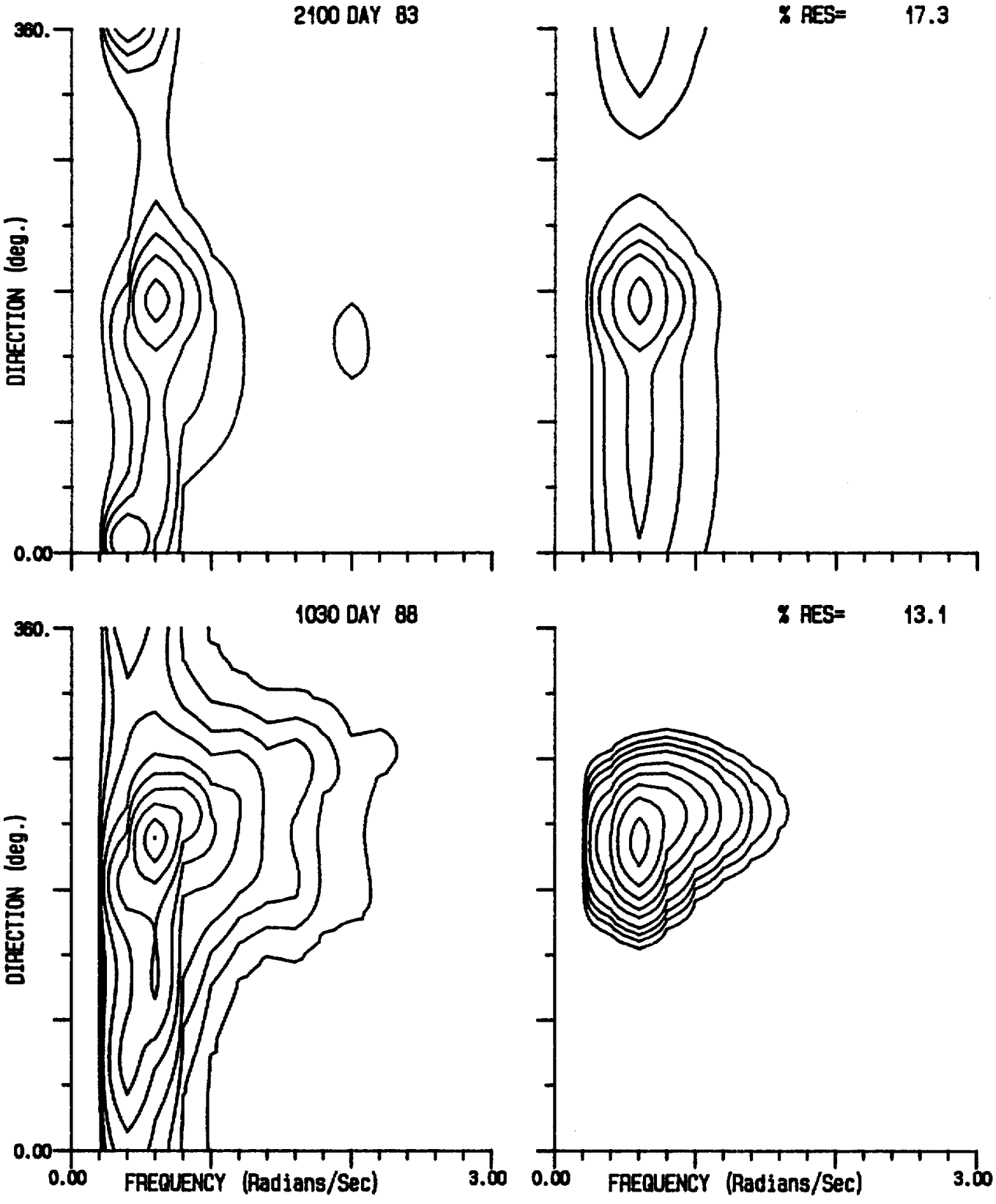

Fig. 21 (continued)

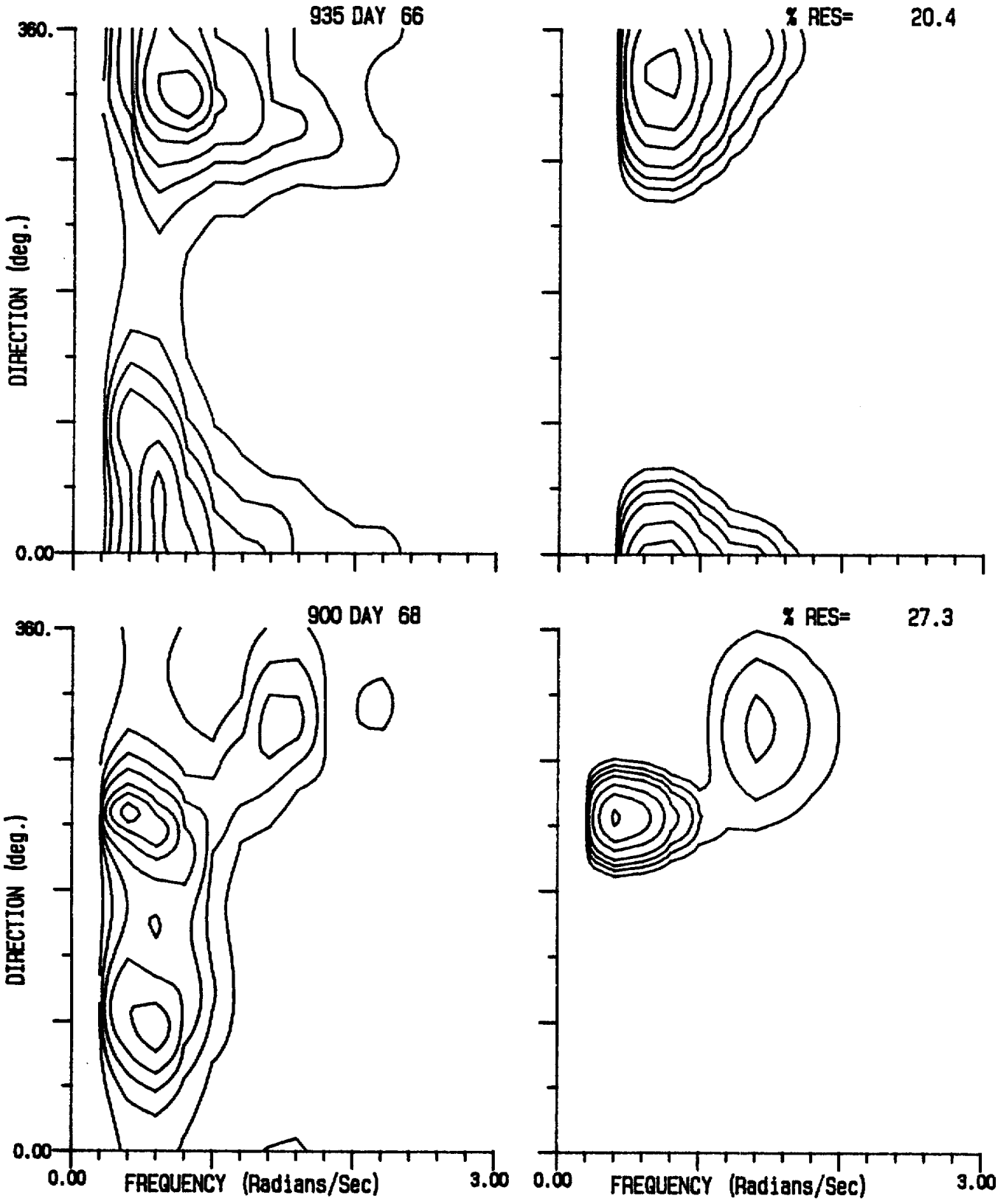

Fig. 21 (continued)

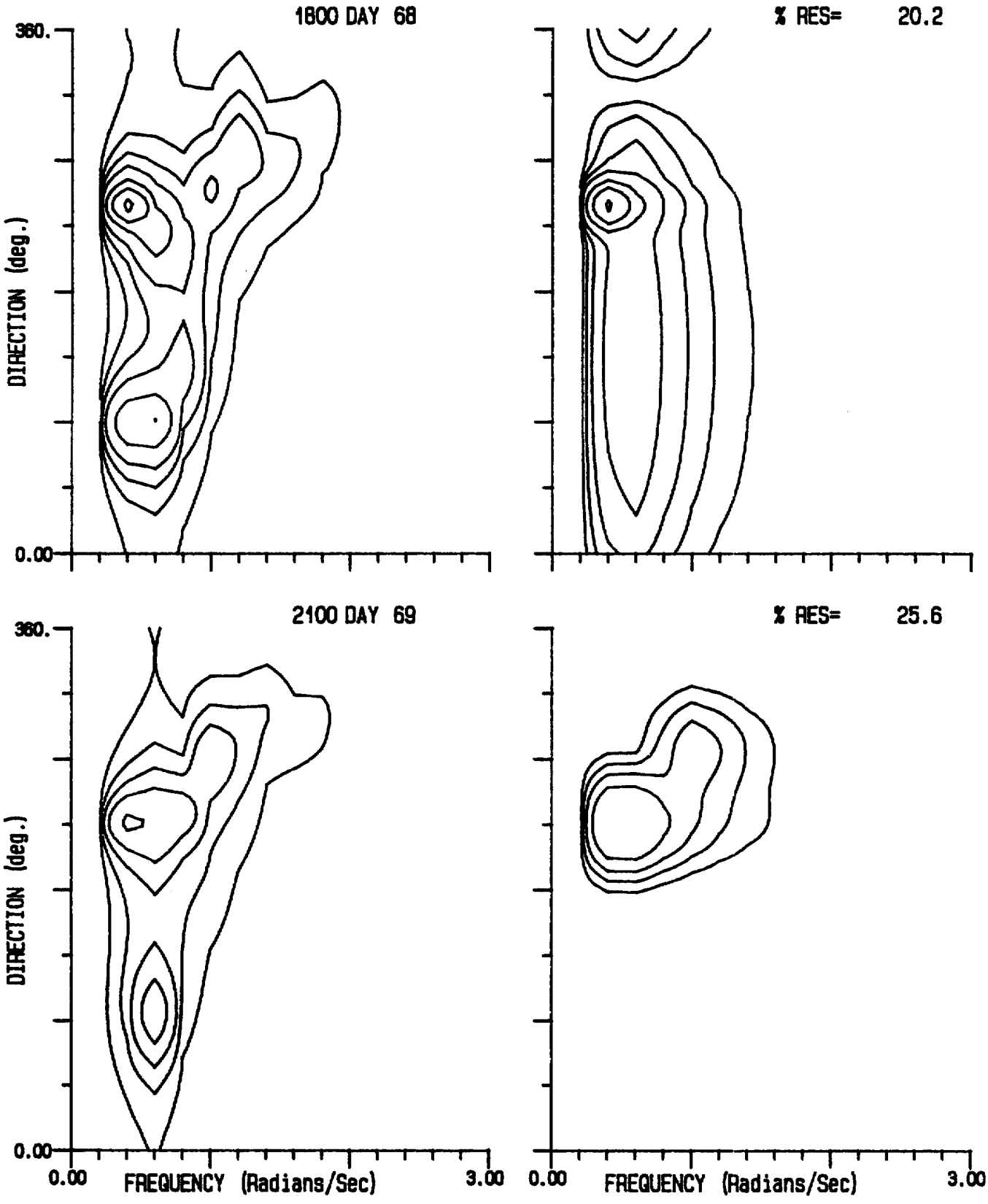

Fig. 21 (continued)

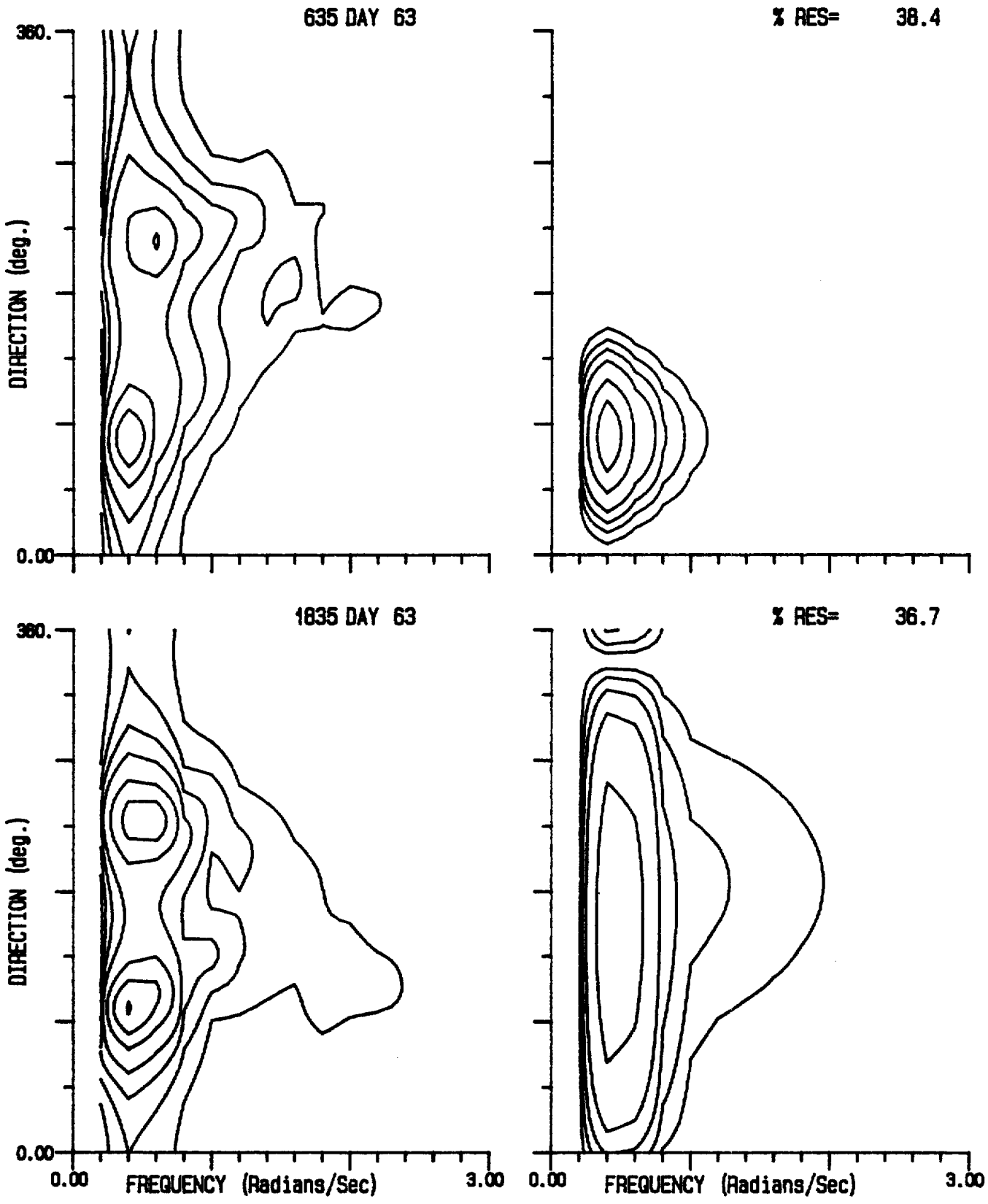

Fig. 21 (continued)

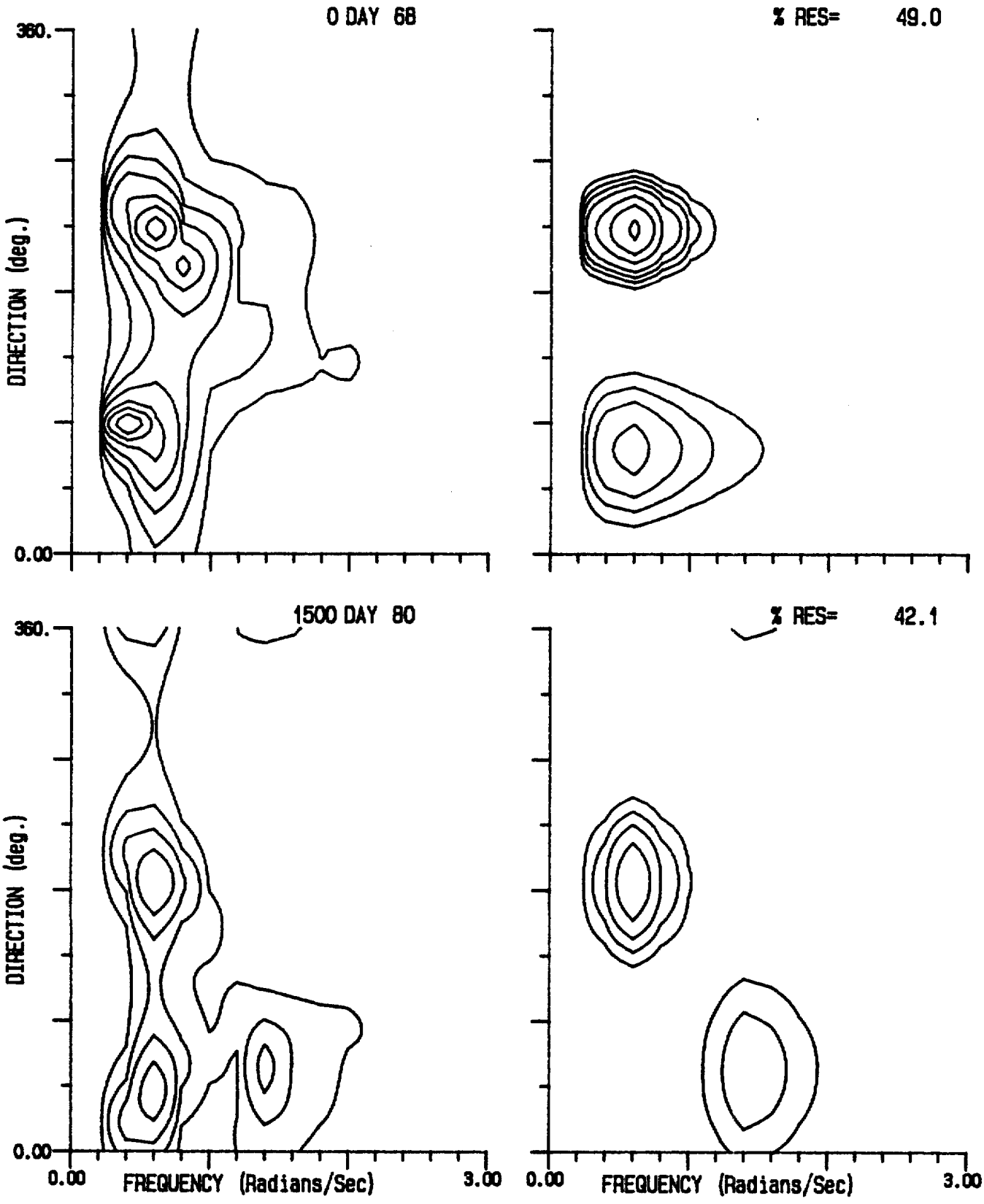

Fig. 21 (continued)

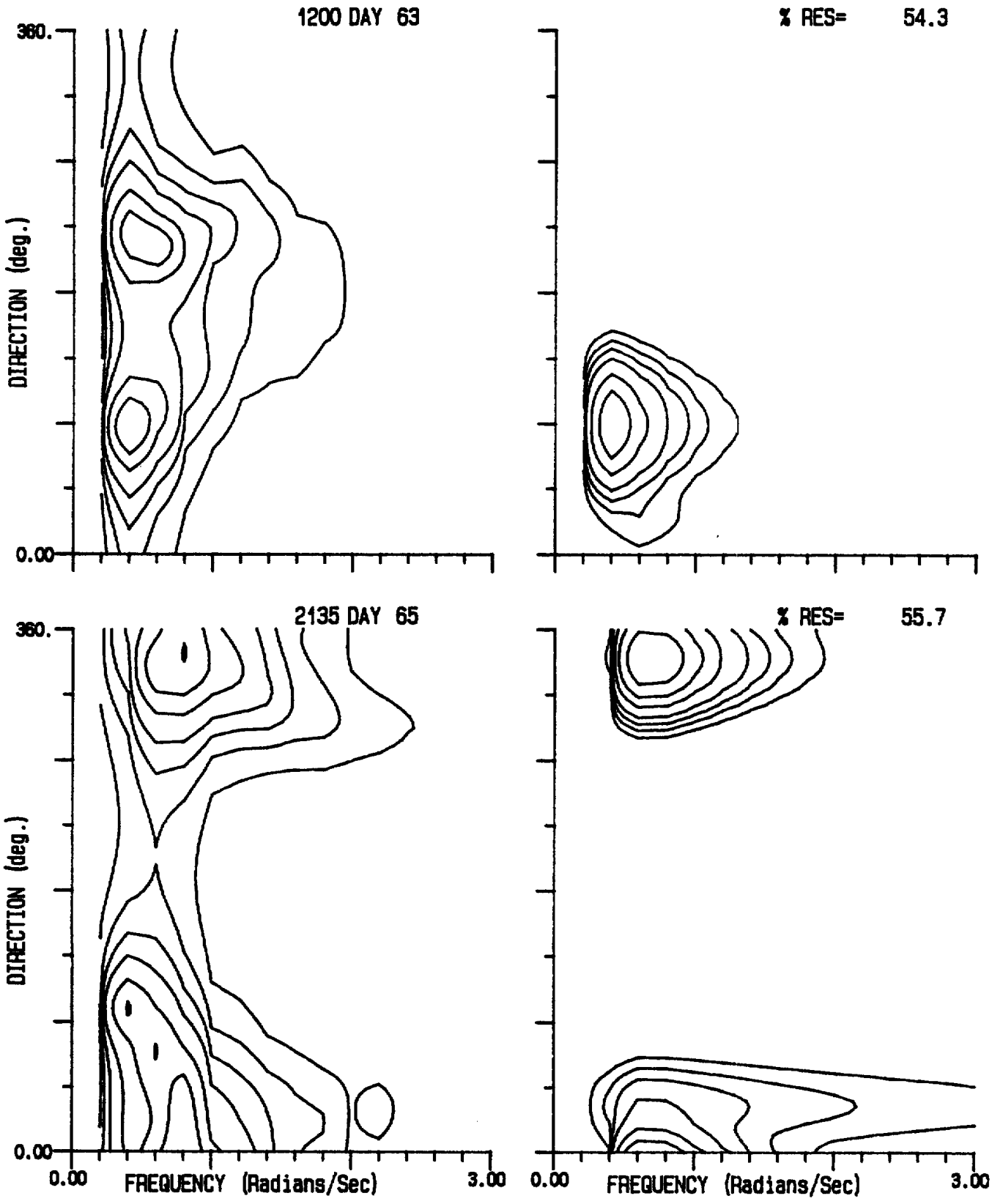

Fig. 21 (continued)

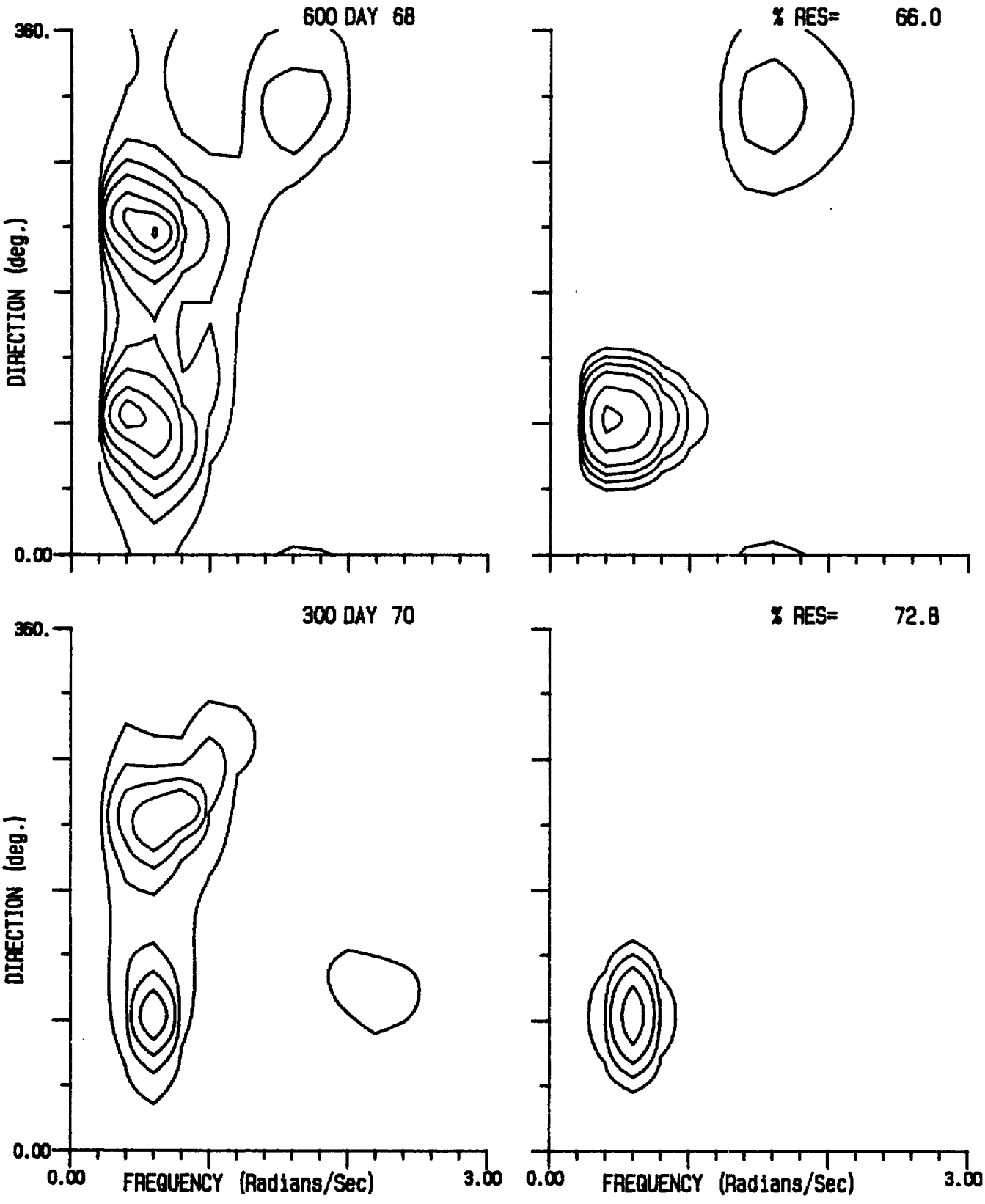

Fig. 21 (continued)

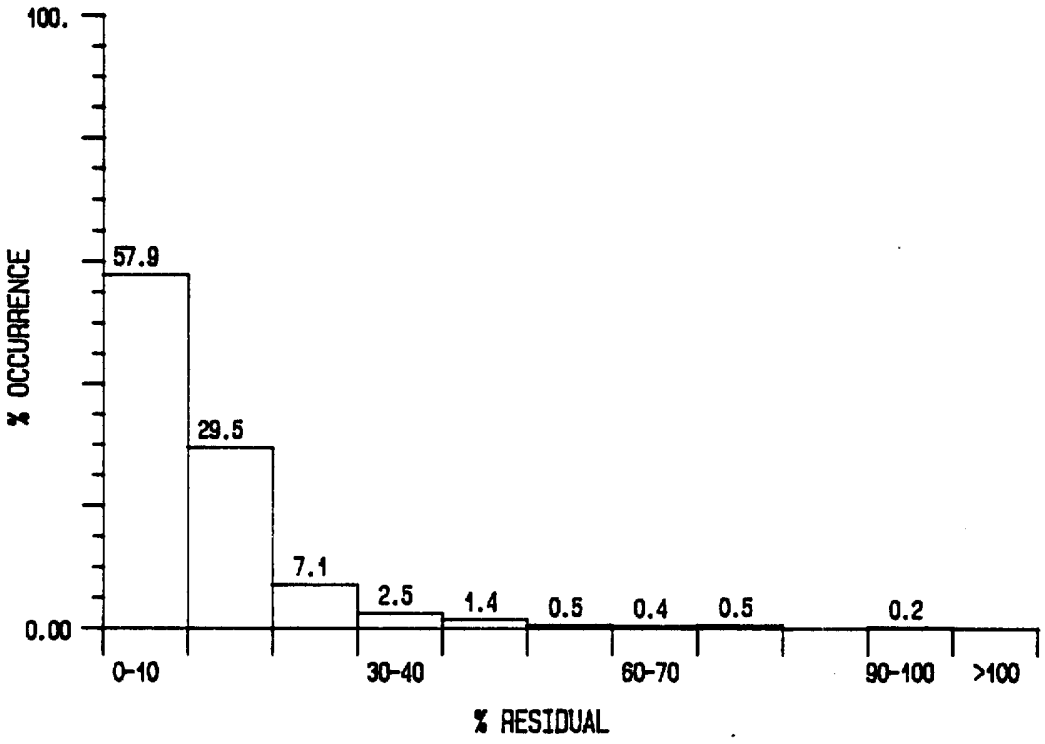

Fig. 22 Percent occurrence of RESD for 10-parameter fit adjusted to swell regime

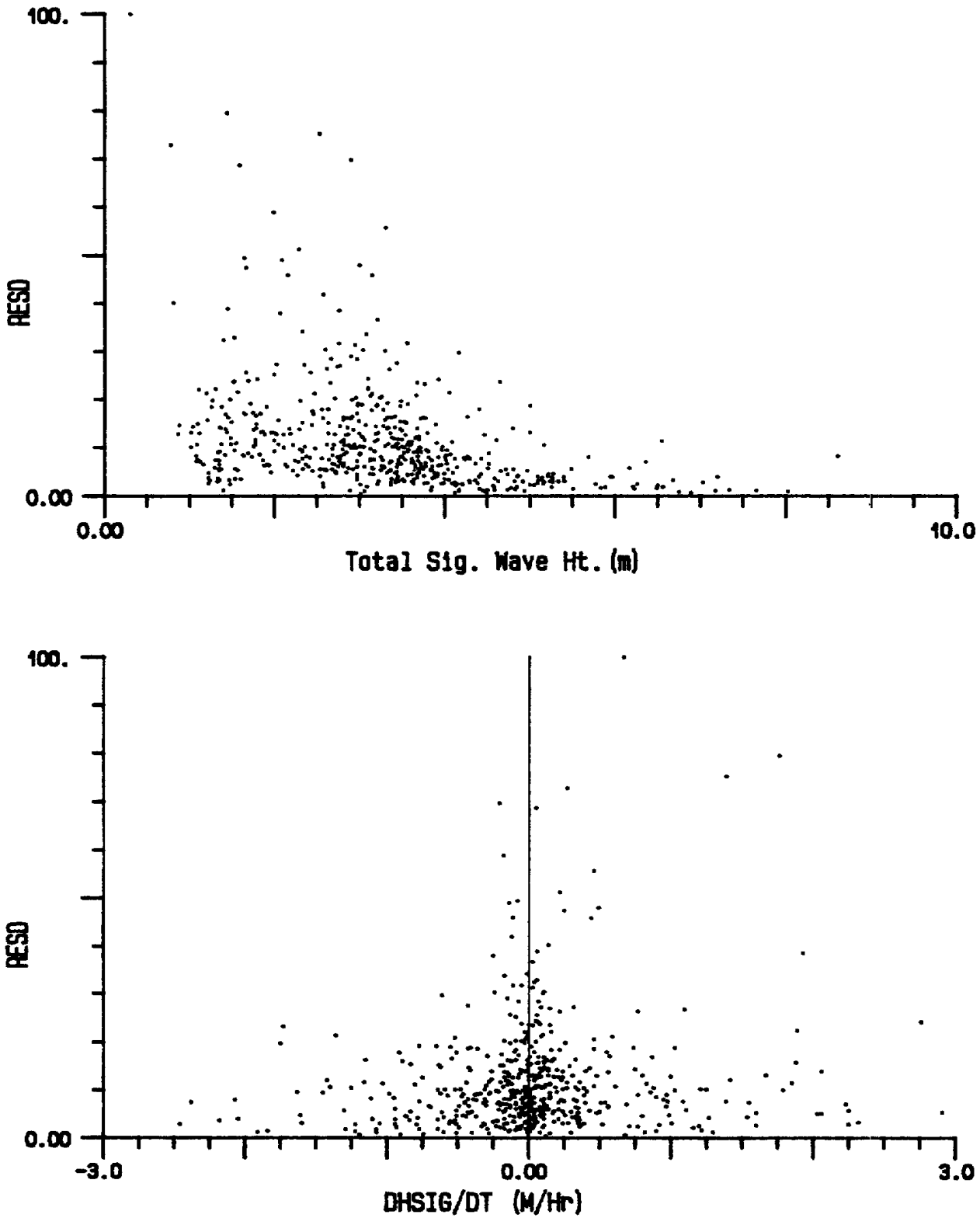

Fig. 23 Distribution of RESD as a function of record significant wave height (upper) and its time rate of change (lower)

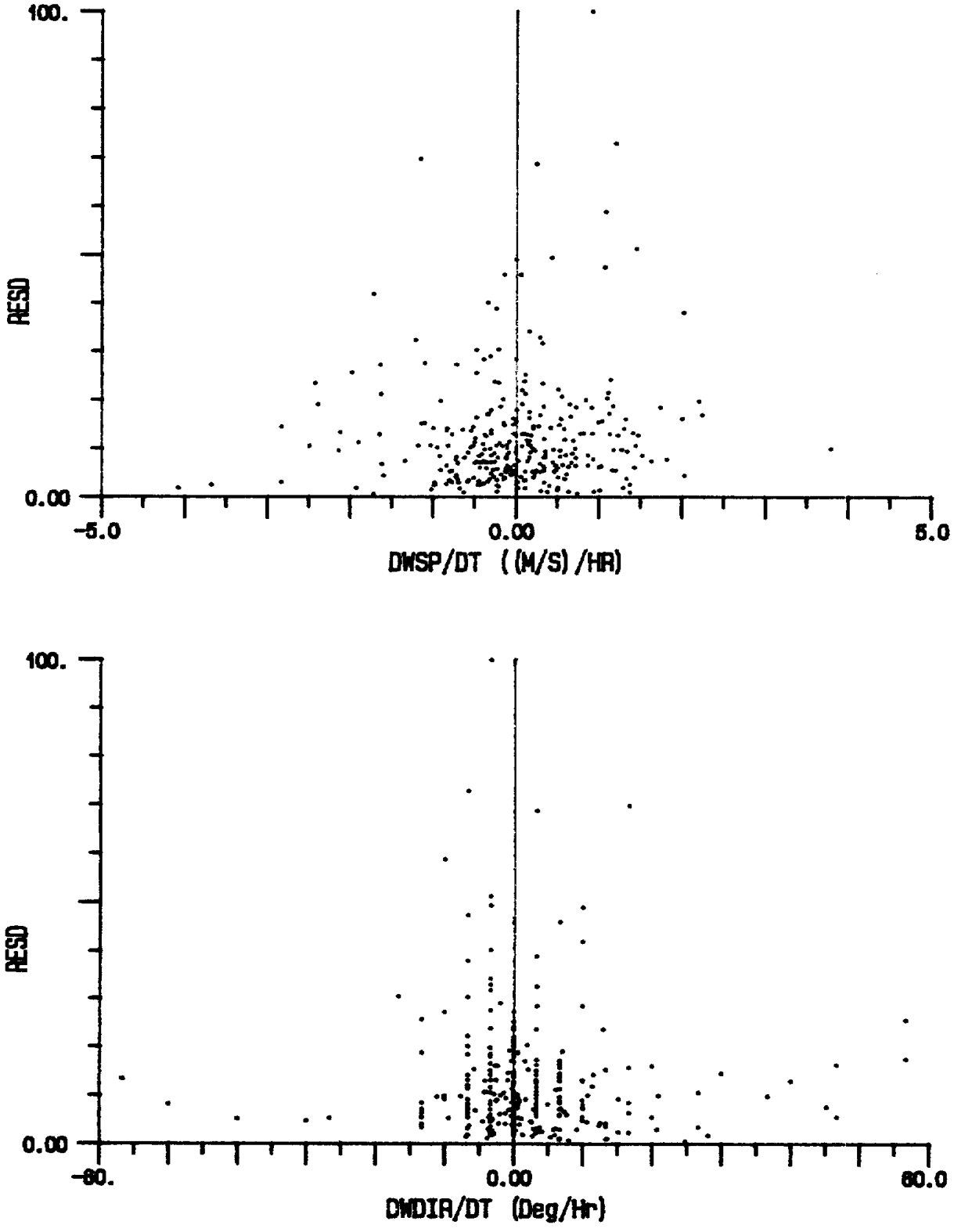

Fig. 24 Distribution of RESD as a function of the rate of change of wind speed (upper) and wind direction (lower)

Selected contoured 10-parameter model results are shown in Figure 21 to illustrate a range of RESD values. Appendix 3 contains plots (labelled F) for the two storms. Large errors are associated with missing a peak at low frequency (ie. more than one swell from different directions) or smoothing two peaks into one and they often are grouped in the time series as the swell signal can last for many hours. In order to handle these situations, one may want to go to a 12-parameter model which allows for two directions at ω_{m1}, while maintaining only one direction at ω_{m2}. If one is interested primarily in the swell regime, one can reprocess the data for cases where the error is greater than, for example, 20% and when scanning indicates that two large swell peaks are present and forcing the fit to the lower frequencies. This was performed and the fit providing the lowest residual was saved. The percent occurrence of these RESD values are shown in Fig. 22 .

An examination of the RESD values with changing environmental parameters was performed to check for the existence of any consistent behavior of the model. Fig. 23 shows a scatterplot of RESD against the total significant wave height in the record and against the rate of change of significant wave height with time (to assess sea build-up and decay). There is a slight tendency for larger RESD values to be associated with lower energies. There was no strong dependence on the rate of change of significant wave height. Fig. 24 shows similar scatterplots of RESD against the rate of change of wind speed and wind direction (to assess veering). Again, there appears to be no strong dependence with these environmental parameters. These results support the contention that the majority of the error results from the handling of the swell signals which may have relatively larger contributions in low energy seas and which are not affected by local atmospheric changes.

7.0 REGRESSION ANALYSIS

7.1 Regression Equations

As the complete 10-parameter model fit is quite time consuming, it is desirable to be able to predict the value for Pi given the six heave parameters. The direction parameter is dependent on the wind sea and swell directions at the time of sampling and hence can never be predicted. A scatterplot of fitted P as a function of the OH model parameters was performed in order to see if a strong functional relationship exists. These plots are shown in Fig. 25 a . b and c . The corresponding distribution of angular half-widths, measured in the data spectrum, are given in Fig. 26 a . b and c . As can be seen, there is considerable scatter in both the P and angular half-width estimates. A regression of the functional forms

$$P = A\omega m^{B}\delta^{C}\lambda^{D} \quad OR \quad P = A\omega m^{B}\delta^{C} \quad OR \quad P = A\omega m^{B}$$

were performed for cases where RESH<8.0%, λi<10 and 0.5<P1<50 and P2<50. These limits were set in order to reduce some of the variance due to extreme values. The lower limit for P1 was chosen to eliminate poorly modelled bi-modal spectra from the regression. All three functional forms could account for 73% (ie. the additional parameters δ and λ did not reduce the variance) of the variance (calculated for 787 pts) with

A =	10.2089	OR	A =	10.1602	OR A = 10.2522
B =	-1.3086		B =	-1.4980	B = -1.3274
C =	1.600E-2		C =	1.588E-2	
D =	-8.344E-3				

These three expressions are explaining the same amount of variance with the fit being dominated by the relationship with frequency. The relatively high percentage of the variance explained, given the amount of scatter obvious in Fig. 25 results from the fit being weighted by the numerous low P2 values and may not be representative of the total range in P encountered. The regression was also performed on P values separated into sea and swell and into frequencies less than or greater than 0.55 radians/sec. In both cases, the explained variance was reduced.

Using these equations with the angular half-widths, which

contain slightly less scatter than the P values, resulted in explaining 83% (ie. again the additional parameters did not improve the regression) of the variance (calculated for 789 pts) in the half-width when the angles were limited to less than 1.745 radians (ie. 100 degrees). The corresponding coefficient values, for a radian calculation, are:

A =	0.5478	OR	A =	0.5321	OR A = 0.5324
B =	0.8012		B =	0.7275	B = 0.7247
C =	2.047E-2		C =	1.947E-3	
D =	-6.766E				

If one limits the analysis to angular half-widths of 50 degrees or less, the formula can explain 87% of the variance (720 pts) with

A =	0.4712	OR	A =	0.4630	OR A = 0.4653
B =	0.6678		B =	0.6230	B = 0.5946
C =	3.128E-2		C =	2.032E-2	
D =	-3.545E-2				

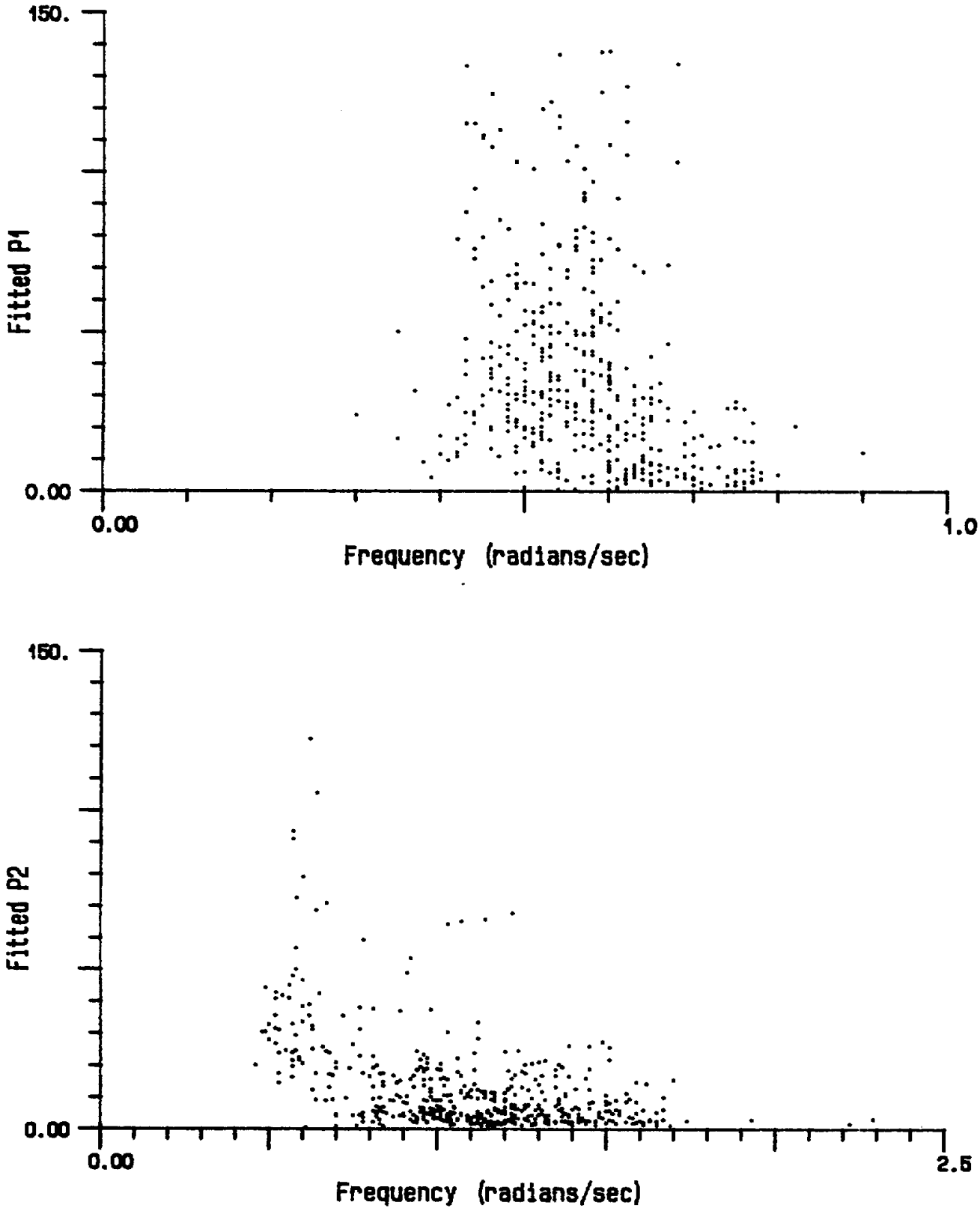

Fig. 25a Distribution of Fitted P as a function of model frequency, ωm1(upper) and ωm2(lower)

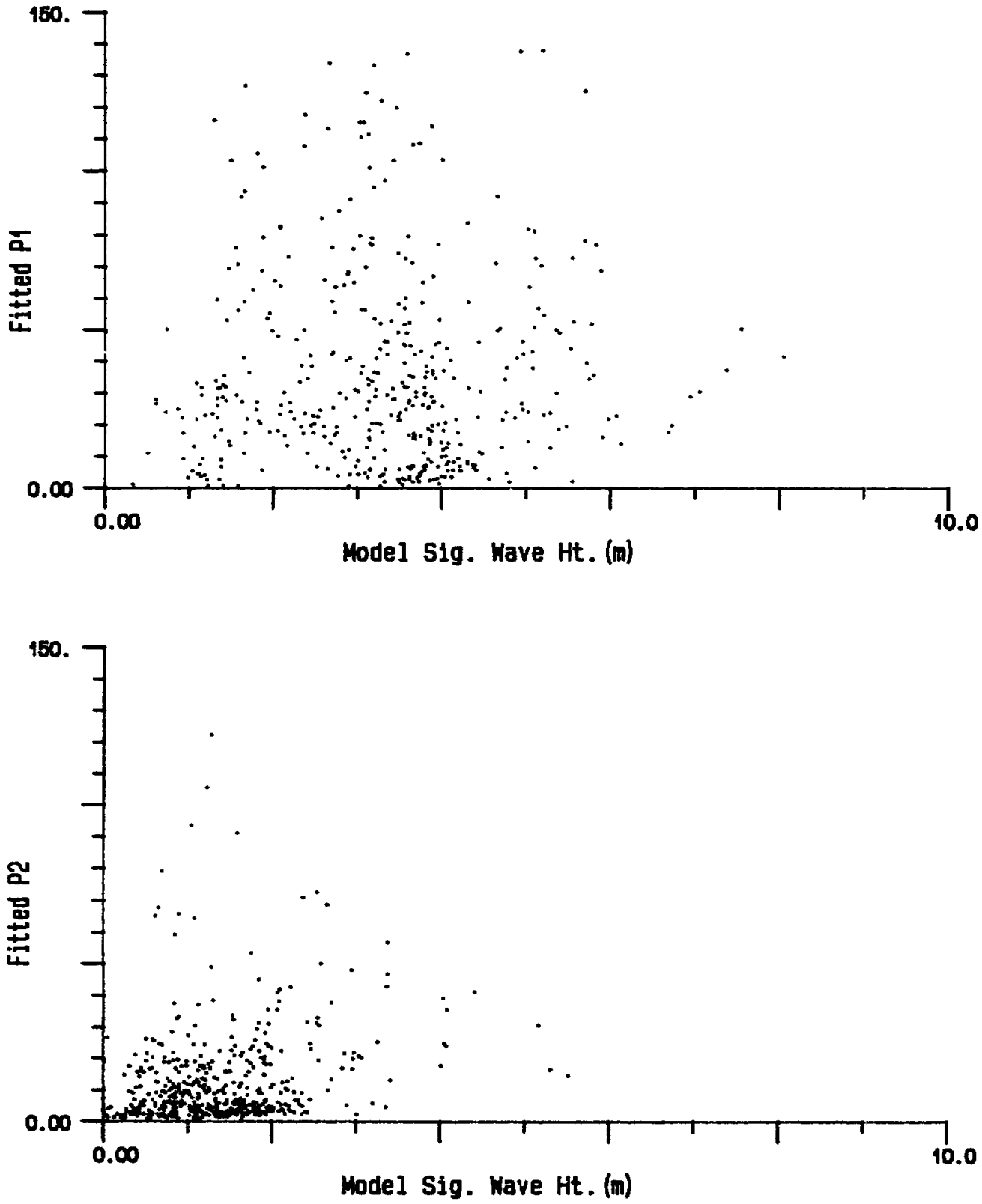

Fig. 25b Distribution of Fitted P as a function of sig. wave height, $\delta 1$(upper) and $\delta 2$(lower)

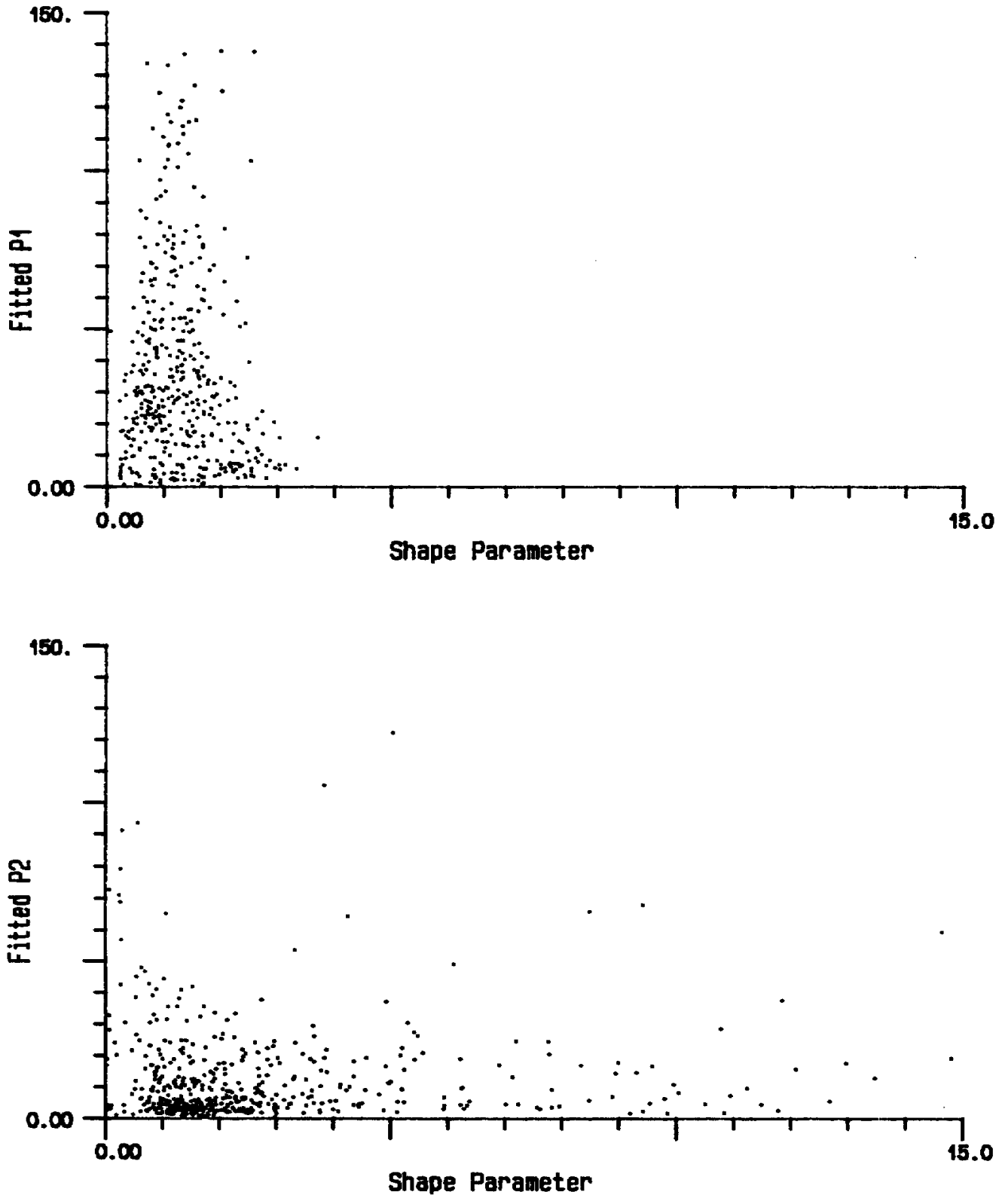

Fig. 25c Distribution of Fitted P as a function of shape parameter, $\lambda 1$(upper) and $\lambda 2$(lower)

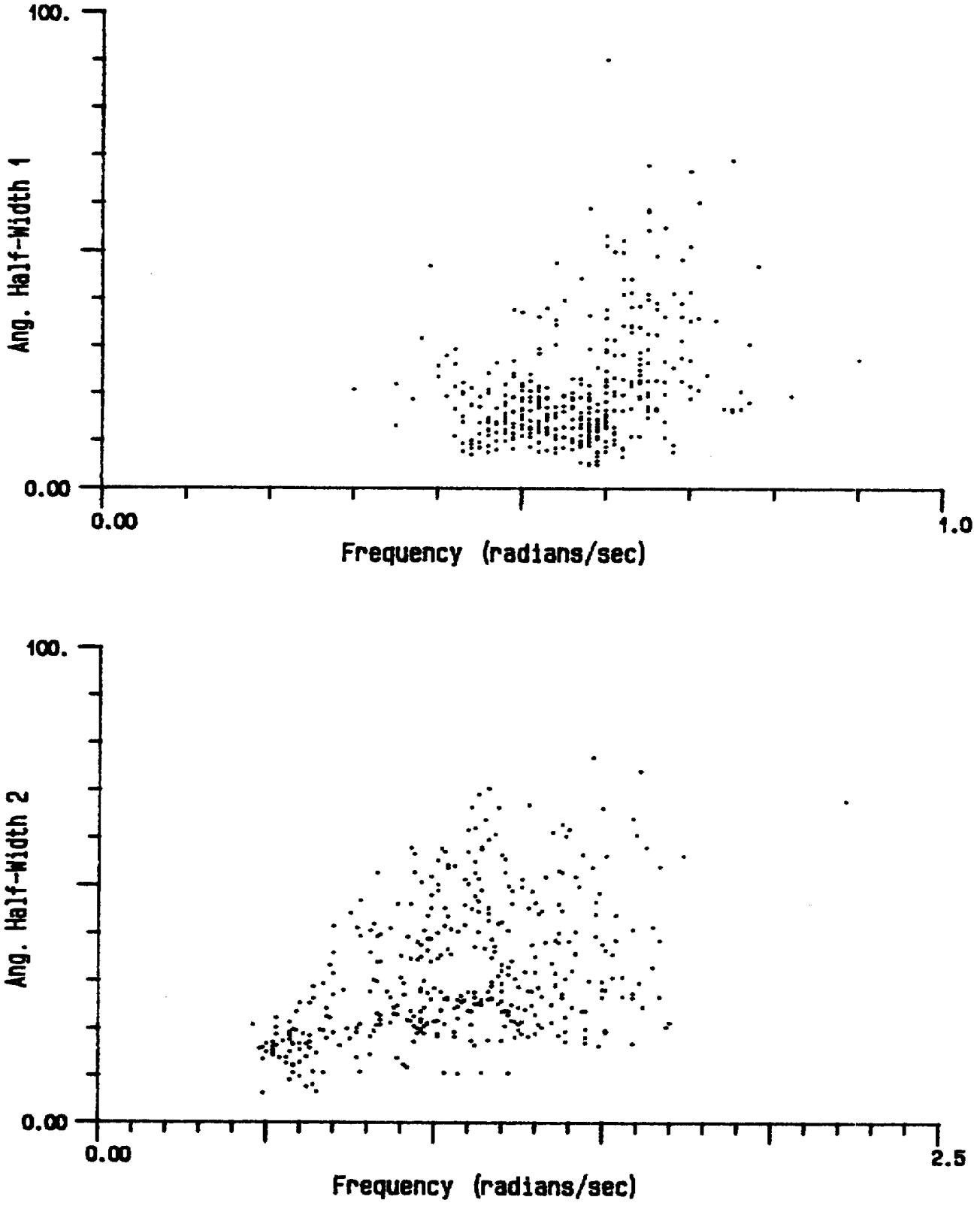

Fig. 26a Distribution of angular halfwidth with model frequency, ω_{m1} (upper) and ω_{m2} (lower)

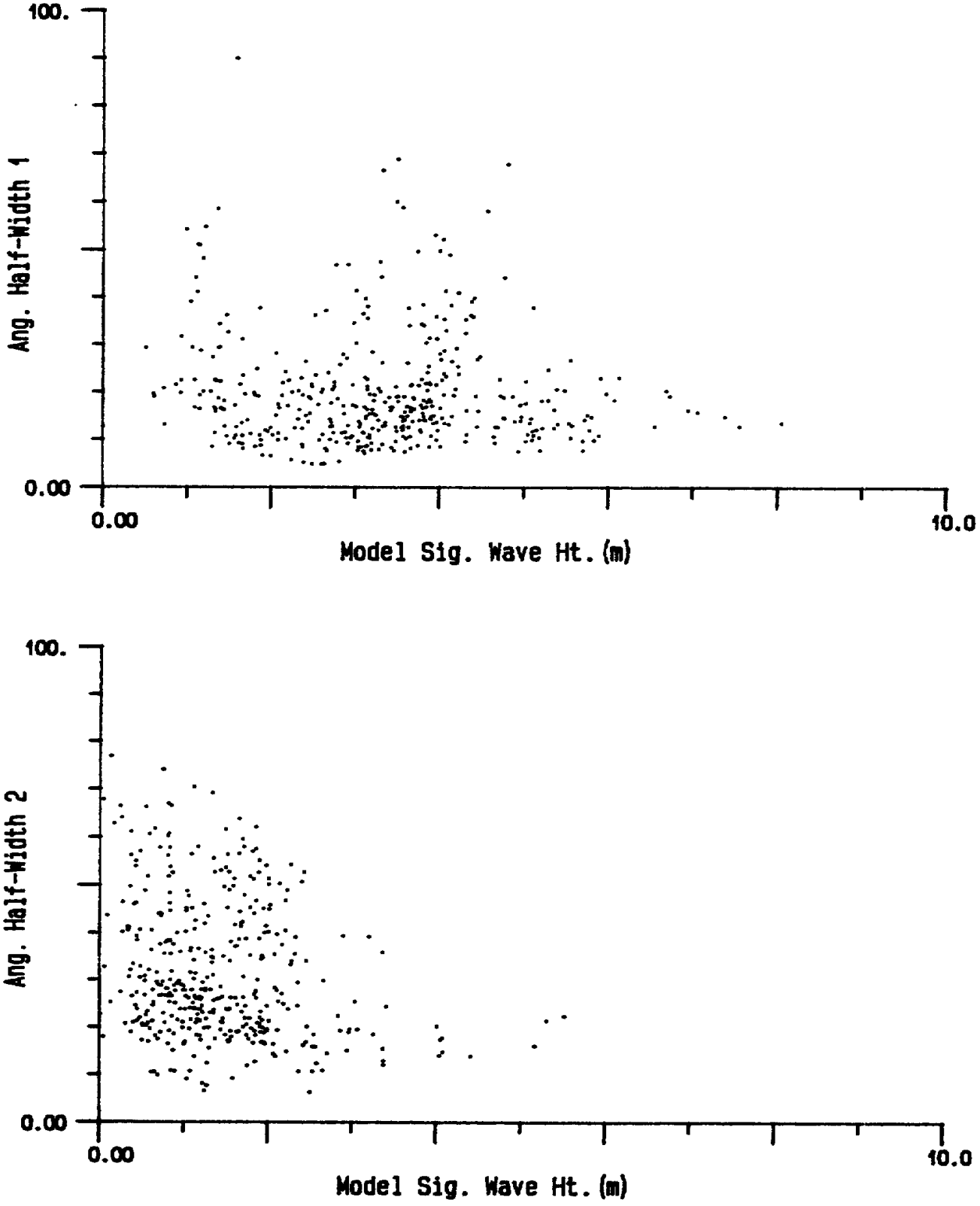

Fig. 26b Distribution of angular halfwidth with sig. wave height, $\delta 1$(upper) and $\delta 2$(lower)

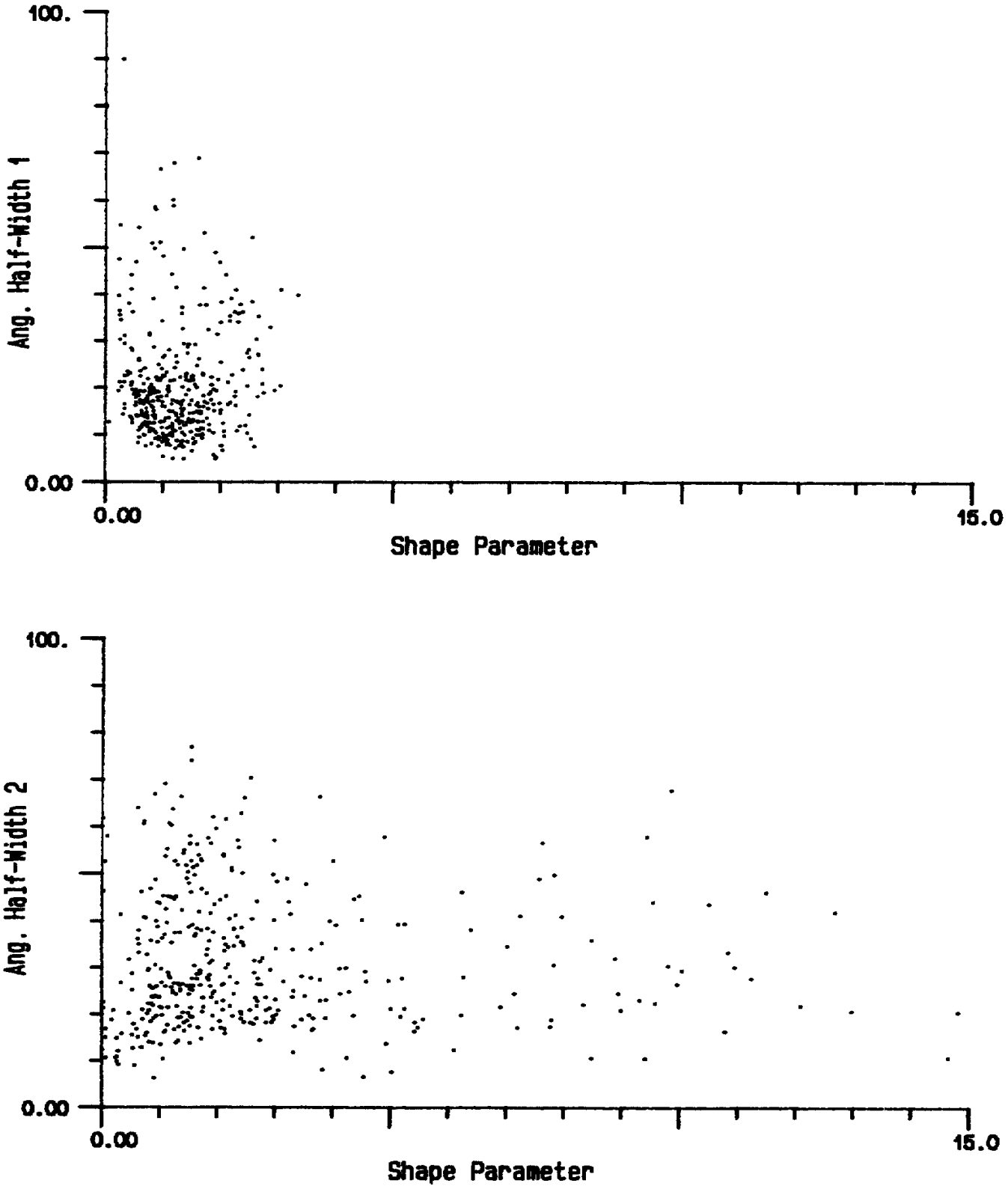

Fig. 26c Distribution of angular halfwidth with shape parameter, $\lambda 1$(upper) and $\lambda 2$(lower)

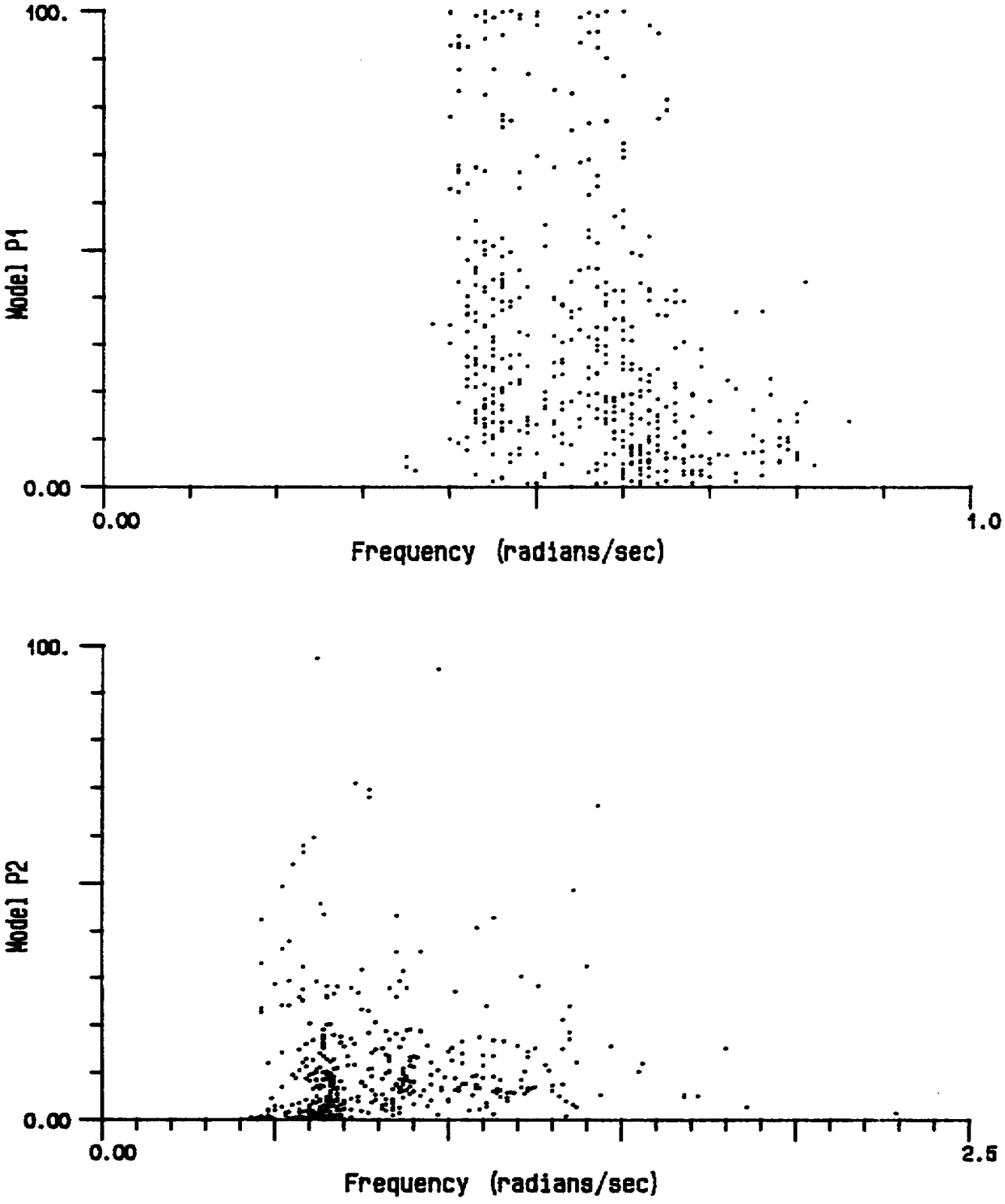

Fig. 27a Distribution of model P as a function of model frequency ωm1(upper) and ωm2(lower)

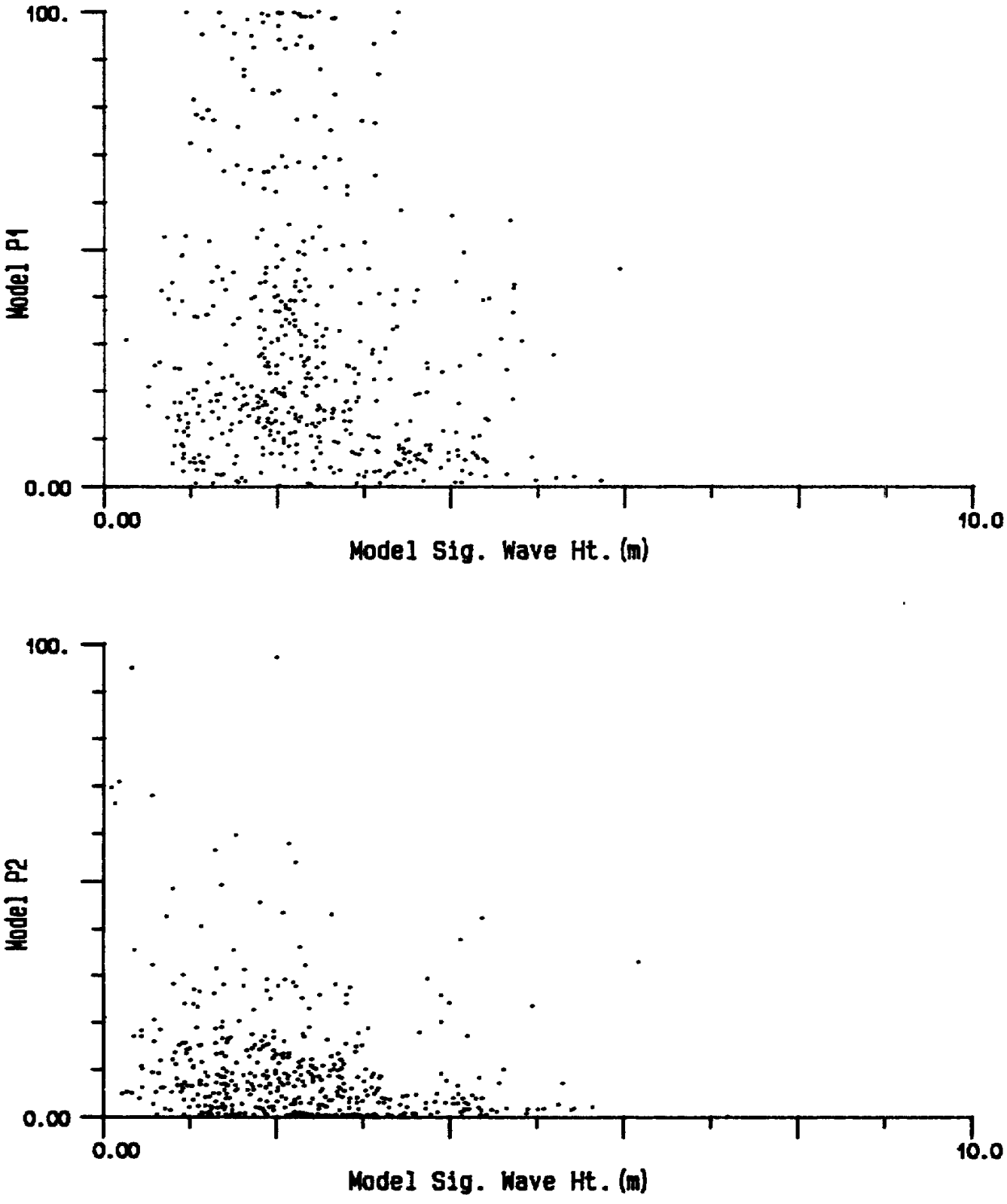

Fig. 27b Distribution of model P as a function of sig. wave height δ1(upper) and δ2(lower)

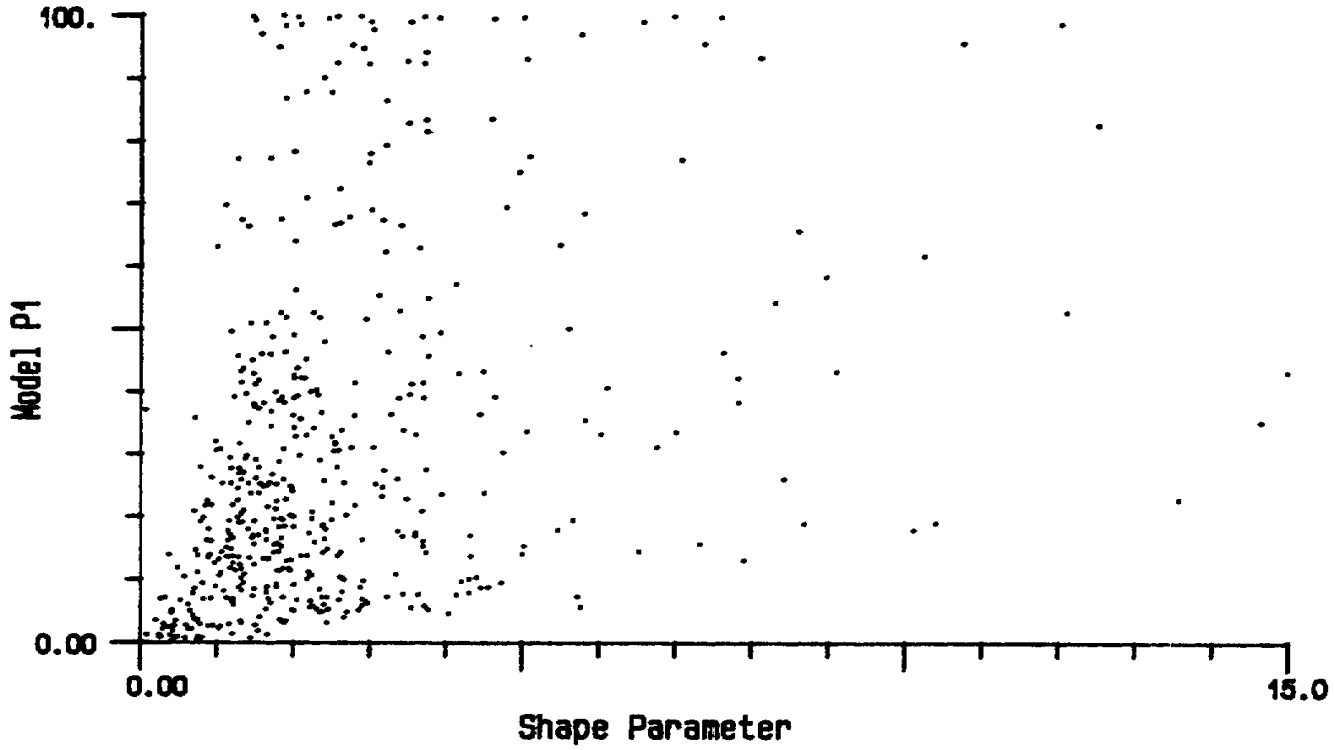

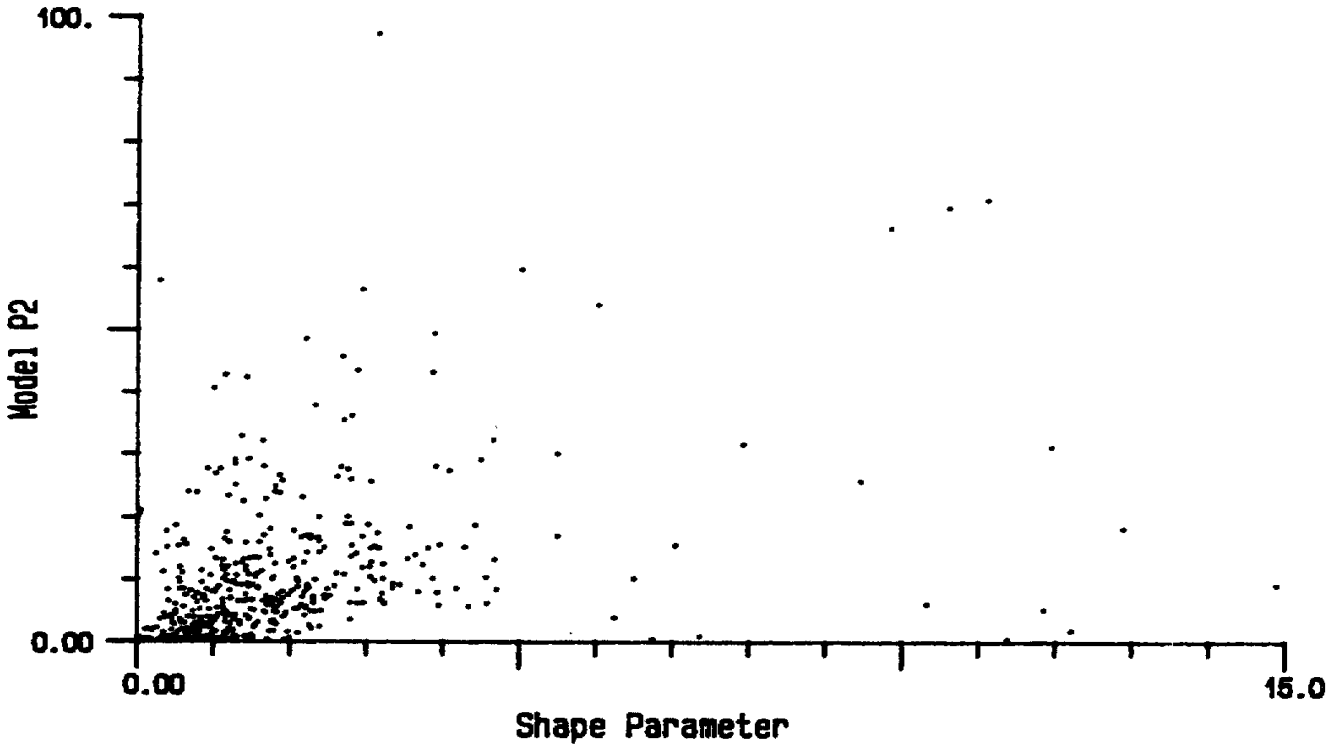

Fig. 27c Distribution of model P as a function of shape parameter $\lambda 1$(upper) and $\lambda 2$(lower)

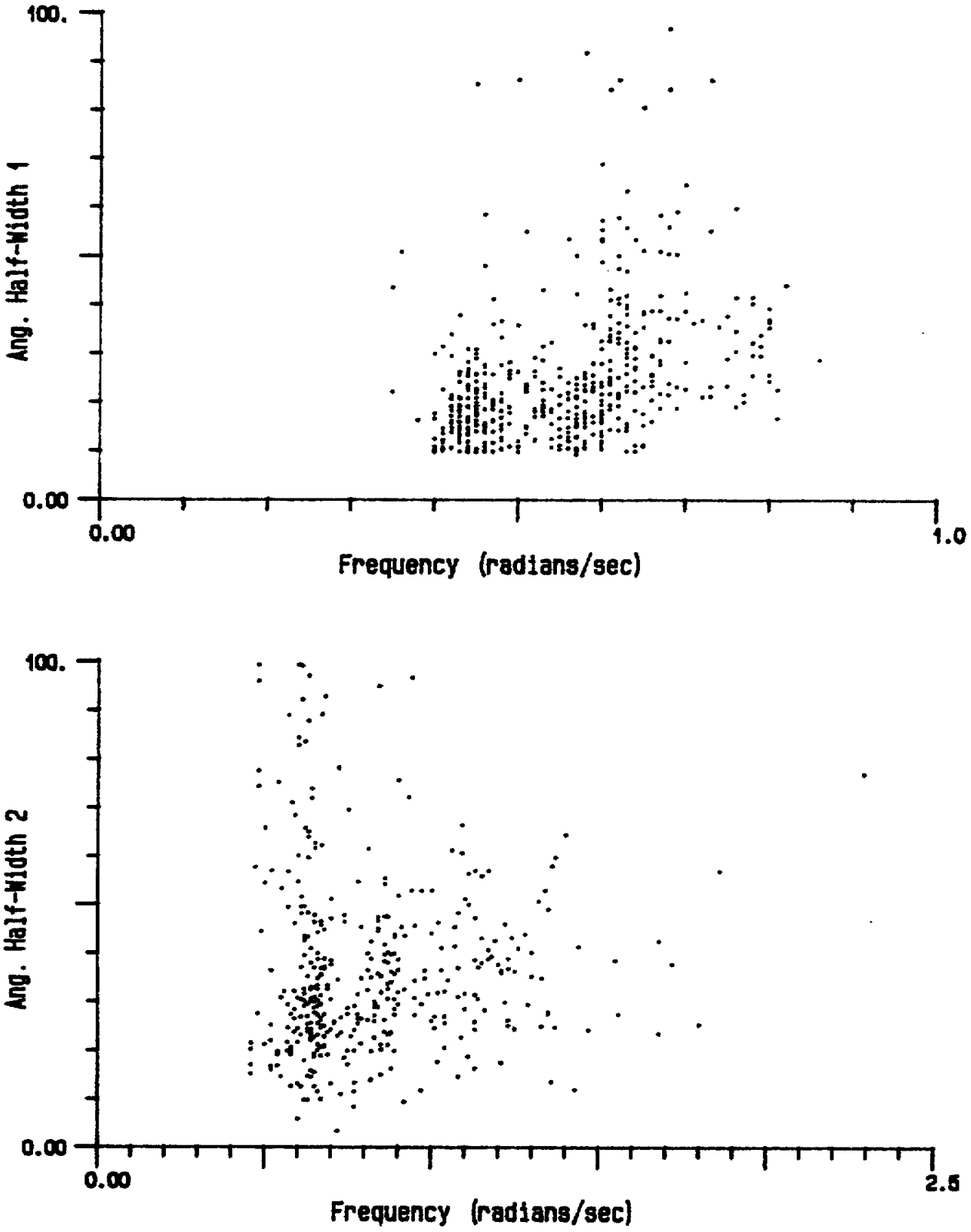

Fig. 28a Distribution of model angular halfwidth with model frequency ω_{m1} (upper) and ω_{m2} (lower)

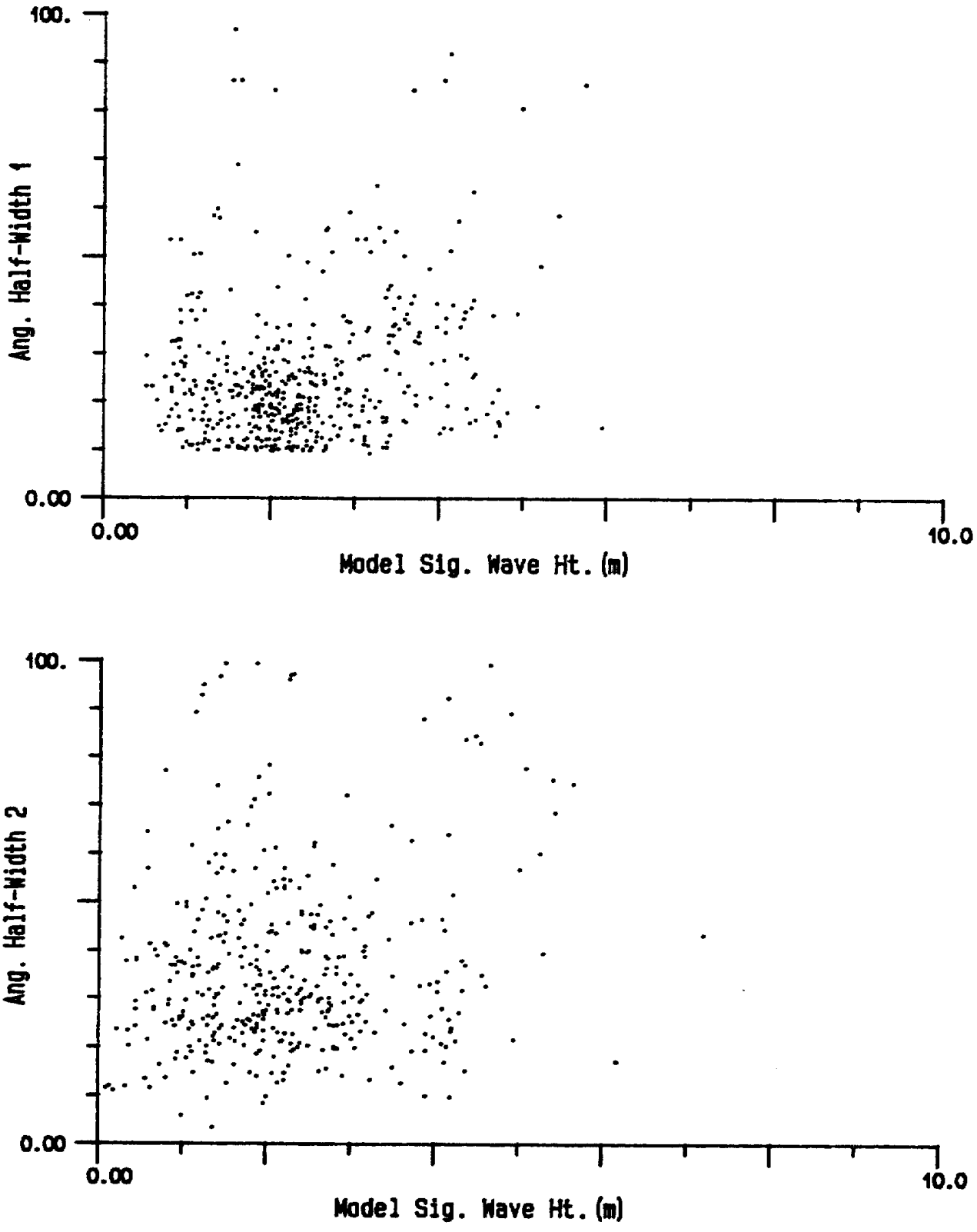

Fig. 28b Distribution of model angular halfwidth with sig. wave height $\delta 1$(upper) and $\delta 2$(lower)

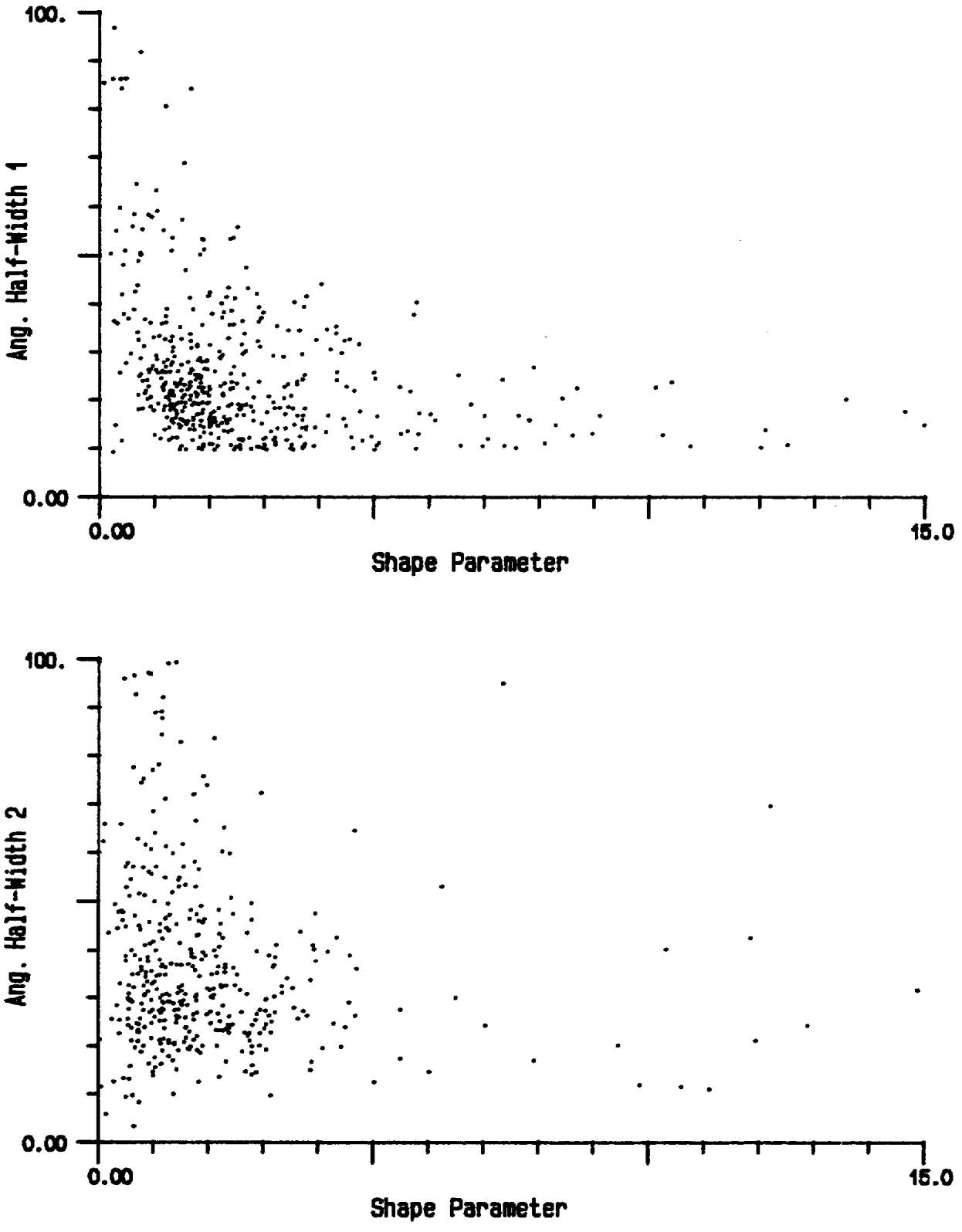

Fig. 28c Distribution of model angular halfwidth with shape parameter $\lambda 1$(upper) and $\lambda 2$(lower)

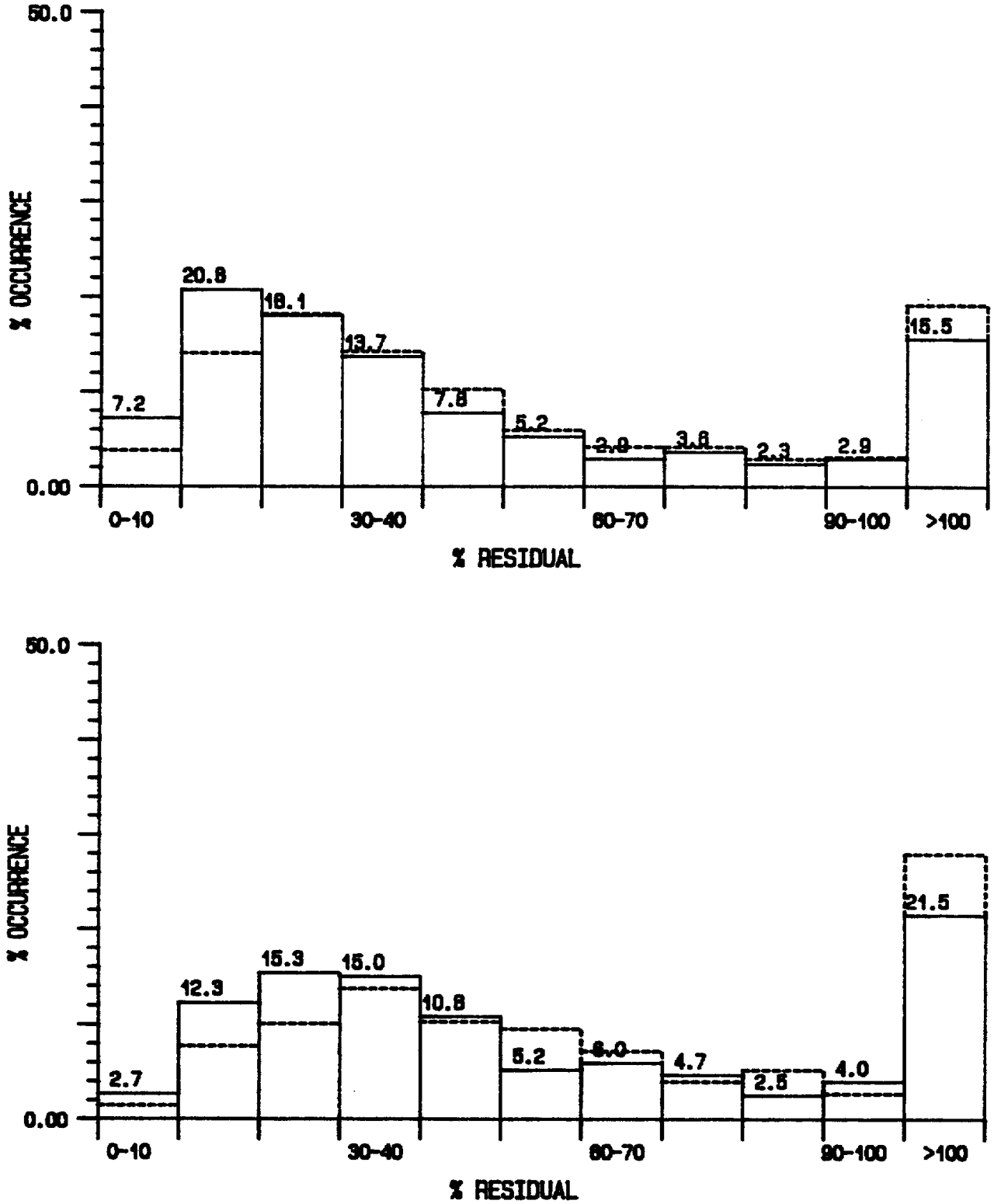

Fig. 29 Percent occurrence of RESD values for Level 2 (Set 2; Upper) and Level 4 (Lower) analyses using predicted P values. Solid (with) and dashed (without) 10% noise.

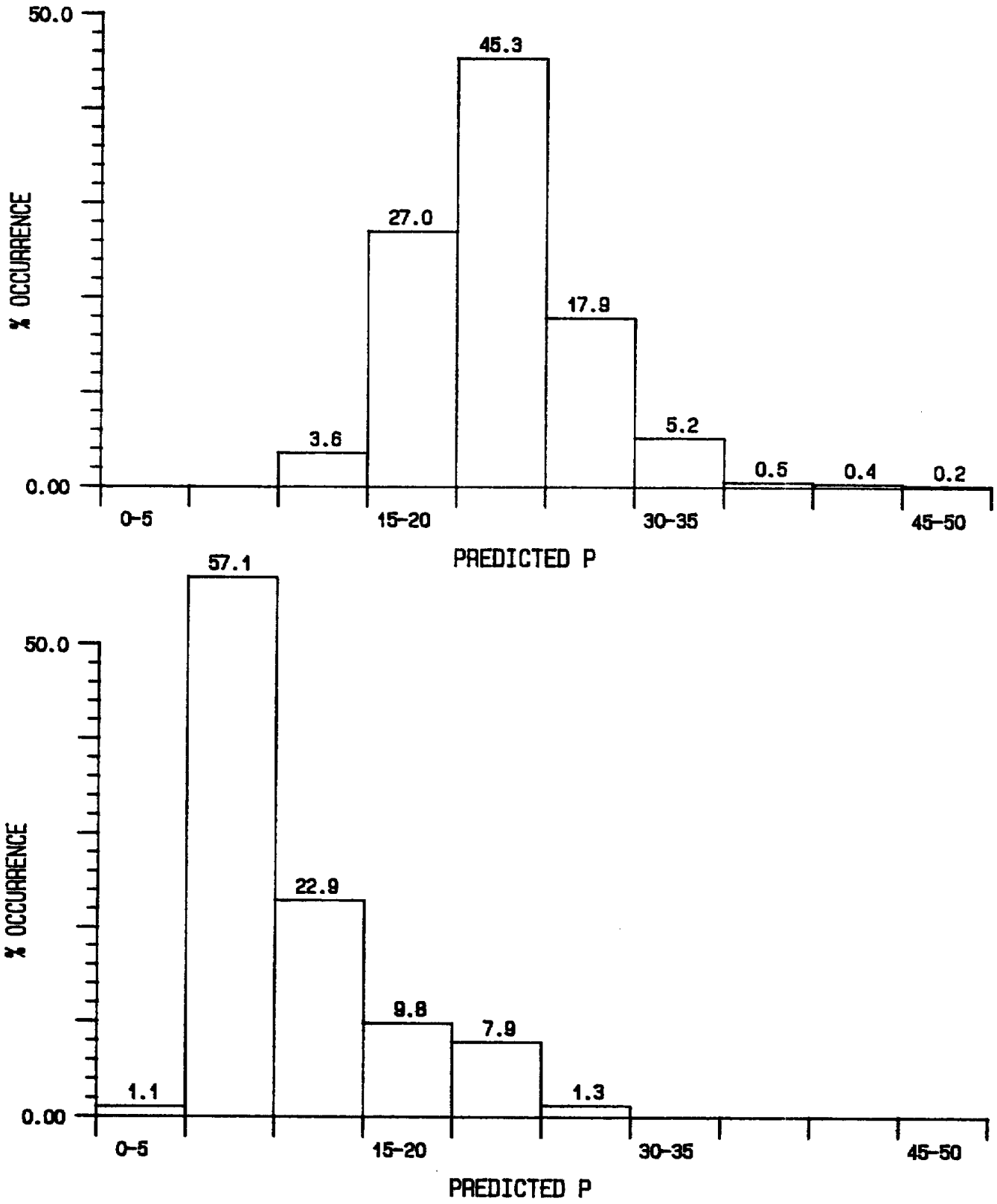

Fig. 30 Percent occurrence of predicted P
(upper: P1 , lower: P2)

A similar analysis was performed using the 10-parameter model values, with corrected significant wave height, and model P values and the angular half-widths measured in the model spectrum. The scatterplot of these P and angular half-widths, as a function of the other model parameters, are shown in Figs. 27 a , b and c and 28 a , b and c . There is still a considerable amount of scatter for both statistics. There does appear to be a slight relationship of P with the shape parameter (Fig. 27c) and of half-width with frequency (Fig. 28b).

Using the same conditions as for the earlier regression analysis, except rejecting records with RESD>20%, the formula could account for 71%, 59% and 58% (for 857 pts) of the variance in P. In this case, the shape parameters appear to be influencing the distribution of P as well as the frequency. The coefficient values were

A =	5.8087	OR	A = 8.1176	OR	A = 7.3321
B =	-1.5667		B = -1.2396		B = -1.2415
C =	-0.2328		C = -0.1264		
D =	0.5518				

Performing the regression on the angular half-widths, again limited to angles less than 1.745 radians, could explain 81%, 79% and 78% (on 852 pts) of the variance with

A =	0.6425	OR	A = 0.5790	OR	A = 0.6488
B =	0.6727		B = 0.6938		B = 0.4920
C =	0.2244		C = 0.2667		
D =	-0.1654				

The regression results for P indicate that, for the 10-parameter fit, the heave related parameters are being adjusted somewhat to compensate for the directional component. The functional relationships for the six-parameter and fitted P and the 10-parameter expression are, therefore, not readily exchangeable. As seen earlier, the angular half-widths are better behaved than the P values.

Using the regression equation

$$P_i = 10.1602 * \omega m_i^{-1.498} \delta_i^{1.588E-2}$$

the Level 2 (with SET 2 values for D) and the Level 4 analysis (P1 and P2 allowed to vary between records but kept constant with frequency) were re-performed with the predicted P1 and P2 values. The corresponding RESD values are shown in Fig. 29 . Again, adding some noise improves the fit. If one compares these results with those using the fitted P1 and P2 (Figs. 13 and 17), the RESD values are poorer than those for the fitted P though similar to Level 3 results (with

P1=20 and P2=7.5). This is explained if one compares the distribution of predicted P values, Fig. 30 and the measured P values, Fig, 11a . as the range of predicted P values is limited.

Appendix 3 contains illustrative contour plots (labelled G) for the directional spectra using the OH model heave energy and the above predicted P1 and P2 values. The P values were allowed to vary with frequency and 10% noise was added.

8. DISCUSSION

The objective of this study was to derive a simple parameterization of the directional wave spectrum using the minimum number of parameters while still accurately portraying the energy distribution in frequency and direction. The approach taken was to extend the Ochi and Hubble (1976) six-parameter amplitude model to include various representations of the directional component through the use of a mean direction and directional spread parameter. In Section 3 , it was shown that the Ochi and Hubble model provided a very good representation of the amplitude spectra that could be used as the foundation. In Section 4 , the baseline (ie, lowest possible) WXS and RESD error statistics were calculated and the latter chosen to provide the best assessment tool. It was noted that the COS2P-FIT directional model, based on the MJ spectrum, was superior to the COS2P-LH model which is a standard model established in the oceanographic literature and that understanding the background noise contribution to the overall energy is important in order to reduce fit errors. In Section 5 , increased restrictions were placed on the direction model parameters and corresponding increases in the RESD error occurred. In Section 6 , a full 10-parameter model fit was performed on the directional spectra and this parameterization provided the lowest RESD values, could accurately describe over 85% of the data spectra encountered and often properly handle bi-modal spectra. In Section 7 , a functional form to predict the directional spread parameter from the heave parameters was established and it was found that the frequency was the prime determining variable. The nature of the scatter in P, weighted the regression such that the prediction formula cannot reproduce the large range in P values that are observed. Prediction of the angular half-widths appeared to be better but the amount of scatter is still significant. From numerous observations, an RESD value of between 20 and 30% appeared to be an appropriate rejection criteria.

The results of the study are summarized in Table 2 . 10% noise has been included in the Level 2, 3, 4 and regression models. The 10-parameter model, in terms of both storage requirements and the low RESD values, is obviously the best candidate to represent the wave

spectrum. As there is no explicit variation of the spread P with frequency nor direct incorporation of background noise, factors examined in the Level 2 through 4 parameterization, the six "heave" parameters must be adjusting in order to compensate for these features which are known to be present in the real data spectrum. The main limitation to this model is the time involved in performing the fit. If computer time is a problem, the best compromise would be to fit the COS2P-FIT direction model only to the distribution at ω_{m1} and ω_{m2} and generate a Level 2 spectrum. Use of the predicted P from the regression analysis was generally no better than using a constant P as the prediction equation only supplies a small range of P values.

TABLE 2. Summary of Results

MODEL	# OF STORED PARAMETERS	P VARIED WITH _	P VARIED BY RECORD	% OCC. OF RESD < 20%	% OCC. OF RESD < 30%
Data	N freq.X M dir.	-	-	-	-
Level 1	6 + N X 3	Y	Y	97.6	98.5
no noise	6 + N X 2	Y	Y	54.3	66.8
Level 2	10	Y	Y	40.1	55.9
Level 3	8	Y	N		
P1=10,P2=4		Y	N	26.9	48.0
P1=20,P2=7.5		Y	N	25.2	46.3
P1=40,P2=7.5		Y	N	12.8	27.2
Level 4					
Fitted P	10	N	Y	29.2	41.1
P1=10,P2=4	8	N	N	25.1	44.6
P1=20,P2=7.5	8	N	N	15.4	32.0
P1=40,P2=7.5	8	N	N	6.9	15.2
10-Parameter Model	10	N	Y	87.4	94.5
Regression					
Level 2	8	Y	Y	28.0	46.1
Level 4	8	N	Y	15.0	30.3

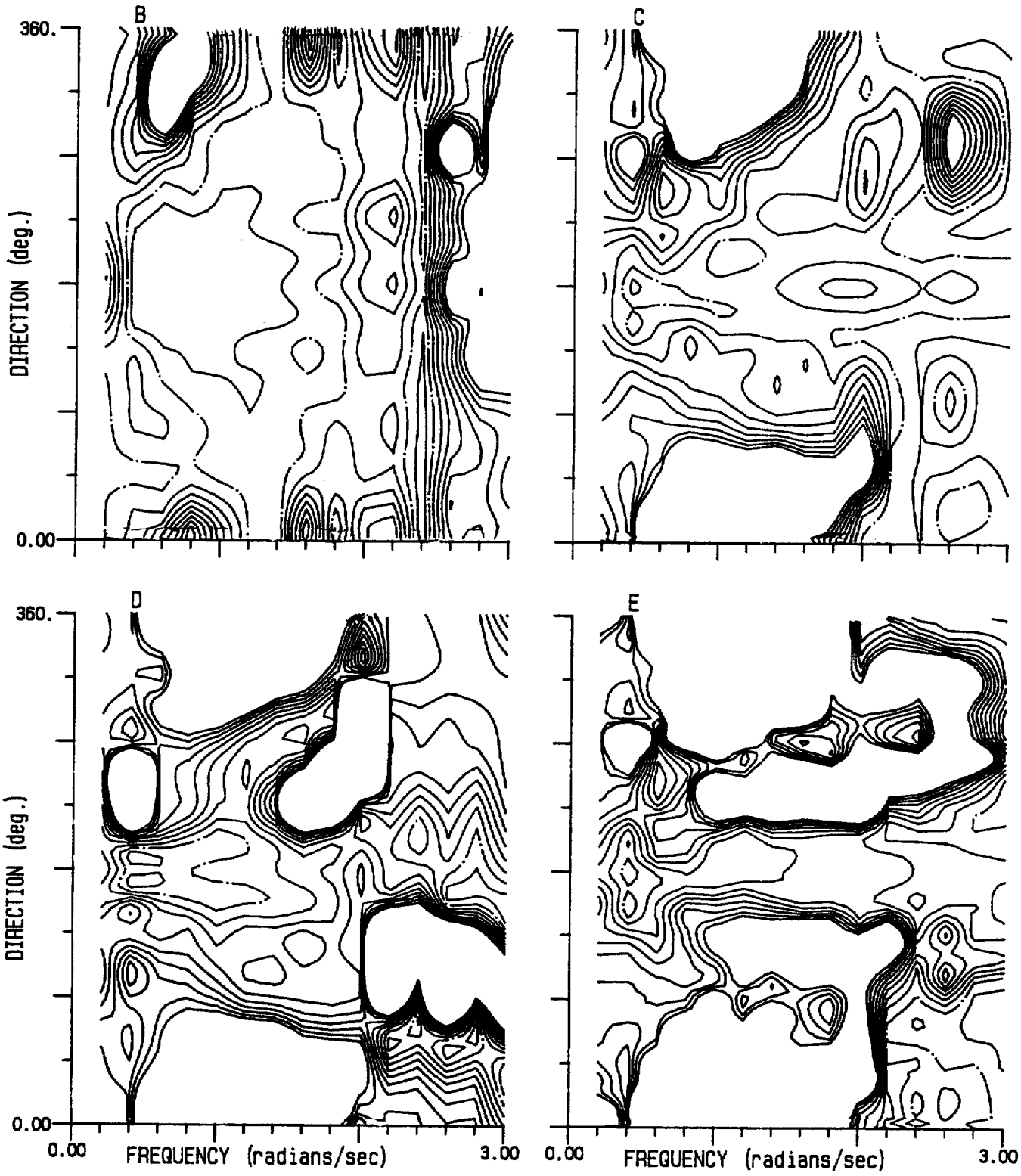

Fig. 31 Contoured residual squared for cases B to G. Contour intervals set to every 10% with the 20% contour dashed.

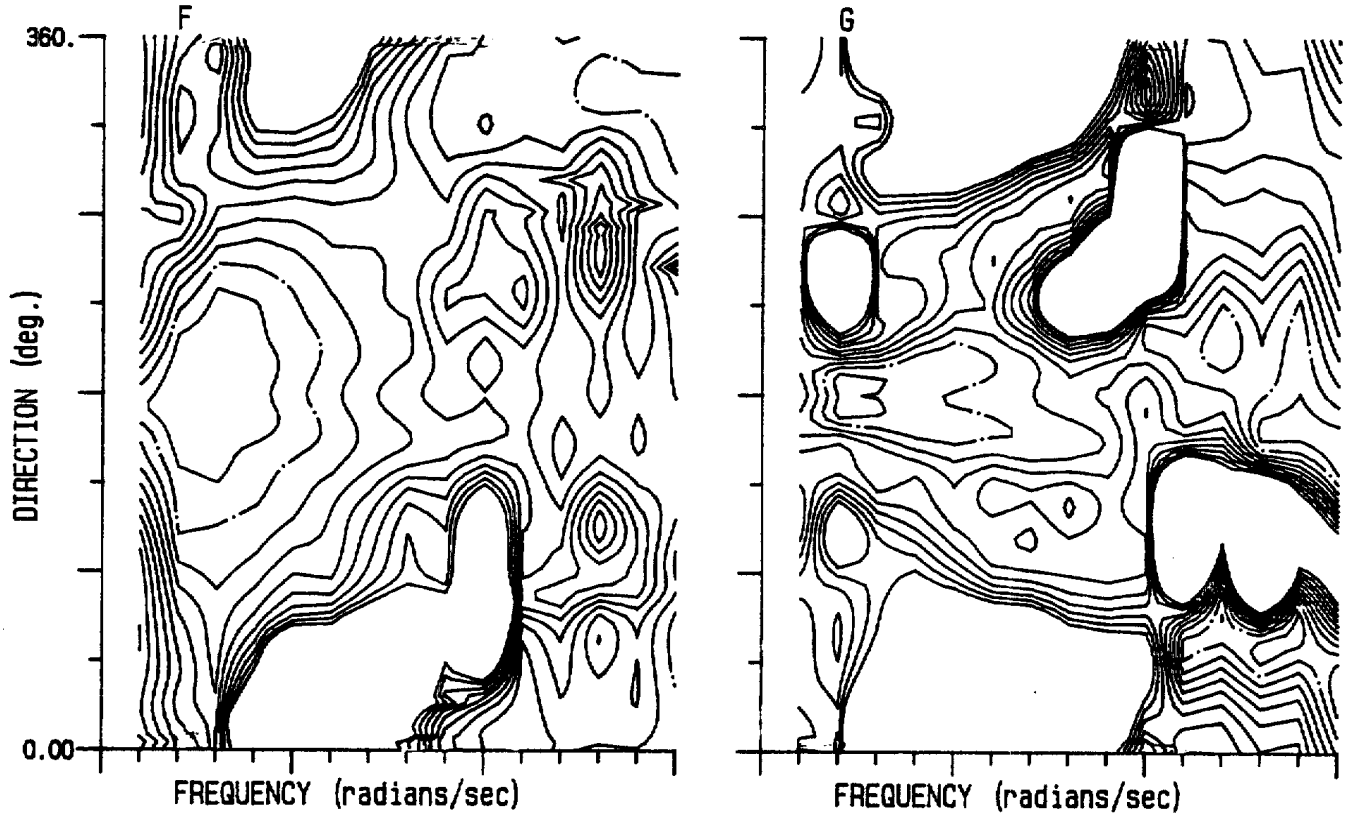

Fig. 31 (continued)

In order to assess the overall frequency/direction behavior about the peak, for cases illustrated in Appendix 3 , the residual squared error in each frequency and direction bin were calculated and summed over all records for which the 10 parameter model had RESD values less than 20%. This is an analysis similar to that performed on the OH model with respect to frequency shown in Fig. 5a . The contoured results are illustrated in Fig. 31 . The contour intervals were set to every 10% while the 20% contour is dashed. The labelling (B to G) is for consistency with Appendix 3 . The analysis was performed after centering the model and MJ data spectrum about the data peak direction at each frequency. This provides a common reference direction of 180 degrees for every record thereby permitting an error assessment in both frequency and direction about the energy peak. It is obvious that Plot B (Level 1) and Plot F (10-parameter model) provide the best fits in both frequency and direction. The increasing error in the directional modelling is implied by the encroachment of the large blank spaces (ie. >100% error) on the mean direction bin (ie. 180 degrees). Some error will be introduced by the presence of bi-modal spectra at low and high frequencies. As in Fig. 5a , large errors at the extremes of frequency and direction may be a result of large relative though small absolute errors in regions of low energy.

All of the results indicate that the 10-parameter model is the best candidate for a simple parameterization of a sometimes complex directional wave spectrum.

9. REFERENCES

Hasselmann D.K., M. Dunckel and J.A. Ewing, 1980. Directional wave spectra observed during JONSWAP 1973. J. Phys. Ocean. 10: 1264-1284.

Hogben N. and F.C. Cobb, 1986. Parametric modelling of directional wave spectra. Presented at the offshore Technology Conference in Houston, Texas, May 5-8, 1986. Paper # 5212, P 489-498.

Juszko B.-A., 1988. Comparison of directional wave spectra. Contractor Report to the Environmental Studies Revolving Fund, Canadian Oil, Gas and Lands Administration. Report #099. 227pp.

Juszko B.-A., 1989. High resolution of the directional wave field on the Grand Banks. Contractor Report SSC File No. 52SS-FP802-7-2719. Unpub. Manuscript.

Long R.B., 1980. The statistical evaluation of the directional spectrum estimates derived from pitch/roll buoy data. J. Phys. Ocean. 10: 944-952.

Longuet-Higgins M.S., D.E. Cartwright and N.D. Smith, 1963. Observations of the directional spectrum of sea waves using the motion

of a floating buoy. In: Ocean Wave Spectra. Prentice-Hall, Englewood Cliffs, N.Y. P 111-136.

Marsden R.F. and B.-A. Juszko, 1987. An eigenvector method for the calculation of directional spectra from heave, pitch and roll buoy data. J. Phys. Ocean. 17: 2157-2167.

Ochi M.K. and E.N. Hubble, 1976. Six-parameter wave spectra. In: Proceedings of the 15th Coastal Engineering conference, Honolulu, Hawaii, P 301-328.

Oltman-Shay J. and R.T. Guza, 1984. A data-adaptive ocean wave directional spectrum estimator for pitch and roll type measurements. J. Phys. ocean. 14: 1800-1810.

Press W.H., B.P. Flannery, S.A. Teukolsky and W.T. Vetterling. 'Numerical Recipes. The Art of Scientific Computing'. 1986. Cambridge University Press, Cambridge. 818pp.

10. ACKNOWLEDGEMENTS

This work was supported by a Department of Supply and Services Contract No. W7707-8-1049/01-OSC, Special thanks to the Scientific Authority, Dr. Ross Graham of the Defense Research Establishment Atlantic, Dept. of National Defense, for his support and helpful comments through the course of this study.

APPENDIX 1. ALGORITHMS USED

SIX-PARAMETER MODEL

The six-parameter model of Ochi and Hubble is given by:

$$S(\omega) = \frac{1}{4} \sum_{I=1}^{2} \frac{\left(\frac{4\lambda_I + 1}{4}\ \omega m_I^4\right)^{\lambda_I}\ \delta_I^2\ e^{-\left(\frac{4\lambda_I+1}{4}\right)\left(\frac{\omega m_I}{\omega}\right)^4}}{\Gamma(\lambda_I)\omega^{4\lambda_I+1}}$$

where ωm represents the modal frequency, δ the significant wave height and λ a spectral shape parameter. The model consists of two parts and the treatment of each is similar.

Let $S(\omega) = S1(\omega) + S2(\omega)$, the fitting procedure requires the first derivatives of $Si(\omega)$ with respect to ωmi, δi and λi. To obtain these derivatives, the log of the model equation is taken and then differentiated. ie.

$$\begin{aligned} \mathrm{Ln}(S_I(\omega)) &= \mathrm{Ln}(1/4) + \lambda_I\, \mathrm{Ln}(\lambda_I + 1/4)(\omega m_I)^4 + 2\mathrm{Ln}\,\delta_I \\ &\quad -(\lambda_I + 1/4)(\omega m_I/\omega)^4 - \mathrm{Ln}\,\Gamma(\lambda_I) - (4\lambda_I + 1)\mathrm{Ln}(\omega) \end{aligned}$$

$$\begin{aligned} \mathrm{Ln}(S_I(\omega)) &= \mathrm{Ln}(1/4) + \lambda_I\, \mathrm{Ln}(\lambda_I + 1/4) + 4\lambda_I\, \mathrm{Ln}(\omega m_I) + 2\mathrm{Ln}\,\delta_I \\ &\quad -(\lambda_I + 1/4)(\omega m_I/\omega)^4 - \mathrm{Ln}\,\Gamma(\lambda_I) - (4\lambda_I + 1)\mathrm{Ln}(\omega) \end{aligned}$$

The derivatives in log space are:

$$\frac{\partial\, \mathrm{Ln}(S_I(\omega))}{\partial\, \omega m_I} = \frac{4\lambda_I}{\omega m_I} - (4\lambda_I + 1)\frac{\omega m_I^3}{\omega^4}$$

$$\frac{\partial\, \mathrm{Ln}(S_I(\omega))}{\partial\, \delta_I} = \frac{2}{\delta_I}$$

$$\begin{aligned} \frac{\partial\, \mathrm{Ln}(S_I(\omega))}{\partial\, \lambda_I} &= \mathrm{Ln}(\lambda_I + 1/4) + \frac{\lambda_I}{\lambda_I + 1/4} + 4\mathrm{Ln}(\omega m_I) - (\omega m_I/\omega)^4 \\ &\quad - 4\mathrm{Ln}(\omega) - \frac{\partial\, (\mathrm{Ln}\,\Gamma(\lambda_I))}{\partial \lambda_I} \end{aligned}$$

The required derivatives are then obtained knowing that

$$\frac{\partial\, S(\omega)}{\partial\, A_I} = S_I(\omega) * \frac{\partial(\mathrm{Ln}(S_I(\omega))}{\partial\, A_I}$$

10-PARAMETER MODEL

The 10-parameter model is a simple extension of the Ochi and Hubble model and given by:

$$M(\omega,\theta) = \frac{1}{4} \sum_{i=1}^{2} \frac{\left(\frac{4\lambda_i+1}{4}\,\omega m_i^4\right)^{\lambda_i} \delta_i^2\, e^{-\left(\frac{4\lambda_i+1}{4}\right)\left(\frac{\omega m_i}{\omega}\right)^4} * \cos^{2P_i}\left(\frac{\theta-\theta m_i}{2}\right)}{\Gamma(\lambda_i)\omega^{4\lambda_i+1}}$$

The fitting procedure was similar to that used on the OH model and the first derivatives of the heave parameters were identical. The first derivatives of the direction parameters used were:

$$\frac{\partial S_i(\omega)}{\partial P_i} = 1/4 * S_i(\omega) * \mathrm{Ln}(\cos^2(\theta-\theta m_i)/2)$$

$$\frac{\partial S_i(\omega)}{\partial \theta m_i} = 1/4 * S_i(\omega) * P_i * \sin((\theta-\theta m_i)/2) * (\cos^2(\theta-\theta m_i)/2)^{(P_i-0.5)}$$

APPENDIX 2. EXAMPLES OF HEAVE MODEL FIT

Solid Data spectrum

Dash OH model fit

Dotted Upper and Lower 95% confidence limits on the data spectrum

Indicated on the plots are day and time and RESH value of model fit. For each time, the original spectrum is on the left and the band-averaged spectrum is on the right.

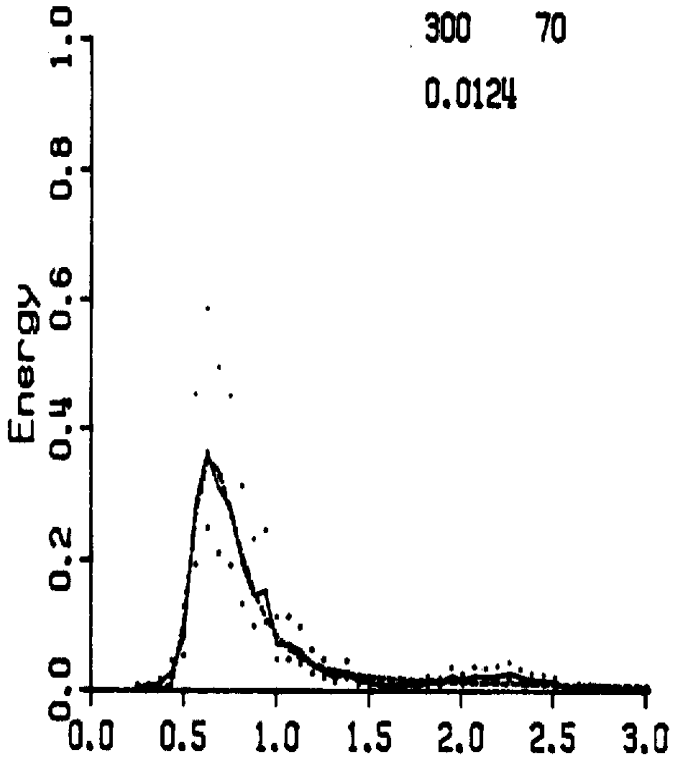
300 70
0.0124
Energy
0.0 0.2 0.4 0.6 0.8 1.0
0.0 0.5 1.0 1.5 2.0 2.5 3.0

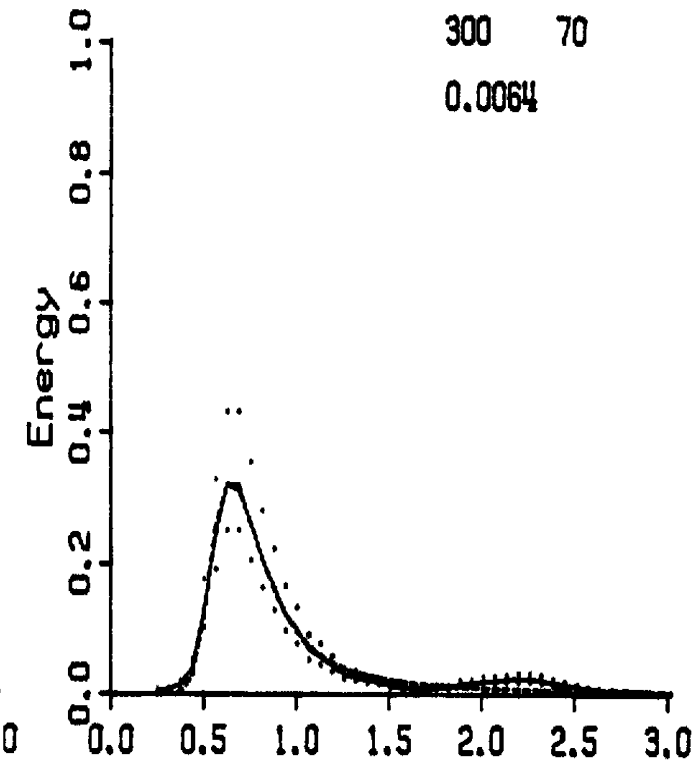
300 70
0.0064
Energy
0.0 0.2 0.4 0.6 0.8 1.0
0.0 0.5 1.0 1.5 2.0 2.5 3.0

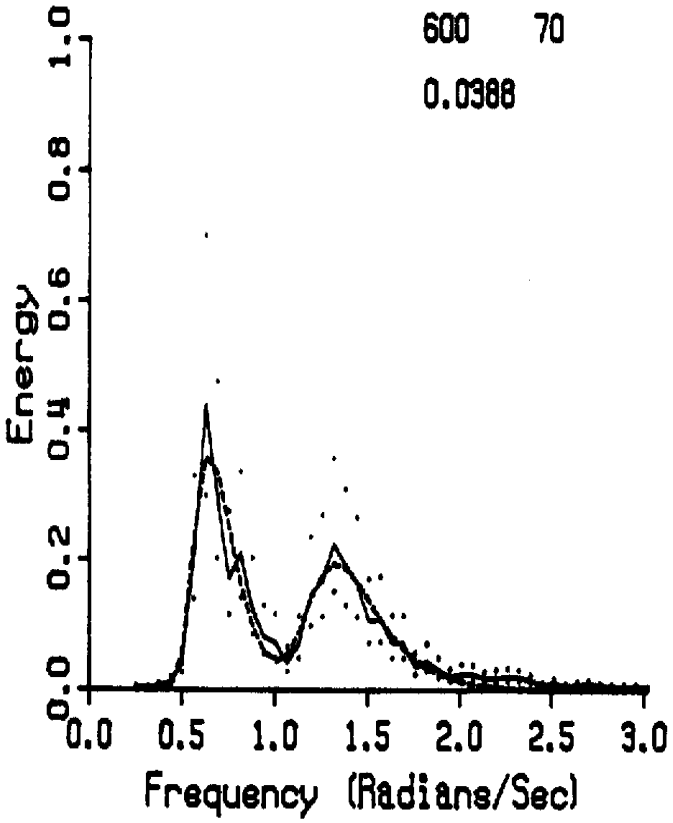
600 70
0.0388
Energy
0.0 0.2 0.4 0.6 0.8 1.0
0.0 0.5 1.0 1.5 2.0 2.5 3.0
Frequency (Radians/Sec)

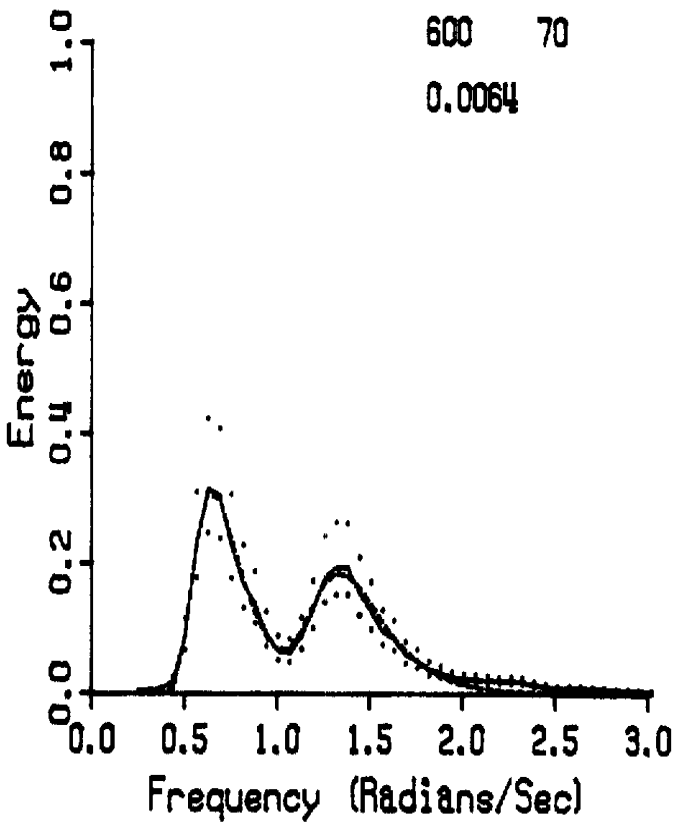
600 70
0.0064
Energy
0.0 0.2 0.4 0.6 0.8 1.0
0.0 0.5 1.0 1.5 2.0 2.5 3.0
Frequency (Radians/Sec)

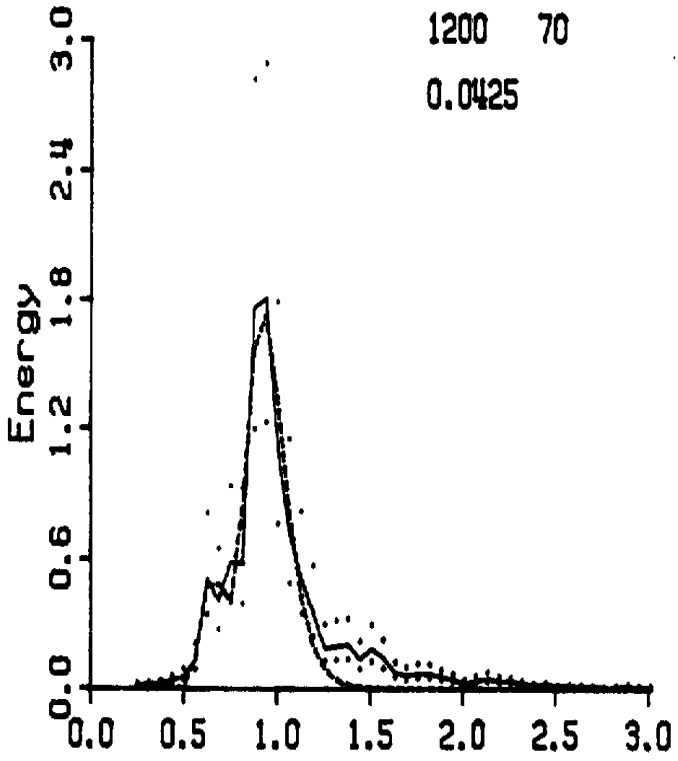
1200 70
0.0425
Energy
0.0 0.6 1.2 1.8 2.4 3.0
0.0 0.5 1.0 1.5 2.0 2.5 3.0

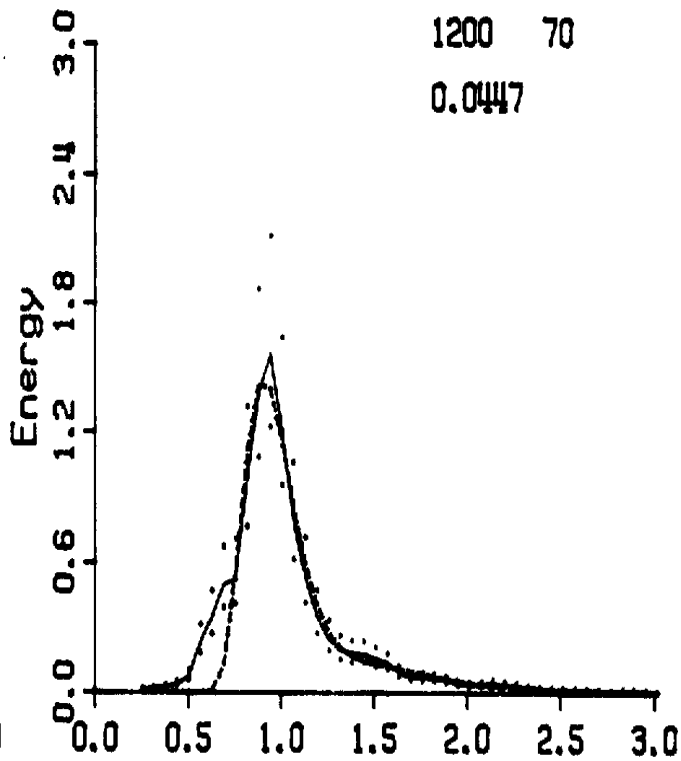
1200 70
0.0447
Energy
0.0 0.6 1.2 1.8 2.4 3.0
0.0 0.5 1.0 1.5 2.0 2.5 3.0

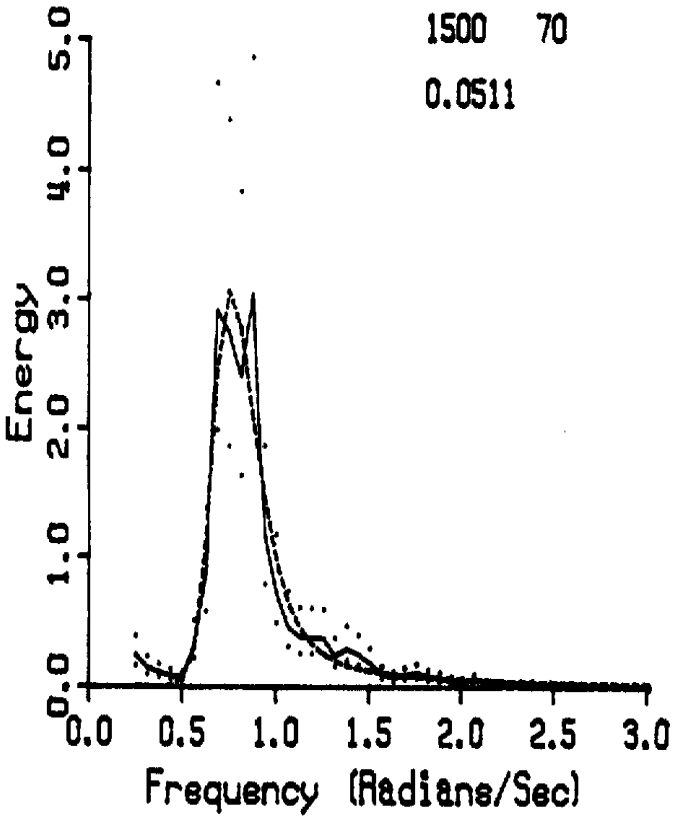
1500 70
0.0511
Energy
0.0 1.0 2.0 3.0 4.0 5.0
0.0 0.5 1.0 1.5 2.0 2.5 3.0
Frequency (Radians/Sec)

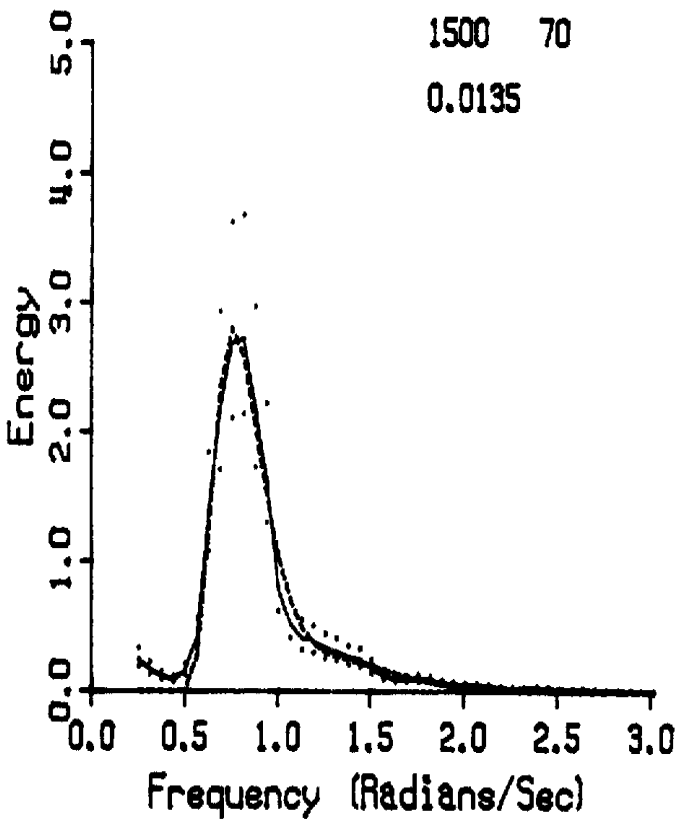
1500 70
0.0135
Energy
0.0 1.0 2.0 3.0 4.0 5.0
0.0 0.5 1.0 1.5 2.0 2.5 3.0
Frequency (Radians/Sec)

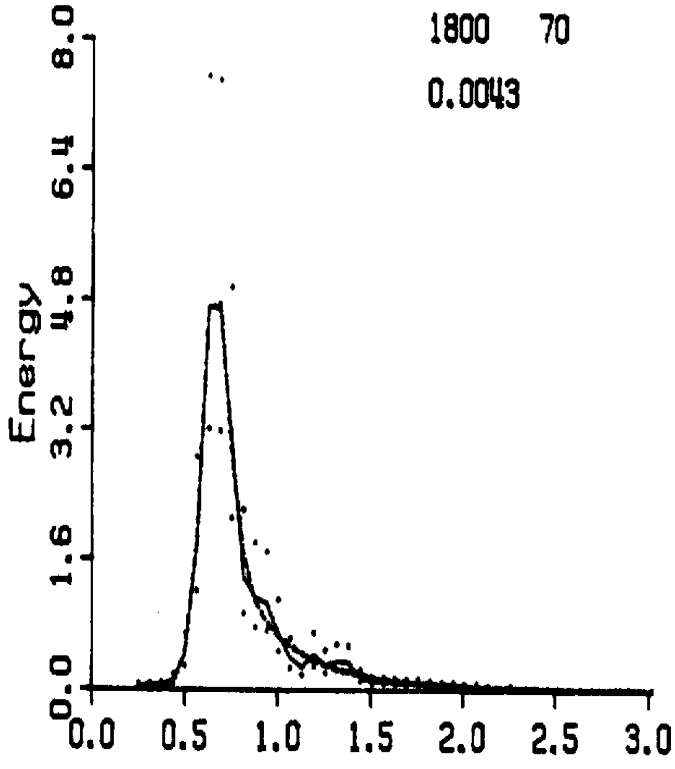
1800 70
0.0043
Energy
0.0 1.6 3.2 4.8 6.4 8.0
0.0 0.5 1.0 1.5 2.0 2.5 3.0

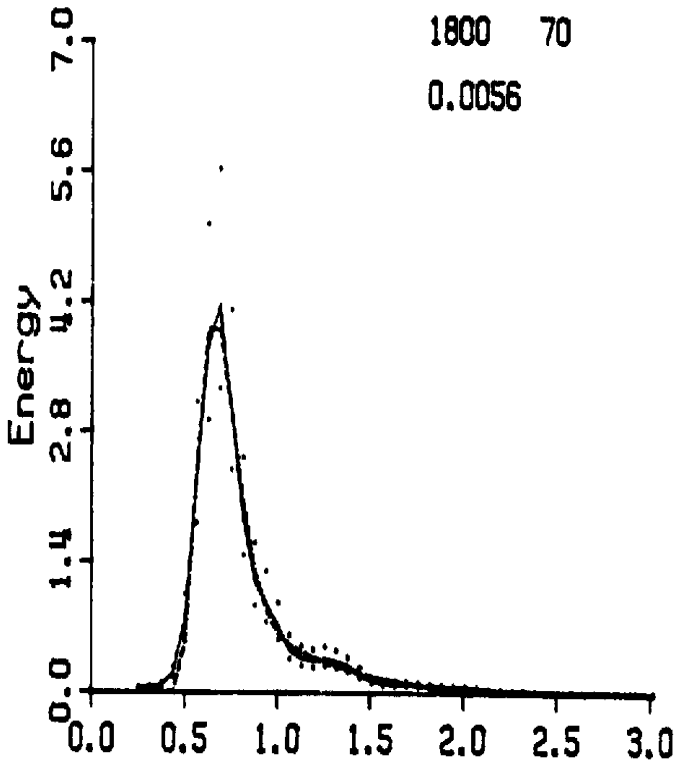
1800 70
0.0056
Energy
0.0 1.4 2.8 4.2 5.6 7.0
0.0 0.5 1.0 1.5 2.0 2.5 3.0

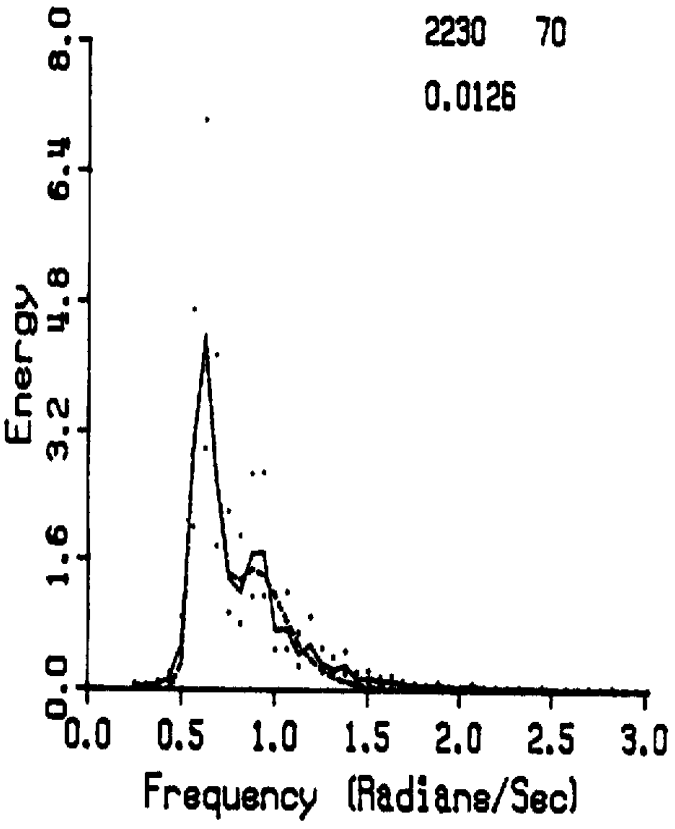
2230 70
0.0126
Energy
0.0 1.6 3.2 4.8 6.4 8.0
0.0 0.5 1.0 1.5 2.0 2.5 3.0
Frequency (Radians/Sec)

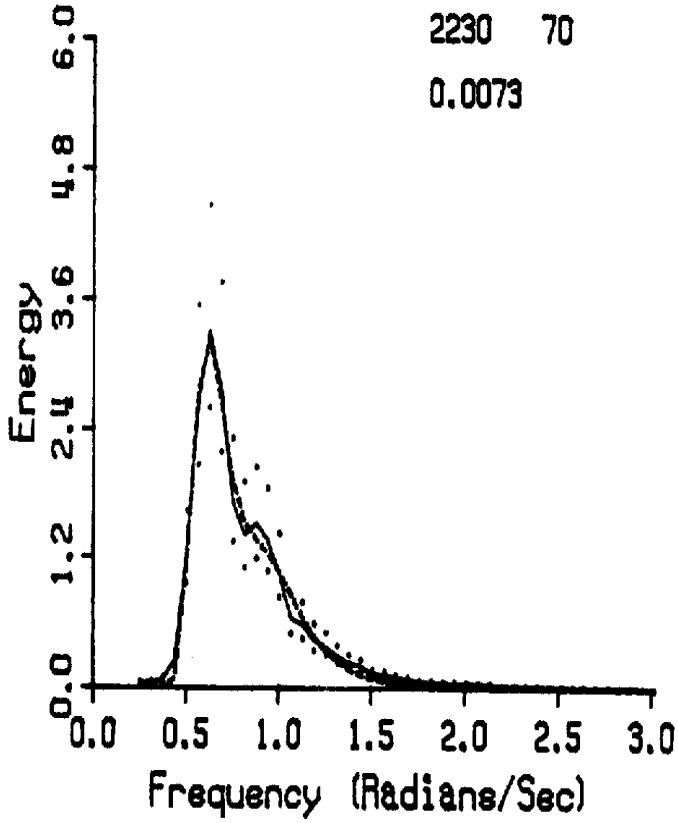
2230 70
0.0073
Energy
0.0 1.2 2.4 3.6 4.8 6.0
0.0 0.5 1.0 1.5 2.0 2.5 3.0
Frequency (Radians/Sec)

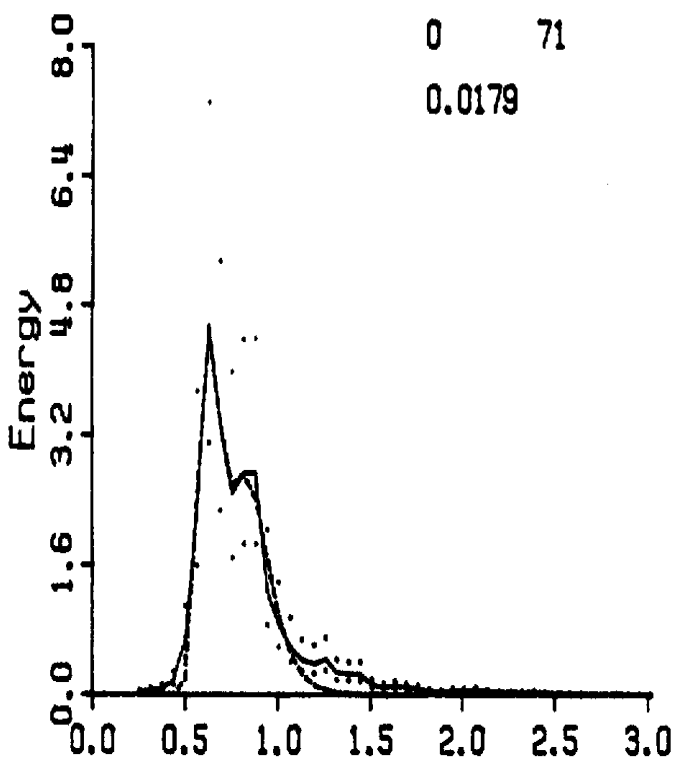
0 71
0.0179
Energy
0.0 1.6 3.2 4.8 6.4 8.0
0.0 0.5 1.0 1.5 2.0 2.5 3.0

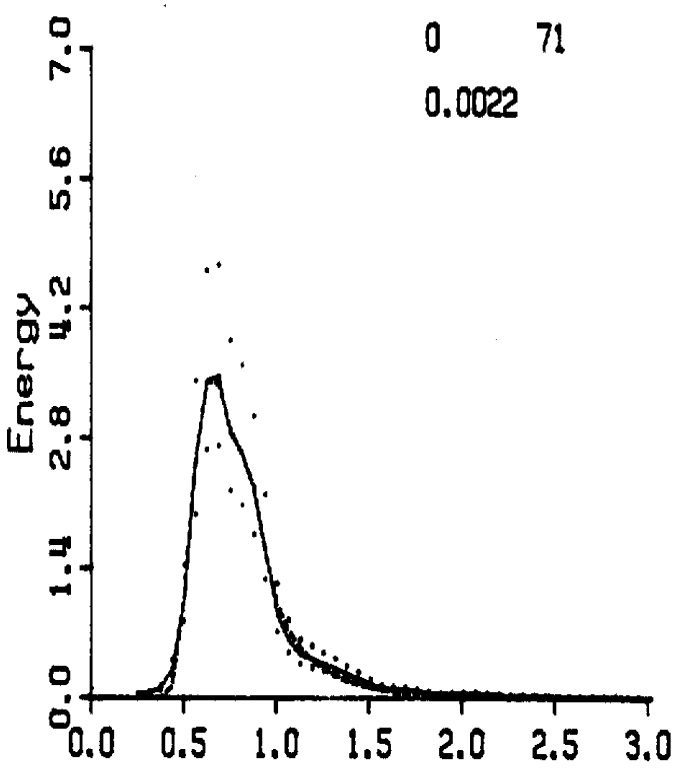
0 71
0.0022
Energy
0.0 1.4 2.8 4.2 5.6 7.0
0.0 0.5 1.0 1.5 2.0 2.5 3.0

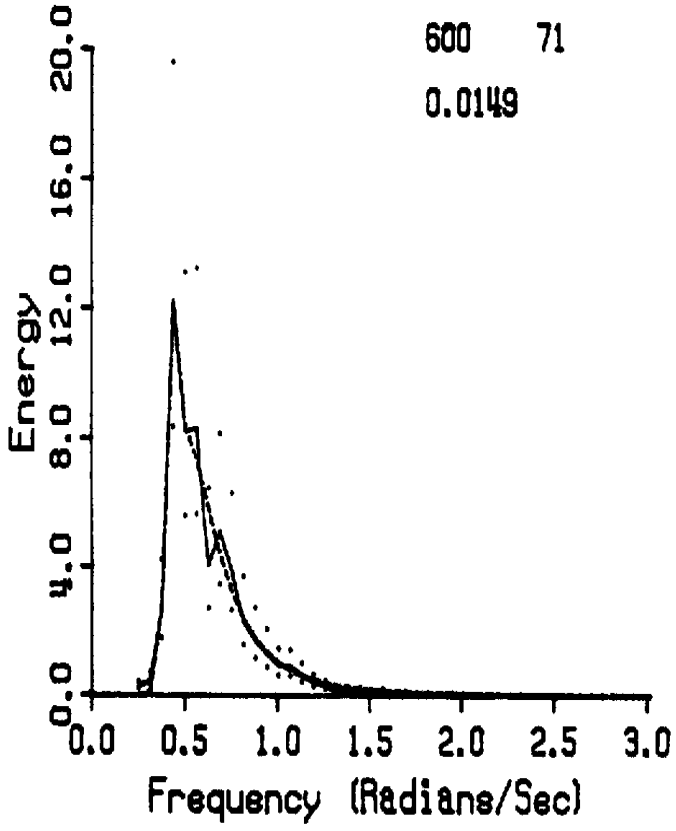
600 71
0.0149
Energy
0.0 4.0 8.0 12.0 16.0 20.0
0.0 0.5 1.0 1.5 2.0 2.5 3.0
Frequency (Radians/Sec)

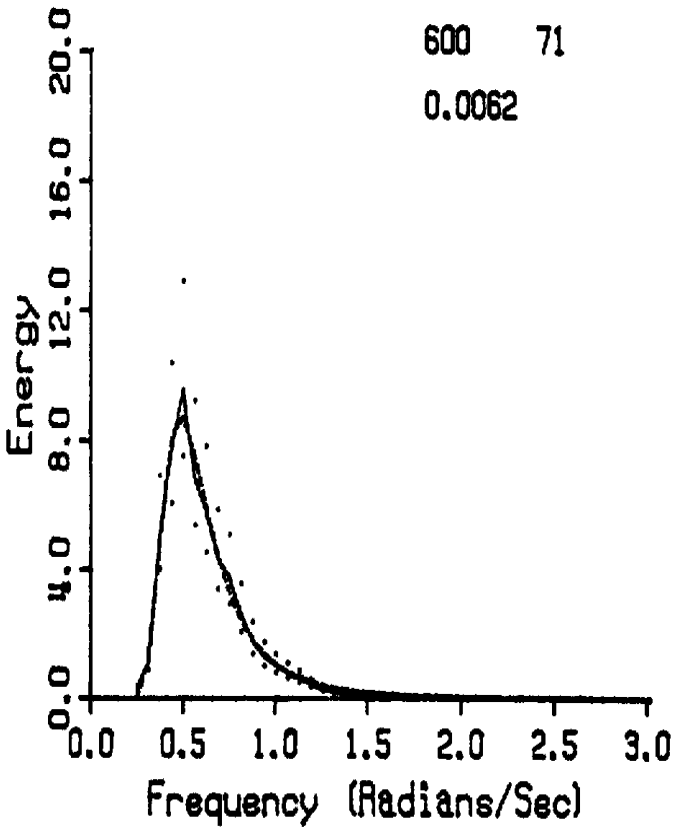
600 71
0.0062
Energy
0.0 4.0 8.0 12.0 16.0 20.0
0.0 0.5 1.0 1.5 2.0 2.5 3.0
Frequency (Radians/Sec)

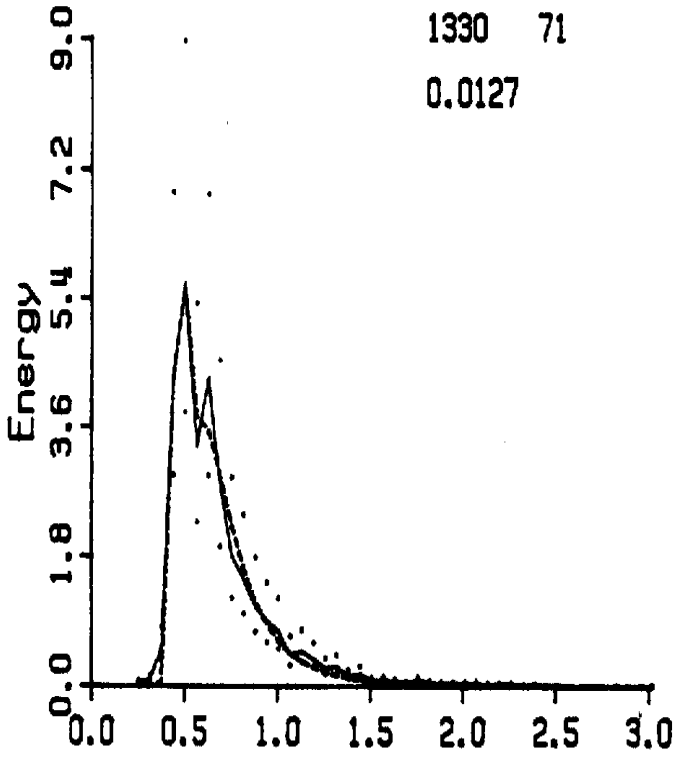
1330 71
0.0127
Energy
0.0 1.8 3.6 5.4 7.2 9.0
0.0 0.5 1.0 1.5 2.0 2.5 3.0

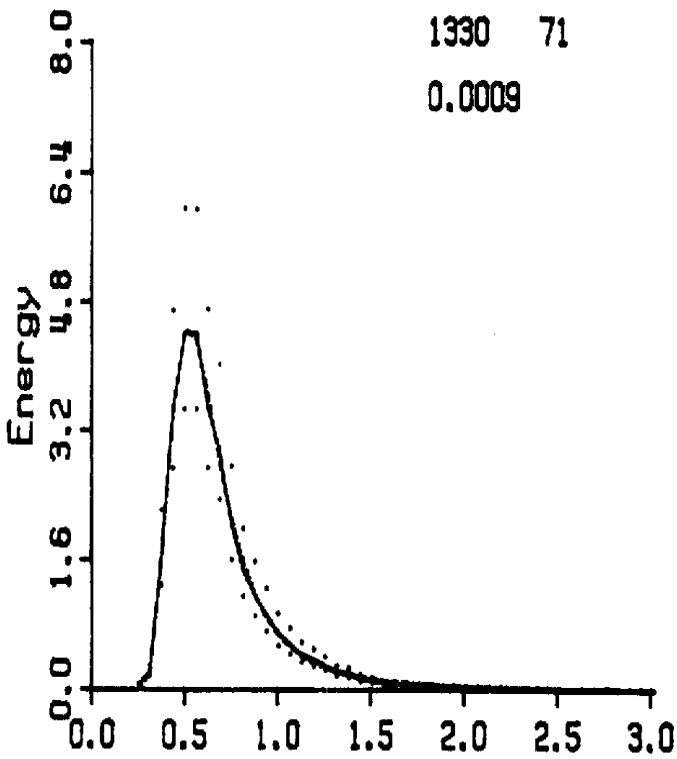
1330 71
0.0009
Energy
0.0 1.6 3.2 4.8 6.4 8.0
0.0 0.5 1.0 1.5 2.0 2.5 3.0

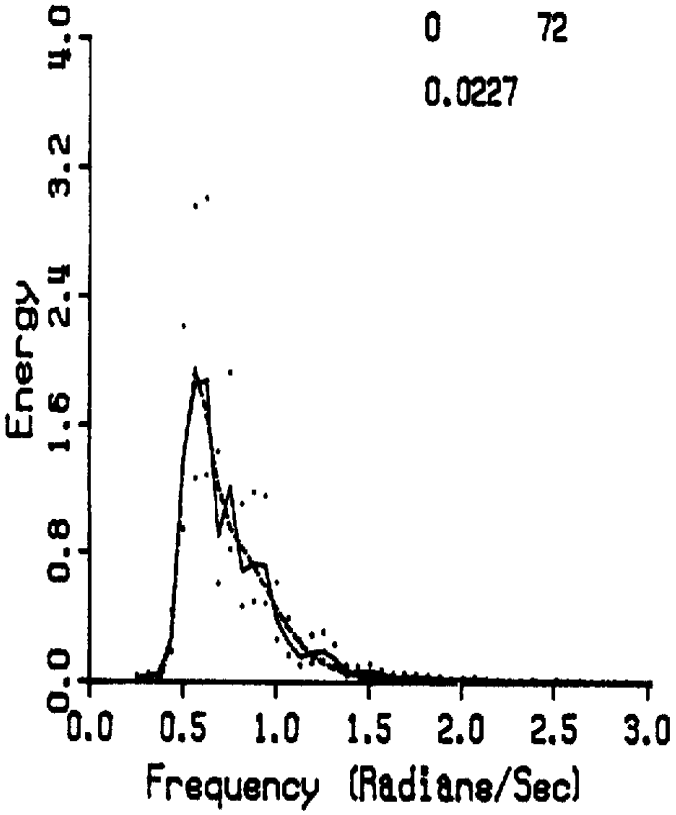
0 72
0.0227
Energy
0.0 0.8 1.6 2.4 3.2 4.0
0.0 0.5 1.0 1.5 2.0 2.5 3.0
Frequency (Radians/Sec)

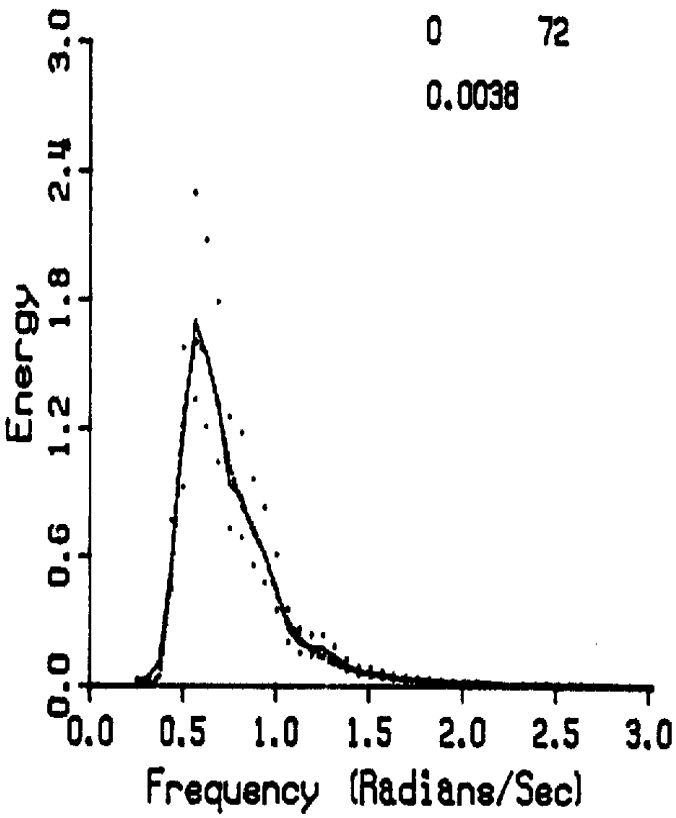
0 72
0.0038
Energy
0.0 0.6 1.2 1.8 2.4 3.0
0.0 0.5 1.0 1.5 2.0 2.5 3.0
Frequency (Radians/Sec)

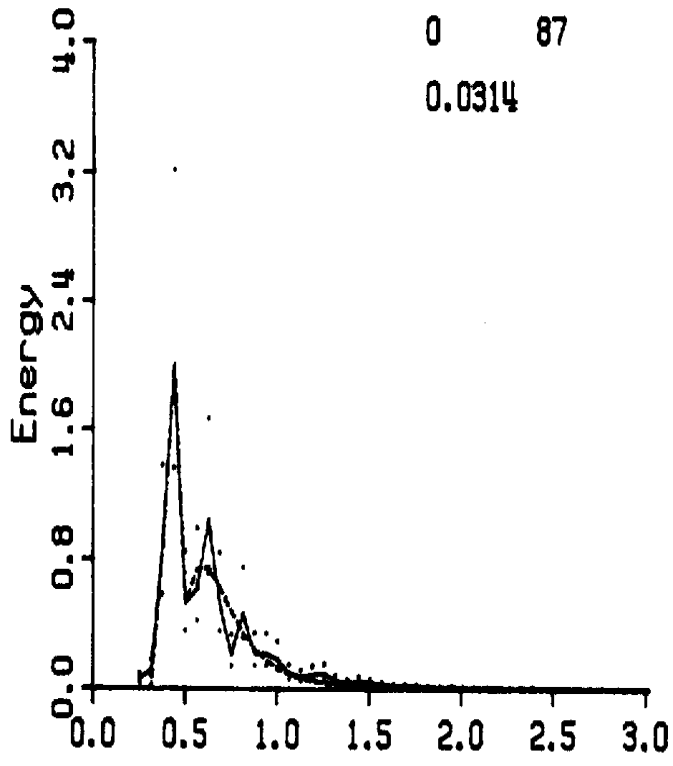
0 87
0.0314
Energy
0.0 0.8 1.6 2.4 3.2 4.0
0.0 0.5 1.0 1.5 2.0 2.5 3.0

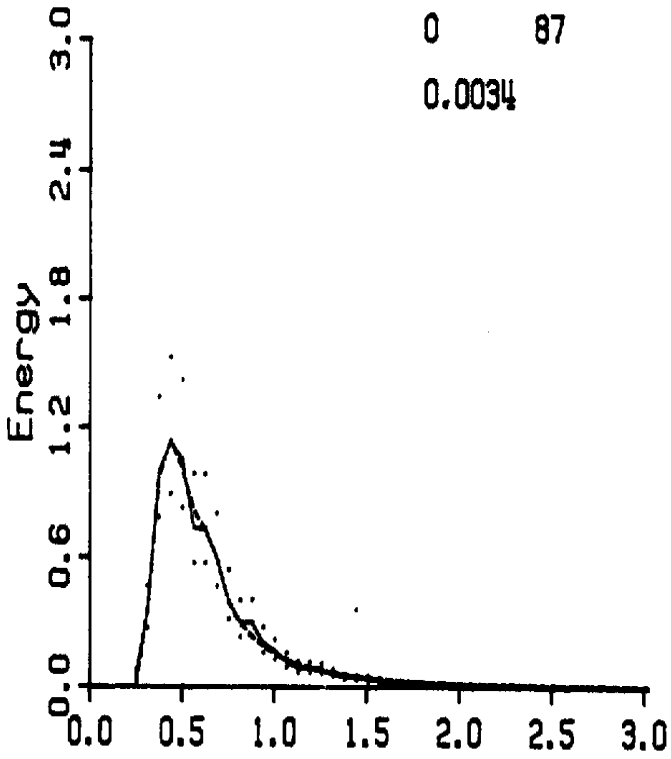
0 87
0.0034
Energy
0.0 0.6 1.2 1.8 2.4 3.0
0.0 0.5 1.0 1.5 2.0 2.5 3.0

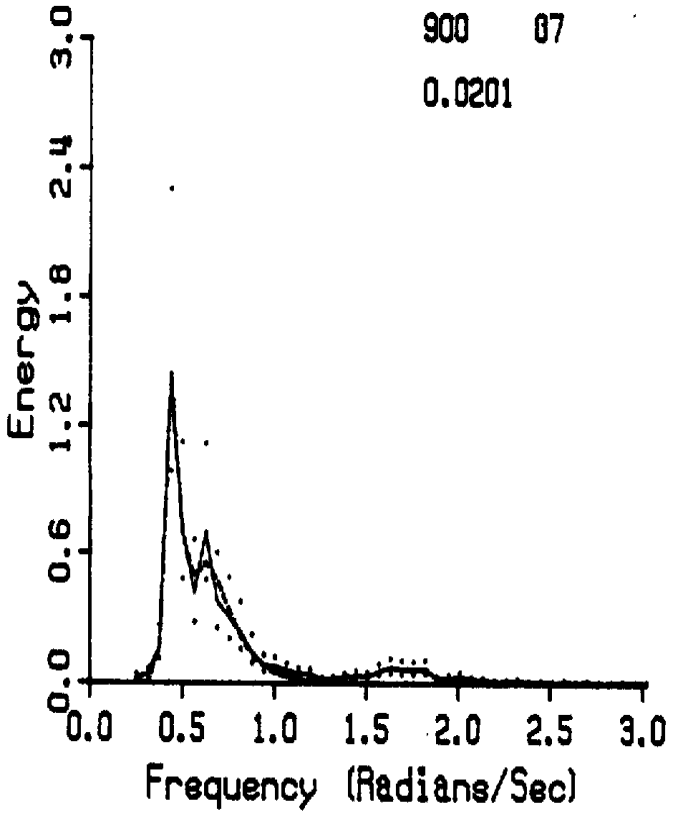
900 87
0.0201
Energy
0.0 0.6 1.2 1.8 2.4 3.0
0.0 0.5 1.0 1.5 2.0 2.5 3.0
Frequency (Radians/Sec)

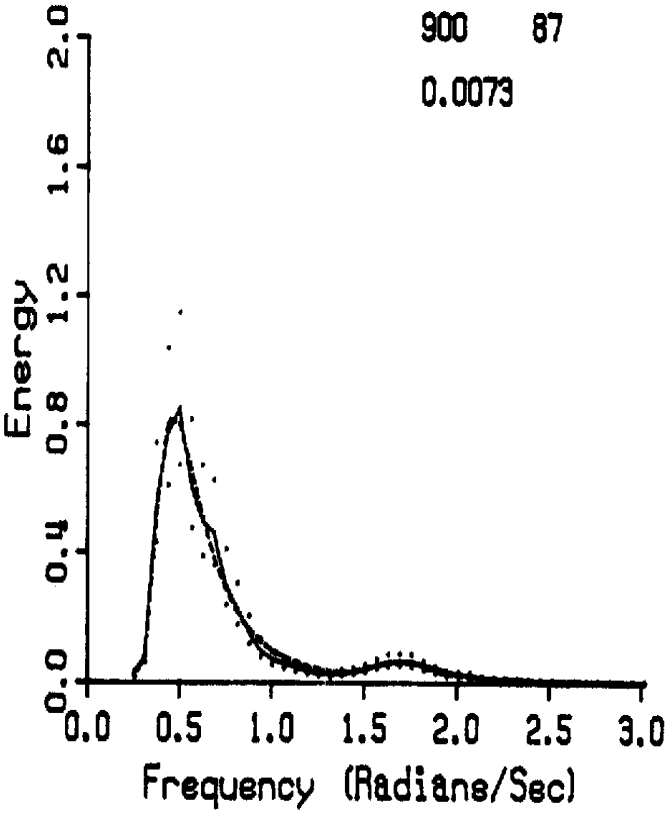
900 87
0.0073
Energy
0.0 0.4 0.8 1.2 1.6 2.0
0.0 0.5 1.0 1.5 2.0 2.5 3.0
Frequency (Radians/Sec)

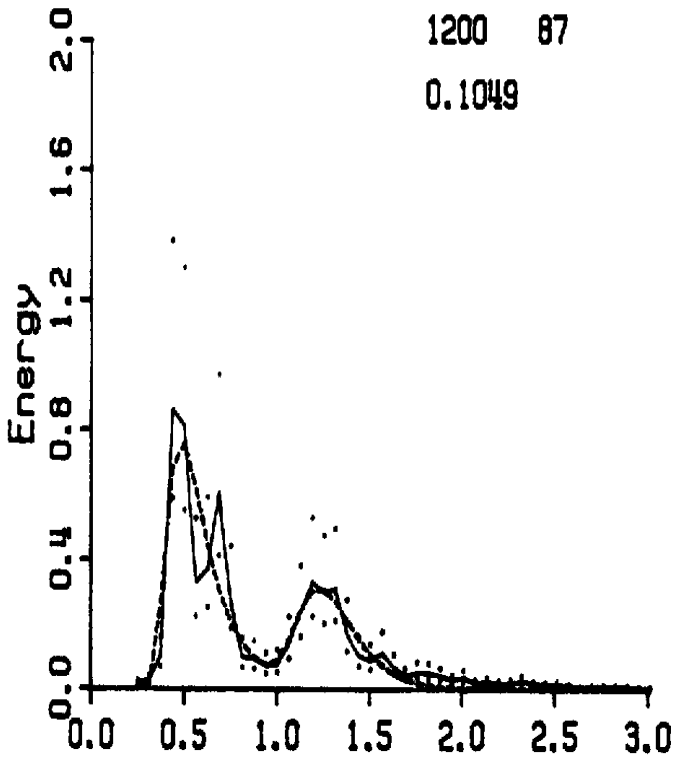
1200 87
0.1049
Energy
0.0 0.4 0.8 1.2 1.6 2.0
0.0 0.5 1.0 1.5 2.0 2.5 3.0

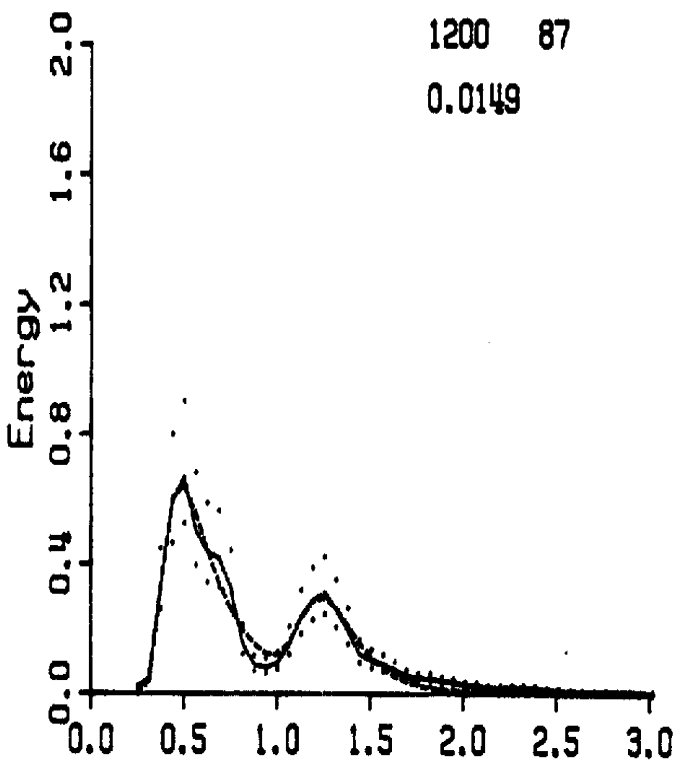
1200 87
0.0149
Energy
0.0 0.4 0.8 1.2 1.6 2.0
0.0 0.5 1.0 1.5 2.0 2.5 3.0

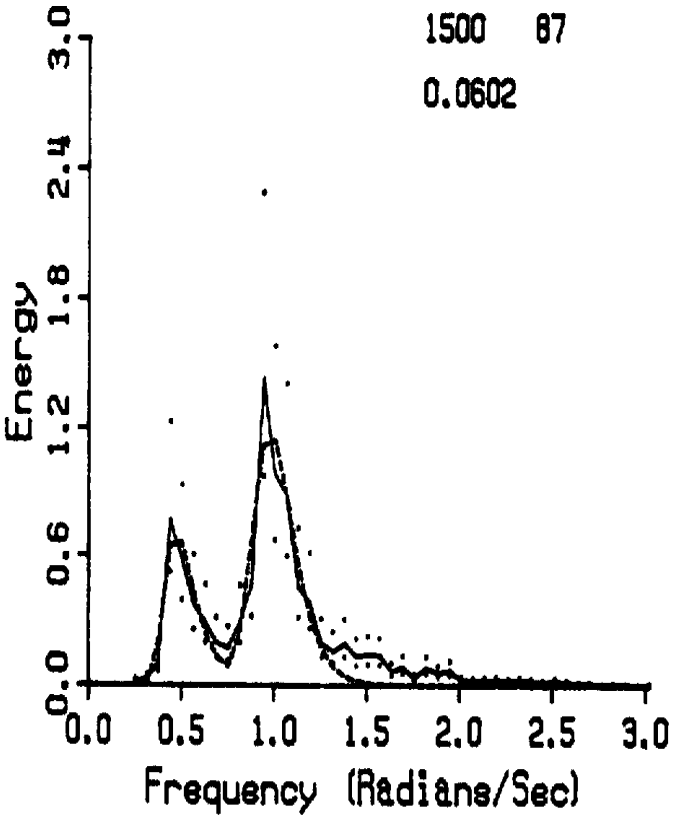
1500 87
0.0602
Energy
0.0 0.6 1.2 1.8 2.4 3.0
0.0 0.5 1.0 1.5 2.0 2.5 3.0
Frequency (Radians/Sec)

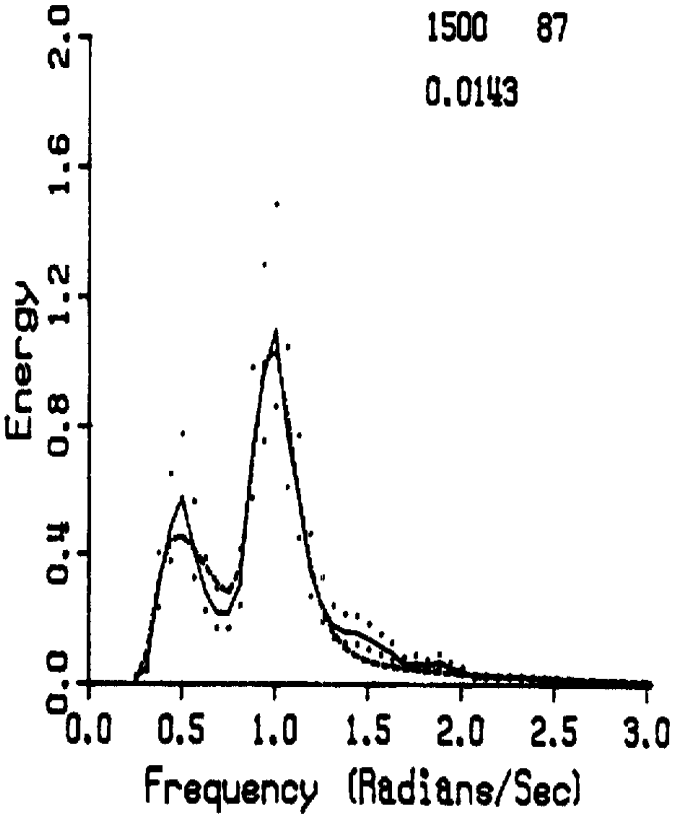
1500 87
0.0143
Energy
0.0 0.4 0.8 1.2 1.6 2.0
0.0 0.5 1.0 1.5 2.0 2.5 3.0
Frequency (Radians/Sec)

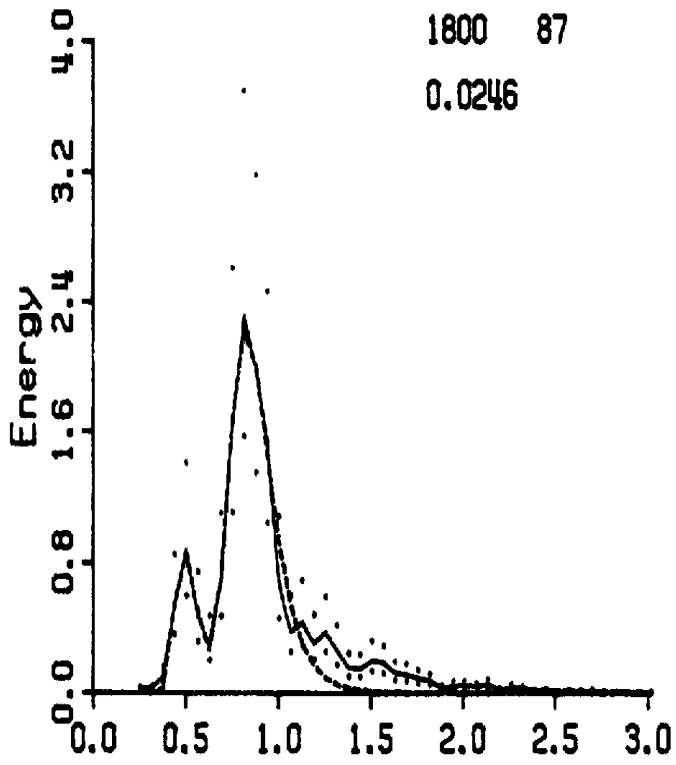
1800 87
0.0246
Energy
0.0 0.8 1.6 2.4 3.2 4.0
0.0 0.5 1.0 1.5 2.0 2.5 3.0

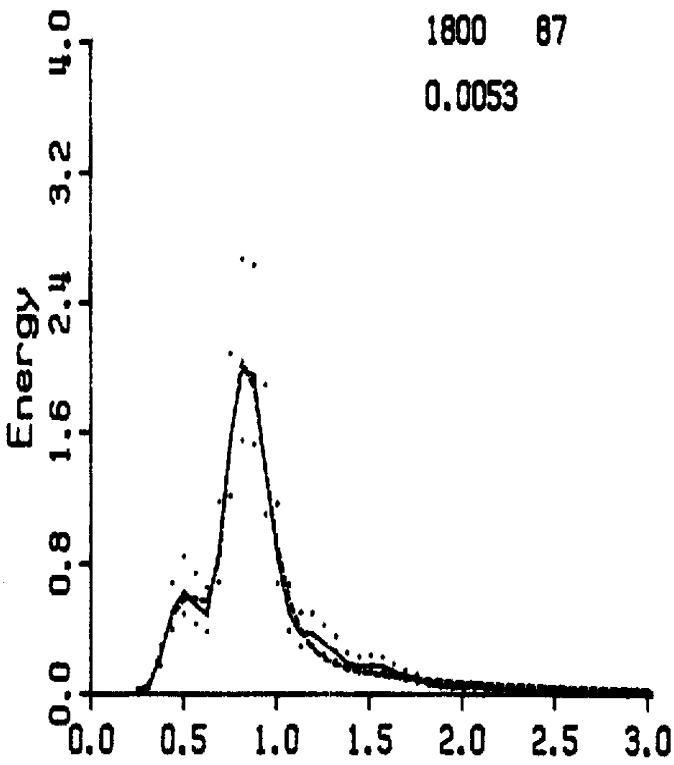
1800 87
0.0053
Energy
0.0 0.8 1.6 2.4 3.2 4.0
0.0 0.5 1.0 1.5 2.0 2.5 3.0

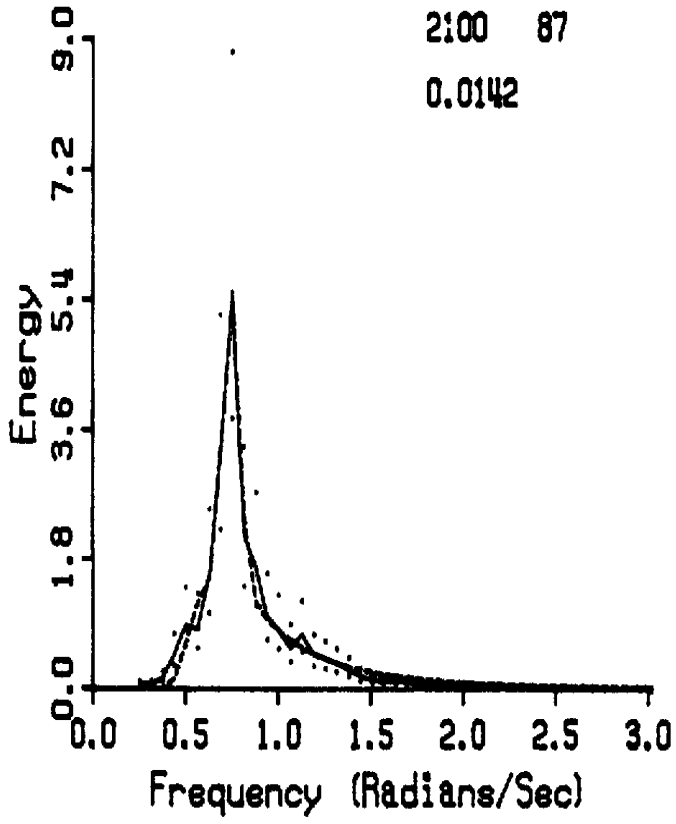
2100 87
0.0142
Energy
0.0 1.8 3.6 5.4 7.2 9.0
0.0 0.5 1.0 1.5 2.0 2.5 3.0
Frequency (Radians/Sec)

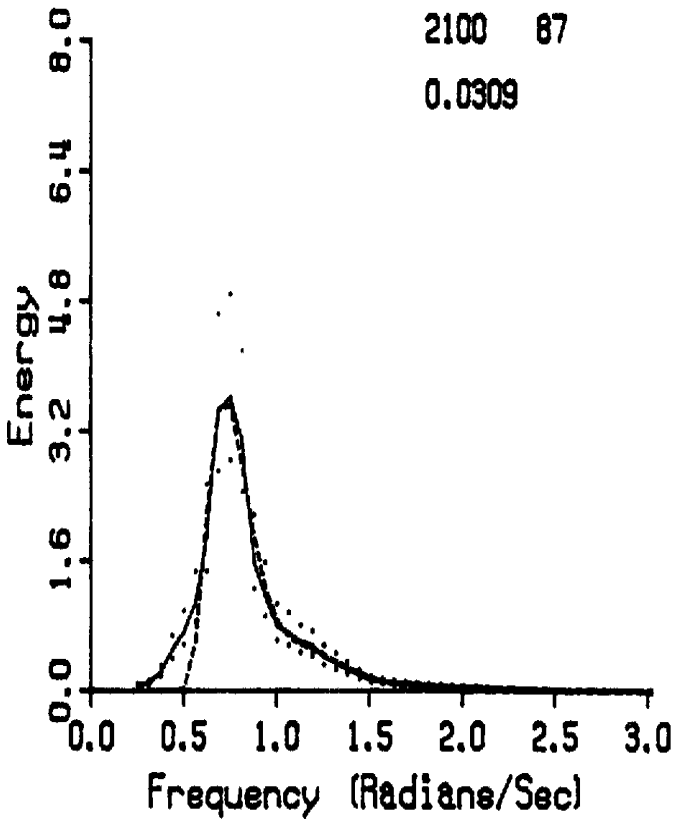
2100 87
0.0309
Energy
0.0 1.6 3.2 4.8 6.4 8.0
0.0 0.5 1.0 1.5 2.0 2.5 3.0
Frequency (Radians/Sec)

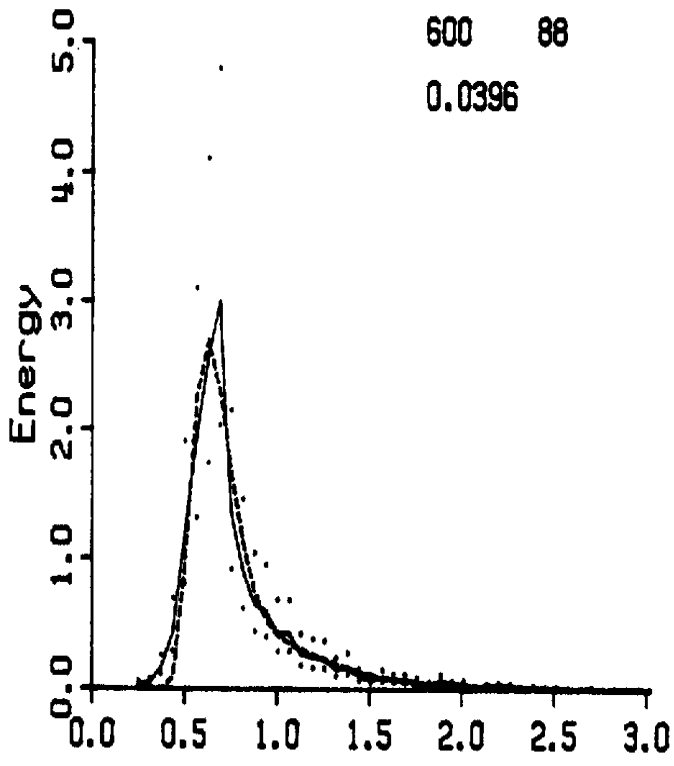
600 88
0.0396
Energy
0.0 1.0 2.0 3.0 4.0 5.0
0.0 0.5 1.0 1.5 2.0 2.5 3.0

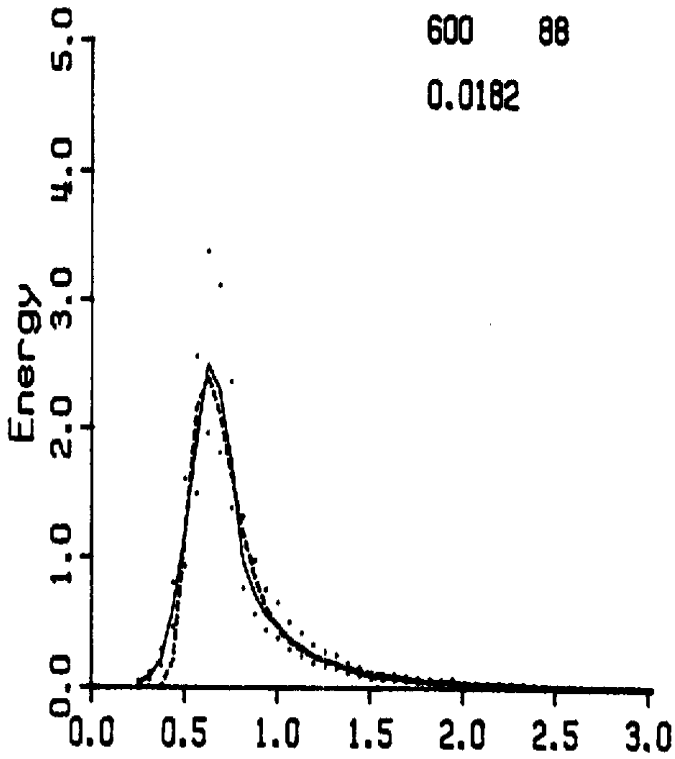
600 88
0.0182
Energy
0.0 1.0 2.0 3.0 4.0 5.0
0.0 0.5 1.0 1.5 2.0 2.5 3.0

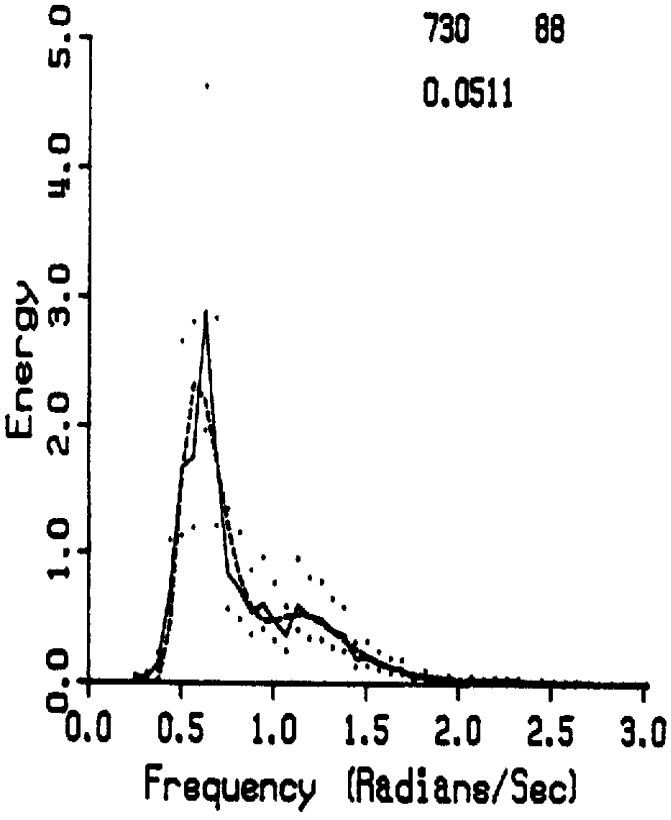
730 88
0.0511
Energy
0.0 1.0 2.0 3.0 4.0 5.0
0.0 0.5 1.0 1.5 2.0 2.5 3.0
Frequency (Radians/Sec)

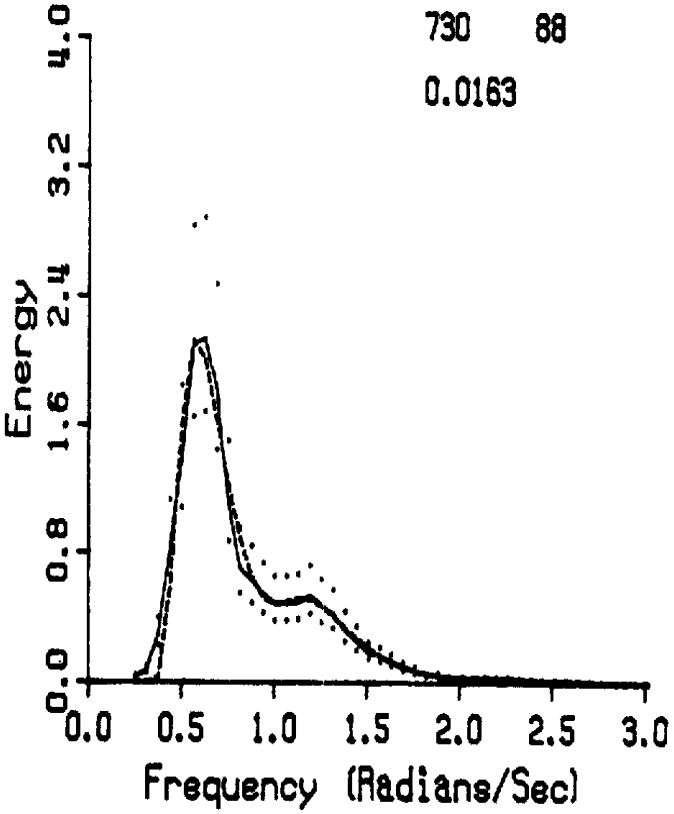
730 88
0.0163
Energy
0.0 0.8 1.6 2.4 3.2 4.0
0.0 0.5 1.0 1.5 2.0 2.5 3.0
Frequency (Radians/Sec)

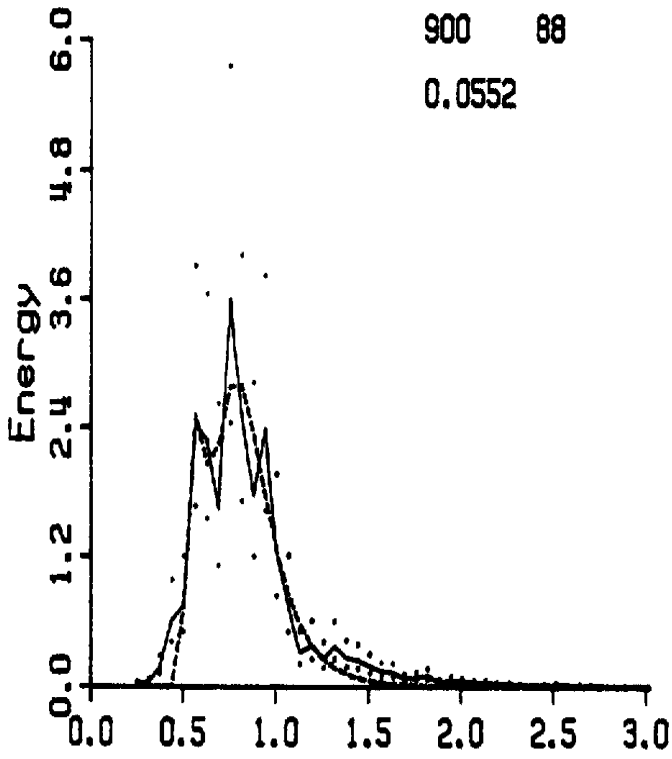
900 88
0.0552
Energy
0.0 1.2 2.4 3.6 4.8 6.0
0.0 0.5 1.0 1.5 2.0 2.5 3.0

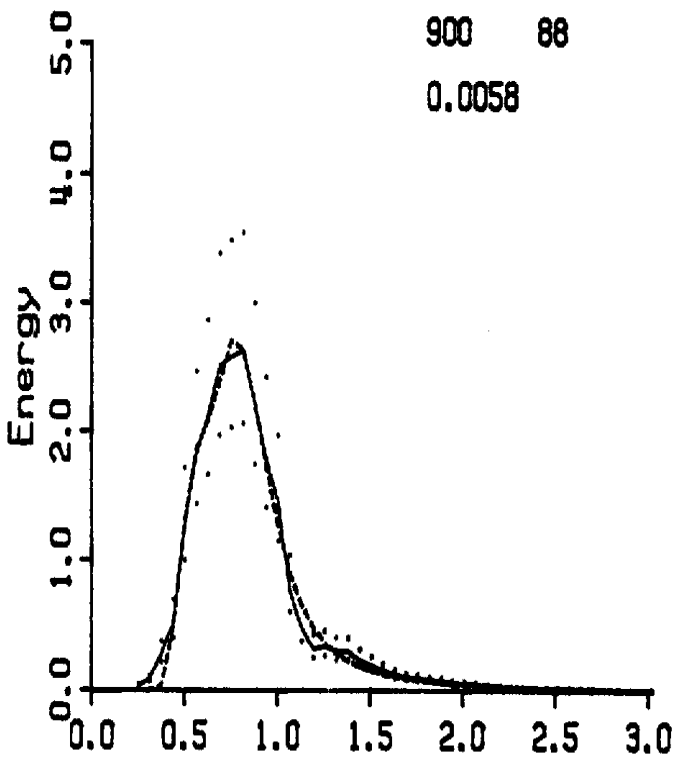
900 88
0.0058
Energy
0.0 1.0 2.0 3.0 4.0 5.0
0.0 0.5 1.0 1.5 2.0 2.5 3.0

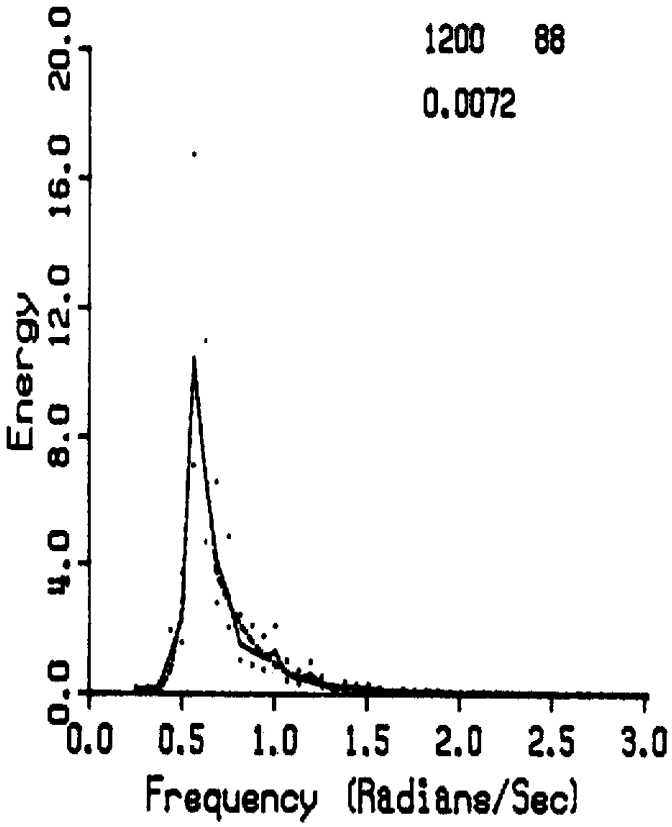
1200 88
0.0072
Energy
0.0 4.0 8.0 12.0 16.0 20.0
0.0 0.5 1.0 1.5 2.0 2.5 3.0
Frequency (Radians/Sec)

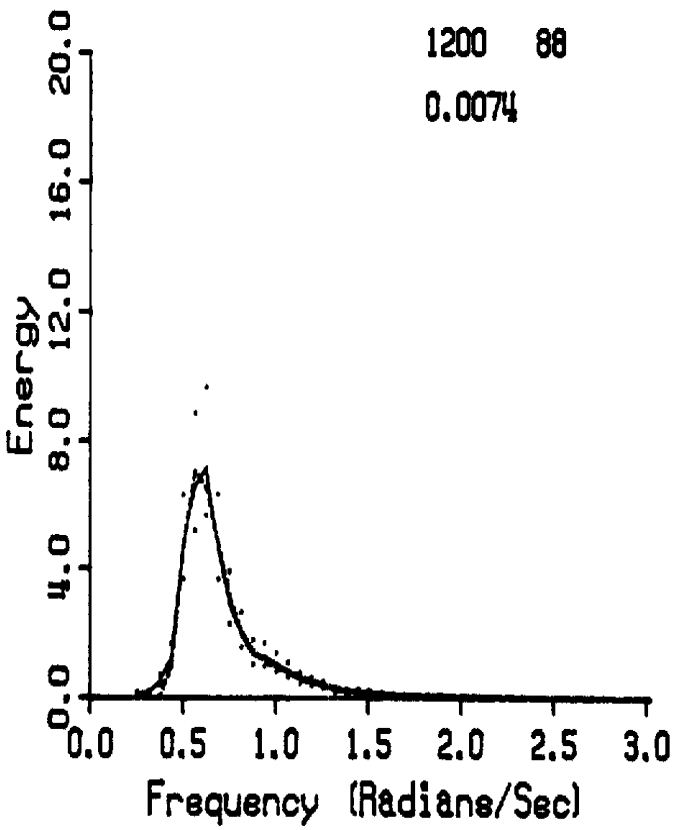
1200 88
0.0074
Energy
0.0 4.0 8.0 12.0 16.0 20.0
0.0 0.5 1.0 1.5 2.0 2.5 3.0
Frequency (Radians/Sec)

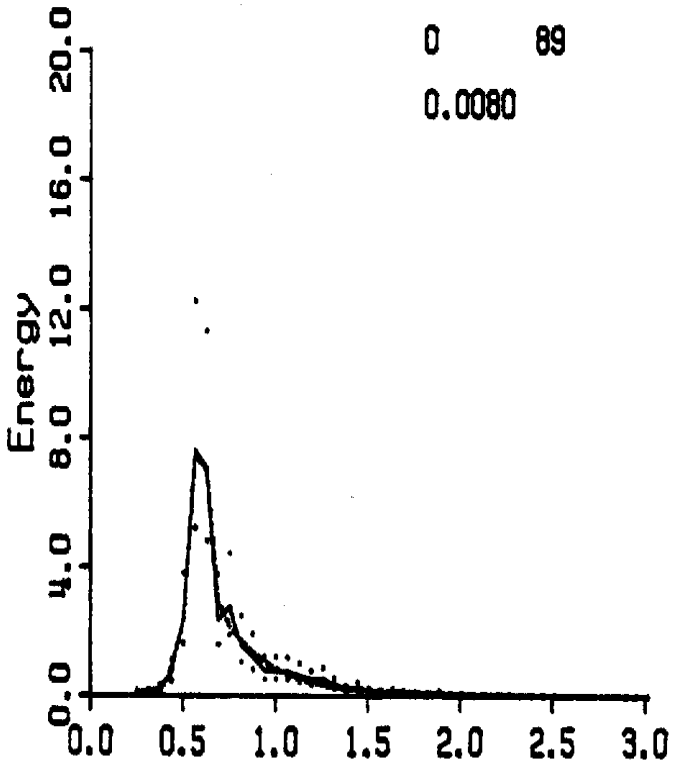
0 89
0.0080
Energy
0.0 4.0 8.0 12.0 16.0 20.0
0.0 0.5 1.0 1.5 2.0 2.5 3.0

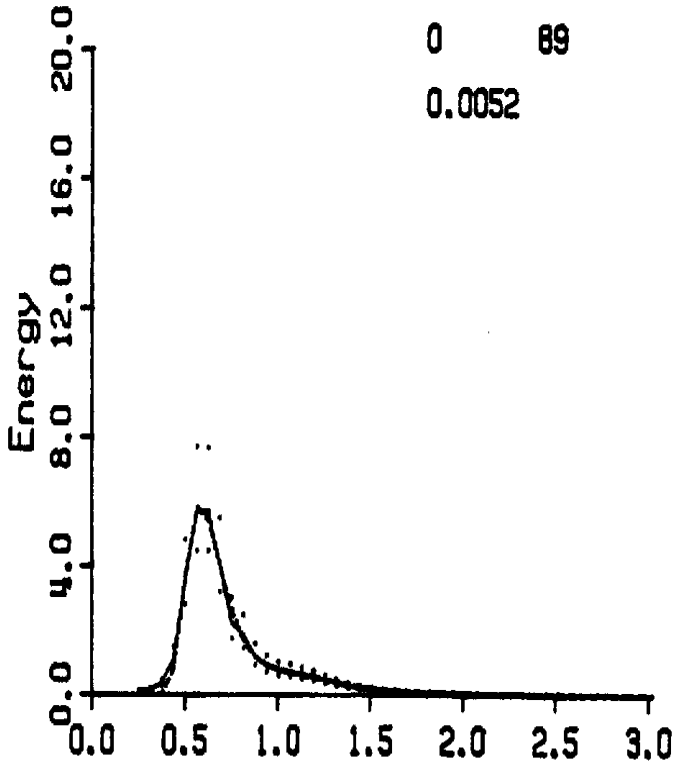
0 89
0.0052
Energy
0.0 4.0 8.0 12.0 16.0 20.0
0.0 0.5 1.0 1.5 2.0 2.5 3.0

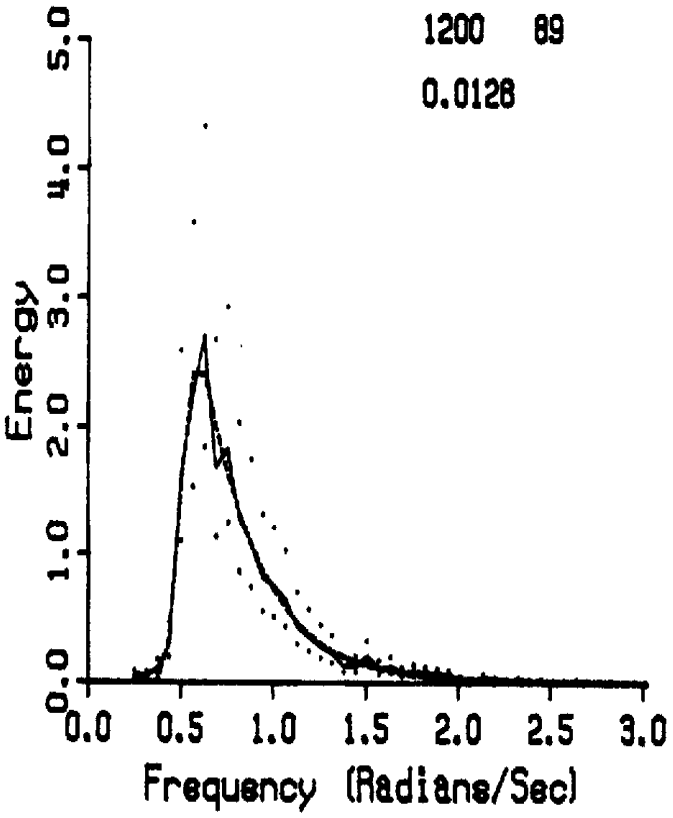
1200 89
0.0126
Energy
0.0 1.0 2.0 3.0 4.0 5.0
0.0 0.5 1.0 1.5 2.0 2.5 3.0
Frequency (Radians/Sec)

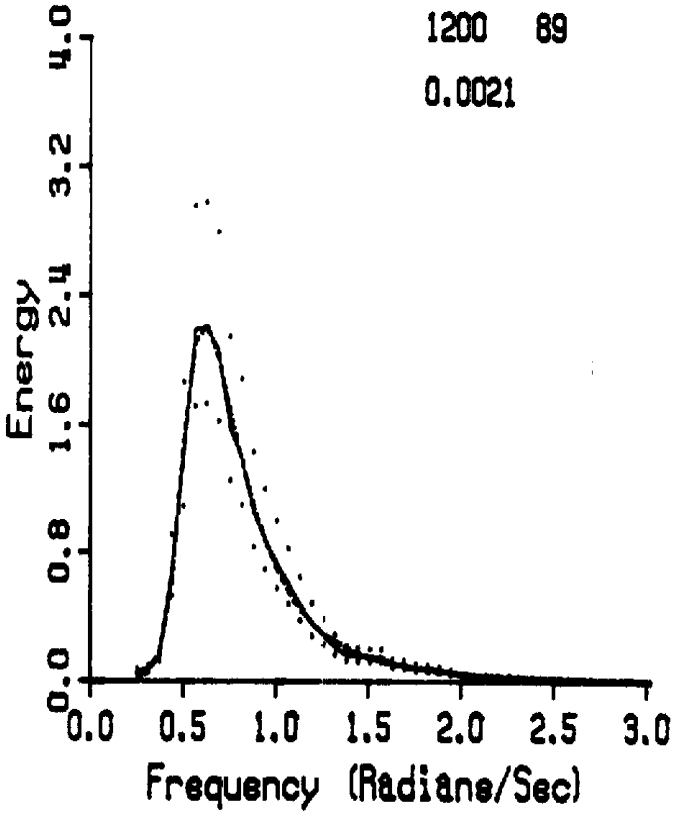
1200 89
0.0021
Energy
0.0 0.8 1.6 2.4 3.2 4.0
0.0 0.5 1.0 1.5 2.0 2.5 3.0
Frequency (Radians/Sec)

APPENDIX 3. SELECTED CONTOURED DIRECTIONAL SPECTRA

Contour Lines at: 0.01, 0.025, 0.05, 0.1, 0.25, 0.5, 1.0, 2.0, 4.0, 6.0, 8.0, 10.0, 15.0, 20.0, and 30.0 M**2/(RPS*Deg)

A Data Spectrum

B Level 1 Spectrum; OH model heave, least squares fitted P at each frequency

C Level 2 spectrum; OH model heave (+10% noise), P1 and P2 from least squares fit to data spectrum at ωm1 and ωm2, P varied by record and with frequency according to P(ω) = Pi(ω/ωmi)**D where D = −2.34 if ω/ωm >or= 1.0, D = 4.06 if ω/ωm < 1.0

D Level 3 spectrum; OH model heave (+10% noise), P1 = 20. and P2 = 7.5 for each record but varied with frequency according to P(ω) = Pi(ω/ωmi)**D

E Level 4 spectrum: OH model heave (+10% noise), P1 and P2 from least squares fit to data spectrum at ωm1 and ωm2, P varied by record but constant with frequency

F 10-parameter model spectrum

G P1 and P2 from regression analysis prediction, OH model heave (+10% noise), P varied by record and with frequency according to P(ω) = Pi(ω/ωmi)**D

S

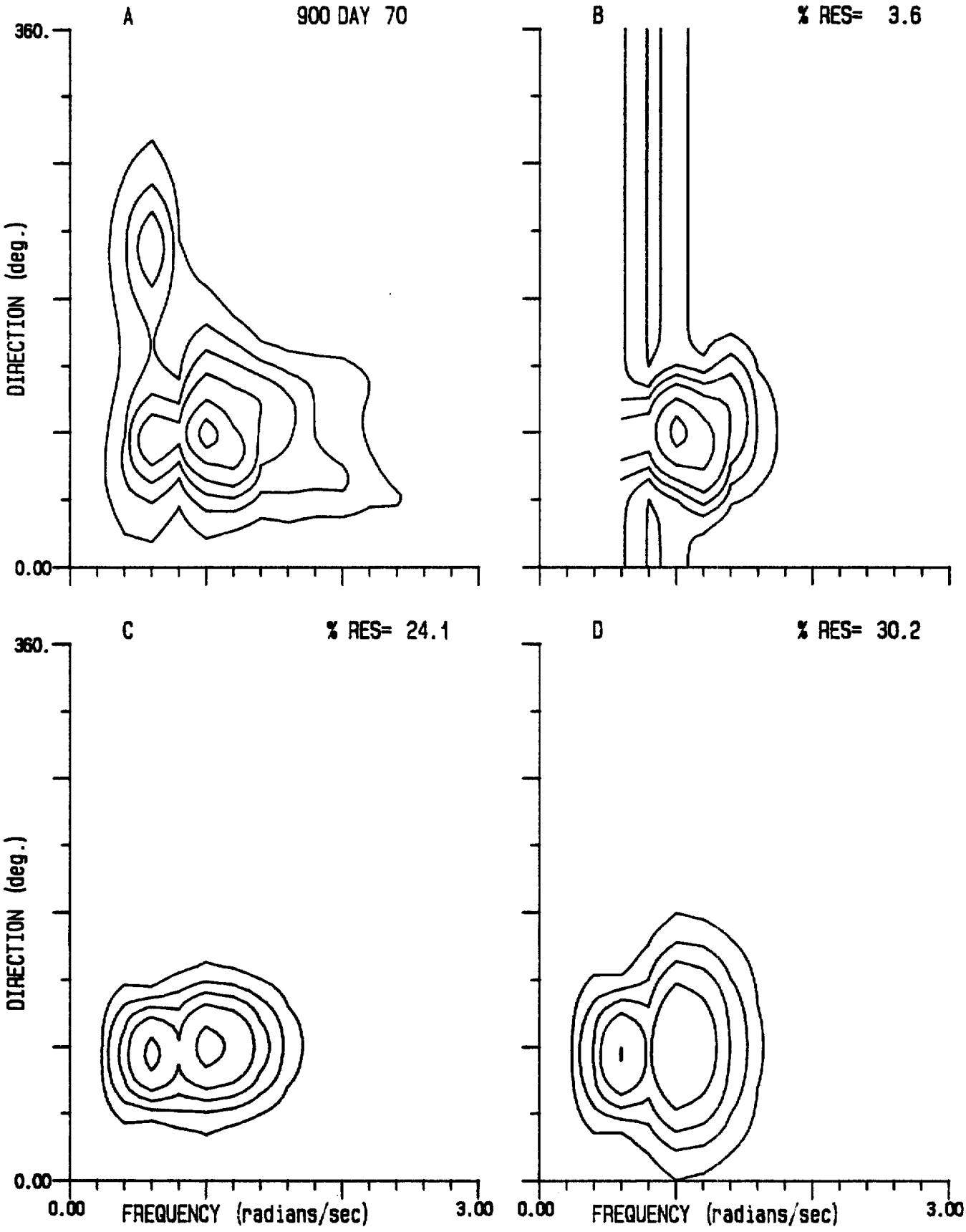
A
900 DAY 70
B
% RES= 3.6
C
% RES= 24.1
D
% RES= 30.2
360.
0.00
DIRECTION (deg.)
0.00
FREQUENCY (radians/sec)
3.00

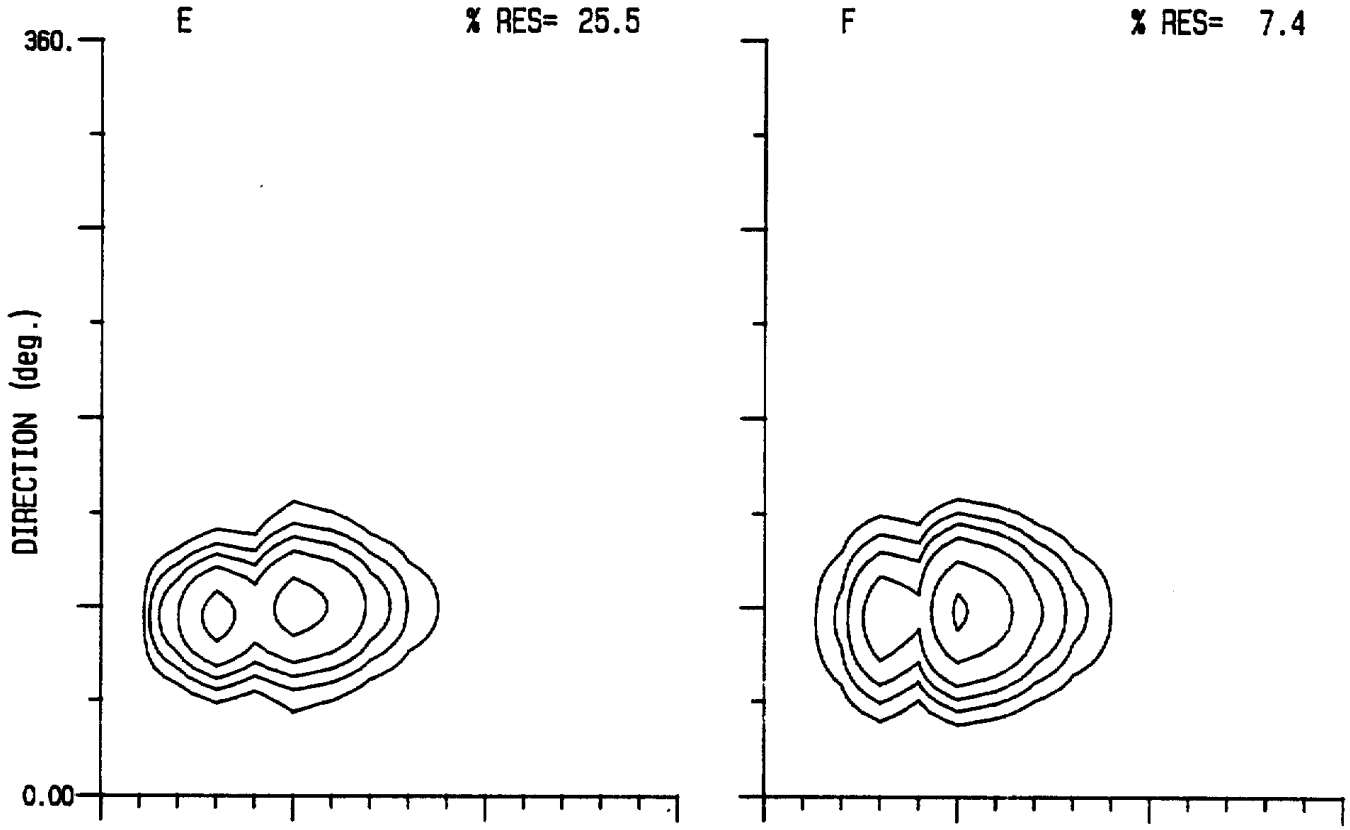
E
% RES= 25.5
360.
0.00
DIRECTION (deg.)
F
% RES= 7.4

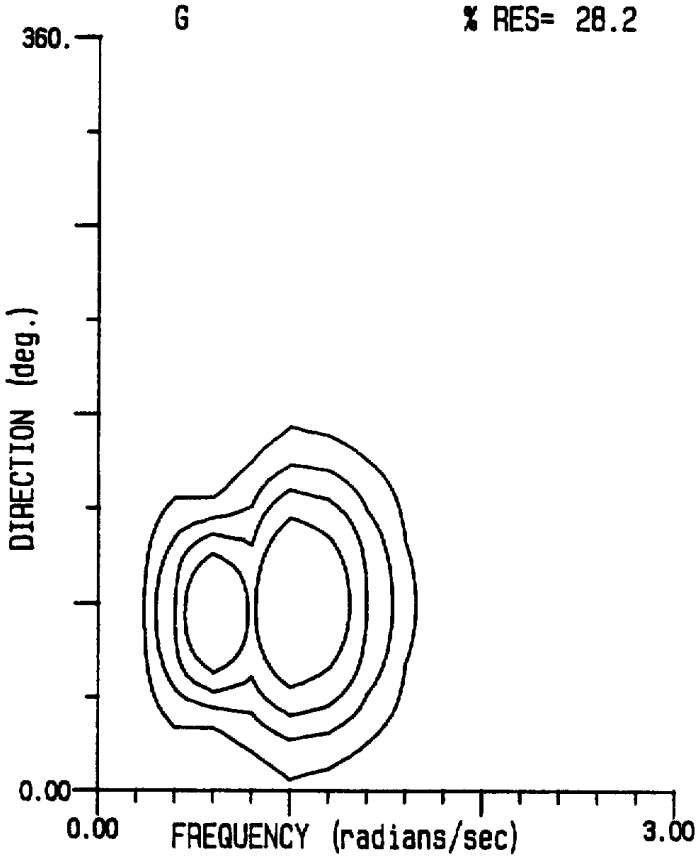
G
% RES= 28.2
360.
0.00
DIRECTION (deg.)
0.00
FREQUENCY (radians/sec)
3.00

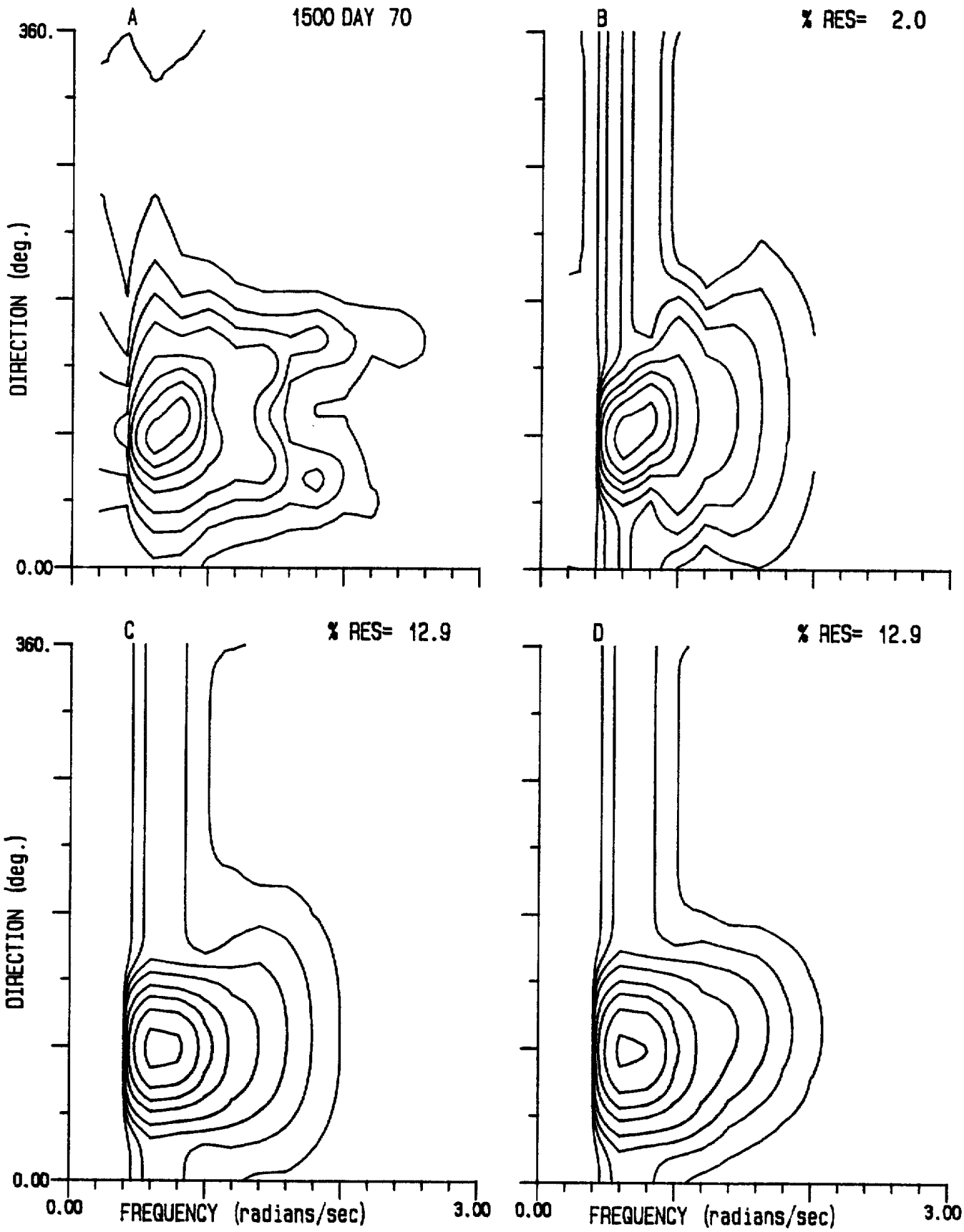
A
1500 DAY 70
B
% RES= 2.0
C
% RES= 12.9
D
% RES= 12.9
360.
0.00
DIRECTION (deg.)
0.00
FREQUENCY (radians/sec)
3.00

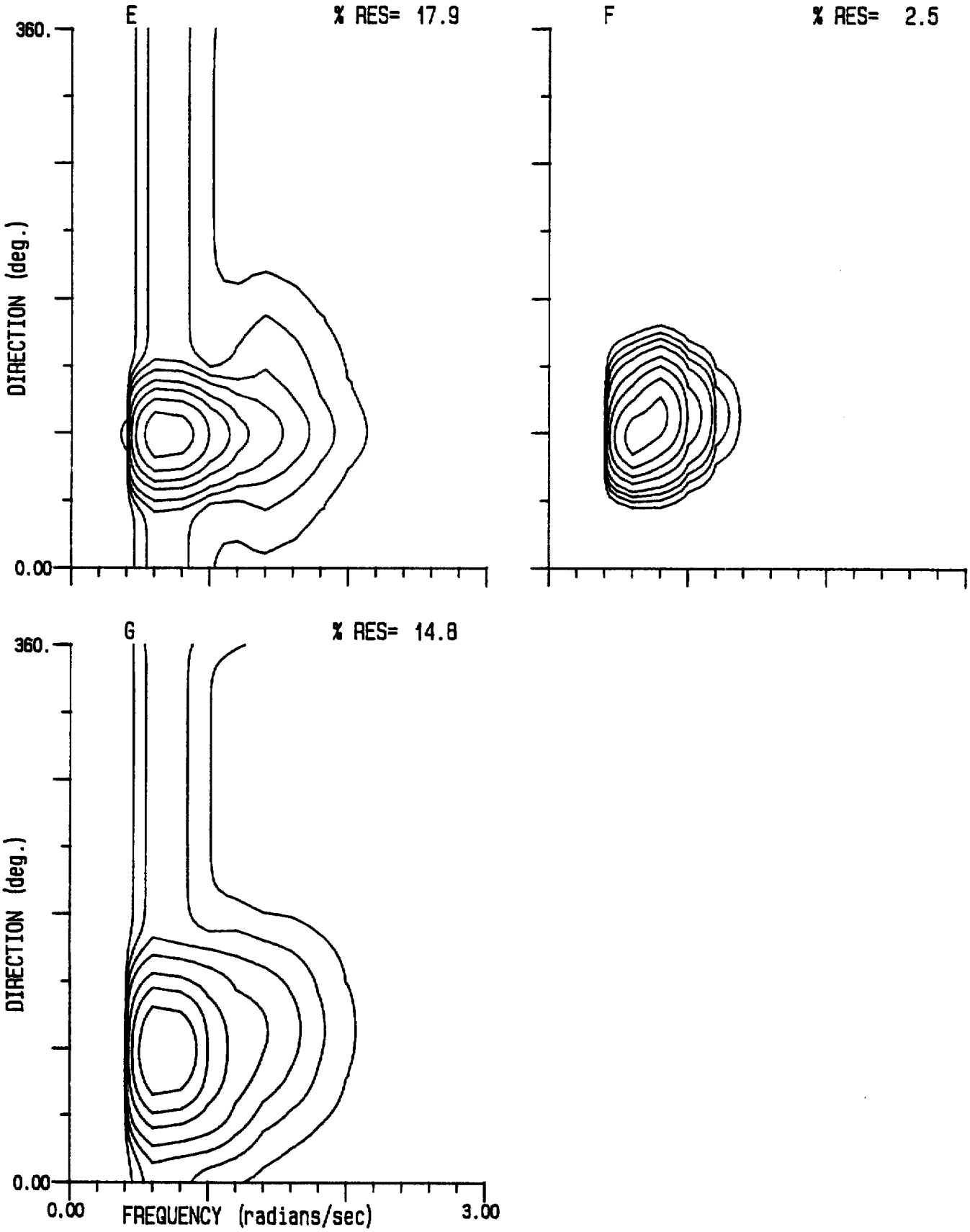
E
% RES= 17.9
F
% RES= 2.5
G
% RES= 14.8
360.
0.00
DIRECTION (deg.)
0.00
FREQUENCY (radians/sec)
3.00

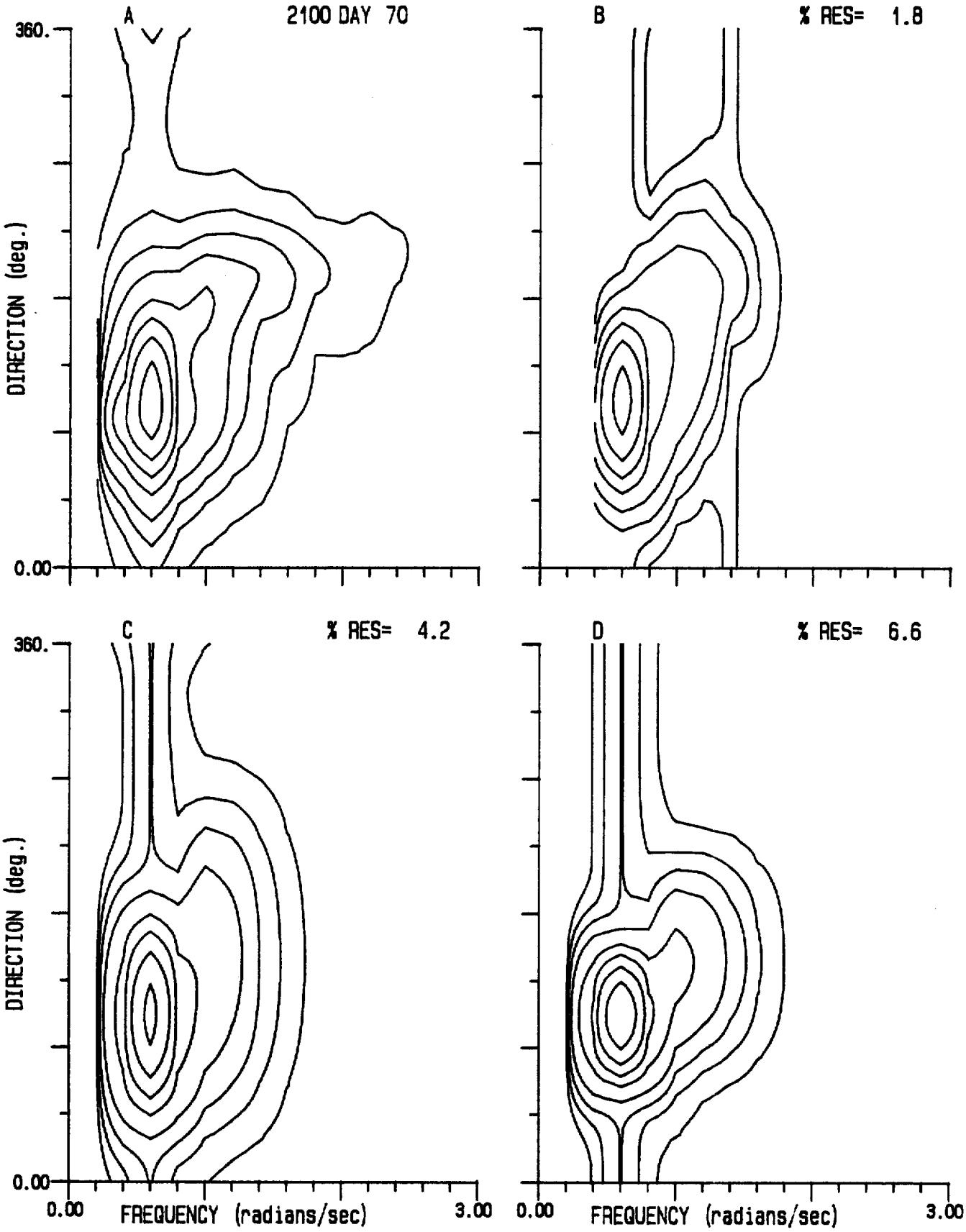
A
2100 DAY 70
B
% RES= 1.8
C
% RES= 4.2
D
% RES= 6.6
360.
0.00
DIRECTION (deg.)
0.00
FREQUENCY (radians/sec)
3.00

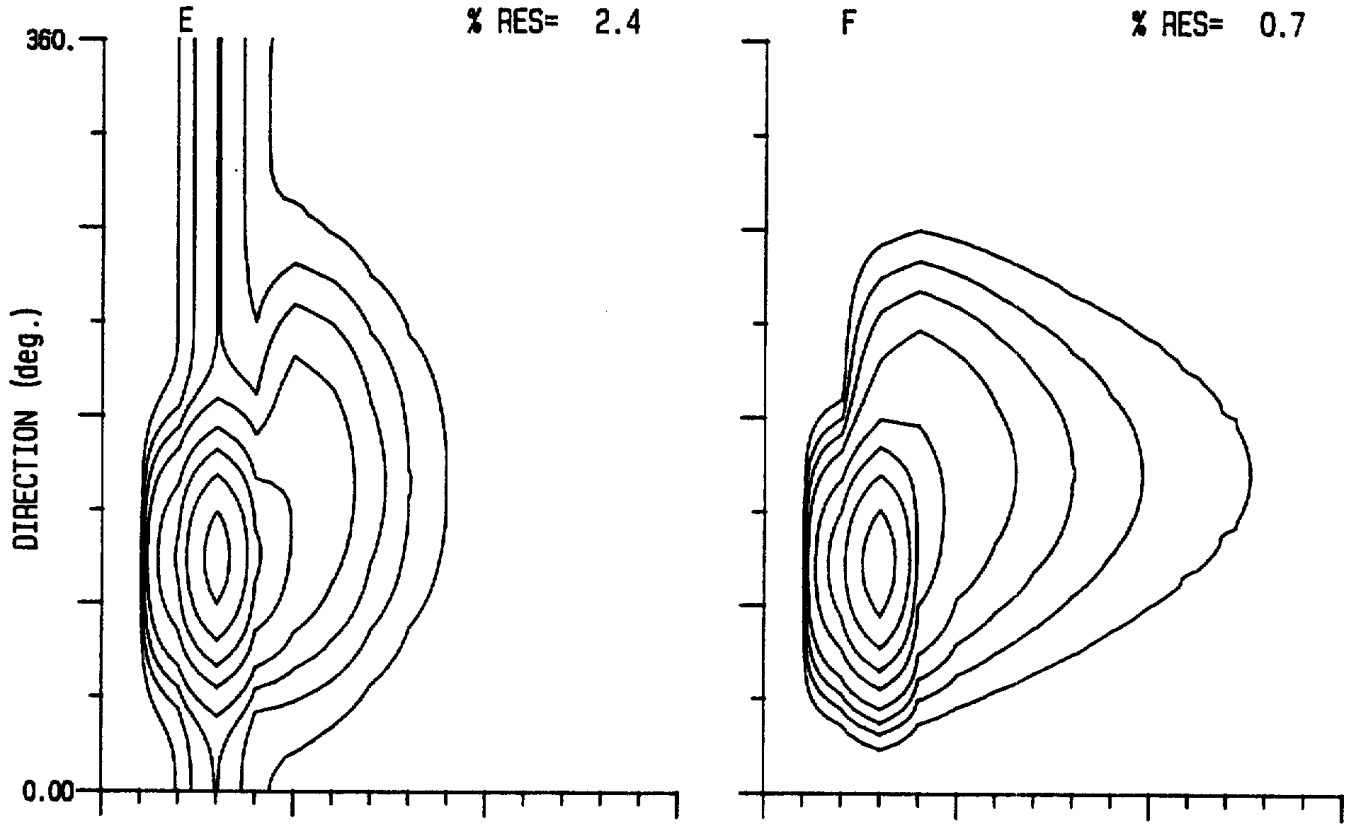
E
% RES= 2.4
360.
0.00
DIRECTION (deg.)
F
% RES= 0.7

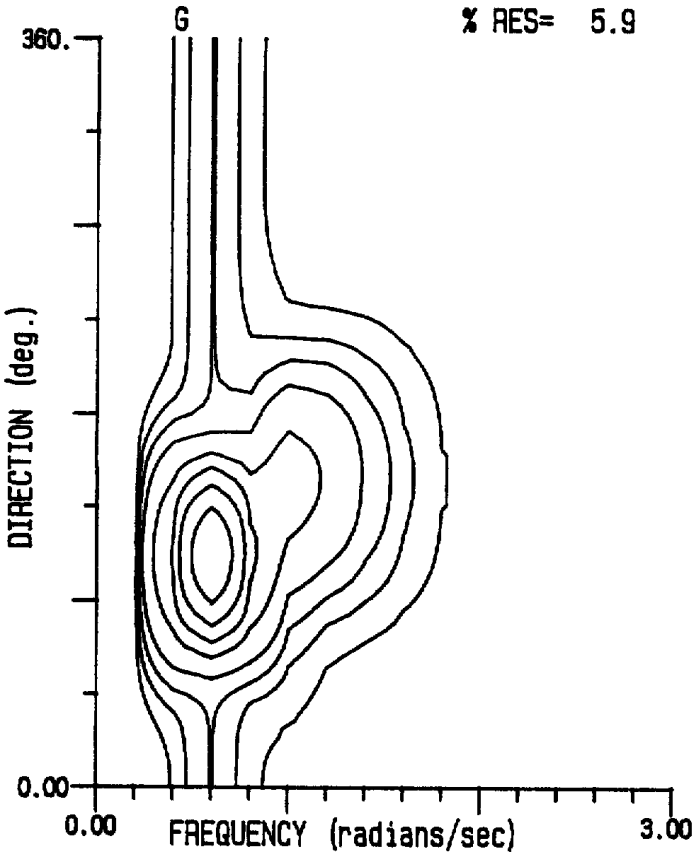
G
% RES= 5.9
360.
0.00
DIRECTION (deg.)
0.00
FREQUENCY (radians/sec)
3.00

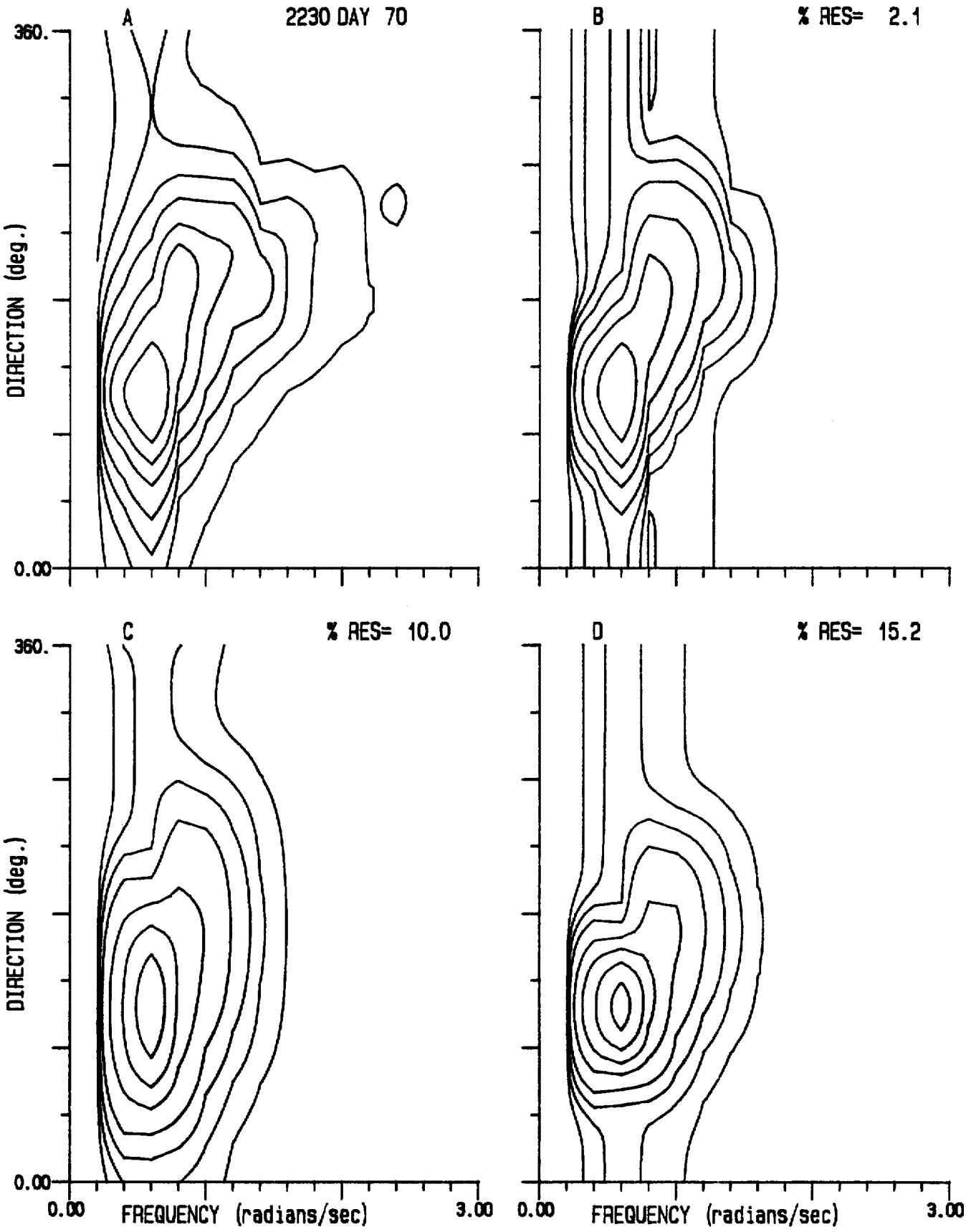
A
2230 DAY 70
B
% RES= 2.1
C
% RES= 10.0
D
% RES= 15.2
360.
0.00
DIRECTION (deg.)
0.00
FREQUENCY (radians/sec)
3.00

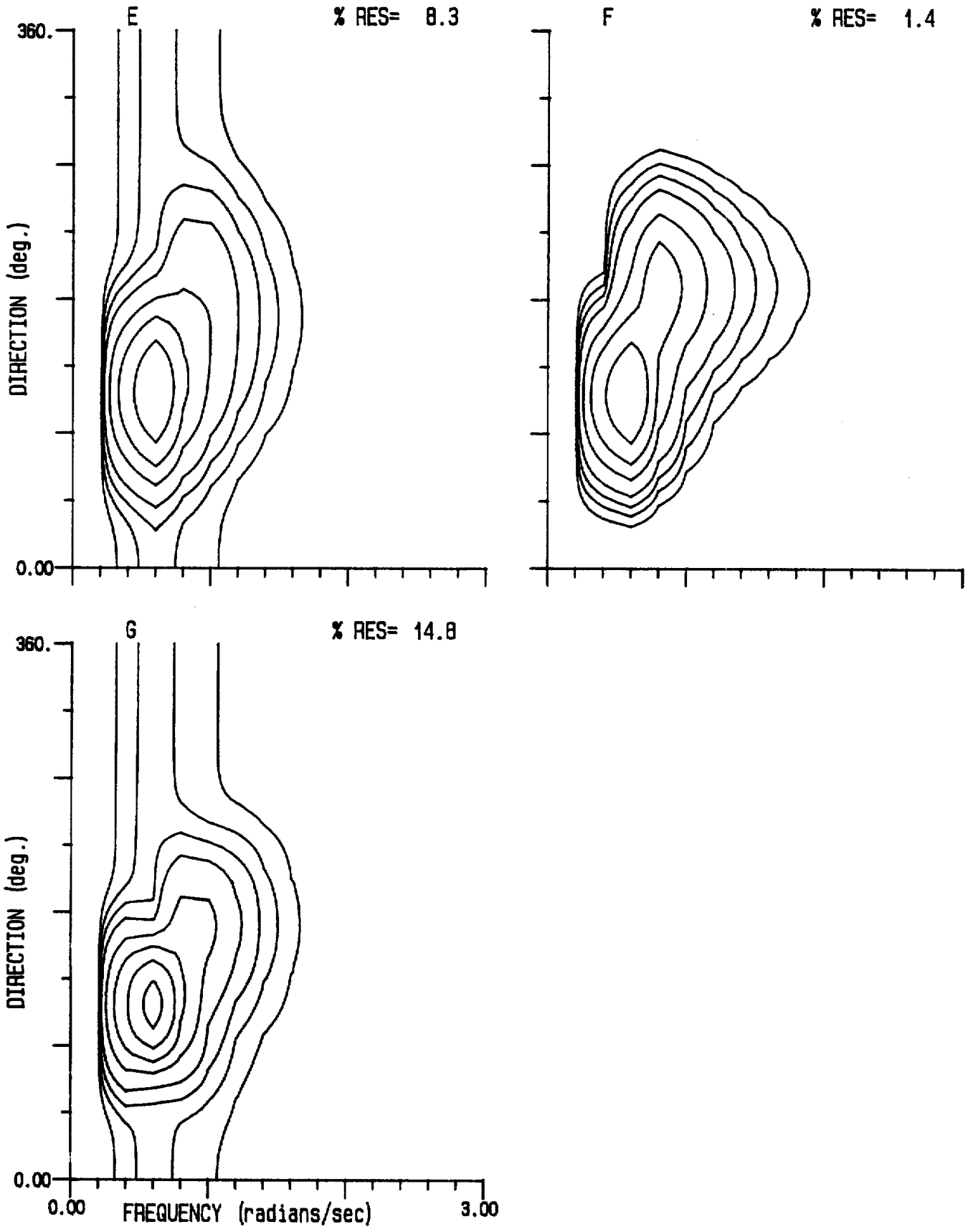
E
% RES= 8.3
F
% RES= 1.4
G
% RES= 14.8
360.
0.00
DIRECTION (deg.)
0.00
FREQUENCY (radians/sec)
3.00

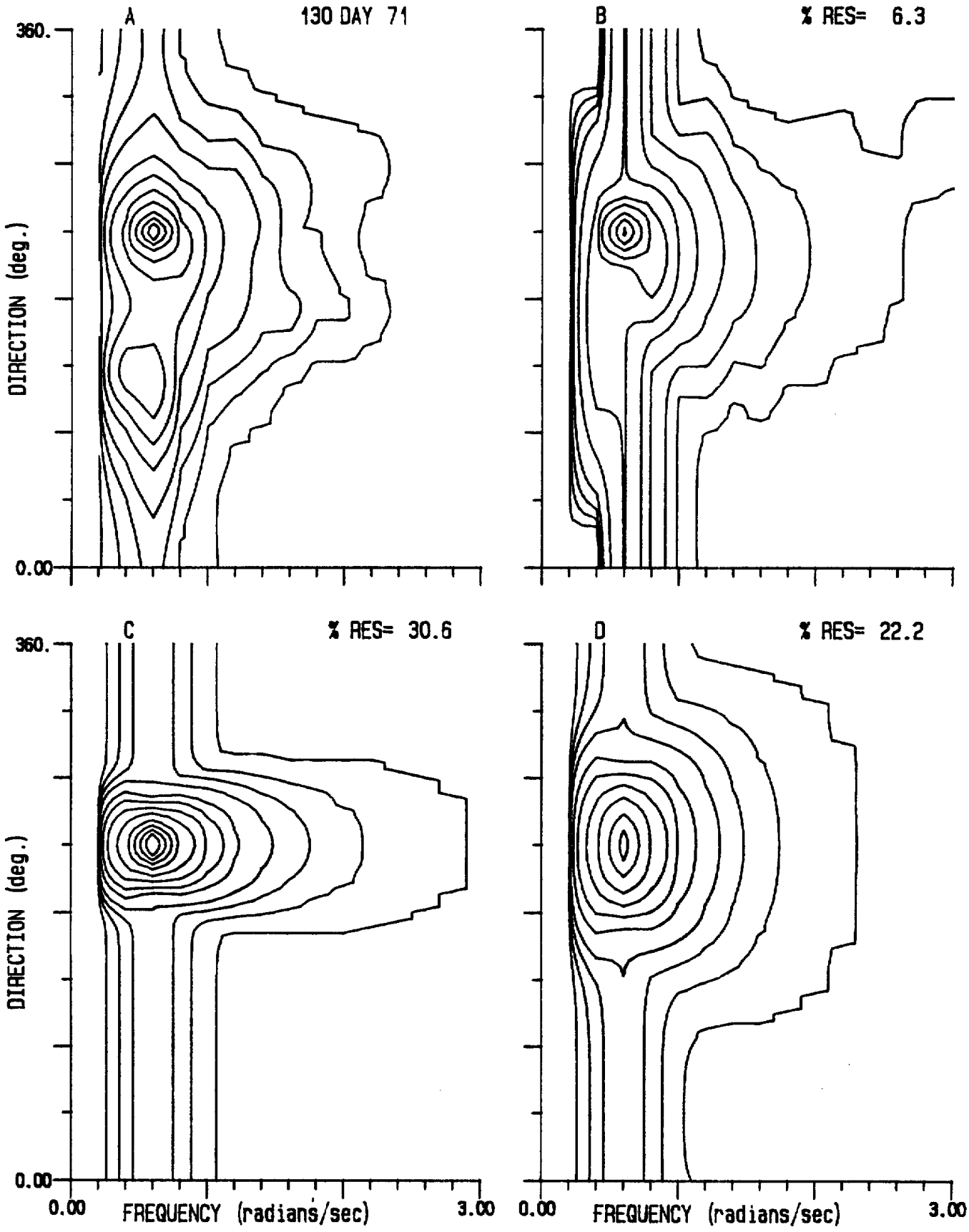
A
130 DAY 71
B
% RES= 6.3
C
% RES= 30.6
D
% RES= 22.2
360.
0.00
DIRECTION (deg.)
0.00
FREQUENCY (radians/sec)
3.00

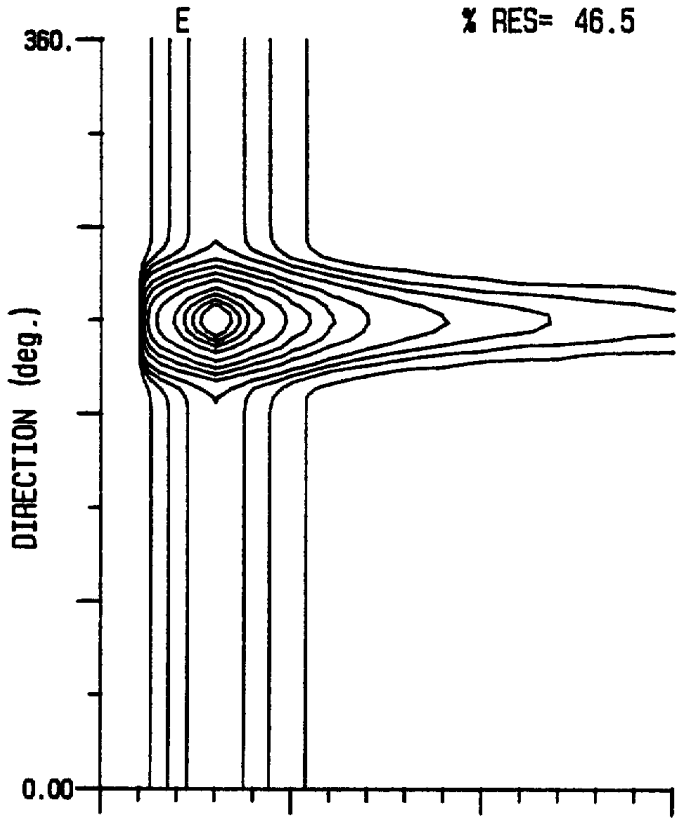
E
% RES= 46.5
360.
0.00
DIRECTION (deg.)

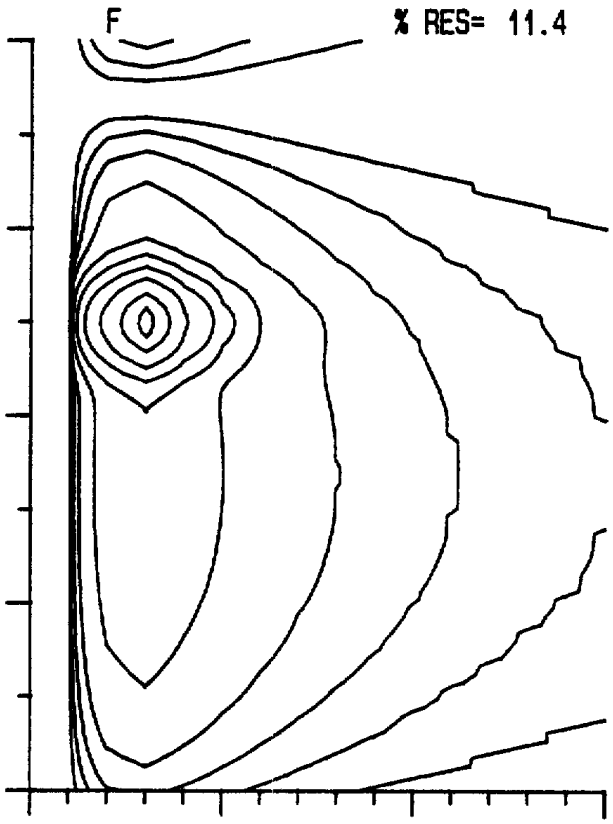
F
% RES= 11.4

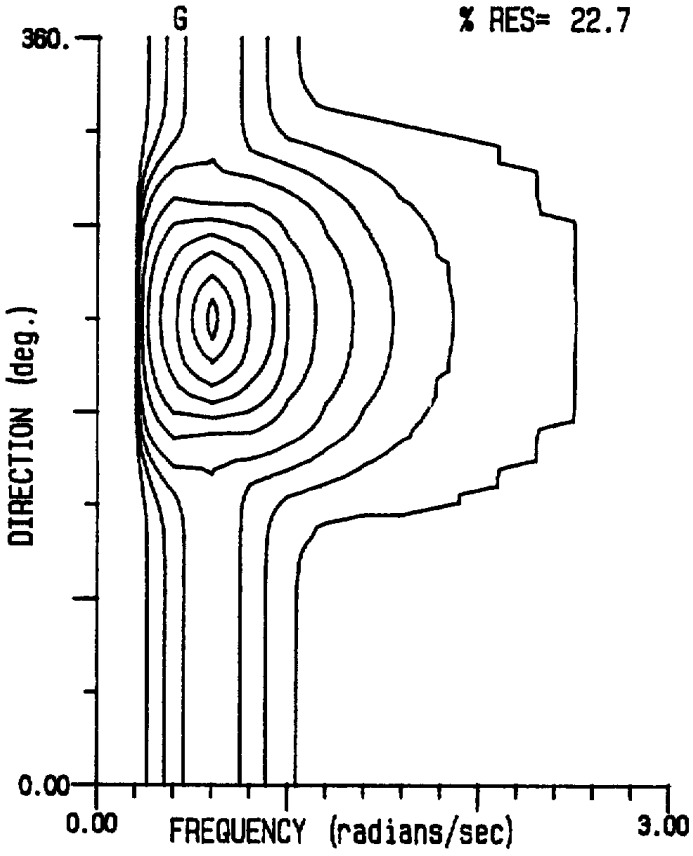
G
% RES= 22.7
360.
0.00
DIRECTION (deg.)
0.00
FREQUENCY (radians/sec)
3.00

DND 1

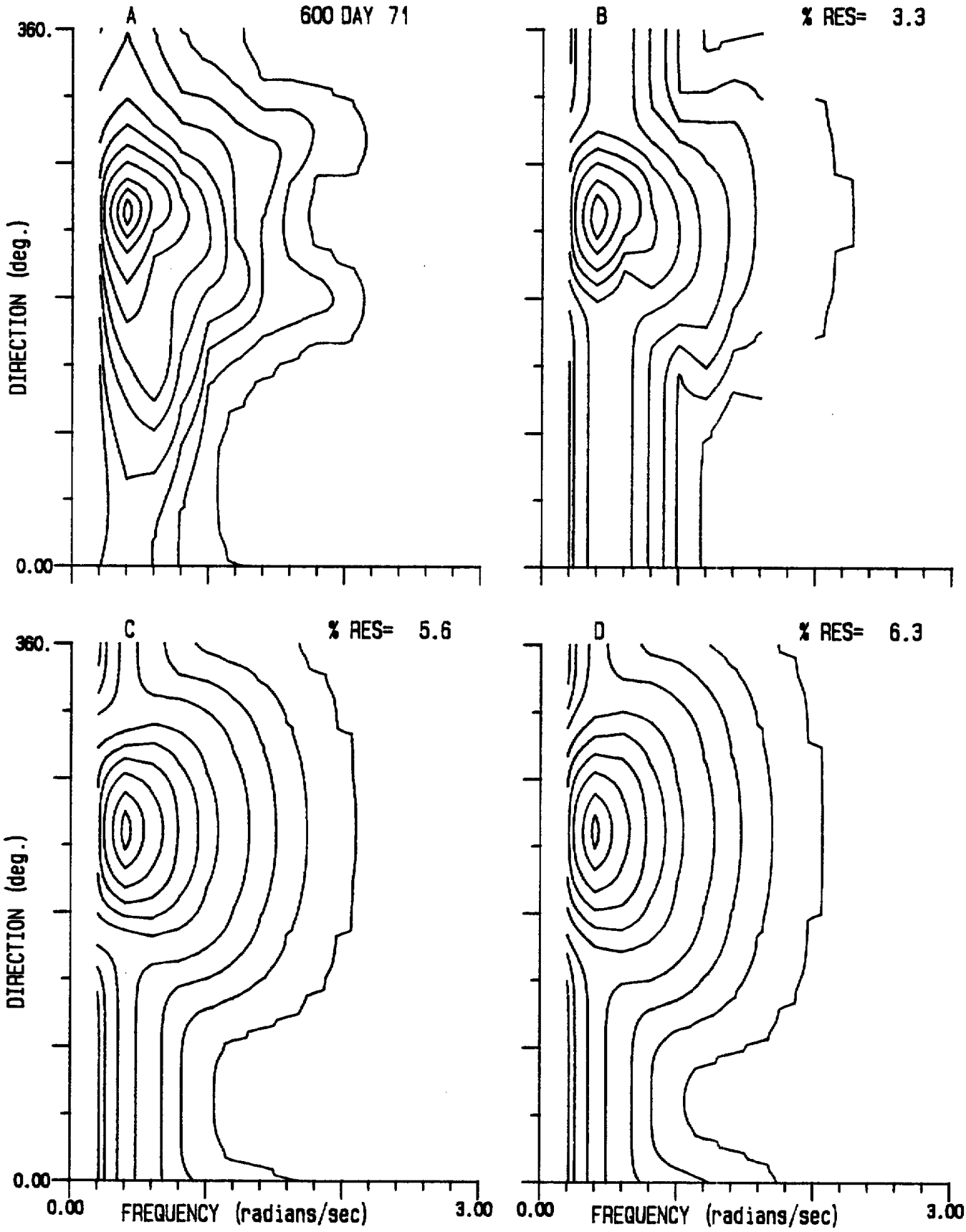
A
600 DAY 71
B
% RES= 3.3
C
% RES= 5.6
D
% RES= 6.3
360.
0.00
DIRECTION (deg.)
0.00
FREQUENCY (radians/sec)
3.00

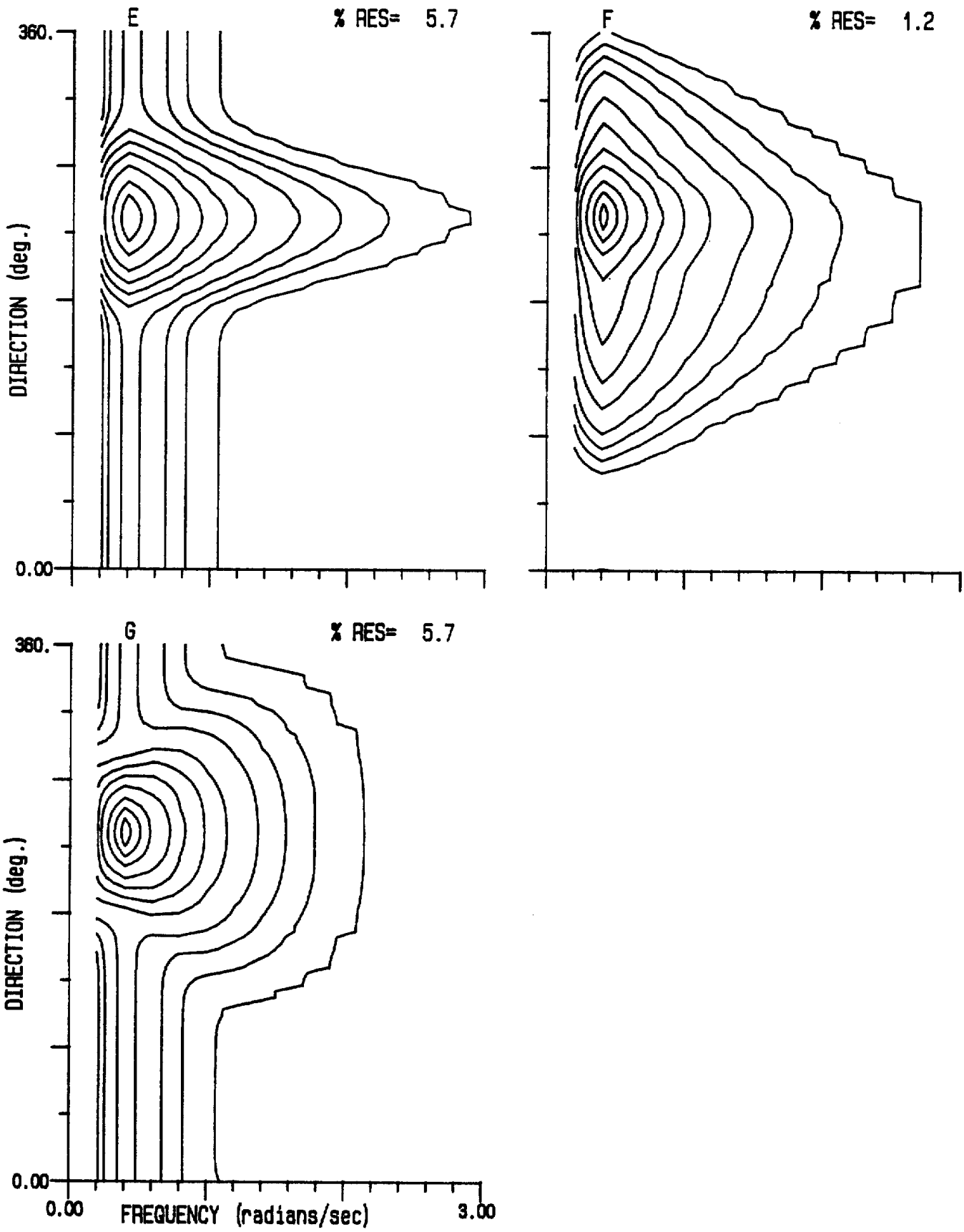
E
% RES= 5.7
360.
0.00
DIRECTION (deg.)
F
% RES= 1.2
G
% RES= 5.7
360.
0.00
DIRECTION (deg.)
0.00
FREQUENCY (radians/sec)
3.00

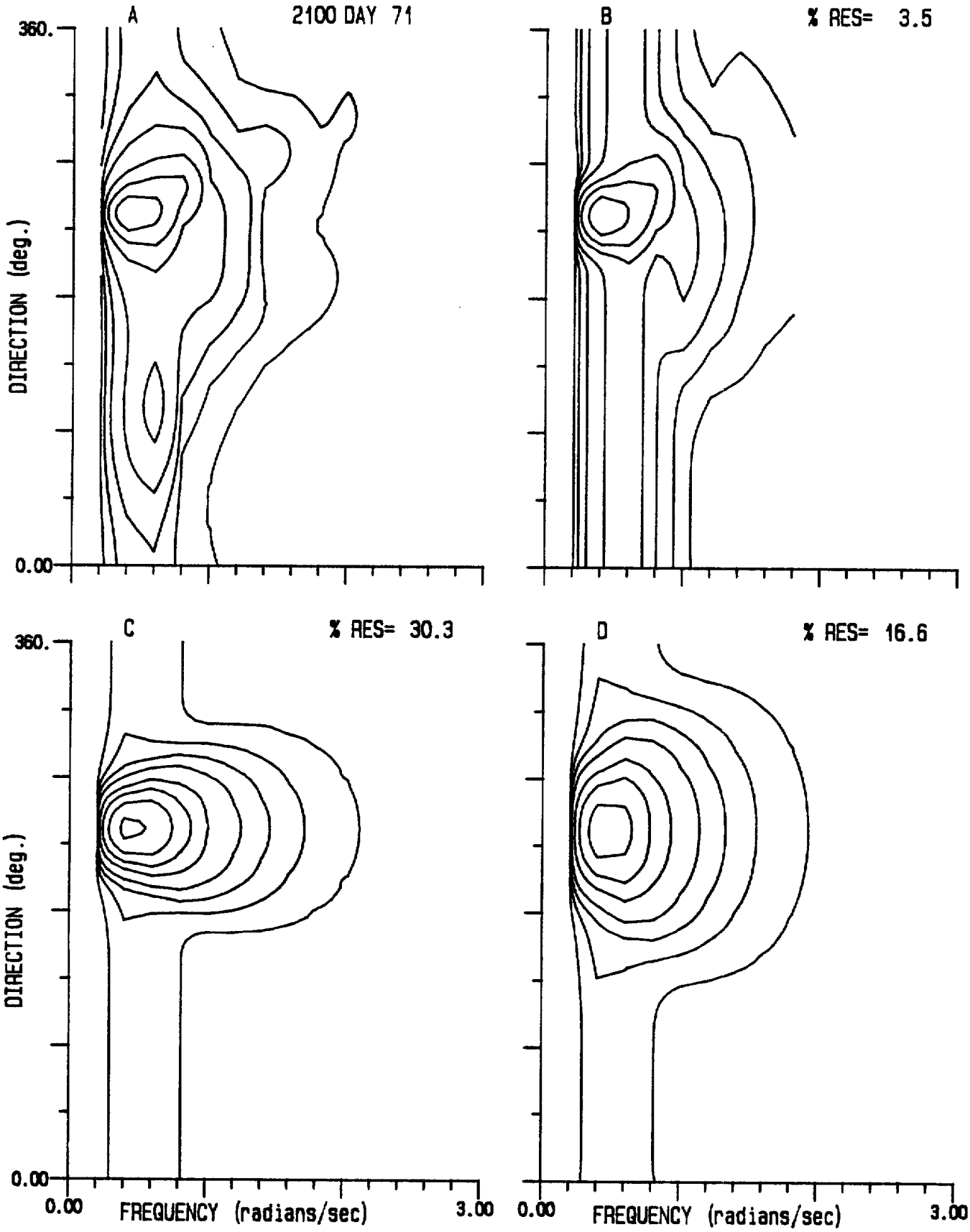
A
2100 DAY 71
B
% RES= 3.5
C
% RES= 30.3
D
% RES= 16.6
360.
0.00
DIRECTION (deg.)
0.00
FREQUENCY (radians/sec)
3.00

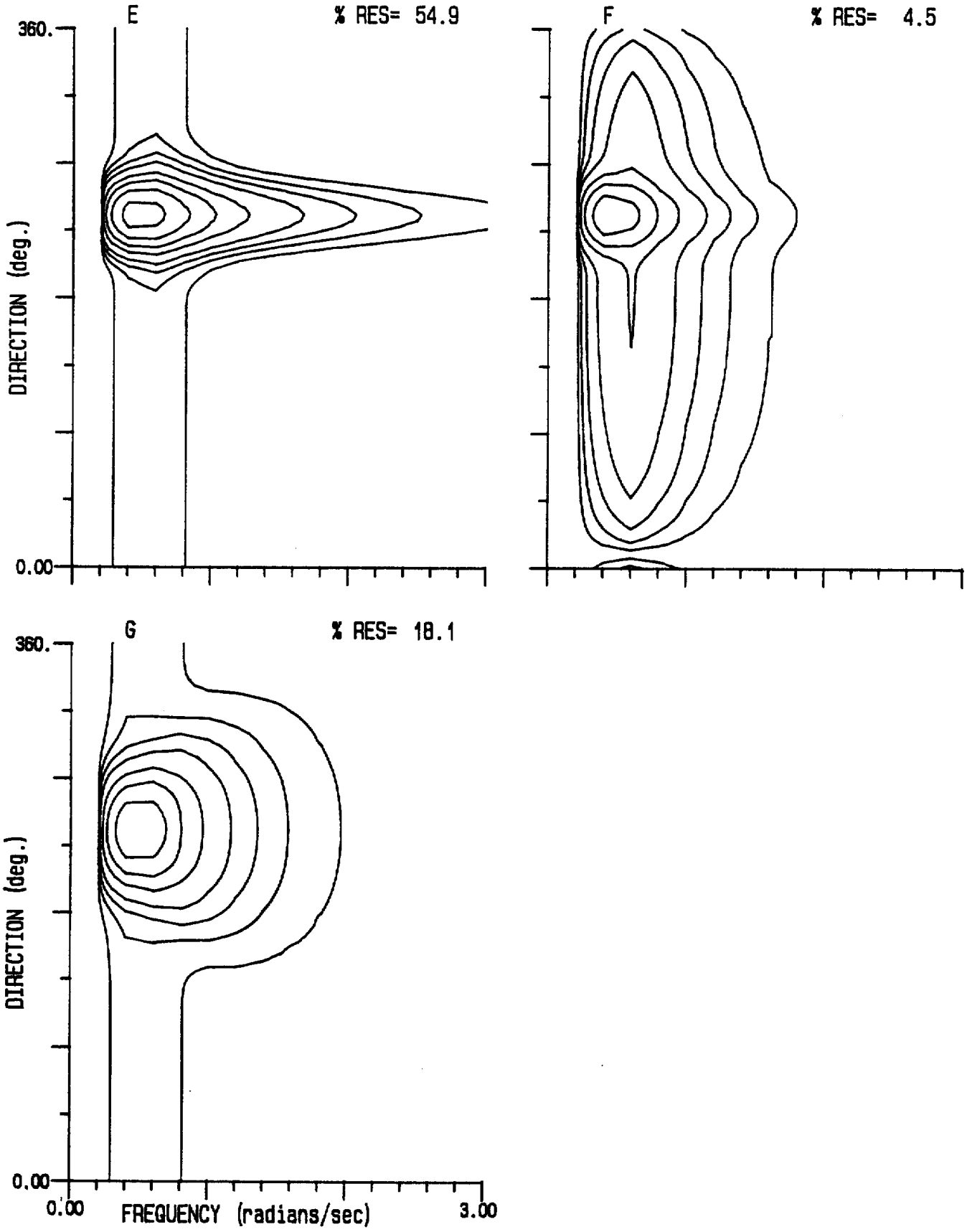
E
% RES= 54.9
F
% RES= 4.5
G
% RES= 18.1
360.
0.00
DIRECTION (deg.)
0.00
FREQUENCY (radians/sec)
3.00

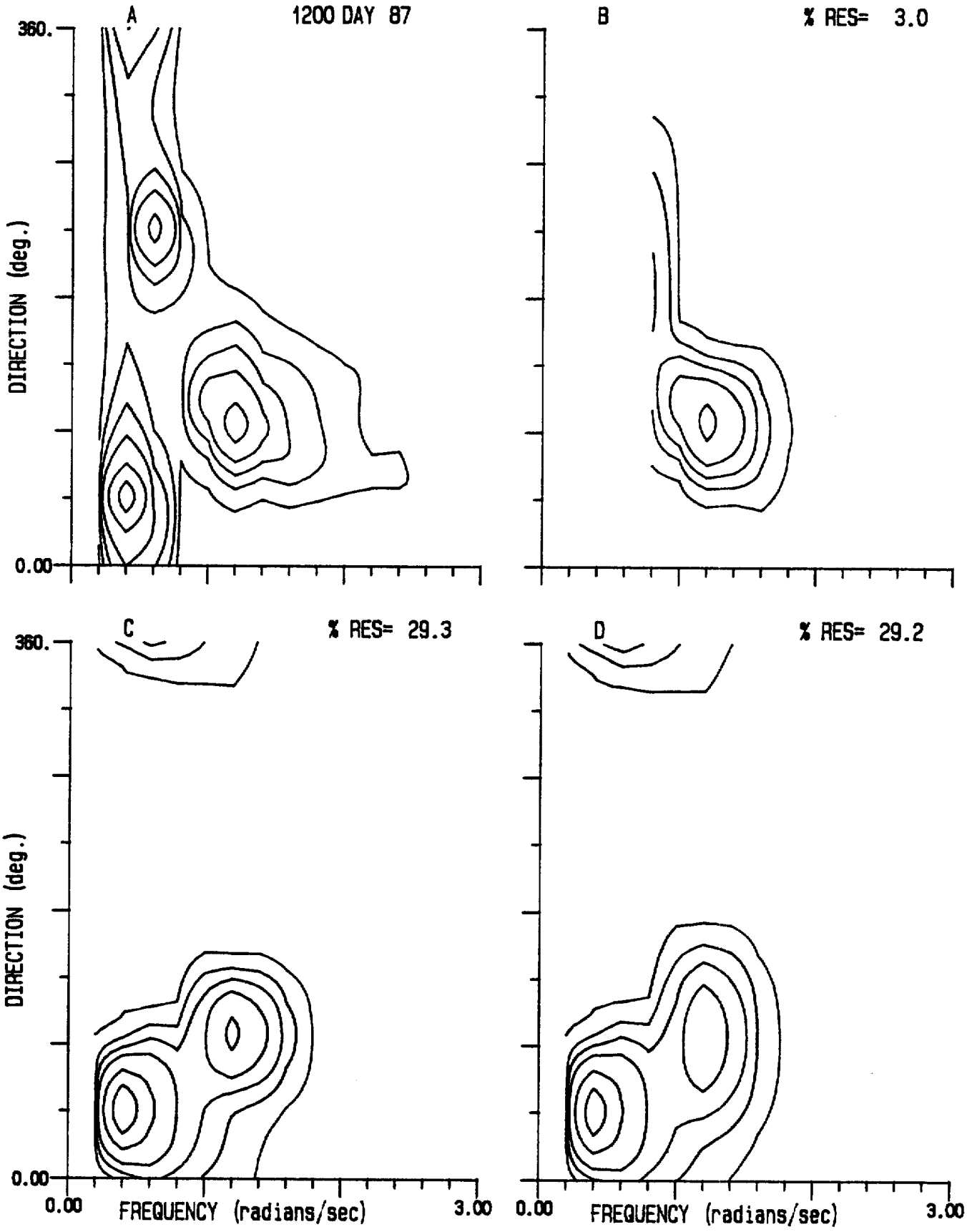
A
1200 DAY 87
B
% RES= 3.0
C
% RES= 29.3
D
% RES= 29.2
360.
0.00
DIRECTION (deg.)
0.00
FREQUENCY (radians/sec)
3.00

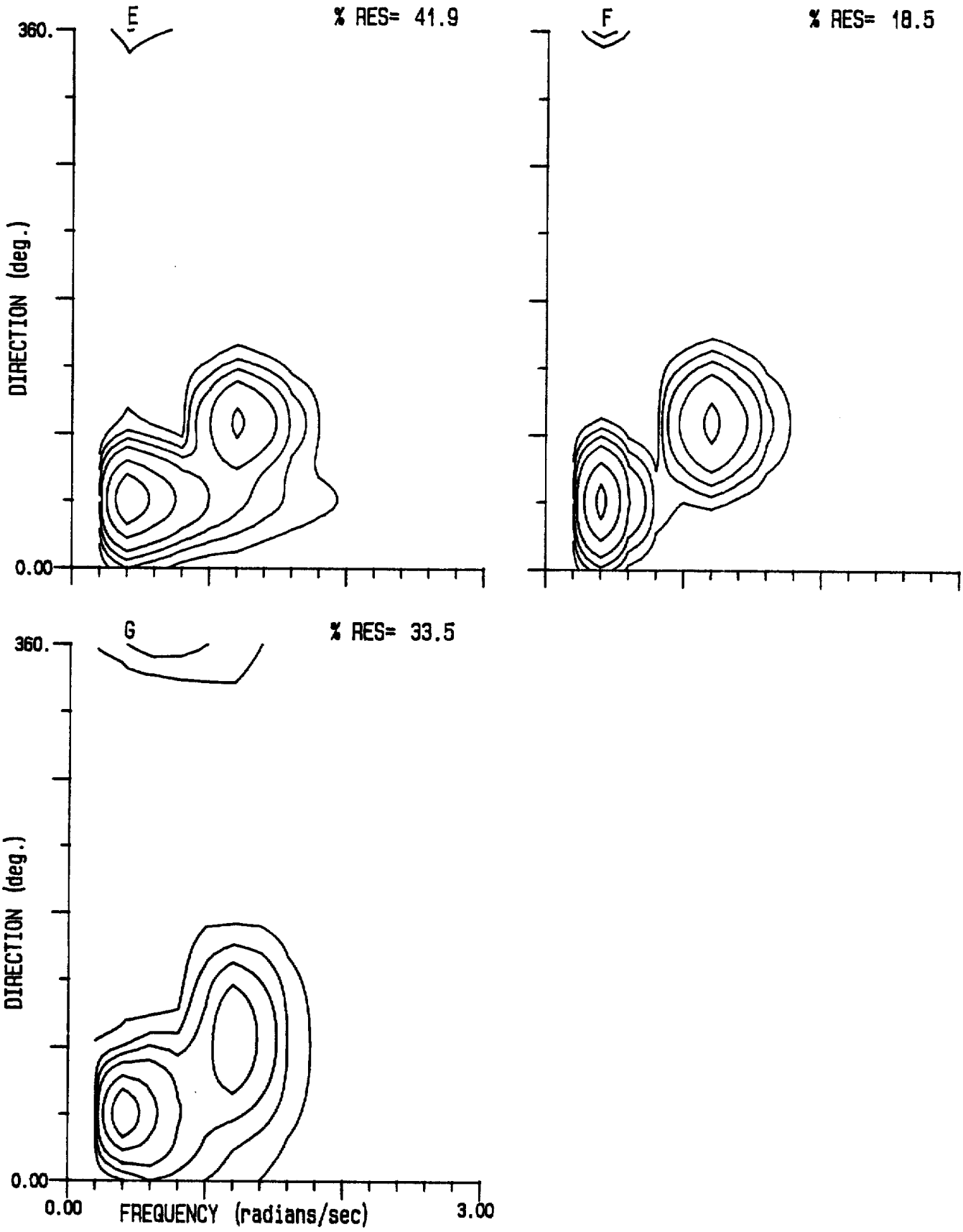
E
% RES= 41.9
F
% RES= 18.5
G
% RES= 33.5
360.
0.00
DIRECTION (deg.)
0.00
FREQUENCY (radians/sec)
3.00

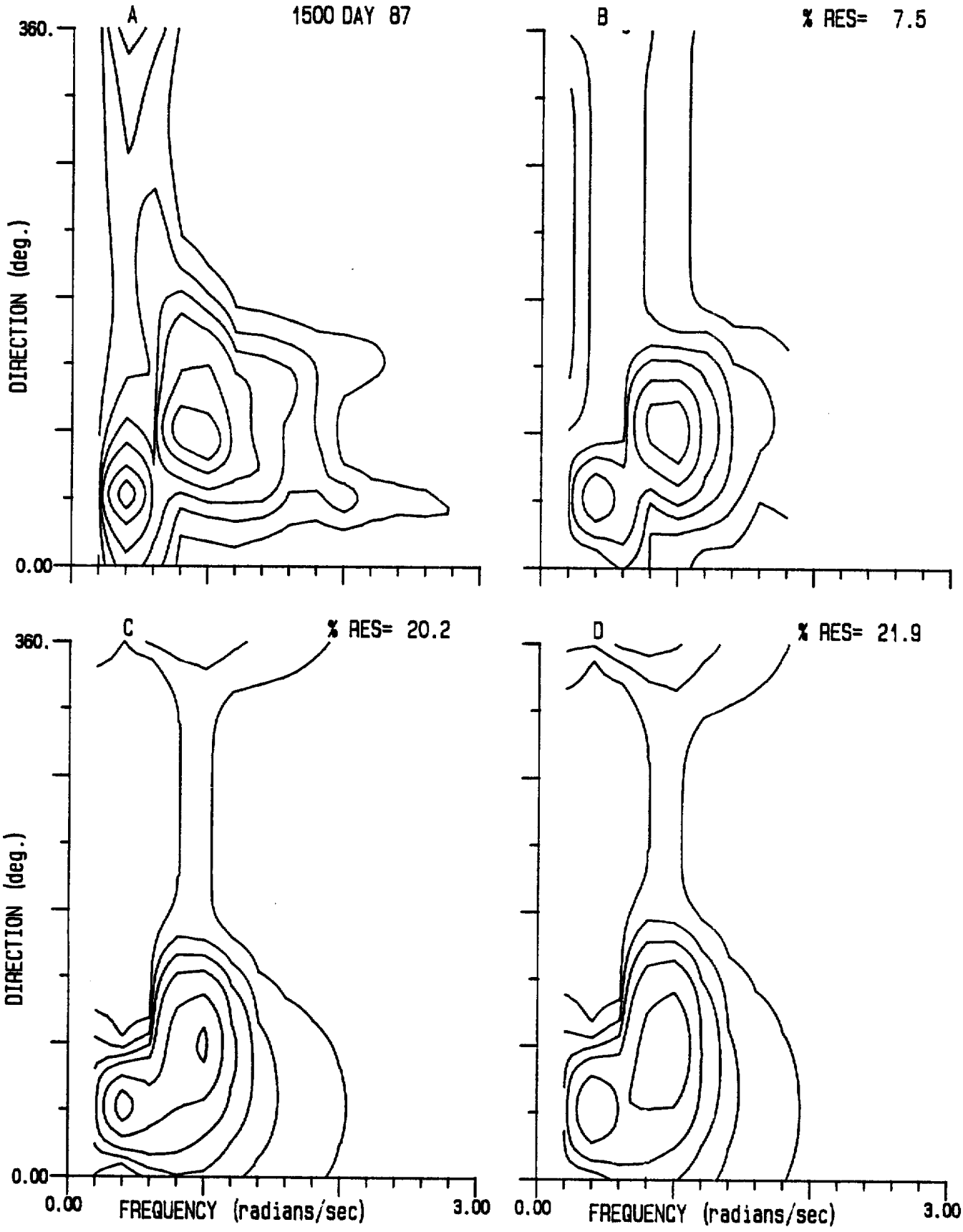
A
1500 DAY 87
B
% RES= 7.5
C
% RES= 20.2
D
% RES= 21.9
360.
0.00
DIRECTION (deg.)
0.00
FREQUENCY (radians/sec)
3.00

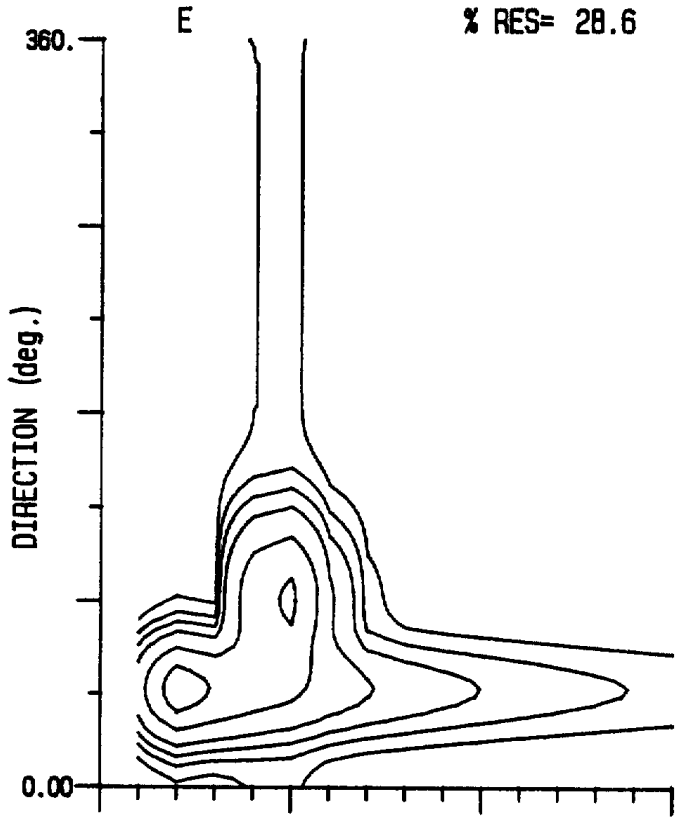
E
% RES= 28.6
360.
0.00
DIRECTION (deg.)

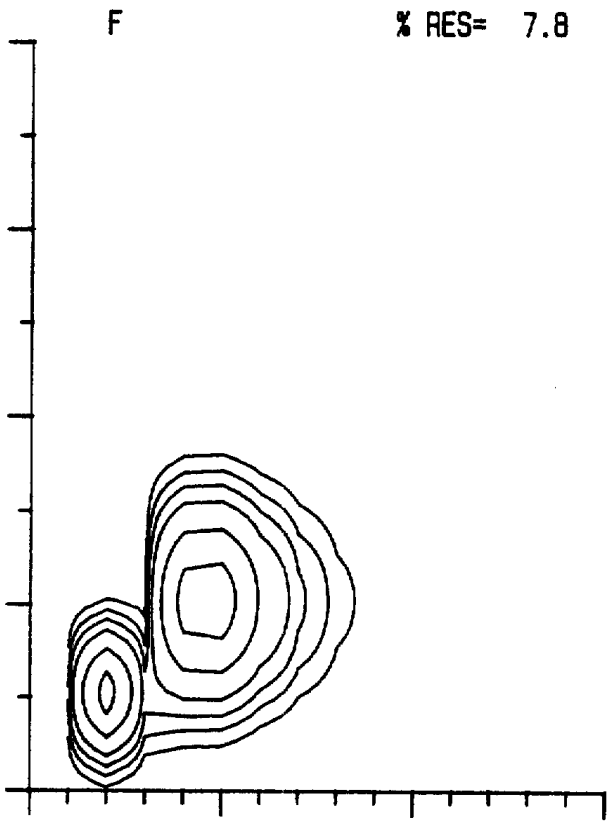
F
% RES= 7.8

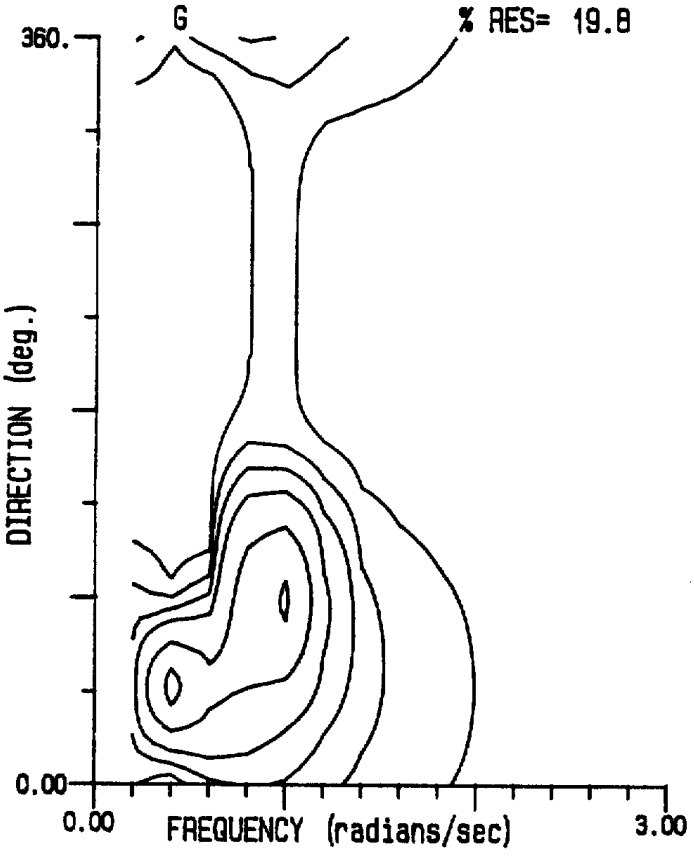
G
% RES= 19.8
360.
0.00
DIRECTION (deg.)
0.00
FREQUENCY (radians/sec)
3.00

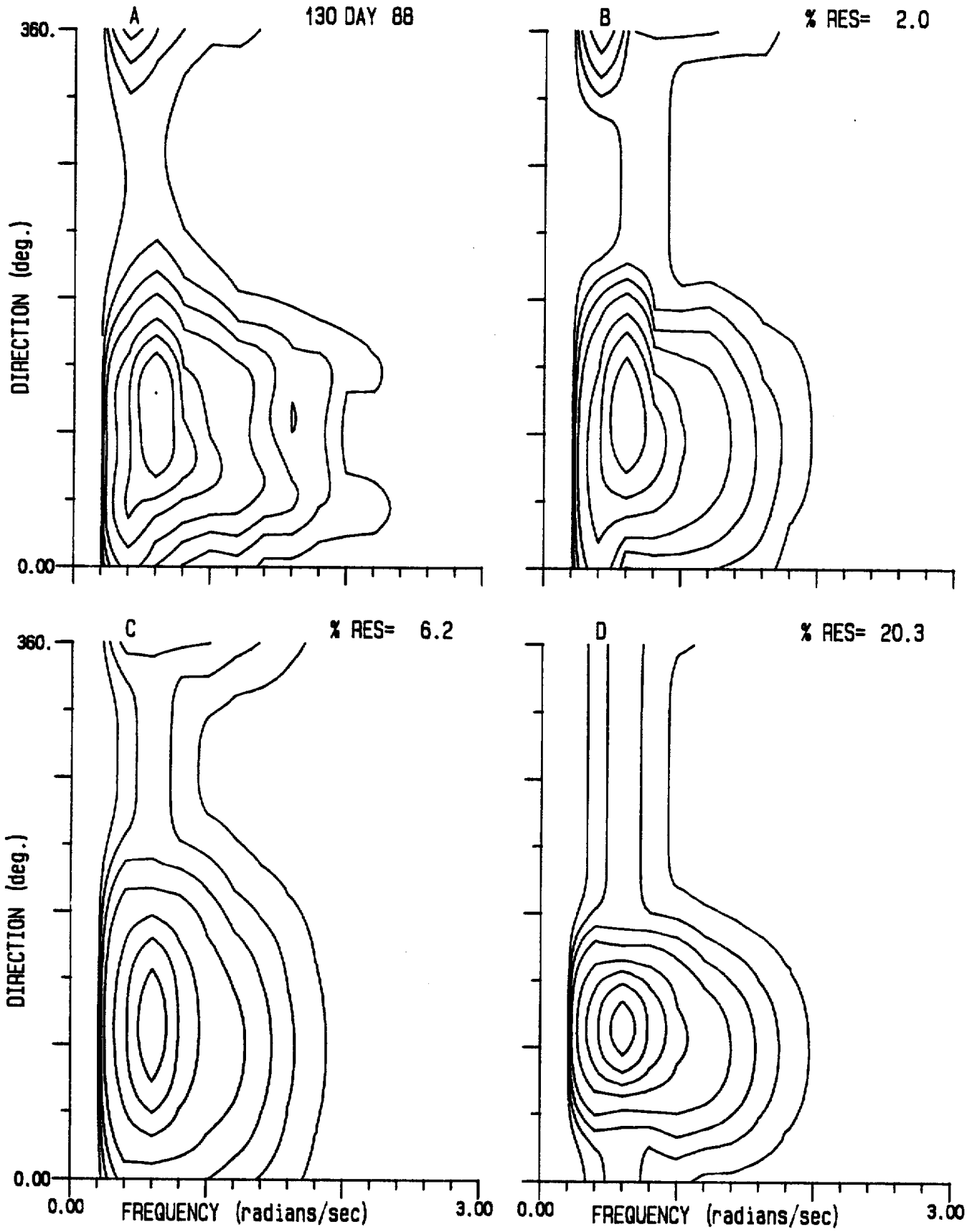
A
130 DAY 88
B
% RES= 2.0
C
% RES= 6.2
D
% RES= 20.3
360.
0.00
DIRECTION (deg.)
0.00
FREQUENCY (radians/sec)
3.00

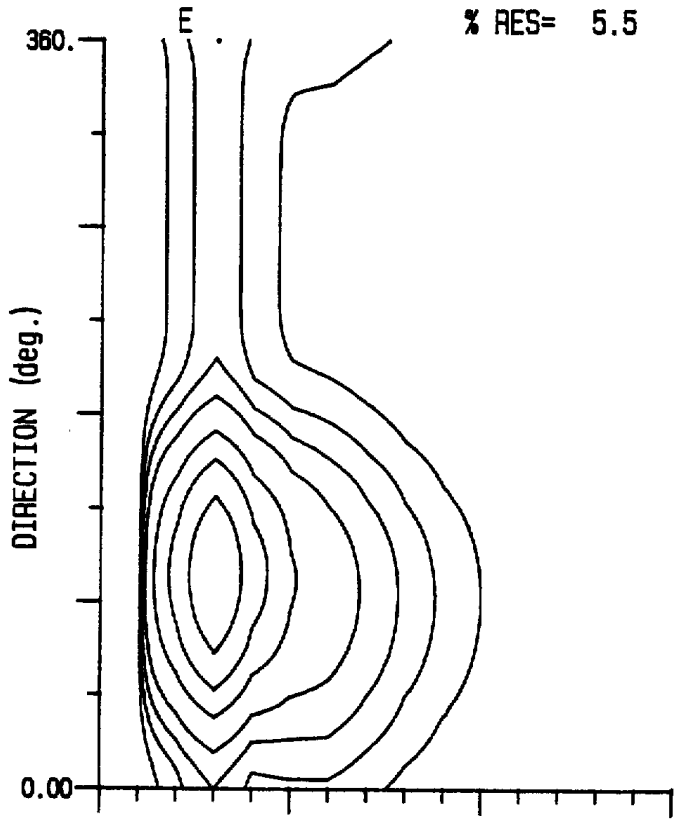
E
% RES= 5.5
360.
0.00
DIRECTION (deg.)

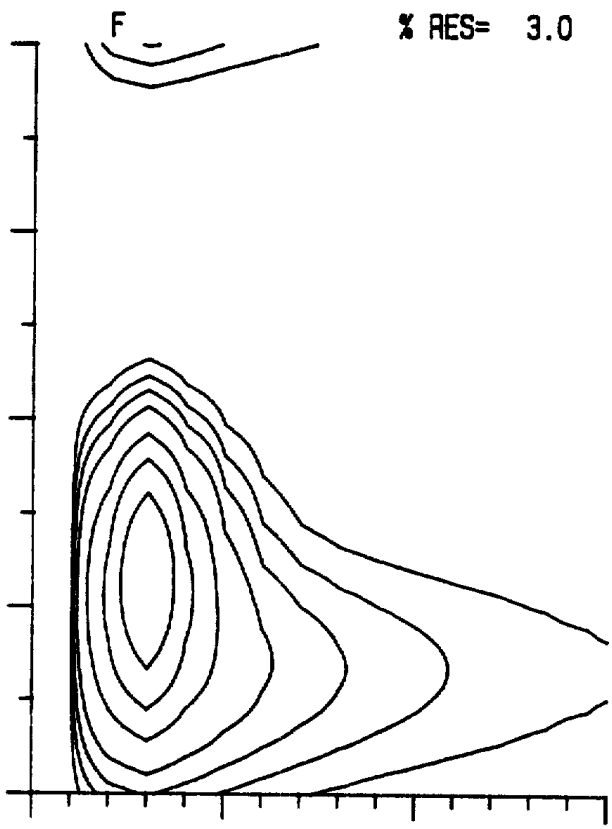
F
% RES= 3.0

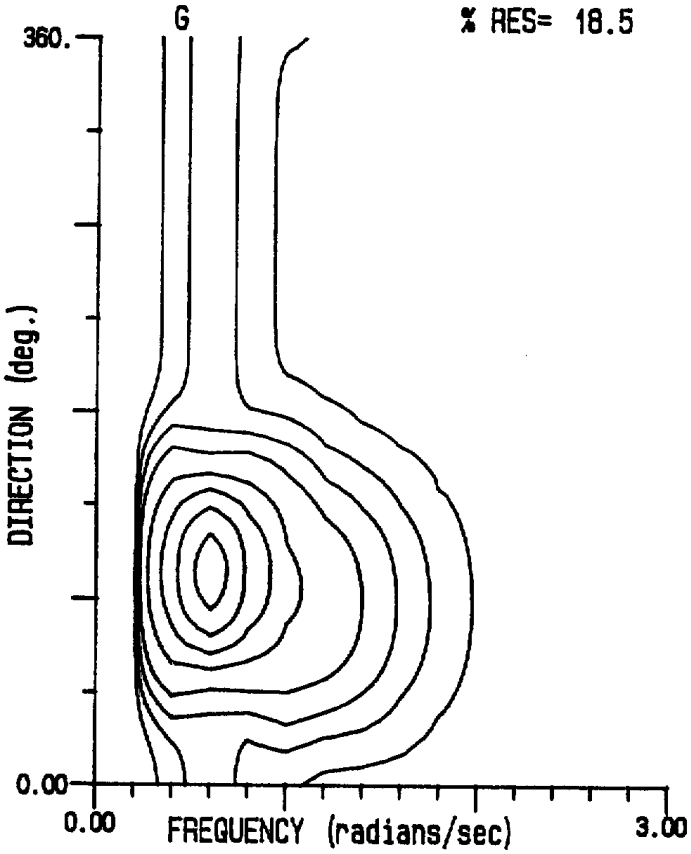
G
% RES= 18.5
360.
0.00
DIRECTION (deg.)
0.00
FREQUENCY (radians/sec)
3.00

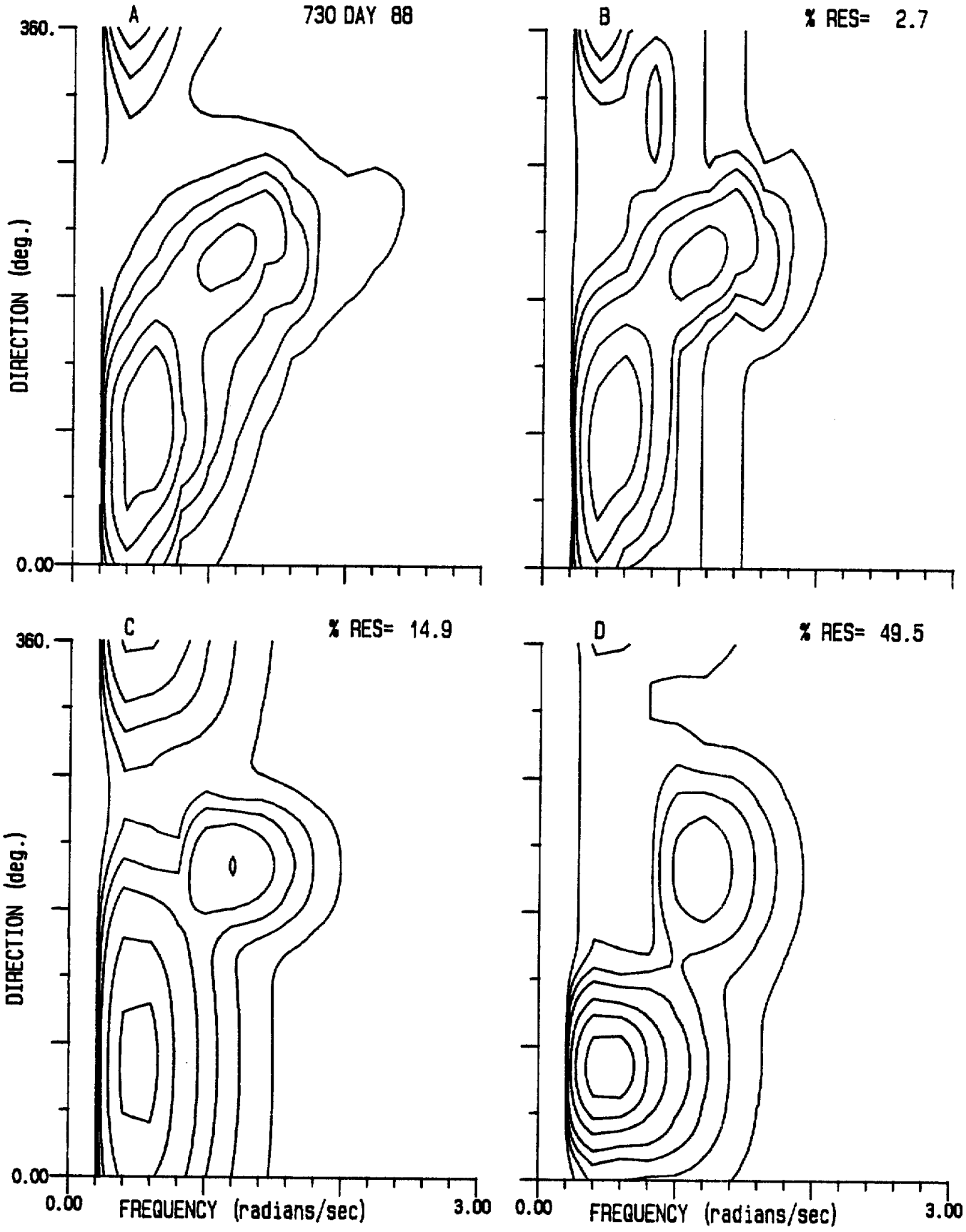
A
730 DAY 88
B
% RES= 2.7
C
% RES= 14.9
D
% RES= 49.5
360.
0.00
DIRECTION (deg.)
0.00
FREQUENCY (radians/sec)
3.00

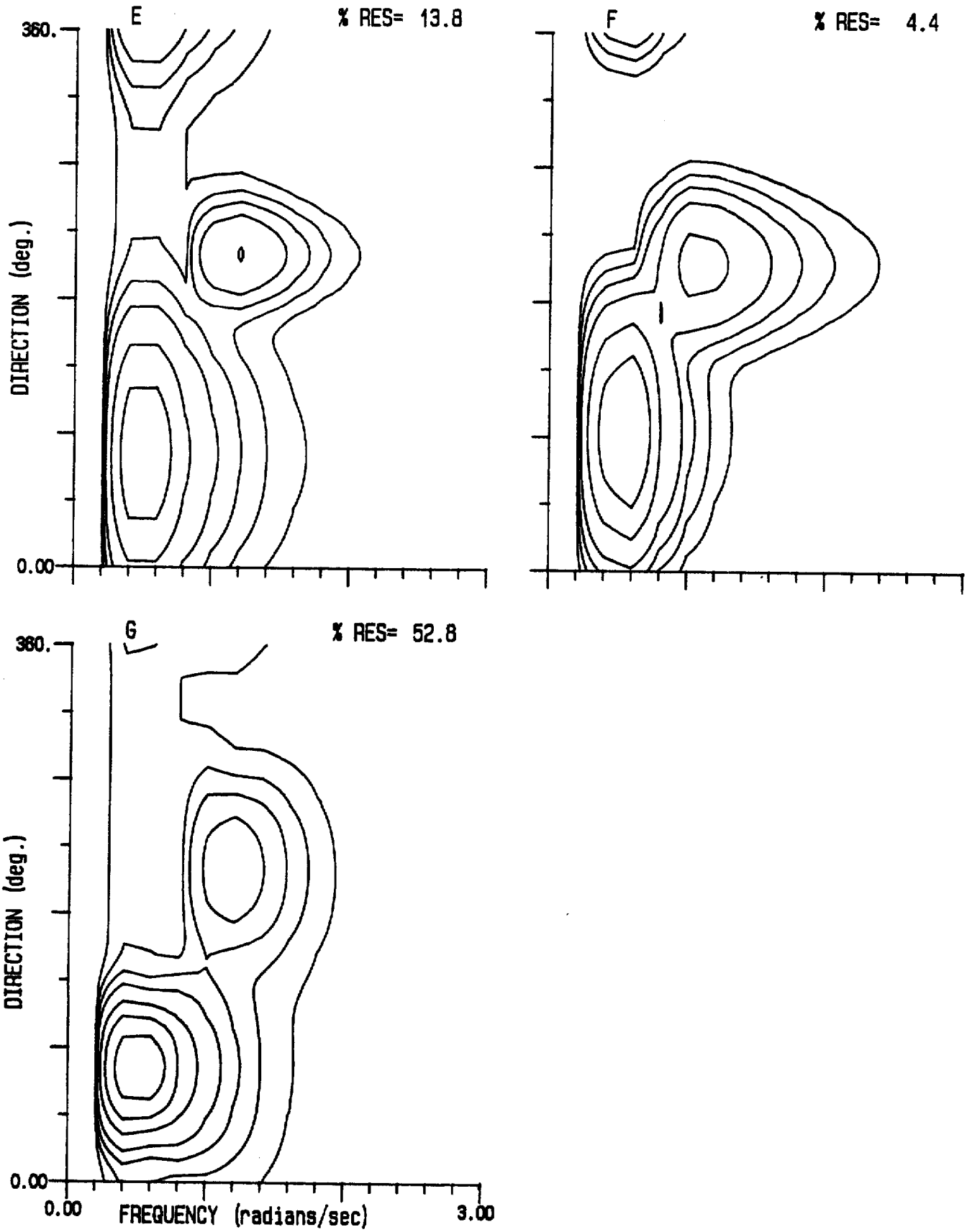
E
% RES= 13.8
360.
0.00
DIRECTION (deg.)
F
% RES= 4.4
G
% RES= 52.8
360.
0.00
DIRECTION (deg.)
0.00
FREQUENCY (radians/sec)
3.00

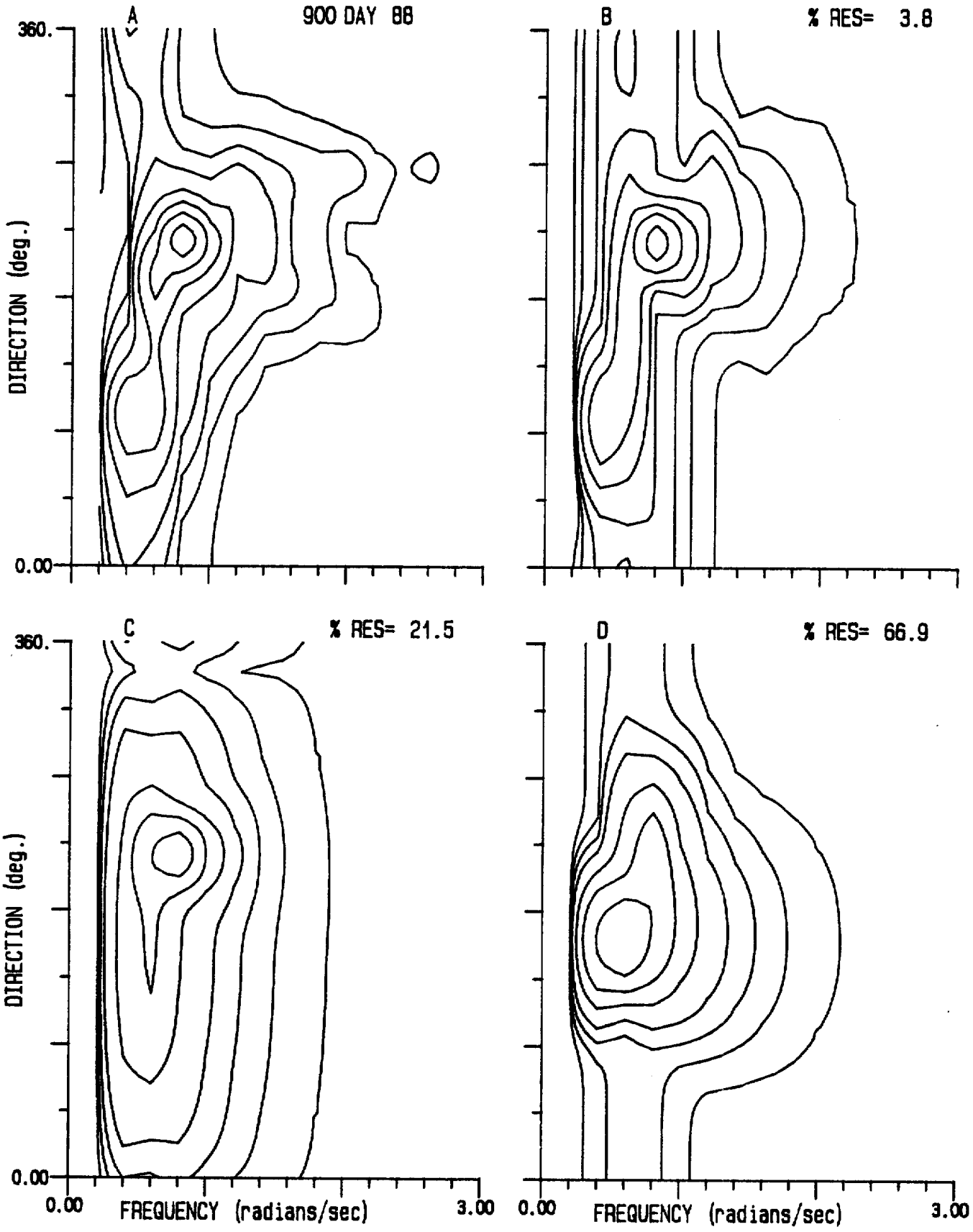
A
900 DAY 88
B
% RES= 3.8
C
% RES= 21.5
D
% RES= 66.9
360.
0.00
DIRECTION (deg.)
0.00
FREQUENCY (radians/sec)
3.00

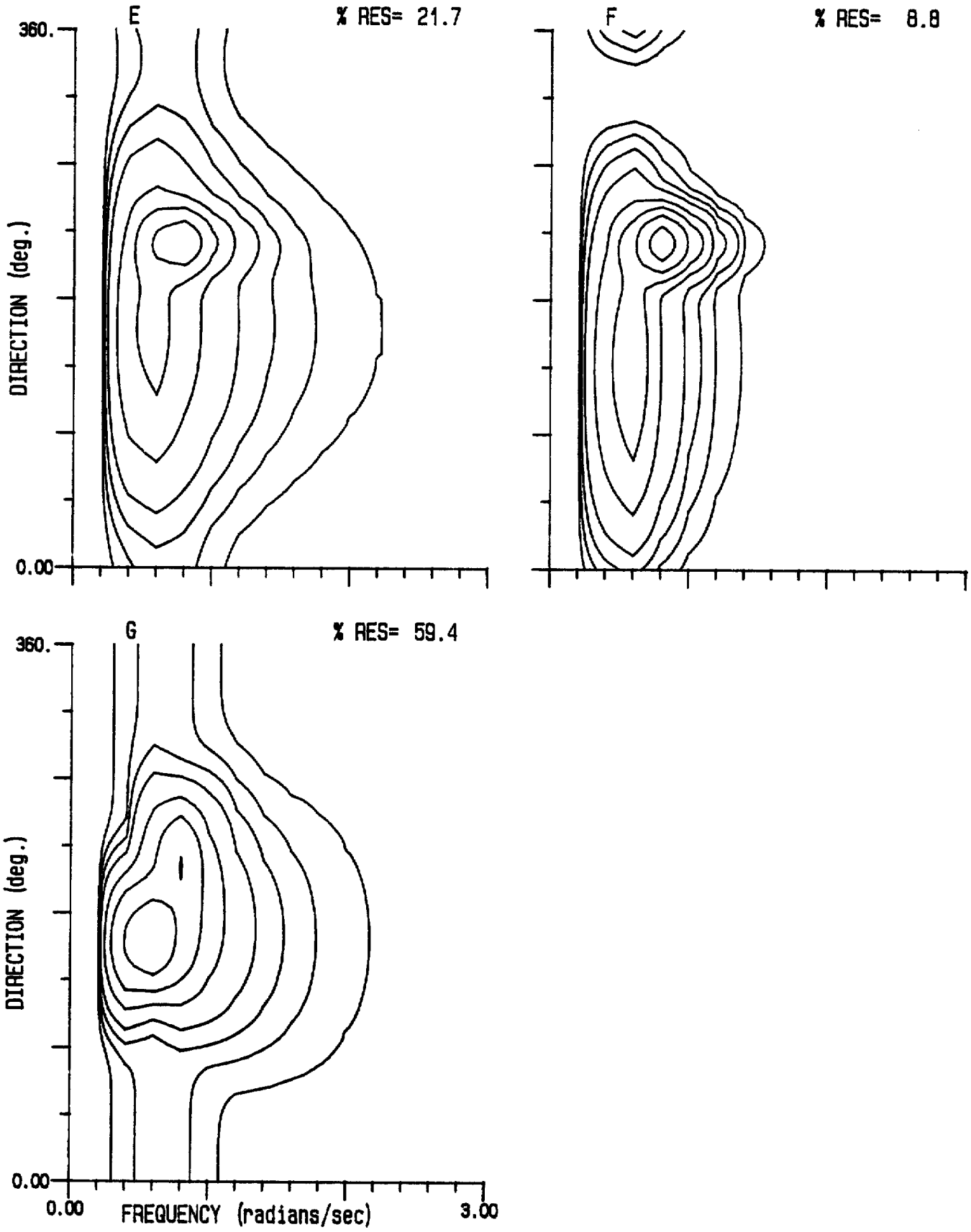
E
% RES= 21.7
F
% RES= 8.8
G
% RES= 59.4
360.
0.00
DIRECTION (deg.)
0.00
FREQUENCY (radians/sec)
3.00

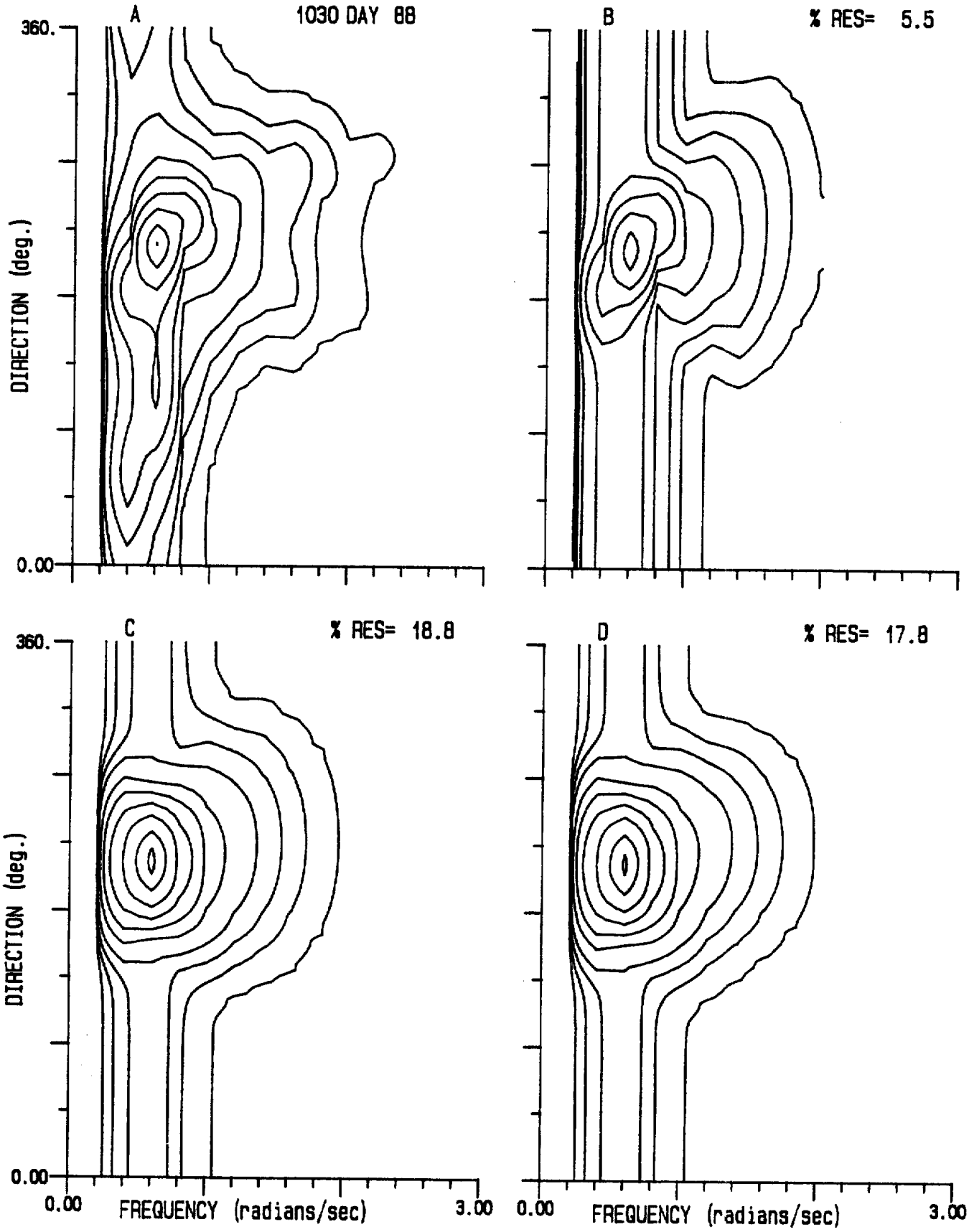
A
1030 DAY 88
B
% RES= 5.5
C
% RES= 18.8
D
% RES= 17.8
360.
0.00
DIRECTION (deg.)
0.00
FREQUENCY (radians/sec)
3.00

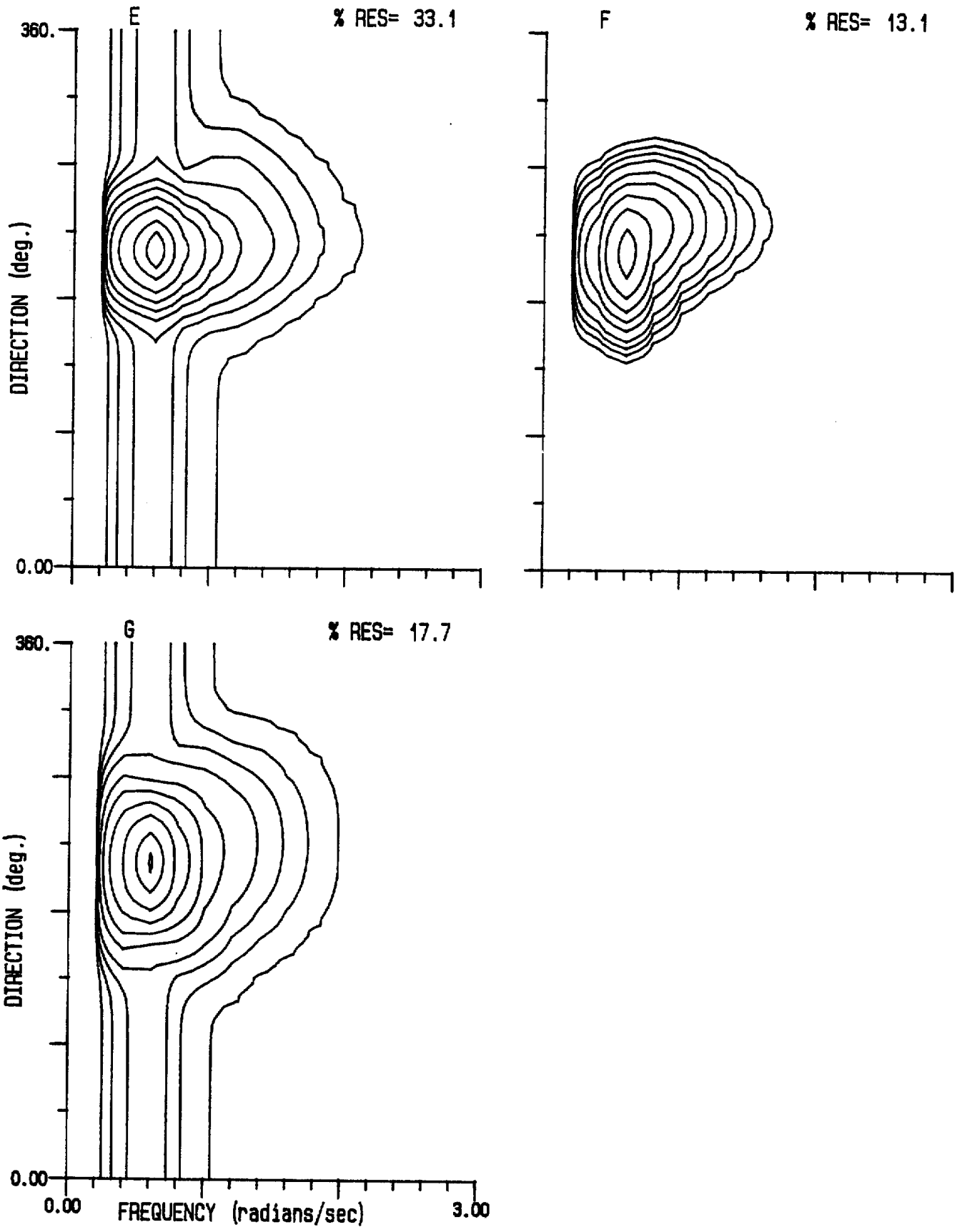
E
% RES= 33.1
360.
0.00
DIRECTION (deg.)
F
% RES= 13.1
G
% RES= 17.7
360.
0.00
DIRECTION (deg.)
0.00
FREQUENCY (radians/sec)
3.00

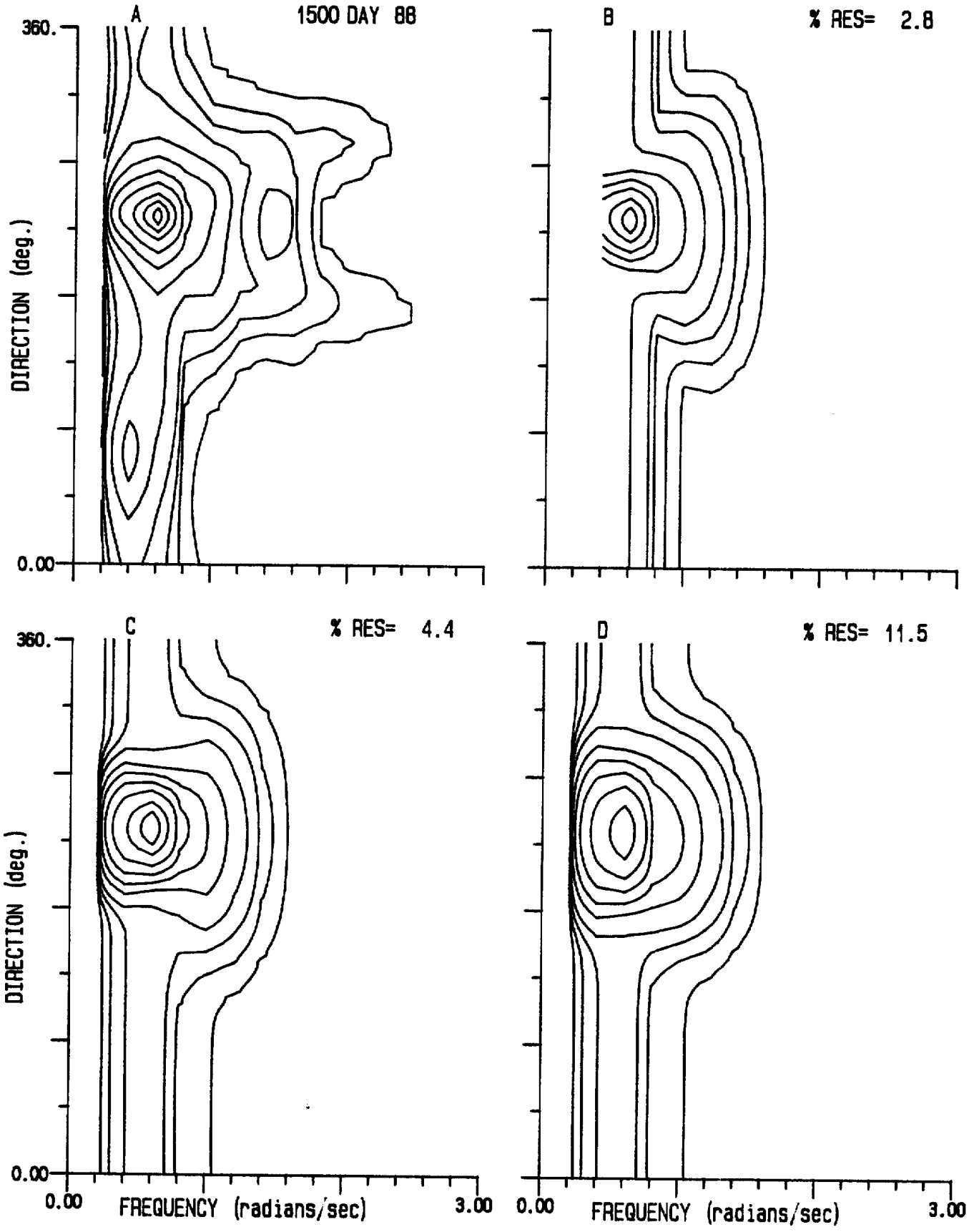
A
1500 DAY 88
B
% RES= 2.8
C
% RES= 4.4
D
% RES= 11.5
360.
0.00
DIRECTION (deg.)
0.00
FREQUENCY (radians/sec)
3.00

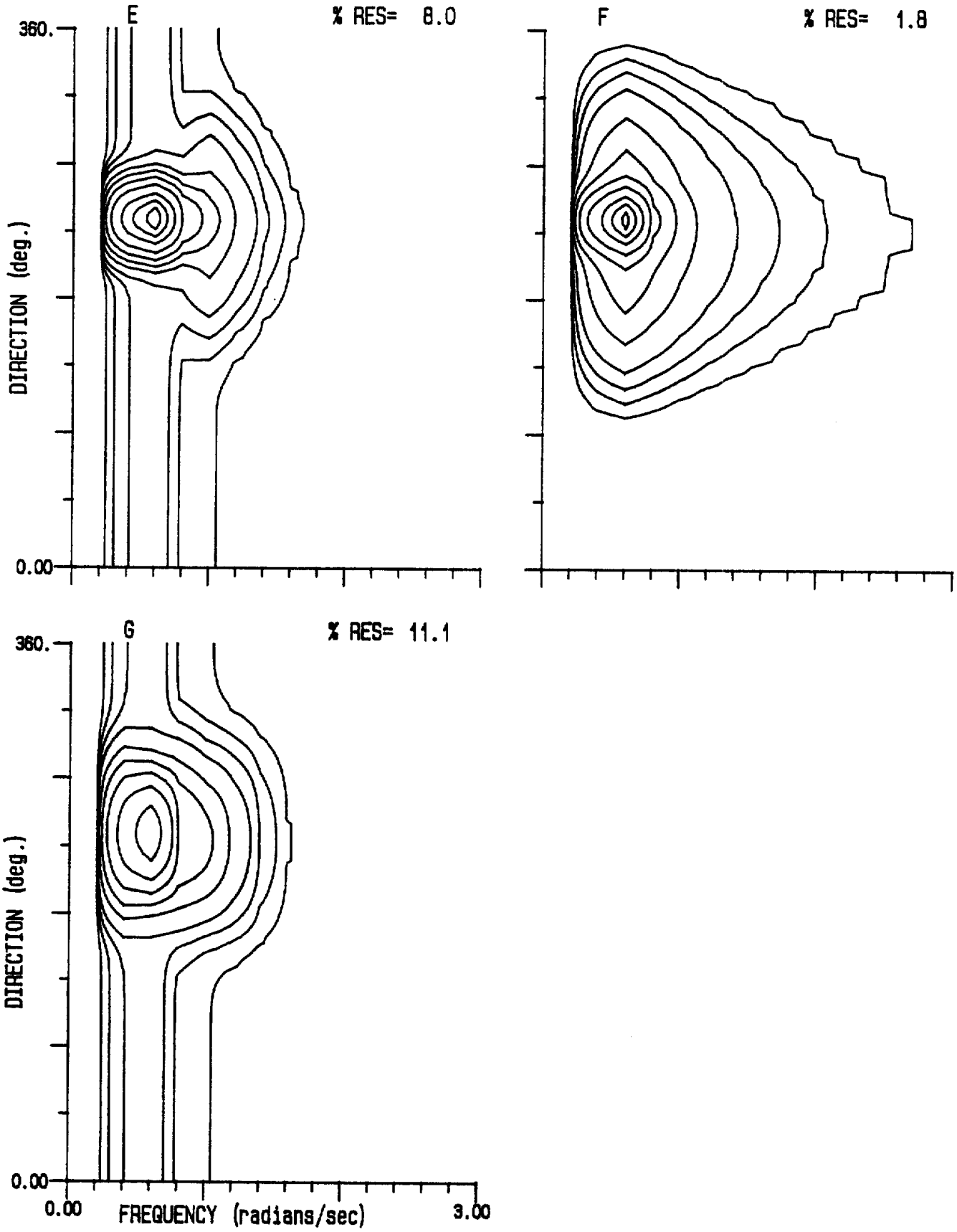
E
% RES= 8.0
F
% RES= 1.8
G
% RES= 11.1
360.
0.00
DIRECTION (deg.)
0.00
FREQUENCY (radians/sec)
3.00

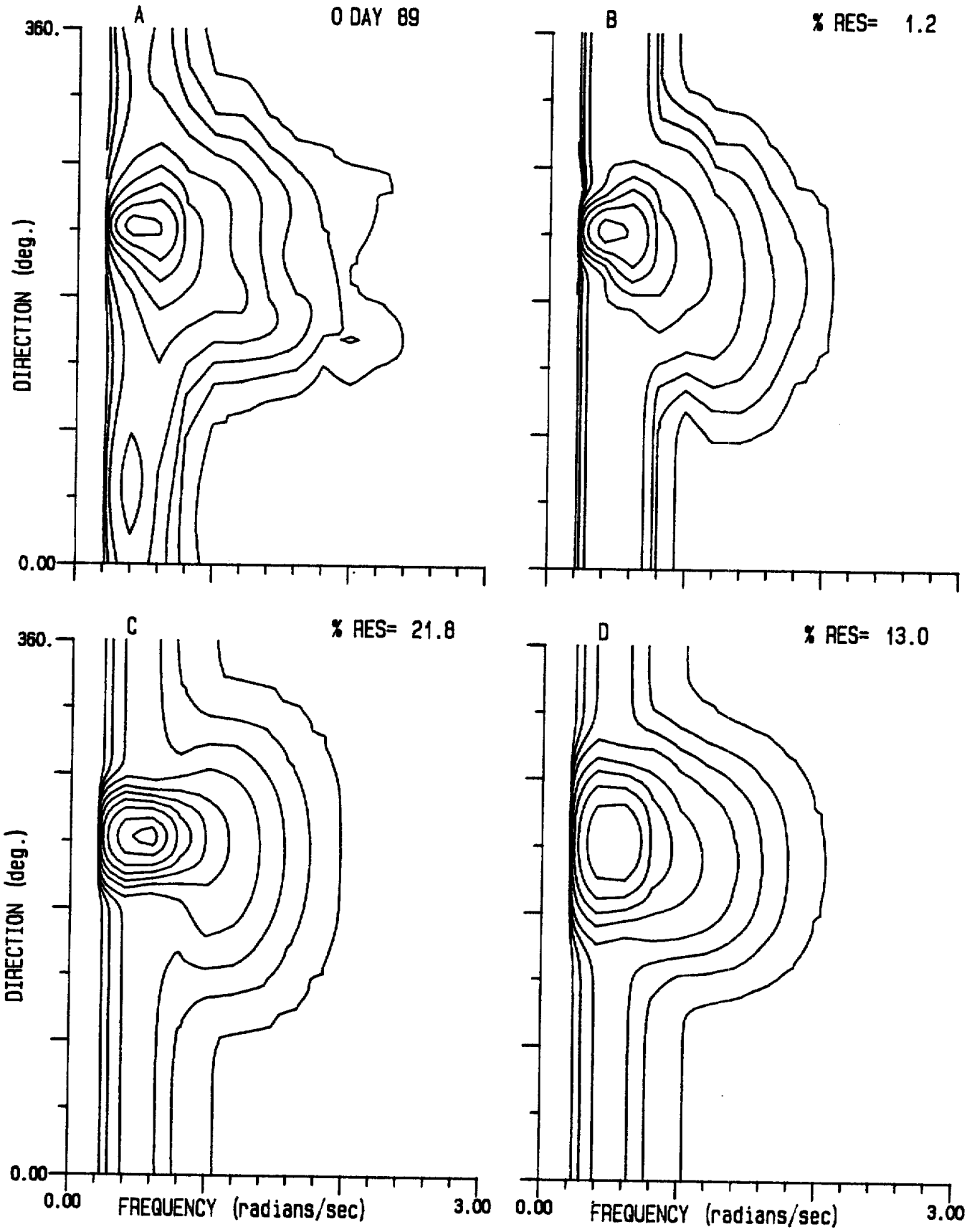
A
0 DAY 89
B
% RES= 1.2
C
% RES= 21.8
D
% RES= 13.0
360.
0.00
DIRECTION (deg.)
0.00
FREQUENCY (radians/sec)
3.00

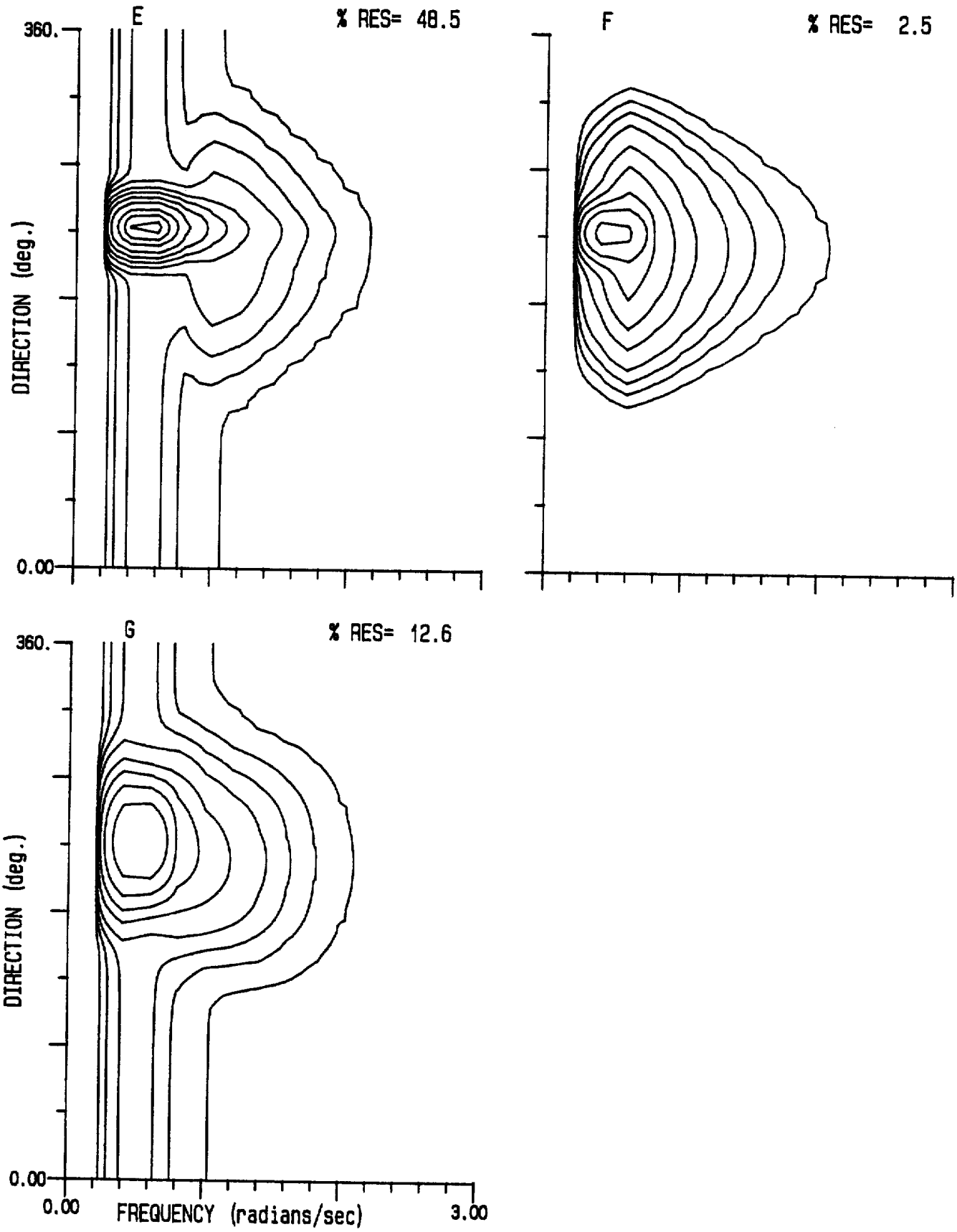
E
% RES= 48.5
360.
0.00
DIRECTION (deg.)
F
% RES= 2.5
G
% RES= 12.6
360.
0.00
DIRECTION (deg.)
0.00
FREQUENCY (radians/sec)
3.00

DND 1

UNCLASSIFIED
SECURITY CLASSIFICATION OF FORM
(highest classification of Title, Abstract, Keywords)

DOCUMENT CONTROL DATA

(Security classification of title, body of abstract and indexing annotation must be entered when the overall document is classified)

1. ORIGINATOR (the name and address of the organization preparing the document Organizations for whom the document was prepared, e.g. Establishment sponsoring a contractor's report, or tasking agency, are entered in section 8.)

JUSZKO SCIENTIFIC SERVICES

2. SECURITY CLASSIFICATION (overall security classification of the document including special warning terms if applicable).

UNCLASSIFIED

3. TITLE (the complete document title as indicated on the title page. Its classification should be indicated by the appropriate abbreviation (S,C,R or U) in parentheses after the title).

PARAMETERIZATION OF DIRECTIONAL SPECTRA

4. AUTHORS (Last name, first name, middle initial. If military, show rank, e.g. Doe, Maj. John E.)

JUSZKO, BARBARA-ANN

5. DATE OF PUBLICATION (month and year of publication of document)

MARCH 1989

6a. NO OF PAGES (total containing information include Annexes, Appendices, etc).

141

6b. NO. OF REFS (total cited in document)

10

6. DESCRIPTIVE NOTES (the category of the document, e.g. technical report, technical note or memorandum. If appropriate, enter the type of report, e.g. interim, progress, summary, annual or final. Give the inclusive dates when a specific reporting period is covered).

CONTRACTOR REPORT

8. SPONSORING ACTIVITY (the name of the department project office or laboratory sponsoring the research and development. Include the address).

DEFENCE RESEARCH ESTABLISHMENT ATLANTIC
P. O. BOX 1012
DARTMOUTH, NOVA SCOTIA B2Y 3Z7

9a. PROJECT OR GRANT NO. (if appropriate, the applicable research and development project or grant number under which the document was written. Please specify whether project or grant).

1AG

9b. CONTRACT NO. (if appropriate, the applicable number under which the document was written).

W7707-8-1049/01-OSC

10a. ORIGINATOR'S DOCUMENT NUMBER (the official document number by which the document is identified by the originating activity. This number must be unique to this document).

DREA/CR/89/414

10b. OTHER DOCUMENT NOS. (Any other numbers which may be assigned this document either by the originator or by the sponsor).

11. DOCUMENT AVAILABILITY (any limitations on further dissemination of the document, other than those imposed by security classification)

(X) Unlimited distribution
( ) Distribution limited to defence departments and defence contractors; further distribution only as approved
( ) Distribution limited to defence departments and Canadian defence contractors; further distribution only as approved
( ) Distribution limited to government departments and agencies; further distribution only as approved
( ) Distribution limited to defence departments; further distribution only as approved
( ) Other (please specify):

12. DOCUMENT ANNOUNCEMENT (any limitation to the bibliographic announcement of this document. This will normally correspond to the Document Availability (11). However, where further distribution (beyond the audience specified in 11) is possible, a wider announcement audience may be selected).

UNCLASSIFIED
SECURITY CLASSIFICATION OF FORM

DCD03 2/06/87-M

UNCLASSIFIED
SECURITY CLASSIFICATION OF FORM

13. ABSTRACT (a brief and factual summary of the document. It may also appear elsewhere in the body of the document itself. It is highly desirable that the abstract of classified documents be unclassified. Each paragraph of the abstract shall begin with an indication of the security classification of the information in the paragraph (unless the document itself is unclassified) represented as (S), (C), (R), or (U). It is not necessary to include here abstracts in both official languages unless the text is bilingual).

High-resolution directional wave spectra, obtained from a WAVEC buoy moored on the Grand Banks in 1984, were modelled using various directional parameterizations. Consistent with most approaches in the literature, a two-part parameterization was attempted. Initially, the Ochi and Hubble (1976) six-parameter amplitude model (OH model) was fitted to the data amplitude spectrum. Parameterization of the directional component was then examined using a basic two-parameter cosine-power model upon which various limitations on the parameters were introduced. The model was assessed by its ability to reproduce the data spectrum based on a least-squares residual statistic. A 10-parameter model, for which the amplitude and direction parameters were fitted simulataneously, was then developed as an extension to the OH model. It was shown to outperform any equivalent, two-part parameterization and could acceptably reproduce over 90% of the data records.

14. KEYWORDS, DESCRIPTORS or IDENTIFIERS (technically meaningful terms or short phrases that characterize a document and could be helpful in cataloguing the document. They should be selected so that no security classification is required. Identifiers, such as equipment model designation, trade name, military project code name, geographic location may also be included. If possible keywords should be selected from a published thesaurus. e.g. Thesaurus of Engineering and Scientific Terms (TEST) and that thesaurus-identified. If it not possible to select indexing terms which are Unclassified, the classification of each should be indicated as with the title).

waves
ocean waves
wave spectra
directional wave spectra